INFORMATION TO USERS

This material was produced from a microfilm copy of the original document. While the most advanced technological means to photograph and reproduce this document have been used, the quality is heavily dependent upon the quality of the original submitted.

The following explanation of techniques is provided to help you understand markings or patterns which may appear on this reproduction.

1. The sign or "target" for pages apparently lacking from the document photographed is "Missing Page(s)". If it was possible to obtain the missing page(s) or section, they are spliced into the film along with adjacent pages. This may have necessitated cutting thru an image and duplicating adjacent pages to insure you complete continuity.

2. When an image on the film is obliterated with a large round black mark, it is an indication that the photographer suspected that the copy may have moved during exposure and thus cause a blurred image. You will find a good image of the page in the adjacent frame.

3. When a map, drawing or chart, etc., was part of the material being photographed the photographer followed a definite method in "sectioning" the material. It is customary to begin photoing at the upper left hand corner of a large sheet and to continue photoing from left to right in equal sections with a small overlap. If necessary, sectioning is continued again — beginning below the first row and continuing on until complete.

4. The majority of users indicate that the textual content is of greatest value, however, a somewhat higher quality reproduction could be made from "photographs" if essential to the understanding of the dissertation. Silver prints of "photographs" may be ordered at additional charge by writing the Order Department, giving the catalog number, title, author and specific pages you wish reproduced.

5. PLEASE NOTE: Some pages may have indistinct print. Filmed as received.

Xerox University Microfilms
300 North Zeeb Road
Ann Arbor, Michigan 48106

A STUDY OF SURFICIAL PROCESSES AND GEOMORPHIC HISTORY OF A BASIN IN THE SONORAN DESERT, SOUTHWESTERN ARIZONA

A dissertation submitted to the

Division of Graduate Studies
of the University of Cincinnati

in partial fulfillment of the
requirements for the degree of

DOCTOR OF PHILOSOPHY

in the Department of Geology
of the College of Arts and Sciences

1976

by

Stephen G. Wells

B.S. Indiana University, 1971
M.S. University of Cincinnati, 1973

UNIVERSITY OF CINCINNATI

June 11 *19* 76

I hereby recommend that the thesis prepared under my supervision by Stephen G. Wells

entitled A Study of Surficial Processes and Geomorphic History of a Basin in the Sonoran Desert, Southwestern Arizona

be accepted as fulfilling this part of the requirements for the degree of Doctor of Philosophy

Approved by:

Form 668—Grad. School—1M—12-69

CONTENTS

	Page
Abstract	xiii
Acknowledgements	xv
Introduction	1
State of Problem, Purpose, and Approach	1
Location	2
Climate	4
General Geology	4
Bedrock Geology	5
Structural Geology	8
Physiography of Sonoran Desert	8
Vegetation	9
Glossary	10
Techniques of Investigation	13
Mapping of Physiographic Units and Landforms	13
Mapping General Drainage Features	16
Hydrologic Studies and Measurements	17
Particle Size Studies for Wash Deposits and Surficial Deposits	19
Soil Studies	20
Mapping Quaternary Surficial Deposits	20
Mapping Geomorphic Parameters	21
LANDSAT Imagery Studies	22
Results of Investigation	23
Harquahala Valley Basin Characteristics and Geomorphology	23

Topography 23

General Drainage Features 36

General Hydrology of Study Area 41

Streamflow Characteristics of Centennial Wash and other Ephemeral Washes 41

Precipitation and Runoff Relationships 46

Comparison of the Study Area to a Semi-Arid Basin Near the Sonoran Desert 48

Quaternary Surficial Deposits of the Harquahala Valley 50

Mapping Units of the Surficial Deposits 51

Particle Size Analyses of the Surficial Deposits 66

Distribution and Form of the Surficial Deposits 67

Relationship of the Surficial Deposits to Topography . . 75

Soils of the Harquahala Valley 86

Stratigraphic Relationahips of Basin Fill Units in the Harquahala Valley 91

Subsurface Units 91

Surficial Deposits 95

Analysis of LANDSAT Imagery and the Surficial Deposits of the Study Area 103

MSS Band 7 103

Color Composite Imagery 106

Geomorphology of Low Order Drainage Basins in the Harquahala Valley 108

Geomorphic Parameters of Low Order Drainage Basins . . . 108

Sedimentology of Ephemeral Washes in Low Order Drainage Basins 124

Hydraulic Geometry and Hydrology of Ephemeral Washes in Low Order Drainage Basins 141

Geomorphic Relationships in Low Order Drainage Basins . 143

Discussion of Results 158

Surficial Processes in Low Order Basins of the Harquahala Valley 158

Hydrologic Behavior of Ephemeral Washes 158

Channel Forming Events and Aggradation in Low Order Drainage Basins 164

Relationships between Wash Processes and Geomorphic Parameters of Low Order Drainage Basins 173

Conceptual Model for Ephemeral Wash Aggradation 177

Processes on Interfluves of Low Order Drainage Basins . 180

Process Geomorphology of the Harquahala Valley Bolson Plain . 186

Geomorphic History of the Harquahala Valley 191

Quaternary History 191

Paleoclimatic and Paleohydrologic Considerations . . . 198

Conclusions and Summary 202

Landforms and Surficial Deposits of the Harquahala Valley . . 202

Dynamics of Surface Runoff in an Arid Basin 204

Factors Controlling Ephemeral Wash Aggradation 205

Factors Influencing Desert Pavement Development 207

Quaternary Geomorphic History of the Harquahala Valley . . . 208

Applications to Land Use and Practical Problems in the Sonoran Desert 211

References 215

Appendix I 221

Appendix II 249

Appendix III 276

Appendix IV 279

Appendix V 285

Appendix VI 290

LIST OF FIGURES

Figure		Page
1	Location map of the study area in Maricopa and Yuma Counties, southwestern Arizona	3
2	Generalized map of study area showing bedrock geology	6
3	Grid system on Harquahala Valley bolson plain used to construct slope and drainage texture map	15
4	Physiography of Harquahala Valley basin and surrounding areas	24
5	Histogram of areal extent of bedrock in mountain ranges and inselbergs of the Harquahala Valley basin	25
6	Selected topographic profiles across alluvial aprons in Harquahala Valley	27
7	Histogram showing frequency of regional slope angles on the Harquahala Valley bolson plain	30
8	In pocket. Slope map of the Harquahala Valley bolson plain	
9	In pocket. Drainage texture map of the Harquahala Valley bolson plain	
10	Histogram showing frequency of drainage texture values	33
11	Longitudinal profile of fan surface and wash on Harquahala Mountain alluvial apron	34
12	Rose diagram of frequency of major drainage line orientations on selected alluvial aprons in the study area	38
13	General drainage patterns on alluvial aprons	30
14	Discharge hydrograph for summer flood events on Centennial Wash, Arizona	42
15	Flow duration curves for selected washes in the Sonoran Desert	44
16	Recurrence interval for Centennial Wash, Arizona	45
17	Logarithmic plot of runoff and precipitation during winter and summer months in the Harquahala Valley	47

Figure		Page
18	Percentage of annual runoff and precipitation for Centennial Wash and Harquahala Valley over a ten year period	49
19	Cumulative curves of particle sizes for selected Quaternary deposits	52
20	Histograms showing frequency of grain sizes in θ intervals for selected Quaternary deposits	53
21	Histogram showing frequency of areal extent of Quaternary surficial deposits on the bolson plain of the Harquahala Valley	55
22	A. Aerial view of fine grained alluvial fan	57
	B. Ground view of fine grained alluvial fan with coppice dunes	57
23	A. Aerial view of eolian dune deposits and their eradication by cultivation	59
	B. Close-up view of eolian dunes showing linguoid form . . .	59
24	Trench in the Quaternary varnished gravels showing a few centimeters thick desert pavement and a mixed gravel and silt layer	62
25	In pocket. Quaternary surficial deposits of the Harquahala Valley bolson plain	
26	Aerial view of alluvial apron flanking Saddle Mountain . . .	64
27	Areal extent of ripple-train phenomena on caliche rubble deposits of alluvial apron flanking Saddle Mountain	70
28	A. Varnished desert pavement surface in mid apron region showing little dissection	72
	B. Varnished desert pavement surface (Qgv) in provimal apron region showing dissection by meandering gullies . .	72
29	Relationship between maximum length and width of desert pavement segments in Harquahala Valley	74
30	Detailed longitudinal profie (BHL-d) and description of surficial deposits on Big Horn Mountain alluvial apron . . .	76
31	Detailed longitudinal profile (BHL-e) and description of surficial deposits on Big Horn Mountain alluvial apron . . .	77

Figure Page

32 Detailed topographic profiles (SMT-a and SMT-b) and descriptions of surfical deposits on Saddle Mountain alluvial apron 78

33 Detailed topographic profile (BHT-j) and description of surficial deposits on Big Horn Mountain alluvial apron 79

34 Detailed topographic profiles (HMT-a and HMT-b) and description of surficial deposits on Harquahala Mountains alluvial apron 80

35 Logarithmic scatter plot showing relationship between micro-relief produced by coppice dunes and amount and concentration of gravels on surface of interfluves 82

36 Bar graph showing range in slope angle on interfluves of different Quaternary deposits 84

37 Curves fitted to longitudinal profiles of alluvial apron surfaces of Harquahala Mountains and valley fill remnants in canyons of Harquahala Mountains 85

38 Generalized soils map of the Harquahala Valley bolson plain . 87

39 Paleosol buried by fine grained alluvial fans (Qff) in the Harquahala Valley bolson plain 90

40 Generalized stratigraphic column of basin fill near Arlington, Arizona 93

41 Subsurface units and their stratigraphic relationships in the Harquahala Valley 94

42 Generalized stratigraphic column of surficial deposits of the Harquahala Valley 96

43 Detailed stratigraphic section along the banks of Centennial Wash south of Saddle Mountains 97

44 Paleosol buried by eolian dune deposits in southern Harquahala Valley 100

45 Quaternary debris flows (Qdf) on proximal portions of alluvial aprons and on hillslopes 102

46 Bar graph illustrating range in densities and mean density for surficial deposits shown on LANDSAT Imagery in the Harquahala Valley 104

Figure		Page
47	Location map for low order drainage basins and areal extent of drainage patterns in Harquahala Valley	109
48	Map of the low order drainage basin LMQ-A and LMQ-B illustrating station locations and drainage systems on the alluvial apron	110
49	Longitudinal profiles of principal washes and station locations for low order drainage basins LMQ-A and LMQ-B . . .	111
50	Map of low order drainage basin LMQ-C and longitudinal profile for principal wash draining basins	112
51	Map of low order drainage basin LMQ-D and longitudinal profile of principal wash draining basin	113
52	Map of low order drainage basin BHMQ-A and longitudinal profile of principal wash draining basin	114
53	Map of low order drainage basin BHMQ-B and longitudinal profile of principal wash drainage basin	115
54	Map of low order drainage basin CPQ-A and longitudinal profile of principal wash draining basin	116
55	Map of low order drainage basin CPQ-B and longitudinal profile of principal wash draining basin	117
56	Map of low order drainage basin CPQ-C and longitudinal profile of principal wash draining basin	118
57	Map of low order drainage basin CPQ-D and longitudinal profile of principal wash draining basin	119
58	Map of low order drainage basin EMQ-A and longitudinal profile of principal wash draining basin	120
59	Map of low order drainage basin EMQ-B and longitudinal profile of principal wash draining basin	121
60	Idealized cross-section of ephemeral wash showing berm and channel in addition to hydraulic geometry of a wash based on high water marks from a previous flood	125
61	Cumulative curves for sediments at selected stations of principal wash draining low order drainage basin LMQ-D . . .	126

Figure Page

62 Cumulative curve for sediments at selected stations on principal wash draining low order drainage basin CPQ-C . . . 127

63 Cumulative curve for sediments at selected stations on principal wash draining low order drainage basin LMQ-A . . . 128

64 Cumulative curves for sediments at selected stations on principal wash draining low order basin CPQ-B 129

65 Cumulative curves for sediments at selected stations on principal wash draining low order basin BHNQ-B 130

66 Relationship between particle size and lithology of the clasts for wash sediments and surficial deposits in the Harquahala Valley 132

67 Histograms showing frequency of grain size in θ intervals for channel and berm sediments in the principal wash draining low order basin LMQ-D 133

68 Histograms showing frequency of grain size in θ interval for channel and berm sediments in principal wash draining low order basin CPQ-C 134

69 Histograms showing frequency of grain size in θ interval for channel and berm sediments in principal wash draining low order basin LMQ-A 135

70 Histograms showing frequency of grain size in θ interval for channel and berm sediments in principal wash draining low order basin CPQ-B 136

71 Histograms showing frequency of grain size in θ interval of channel and berm sediments in principal wash draining low order drainage basin BHMQ-B 137

72 Logarithmic plot of maximum particle diameters and tractive forces for selected stations of principal washes in low order basins 140

73 Logarithmic plots of local maximum channel width and length of wash and drainage area above the maximum width for principal washes in low order drainage basins 144

74 Relationship between wash length and drainage area above local maximum channel width for principal washes in low order drainage basins 146

Figure Page

75 Logarithmic plot of drainage area and length of wash above local maximum channel width of principal washes in low order drainage basins in the Harquahala Valley 148

76 Logarithmic plots and regression analyses of computed maximum discharge and drainage area at the local maximum channel width in low order basins with and without caliche rubble 151

77 Flood deposits resulting from a summer thunderstorm on Big Horn Mountain alluvial apron 154

78 Relationship between width-depth ratio and distance from head of principal wash for selected low order drainage basins 155

79 Logarithmic plot and regression analysis of wash length and drainage area above that point on the wash where the width-depth ratio increases rapidly 157

80 Relationship between peak discharge and distance down channel for a single flood event on New River, Arizona . . . 160

81 Relationship between computed velocity, grain diameter of berm sediments (d_{50}) and channel sediments (d_{75}), and state of sediment 165

82 Channel aggradation in ephemeral washes 169

83 Berm aggradation in distal portion of Harquahala Mountains alluvial apron and Big Horn Mountains alluvial apron 171

84 Hypothetical series of hydrographs on an ephemeral wash in the Sonoran Desert 178

85 Relationship of geomorphic parameters which influences channel and berm aggradation in washes of low order drainage in the Harquahala Valley 181

86 Idealized sketches illustrating processes which destroy desert pavement surfaces in the Harquahala Valley 185

87 A. Local erosional surface on coarse grained alluvial fan deposits (Qfc) of Harquahala Mountains alluvial apron . 194

B. Local erosional surface of coarse grained alluvial fan deposits (Qfc) on alluvial apron south of Saddle Mountain 194

Figure Page

88 Relationship of mean annual runoff and precipitation for semi-arid Sycamore Creek basin near Sonoran Desert 201

89 Accelerated erosion and caputre of major drainage lines as a result of lowering base level by excavating a borrow pit . 214

LIST OF TABLES

Table		Page
1	Selected geomorphic parameters of the Harquahala Valley Mountains and associated alluvial aprons	28
2	Rank of flanking alluvial aprons according to their highest frequency and drainage texture value in the Harquahala Valley	35
3	Selected geometric parameters of well developed desert pavement segments in the Harquahala Valley	73
4	Density measurements from color composite transparencies of MSS Bands 4, 5, and 7 of LANDSAT Imagery of the Harquahala Valley	107
5	Maximum particle diameter in cm at selected stations on principal washes draining low order drainage basins	139
6	Selected hydraulic geometry parameters and tractive forces for principal washes draining low order drainage basins in the study area	149
7	Regression equation and coefficients for relationship between width-depth ratio and length of wash from divide in selected low order drainage basins	163

ABSTRACT

The bolson plain of the Harquahala Valley in the Sonoran Desert of southwestern Arizona, is composed of coalescing alluvial aprons (fans and buried pediments) which flank major mountain ranges. The shape and slope of these alluvial aprons are influenced by the size and lithology of the contributing bedrock areas. Quaternary surficial deposits, which form the aprons, can be differentiated and mapped on the basis of particle size and alteration due to weathering. These deposits include coarse and fine grained alluvial fans, varnished gravels, caliche rubble, and eolian sand dunes. Coarse grained alluvial fans occur on the mid to upper apron regions and cover 62 percent of the bolson plain. Fine grained fans are on the lower apron regions and cover 16 percent of the bolson plain.

Runoff is channelized (streamflow) in tributary drainage systems when it occurs on the coarse grained alluvial fans. Runoff is unchannelized (sheetflood) in anastomosing-distributary drainage systems when it develops on the fine grained fans. Runoff on coarse grained alluvial fans is basically erosional, and runoff on fine grained alluvial fans is generally aggradational. Erosion and aggradation in the bolson plain are influenced by short, intense, summer rainfall which produces eighty percent of the runoff.

Sheetwash on interfluves in the coarse grained alluvial fans removes fine sediments and leaves desert pavements on the interfluves and berms in the ephemeral washes. Fine grained alluvial fans result from the coalescing and aggrading of berm deposits. Berm aggradation, or fine

grained fan deposition, is proportional to the length of overland flow on the interfluves and is inversely proportional to drainage density. Berm aggradation is almost in a steady state condition on the bolson plain.

Aggradation on the coarse grained alluvial fans is less extensive than on the fine grained fans and can be expressed as local maximum channel width. The position of the maximum channel width is influenced by the drainage area and channel length above this point. Aggradation and channel widening are related to thresholds in channel slope and depth of flow.

The late geomorphic history of the bolson plain is recorded in the surficial deposits. Changes between dominantly erosional and dominantly aggradational processes are recorded as changes in the particle size and extent of weathering on these deposits. Climatic changes appear to have caused erosion of the initially-deposited coarse grained fans. Climatic changes and piracy of drainage outside the bolson plain have induced deposition of fine grained fans and have shifted the zero edge of aggradation up the apron slopes. Relict surficial deposits and soils have reduced channel erosion of hillslopes and alluvial apron surfaces.

LANDSAT imagery is useful for delineating certain surficial deposits and their associated processes on the bolson plain. Areas of rapid ground-water recharge, and channelized and unchannelized flow can be distinguished by this method. Understanding these processes and their appearance on aerial imagery provides a basis for solving pragmatic problems related to land use in the Sonoran Desert.

ACKNOWLEDGEMENTS

The author wishes to express his deepest thanks to his advisor, Dr. L. H. Lattman (University of Utah) for his suggestions and advice regarding this study. Dr. Robert Fleming (U.S.G.S.), Dr. Wayne A. Pryor, Dr. Warren Huff, Dr. Paul E. Potter, and Dr. Louis Laushey (University of Cincinnati) were most helpful in sharing their comments and ideas related to this study.

I am grateful to the following people for their time shared in the field or in discussions related to this study: Mr. J. Carter, Mr. T. Gardner, Mr. T. Belchak, Mr. B. Umstead, Mr. J. Harrell, Mr. R. Lenhart, Mr. R. Spohn, Ms. J. Grover, and Mr. R. Bacon. Thanks are given to the Soil Conservation Service of Arizona and the Arizona Department of Highways for their assistantce. Ms. R. Martin is thanked for her drafting assistance.

Assistance provided by Sigma Xi, the Research Society of North America; Ohio Academy of Science; Summer Research Fellowship, University of Cincinnati Research Council; Fenneman Fellowship, Department of Geology; and the Fenneman Fund is gratefully acknowledged.

My deepest thanks and appreciation go to my wife who assisted in the field and had patience during my writing.

INTRODUCTION

STATEMENT OF PROBLEM, PURPOSE AND APPROACH

The nature, distribution, and frequency of surficial processes typical of arid basins in the southwestern United States are of significant concern if effective utilization of these basins is to occur. Practical problems in these desert basins, such as devastating flash floods, accelerated erosion of valleys, and lowering ground-water tables, are related to the interaction between man and surficial processes. General and detailed accounts of such problems have been outlined by numerous investigators (Peterson, 1953; Lewis, 1963; Stulik, 1964; Dunbier, 1958; Roeske, 1971; Cooley et al., 1973; Clancy and Harmsen, 1975). These practical problems result, in part, from an incomplete understanding of the behavior and interrelationship of surficial processes within an arid drainage basin.

The primary purpose of this study is to determine those surficial processes which operate basin-wide and those which operate in isolated portions within a basin in the Sonoran Desert of southwestern Arizona. Of major concern in this study are: 1) to determine types and distribution of surficial landforms and sediments, 2) to delineate types and distribution of surficial runoff, and 3) to distinguish processes and areas of net aggradation and erosion.

A secondary purpose is to establish the geomorphic history of the basin and thus to determine the location and variation in intensity of

these processes through time. The delineation of spatial and temporal relationships between landform characteristics and processes in a basin may form a basis for effective land management and land use restrictions. This investigation will focus on processes operating on the bolson plain and will not concentrate on those processes operating on the bedrock of the surrounding mountain ranges.

In this investigation, the drainage basin is studied as a process response model. Chorley (1962) gives the advantages of applying a process response model to geomorphic problems; however, the most important advantage of a process response model is that it emphasizes landscape as a continuous interaction between form and process. This method of approaching the problem is very useful in arid regions because investigators are confronted with processes which are short in duration and difficult to measure, for example, flash floods. In order to decipher these processes, the static, or post facto results must be examined and interpreted.

LOCATION

The study area is the Harquahala Valley, located in western Maricopa and eastern Yuma counties of southwestern Arizona (Fig. 1). The Harquahala Valley is in the Sonoran Desert, a sub-division of the Basin and Range province (Fenneman, 1931), approximately 110 km east of the Colorado River and 50 km west of Phoenix, Arizona (Fig. 1). The Harquahala Valley is characterized by through-flowing drainage which is tributary to the Gila River. The Hope, Lone Mountain, Big Horn Mountain, Cortez Peak, Eagletail Mountains, and Arlington 15-minute topographic quadrangles cover the area.

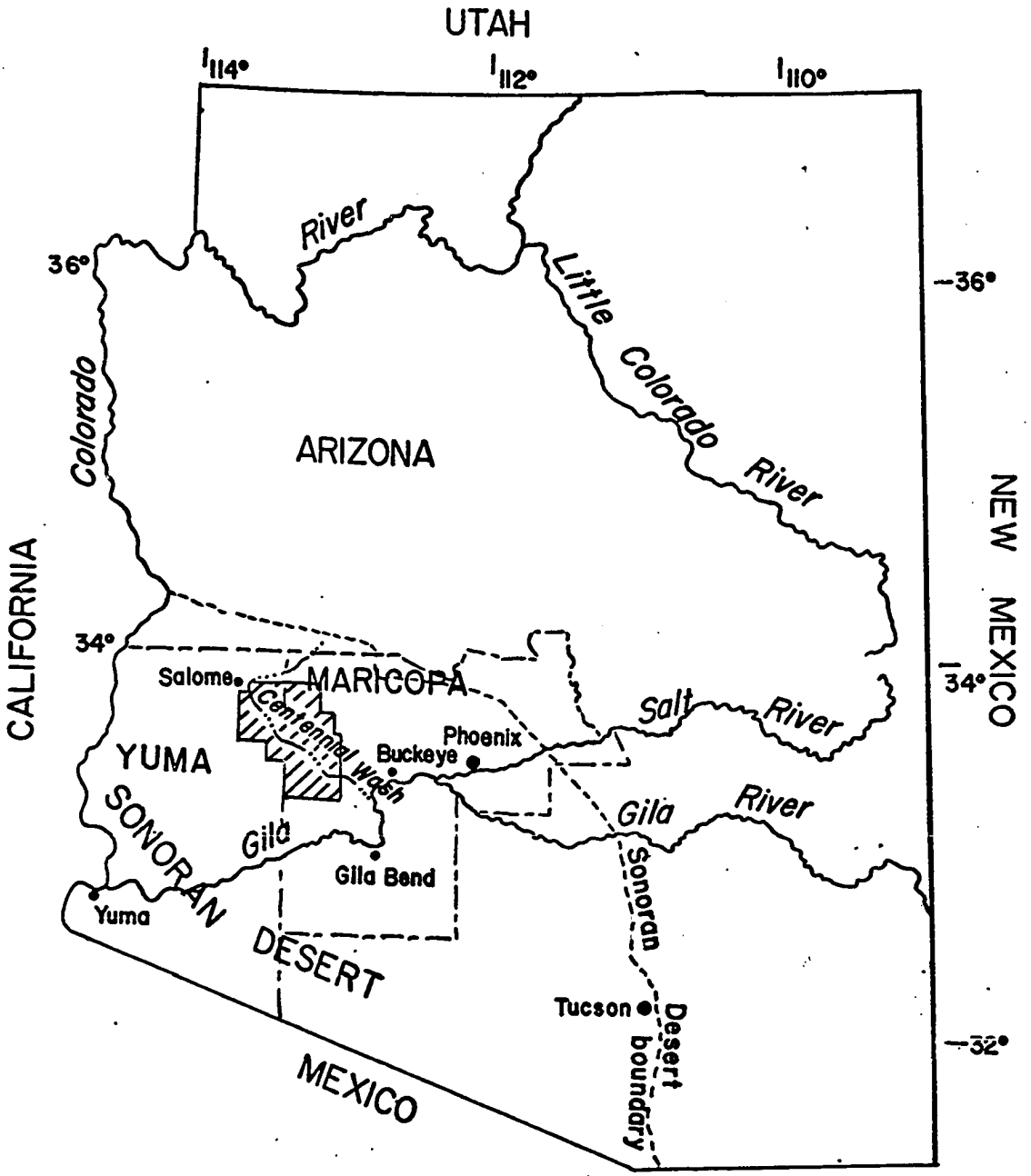

Figure 1. Location map of the study area in Maricopa and Yuma Counties, southwestern Arizona.

CLIMATE

The climate of the Harquahala Valley is hot and arid. The mean annual precipitation is 15.5 cm (less than 7 inches) per year. The wettest months of the year are July, August, September, December, and February, each with a mean monthly rainfall over 1.5 cm (Sellers and Hill, 1973). The months of April, May, and June are the driest, each receiving less than 0.50 cm of rainfall. Rainfall intensity and duration varies in two seasons: winter months (November through April) and summer months (May through October). The rainfall in the winter months is long and light, and the summer rainfall is short and intense.

Summer months in the Harquahala Valley are hot and dry, and the winter months are cold and slightly more humid. Mean daily temperatures for the Harquahala Valley average 41.3°C (106.3°F) for July and 18.9°C (66°F) for December. The lowest recorded temperature is -12.8°C and the highest is 51.1°C. The mean annual pan evaporation for the Harquahala Valley ranges from 180 to 250 cm. The highest evaporation period is from May through August, with monthly averages above 23 cm (Sellers and Hill, 1973).

Wind conditions of the Sonoran Desert are complex, but the months of April through August have the greatest monthly wind movement. Local, high winds and blowing dust occur prior to summer thunderstorms.

GENERAL GEOLOGY

The general bedrock geology, stratigraphy, and structure have been mapped by Darton (1926), Metzger (1957), and Wilson (1960). The

geologic structure and bedrock stratigraphy of the Harquahala Valley are complex. The stratigraphy is discussed below in terms of the age and occurrence of the predominant lithologies in each mountain range. The general structural geology is summarized separately. The Quaternary surficial deposits have been mapped in detail during the present study and are presented later.

Bedrock Geology

Precambrian Metamorphic and Igneous Rocks: the predominant lithology of Precambrian age rocks is granitic gneiss (Metzger, 1957) (Fig. 2). Other rock types of this age include gneisses, schists, and granites. Granitic gneisses, in addition to schists and alaskite intrusions, are common to the Harquahala and the Little Harquahala mountains. The granitic gneisses are extensive in the northern portion of the Big Horn Mountains. The Eagletail Mountains have contorted gneisses and granitic gneisses characterized by feldspar phenocrysts over 0.4 cm long. The northern portion of the Gila Bend Mountains is composed of the granitic gneisses. Foliated, chloritic schists form the northern portion of Saddle Mountain.

Paleozoic/Mesozoic Sedimentary and Igneous Rocks: These rocks are typically shale, sandstone, and limestone, which are locally metamorphosed to phyllites, quartzites, and marbles. These lithologies occur mainly in the Harquahala and the Little Harquahala mountains and also occur as inselbergs near these mountains (Fig. 2). They are found resting on the granitic gneisses described above (Metzger, 1957). Smaller exposures of the Paleozoic rocks occur in the Eagletail Mountains. Granite and

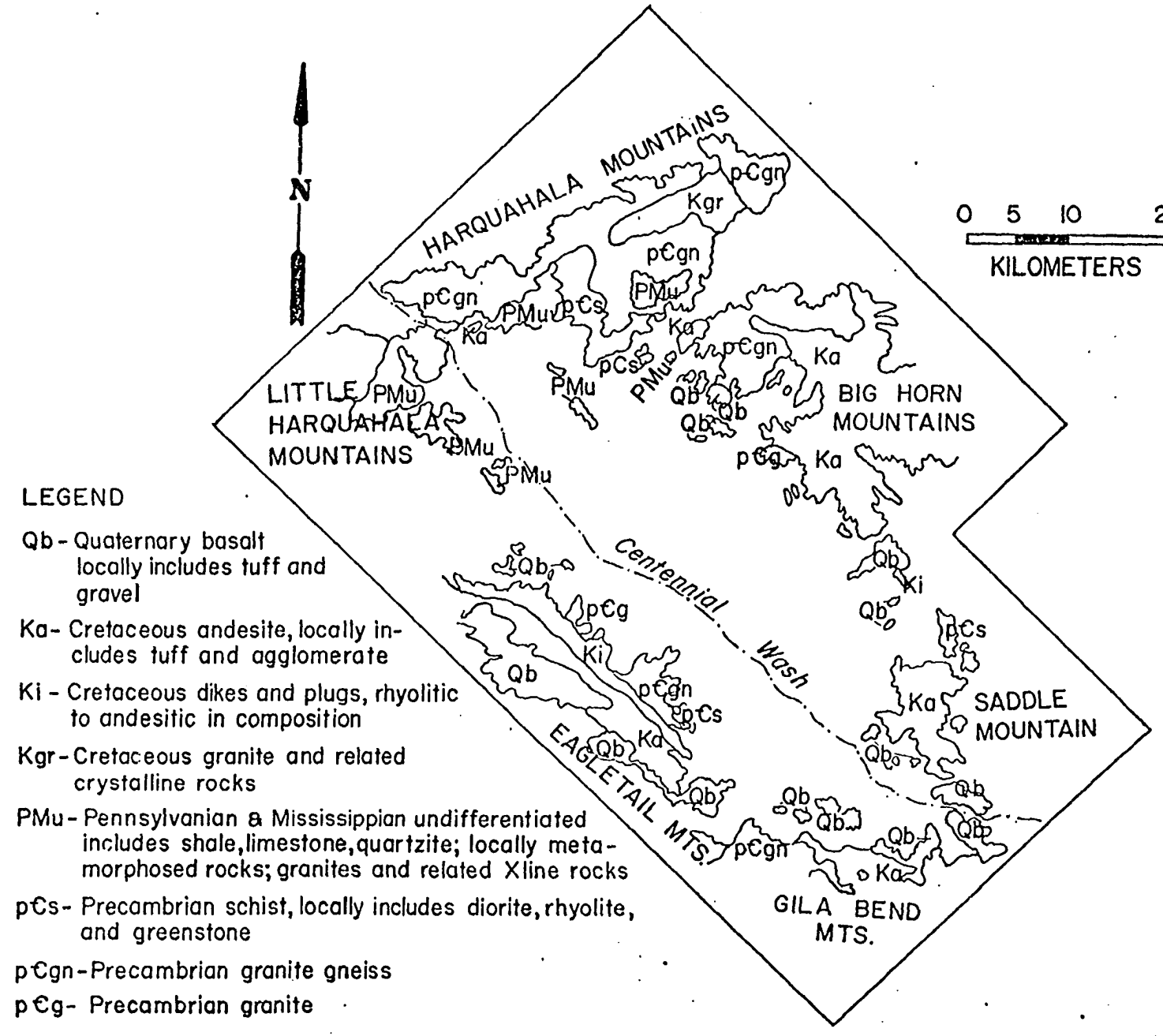

Figure 2. Generalized map of study area showing bedrock geology. Modified from Metzger (1957) and Wislon (1960)

related crystalline rocks of Mesozoic Age crop out in the Little Harquahala mountains (Wilson, 1960).

Cretaceous and/or Tertiary Sedimentary Rocks: These rocks are primarily arkosic conglomerates which have been intruded by Cretaceous and Tertiary volcanic rocks (Fig. 2). The conglomerates include fragments of schist and quartzite and occur in the Harquahala Mountains. The Eagletail Mountains, near Courthouse Butte, have a fanglomerate consisting of ninety percent Paleozoic carbonate rocks and ten percent granitic rocks. These coarse grained sedimentary rocks have been assigned Cretaceous age (Metzger, 1957) based on similar conglomerates which have been described by McKee (1947) and Wilson (1933). Kam (1961) has assigned Tertiary age to similar rocks found just north of the Harquahala Valley.

Cretaceous and/or Tertiary Volcanic Rocks: Andesites and basalts are the common rock type and occur in all mountain ranges except the Little Harquahala Mountains. Volcanic rocks of the Big Horn, Saddle, Eagletail, and Gila Bend mountains are agglomerates, tuffs, and lava flows (Metzger, 1957) (Fig. 2). Black, brown, and dark red obsidian is common in the Big Horn Mountains.

Tertiary Intrusive Rocks: Fine grained, light colored, acidic rhyolites occur in three locations in the western Harquahala Mountains and in two locations in the Eagletail Mountains (Fig. 2). Courthouse Butte (Fig. 4) represents one of these locations in the Eagletail Mountains and has been interpreted as an exposed volcanic neck (Metzger, 1957).

Quaternary Volcanic Rocks: Dark gray to black, highly vesicular, olivine basalt occurs throughout the Harquahala Valley (Fig. 2). The

basalt is extensive at Burnt Mountain (Fig. 4) and rests conformably on tuffs.

Structural Geology

Faulting has been the predominant form in the Harquahala Valley (Metzger, 1957). The following major structural events have been worked out in the study area by Metzger (1957): 1) a period of faulting and folding between deposition of the Paleozoic rocks and deposition of the arkosic conglomerate (numerous high angle faults cut the overturned Paleozoic rocks), 2) a period of uplift in the Cretaceous, and 3) block faulting and tilting in the late Cretaceous and Tertiary.

PHYSIOGRAPHY OF THE SONORAN DESERT

The physiography of the Sonoran Desert has been described by Fenneman (1931) and Dunbier (1968). This desert is a sub-division of the Basin and Range province with sub-parallel and disconnected mountain ranges trending northwest-southeast. These isolated, block-faulted mountain ranges are surrounded by desert plains called bolson plains (Tight, 1905; Tolman, 1909). The width of the bolson plain is typically greater than the width of the flanking mountain ranges. In the western Sonoran Desert, the bolson plains cover between 50 to 80 percent of the total surface area (Bryan, 1925; Dunbier, 1968), and in the eastern portions, the basins cover a smaller percent of the area. Elevations of the bolson plains in the western Sonoran Desert are less than 600 m, and elevations in the eastern plains are between 600 and 1200 m. The mountain ranges typically have maximum elevations of 900 m; however, some ranges,

including the Harquahalas, have maximum elevations of about 1200 m.

The slopes of the mountain ranges are usually not less than 20° and are controlled by the joint spacing and rock type (Bryan, 1925; Rahn, 1965). The mountain ranges are usually surrounded by pediments (Fenneman, 1931) which may be covered by various thicknesses of alluvium or colluvium. These pediments and alluvial fans, which coalesce to form the bolson plain, have slopes less than 10°. The alluvial fans are usually distinct near the mountain front and are indistinct near the center of the bolson plain. Arroyos, or washes, draining the fans are typically incised near the mountains and become shallower toward the basin axis until they are difficult to discern in the field. The majority of basins in the Sonoran Desert, including the Harquahala Valley, are drained by through-flowing, ephemeral washes.

VEGETATION

The landscape of the Sonoran Desert is dominated by extensive areas of giant cacti and xerophytic trees. Due to the widespread distribution and size of this vegetation, this region has been called an "arborescent desert". The distribution of the desert vegetation is related to the soil and moisture conditions in the bolson plains of the Sonoran Desert.

The most widespread vegetation over the bolson plain is mixed stands of creosote bush (Larrea divaricata) and burro bush (Franseria dumisa). Creosote and burro bushes are most common to the center of the bolson plain. The vegetation along the drainage lines is typically mesquite (Prosopis juliflora), blue palo verde (Cercidium floridum),

and ironwood (Olneya tesota) trees (Dunbier, 1968).

The better drained areas of the upper bahada slopes are characterized by giant saguaro cacti (Carnegiea gigantea), as well as ocotillo (Fouquieria splendeus) and catclas (Acacia greggii). Various cholla cacti (Opuntia) frequent the interfluves of dissected alluvial fans. The teddy bear cholla (Opuntia bigelovii) is also common in the study area. On alluvial apron slopes higher than 600 m in elevation, the prickly pear (Opuntia engelmannii) cacti are prevalent.

GLOSSARY OF GEOMORPHIC TERMS

1. Alluvial apron - sloping desert plain that lies between mountain front and axial drainage and may include erosional (buried pediments) and aggradational surface.
2. Berm of wash - topographically higher overbank area which is typically composed of fine sediment.
3. Bolson plain - surface of desert basin formed by coalescing alluvial aprons and surrounded by mountains; may be drained by ephemeral stream.
4. Caliche rubble - angular rubble derived from mechanical breakup of nonpedogenic, secondary accumulations of calcium carbonate.
5. Channel of wash - topographically higher talweg which is typically composed of coarse sediment.
6. Coppice dunes - wind deposited mounds which are commonly formed around vegetation.
7. Desert pavement - surface feature developed on alluvial aprons which is composed of pebbles and cobbles. These fragments form an armor when

they are tightly interlocking and typically have a thick layer of silt below armor. Segments of desert payment are either individual or composite interfluves, which are covered with the armor.

8. Desert varnish - dark coating or film of iron and manganese oxides on rock surfaces.

9. Drainage density - ratio of total channel lengths cumulated for all order streams within a basin, to the basin area. In the present study, drainage density refers to only those streams developed on the alluvial apron and not the bedrock surface.

10. Drainage frequency - number of stream segments per unit area, and in the present study, is only measured on the alluvial apron.

11. Drainage texture - a measure of the cumulative length and frequency of streams per unit area.

12. Gravity wave velocity - velocity of shallow wave controlled by gravitational and inertial forces.

13. Hydraulic geometry - channel or stream characteristics expressed by relations of width, depth, velocity, channel roughness, and slope.

14. Low order drainage basin - a basin, varying in size, which is tributary to axial drainage of a much larger basin. A low order basin may be drained by ephemeral streams draining mountain ranges or may be drained by ephemeral tributaries on alluvial aprons.

15. Micro-relief - small-scale differences in relief such as minor undulations on the land surface, which would not show on a normal topographic map. In the present study, micro-relief is defined as

any relief less than one meter.

16. Overland flow - unchannelized surface runoff which follows downslope paths from drainage divide to nearest channel.

17. Relief ratio - the maximum basin relief divided by the longest horizontal dimension of a basin, which is parallel to principal drainage line.

18. Tractive force - shear stresses produced on streambed which are proportional to slope of channel and depth of flow.

19. Transmission loss - water which is lost through infiltration into the floor of stream.

20. Trunk or principal wash - major drainage line that drains nearly the entire length of a low order drainage basin.

TECHNIQUE OF INVESTIGATION

This investigation utilizes all published data on the Harquahala Valley. These include discharge and runoff data (U.S.G.S. Water Supply Papers, 1970 and 1975) and climatological data (National Oceanographic and Atmospheric Administration, 1961-1970; Sellers and Hill, 1973). Geologic maps of the Harquahala Valley have been published by Metzger (1957) and Wilson (1960). Portions of the bedrock geology in the Harquahala Valley have also been mapped by Denis (1971).

MAPPING OF PHYSIOGRAPHIC UNITS AND LANDFORMS

Alluvial apron units are delineated on the basis of areal extent from the mountain front to a major drainage line and are mapped on the Phoenix, Arizona 2° topographic sheet. These alluvial apron units are given in Figure 4.

The alluvial apron-bedrock contact is based on the geologic maps published by Metzger (1957), Wilson (1960), and Denis (1971) and on field observations and aerial photographic analysis. The divide between the Harquahala Valley basin and surrounding basins is measured from 15-minute topographic quadrangles, and the area between this divide and each mountain front constitutes the areal extent of the bedrock in Figure 5. The cumulative area of inselbergs is determined from the geologic and topographic maps and is given in Figure 5. Maximum relief for each mountain range is based on the difference in elevation from the highest point in the mountains to the lowest point at the apron-bedrock contact.

Mean alluvial apron length (that distance from the apron-bedrock contact to the axial drainage, measured parallel to the regional slope) is determined by averaging a minimum of 5 measurements per apron. Mean apron length is given for each apron in Table 1. Mean apron relief (that difference in elevation from the apron-bedrock contact to the axial drainage) is determined by averaging 5 measurements per apron and is given in Table 1.

Details for constructing a slope map (Fig. 8) are given by Strahler (1956) and Chow (1964). The general procedure used on the bolson plain of the Harquahala Valley is as follows: 1) slopes of short segments of a line normal to the contours are determined for each section of a 15-minute topographic map (approximately 2.5 km^2) (Fig. 3); 2) the tangent of the slope is calculated, converted to degrees, and plotted at the center of each section shown in Figure 3; and 3) isopleths of equal slope are drawn at an interval of 0.25° for this data. The frequency of the slope angles on the Harquahala Valley bolson plain is based on the cumulative measurements of slope angles in each section (Fig. 7).

Construction of a drainage texture map (Fig. 9) is based on methods devised by Ruhe (1967) and methods developed in the present study. The procedure is as follows:

1. A curve is fitted to the longest contour in each section of the topographic maps shown in Figure 3, according to those procedures given by Ruhe (1967).

2. Lengths are measured from the fitted curve to the actual contour line parallel to axis of drainage lines. These lengths are totalled for each section, and the result is L_D, or the cumulative length of drainage

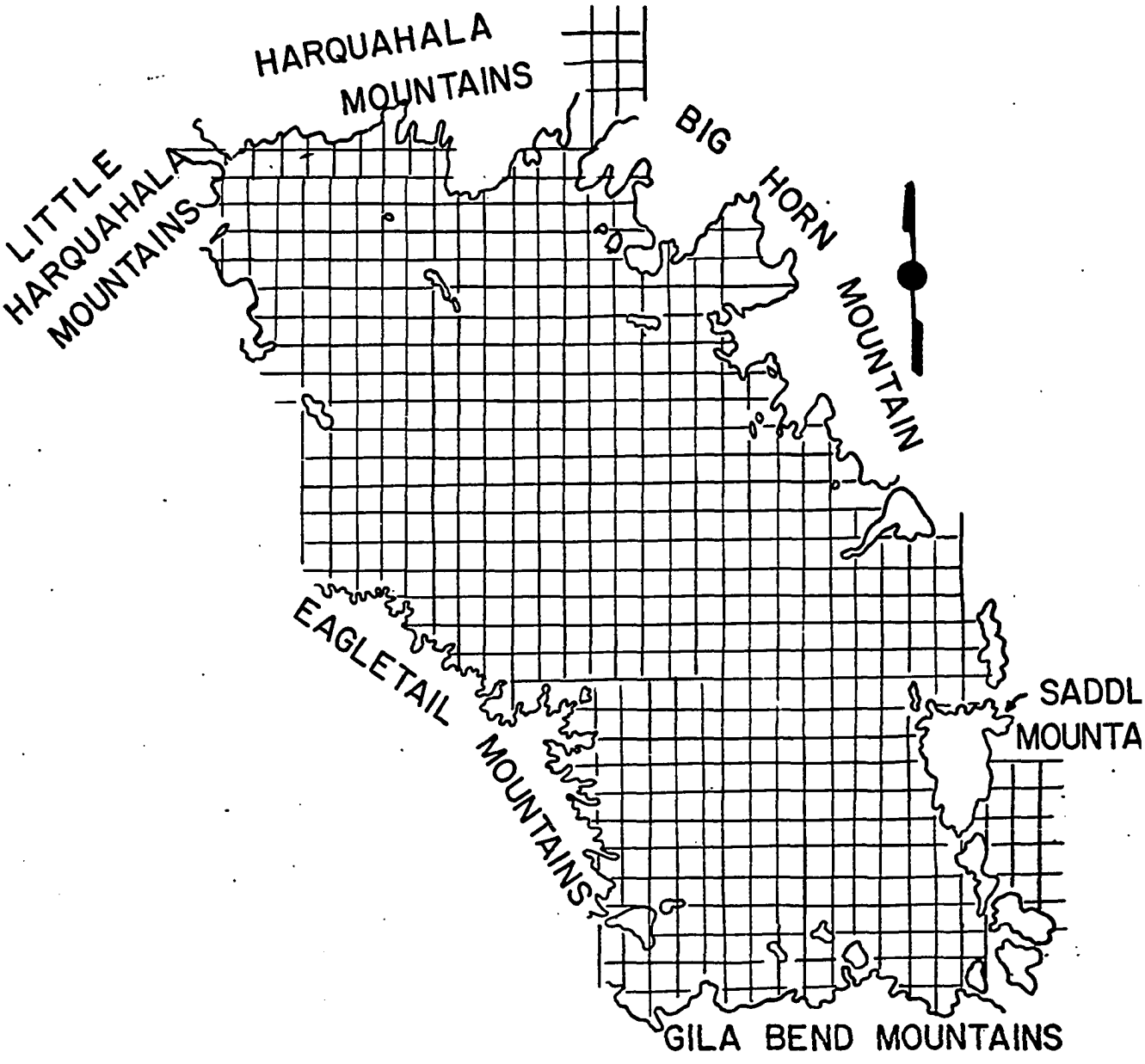

Figure 3. Grid system on Harquahala Valley bolson plain used to construct slope and drainage texture map. Each square is 2.5 km^2 in area.

lines produced by erosion.

3. Frequency of the drainage lines for each section, or N_D, is multiplied by L_D. This number is then calculated for an area of 1 km^2, rather than 2.5 km^2, and is a measure of the drainage texture.

4. The drainage texture value is plotted in the center of each square in Figure 3, and isopleths of equal drainage texture are drawn at an interval of 2 km of eroding channel per km^2.

The frequency of the drainage texture values (Fig. 10) is based on the measurements from each square as illustrated in Figure 3.

MAPPING GENERAL DRAINAGE FEATURES

The regional drainage patterns and features of the ephemeral washes in the Harquahala Valley are based, in part, on aerial observations from a single engine plane during the 1975 field season.

Regional drainage patterns are studied from black and white, vertical aerial photographs at a scale of 1:60,000 and color Skylab photography (S190B) at a scale of 1:125,000. The patterns are based on whether they bifurcate up regional slope (tributary), bifurcate down regional slope (distributary), or a combination of both (anastomosing).

The orientation of major drainage lines for each apron is measured from the Phoenix, Arizona 2° topographic sheet. The orientation of a stright line best fit to the drainage line is measured and plotted in 20° class intervals. The frequency of the class intervals for selected aprons is illustrated in Figure 12.

HYDROLOGIC STUDIES AND MEASUREMENTS

Data are obtained from the U.S.G.S. Water Supply Papers (1970, 1975) for runoff and discharge measurements on Centennial Wash. Additional data on the surfical hydrology are based on flood records published by Wehro (1967).

The recurrence interval for Centennial Wash is calculated according to those procedures of Dalrymple (1960). The equation for recurrence interval used by the U.S.G.S. is: $T = \frac{n + 1}{m}$ where T is the recurrence interval in years, n is the number of years record, and m is the magnitude of flood with the highest being 1. Cumulative flow duration curves for the various washes are plotted by the same methods used by the U.S.G.S. (Leopold and Maddock, 1953).

Calculations for the percent annual runoff and precipitation at the gauging station on the lower Centennial Wash (Fig. 18) are as follows: 1) runoff and precipitation are accumulated monthly for the period between 1961 and 1970; 2) runoff and precipitation accumulated for each month is divded by the total runoff, or precipitation, for the ten year period; and 3) this percentage is plotted in Figure 18.

Major washes of low order drainage basins in the Harquahala Valley are studied to determine the velocity, discharge, and tractive force at a cross-section. The computed values for these hydrologic parameters are given in Appendix VI. They are based on measurements from the hydraulic geometry of washes taken from high water marks rather than actual flood events (Fig. 60). Types of high water marks used in this study include: perched flotsom in vegetation and along the banks of washes; and mud and

silt, carried by previous floods, as lines along the banks or vegetation (Fig. 60). Another method used in this study consists of measuring the high water mark from the edge of disturbed varnish. This method was first suggested by Rahn (1967). Varnished gravels may be disturbed by floods, which cover them with silt or erode them. Field procedures for measuring the hydraulic geometry of washes are based partially on those given in the U.S.G.S. Techniques of Water-Resources Investigation (Benson and Dalrymple, 1967). Maximum depth is computed from a minimum of three high water marks at a station and averaged. Different types of high water marks are compared for accuracy, and maximum error for depth is 25 cm.

Maximum cross-sectional area is determined by multiplying maximum depth of flow by maximum width of flow (Appendix VI). Hydraulic radius is computed by cross-sectional area by the wetted perimeter. Channel slopes are measured by an inclinometer and from topographic maps.

Velocities are computed from physical parameters of the wash and are averaged for steady flow conditions for the Mannings equation ($V_m = 1.49 \frac{R^{.66} S^{.5}}{n}$ where R is the hydraulic radius; S is the water slope, but channel slope is substituted; and n is the roughness coefficient which is based on values for ephemeral streams given by Renard and Keppel in 1966) and for the gravity wave ($V_g = \sqrt{g\ D}$ where g is the gravity constant and D is the depth of flow). Averaged velocity times the maximum cross-sectional area gives the maximum discharge for each station given in Appendix VI.

Tractive forces are computed from the expression: $T = \gamma\ RS$ where γ is the specific weight, R is the hydraulic radius, and S is the channel slope. In this study, hydraulic radius is substituted for depth in the

conventional equation since the entire wash surface is under consideration and the width-depth ratios are high. Specific weight is held constant in the calculations of tractive forces.

PARTICLE SIZE STUDIES FOR WASH DEPOSITS AND SURFICIAL DEPOSITS

Maximum particle diameter is measured for each station along major washes in low order drainage basins in the Harquahala Valley, and these measurements are given in Table 5. These measurements are taken in the wash channel within 3 m of the station location.

Sediment samples are taken at each station for selected washes in the low order drainage basins by the following procedure: 1) an imaginary square approximately 2 m in width and length is superimposed on the channel of the wash, 2) samples are taken from each corner of the square, and 3) only the upper 10 to 15 cm are sampled. Additionally, at each station, grab samples are taken from the berm of the wash due to obstructions by vegetation.

Grab samples of surficial deposits are taken at each station during geomorphic mapping of the Harquahala Valley.

Particle sizes of the sediment samples collected during the field studies are analyzed by sieving. Sieve analyses are conducted for selected surficial deposit samples and both berm and channel sediments according to those methods given by Ingram (1971). The analyses include intervals for the following ϕ values: -3, 1-, 0, 1, 2, 2.75, 3, 3.25, and 4. The samples are not treated for organics prior to the sieving. Results of the sieve analyses are given in Appendix II.

SOIL STUDIES

Soil profiles are described during the geomorphic mapping of the Harquahala Valley and are summarized in Appendix IV. The soils are described according to methods outlined by Birkeland (1974). These descriptions include: horizon thickness, texture, relative amount of calcium carbonate, and color. Color for selected soil profiles are given under dry laboratory conditions, and chroma and hue values are based on the Munsell Soil Color Chart.

Soil maps provided by the Soil Conservation Service (Hartman, 1973; Chamberlin (in preparation)) are compiled and given in Figure 38.

MAPPING QUATERNARY SURFICIAL DEPOSITS

The surficial deposits of the Harquahala Valley bolson plain are not mapped according to conventional procedures because of the special purposes of this investigation. Rather, two parameters are used to meet the special purposes of this study. These parameters are particle size and distribution, and degree of secondary deposition and weathering. Data used in the field mapping of these deposits are given in Appendix IV. Vertical, black and white, aerial photography at a scale of 1:60,000 is used as the base for field mapping. Compilation of the final surficial deposit map (Fig. 25) is according to those procedures given by Lattman and Ray (1965).

Detailed topographic transects and profiles are used to illustrate relationships between surficial deposits and topography. These profiles are selected across various reaches of the bolson plain and are given in

Figures 30 through 34. Horizontal and vertical control during profile measurements is maintained by a transit and stadia rod. Detailed sketches and bearings between stations are also taken during the profiles.

MAPPING GEOMORPHIC PARAMETERS

Slope measurements are taken with a transit and stadia rod and are given in Appendix III. Additional slope measurements are taken with an inclinometer.

Micro-relief is measured with a one-man surveying instrument. This instrument is a piece of wood with a level and retractable measuring tape at one end. Holding the instrument level, the amount of relief can be measured on such features as coppice dunes or abandoned bar deposits.

The amount of gravel and its concentration on alluvial fan surfaces are measured from a comparison chart. Selected results of these measurements are given in Appendix IV.

Geomorphic parameters of several low order drainage basins in the Harquahala Valley are given in Appendix VI. Relief ratio is measured for these basins according to Schumm's definition (1956) and is measured from 15-minute topographic maps. The drainage lines for each basin are mapped from 1:60,000 vertical, black and white, aerial photographs. Only the major drainage lines are mapped in the bedrock regions of these basins. Drainage density and frequency are measured from these maps on the alluvial apron portion of the low order basins.

Drainage divides of these low order basins are mapped from the 1:60,000 aerial photographs. The maps of these low order basins are given in Figures 48, and 50 through 59. Mean basin width is taken from these

maps and is the average of basin width taken perpendicular to regional slope at each station given in Appendix VI.

LANDSAT IMAGERY STUDIES

The procedure for measuring the density on positive, LANDSTAT transparencies is to use a MacBeth Transmission Densitometer (TD-504). This measures the density of an area on the transparency 1 mm in diameter, which represents nearly 31,000 m^2 on the surface. Each major surficial deposit in the Harquahala Valley has had three runs (tests) of eight measurements each for MSS Band 7. For color composite of Bands 4, 5 and 7, only one run of eight measurements is taken. These data are summarized in Appendix I and Figure 46. The method for comparing various density measurements on LANDSAT imagery is based on the contrast method established by Lenhart (1974). Statistical analyses of these comparisons are given in Appendix I.

RESULTS OF THE INVESTIGATION

HARQUAHALA VALLEY BASIN CHARACTERISTICS AND GEOMORPHOLOGY

Topography

The Harquahala Valley is an elongate basin which trends N55°W (Fig. 4). This valley covers approximately 2000 km^2. Total basin length is 75 km. The average basin width is 20 km and it has a maximum width of 35 km. Two thirds of the basin's area is represented by coalescing alluvial aprons which form the bolson plain (Fig. 4). Elevation of the bolson plain ranges from over 600 m to slightly less than 300 m above mean sea level. The remaining one third of the basin's area is composed of bedrock outcrops of mountains and inselbergs (Fig. 4). The bolson plain of the Harquahala Valley is flanked by six major mountain ranges (Fig. 4). These ranges, in order of decreasing maximum relief, are the Harquahala, Big Horn, Eagletail, Little Harquahala, Saddle, and Gila Bend mountains. The exposed bedrock area in these mountain ranges and associated inselbergs is given in Figure 5. The two largest ranges, the Harquahala and Big Horn mountains, contribute 60 percent of the total bedrock area.

The bolson plain can be divided into six different alluvial aprons, which flank those mountain ranges given above. These aprons flank the southern Harquahala and the Little Harquahala mountains, northeastern Eagletail and Gila Bend mountains, southwestern Big Horn Mountains, and the northern, western, and southern edges of Saddle Mountain (Fig. 4). The amount of relief and length of these alluvial aprons, as measured perpendicular to the mountain front, varies considerably across the Harquahala

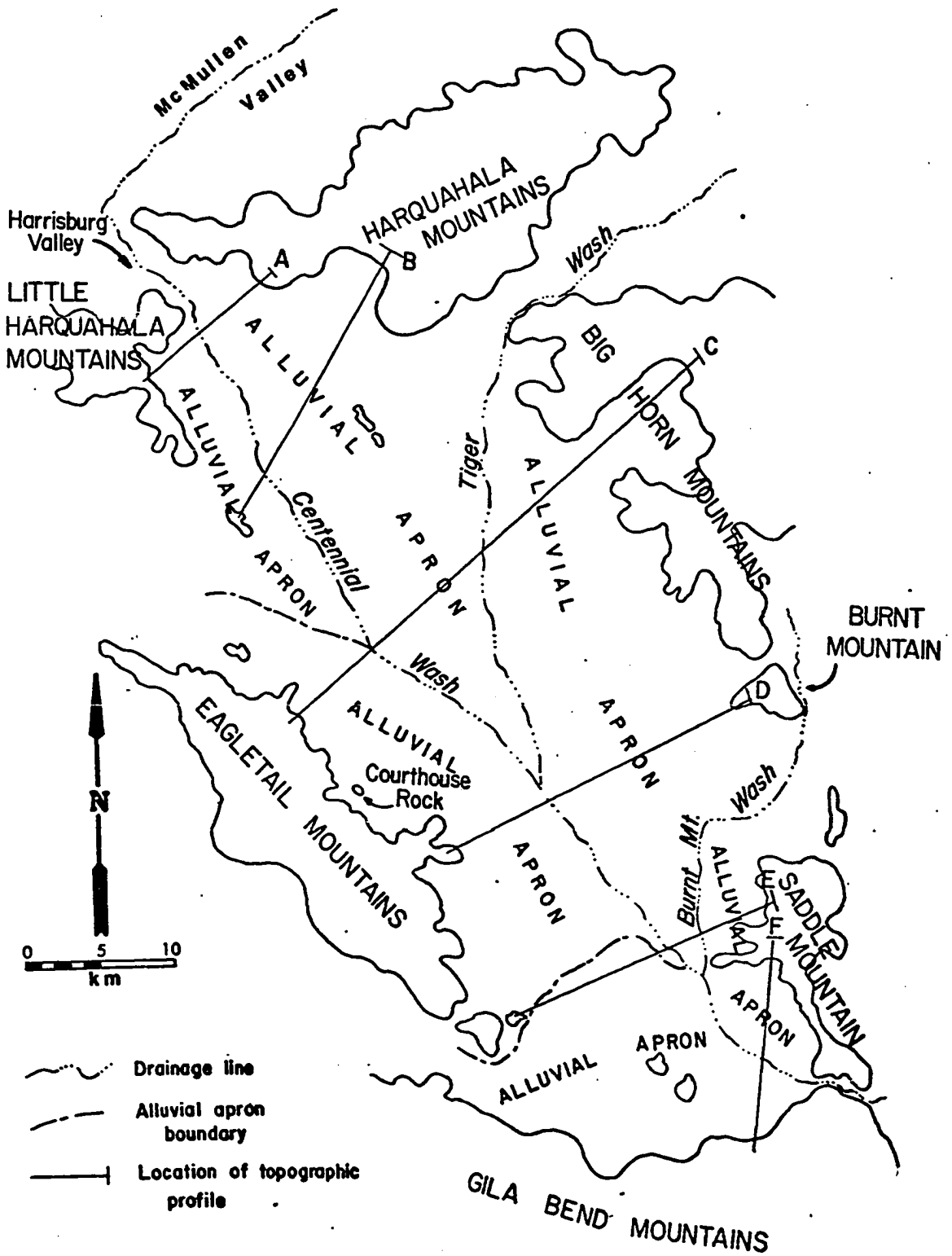

Figure 4. Physiography of Harquahala Valley basin and surrounding areas. Topographic profiles whose locations are given above are shown in Figure 6.

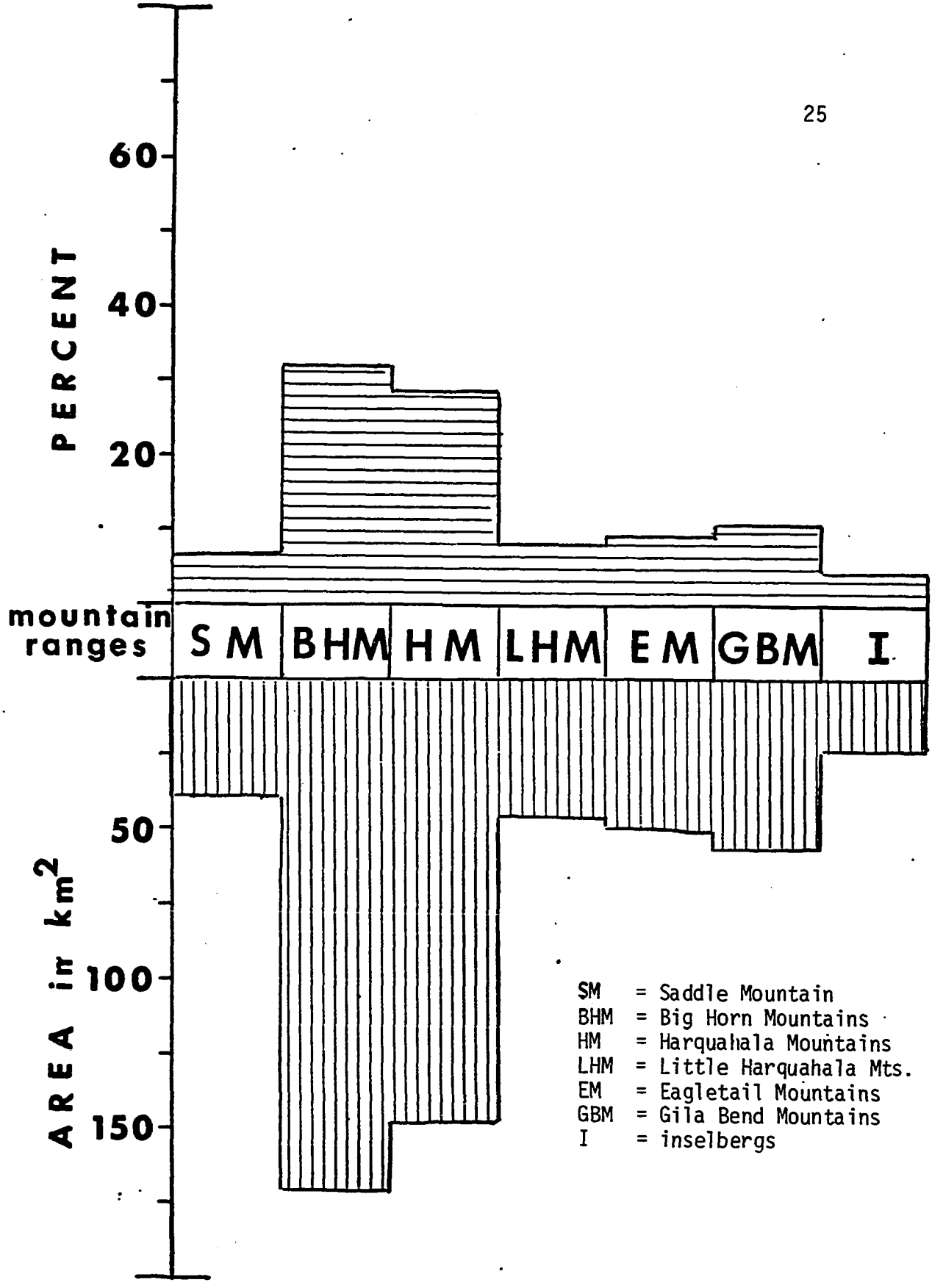

Figure 5. Histogram of areal extent of bedrock in mountain ranges and inselbergs of the Harquahala Valley basin.

Valley. A series of topographic profiles orthogonal to the trend of the basin illustrate this variety (Fig. 6).

Runoff and amount of sediment yielded from a source area affect the size of an alluvial apron; therefore, the mean length of the alluvial apron should be related to the contributing bedrock area. Table 1 compares mean alluvial apron length, contributing bedrock area, mean apron relief, and maximum bedrock relief for each alluvial apron and its associated mountain range. The Spearman Rank correlation coefficient, r_S, (Siegel, 1956) for the relationship between mean apron length and bedrock area above the apron is 0.89 which is significant at $\alpha = 0.05$ (Appendix I). However, r_S for the relationship between maximum bedrock relief and mean apron length is 0.03 at $\alpha = 0.05$ which indicates a lack of significant relationship between maximum relief in the mountain ranges and alluvial apron length (Appendix I). The relationship between mean alluvial apron relief and maximum bedrock relief is not statistically significant at $\alpha = 0.05$ (Appendix I). The Spearman Rank correlation coefficient for the latter variables is equal to 0.77, and the accepted table value, p, is 0.829. Although there is no significant correlation, the mountain ranges with the highest relief exhibit alluvial aprons with the highest relief.

In summary, the lengths of the alluvial aprons are directly correlated with the size of the source area, and the relief of the aprons is not correlated with the relief of the mountain ranges.

Another major characteristic of the bolson plains in the arid southwestern U.S. is very low regional slope angles. Slopes in desert regions have been discussed by Carson and Kirkby (1971) and Cooke and Warren (1973). In the Harquahala Valley, slope angles on the bolson plain range from 0.17°

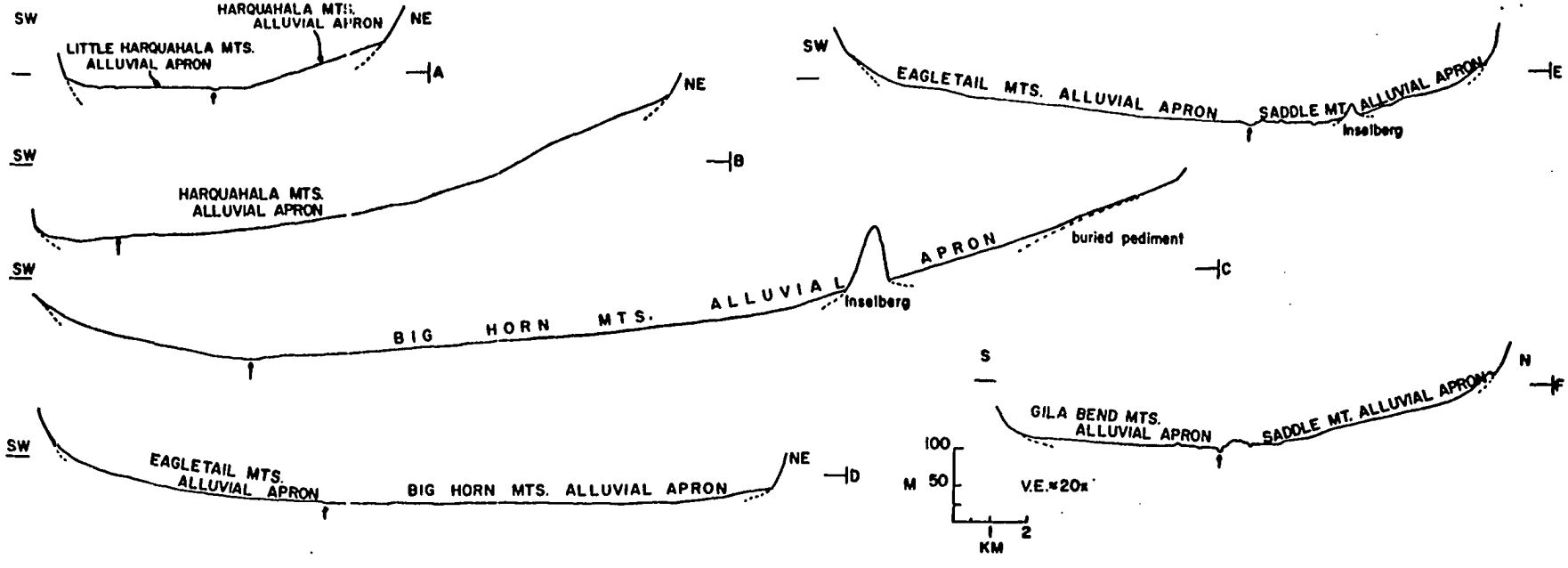

Figure 6. Selected topographic profiles across alluvial aprons in Harquahala Valley. For location see Figure 4. Arrow indicates Centennial Wash.

GEOMORPHIC PARAMETERS	MOUNTAIN RANGES AND ASSOCIATED ALLUVIAL APRONS					
	Eagletail	Big Horn	Harquahala	Little Harquahala	Saddle	Gila Bend
Maximum Bedrock Relief (m)	420	510	1060	280	255	220
Mean Alluvial Apron Length (km)	8	16.7	11.5	4.8	5.2	13.4
Bedrock Area (km^2)	49	171	148	40	38	56
Mean Total Alluvial Apron Relief (m)	86	210	200	18	91.5	15

Table 1. Selected geomorphic parameters of the Harquahala Valley Mountains and associated alluvial aprons.

to nearly 4.0°. Typically, the lower slope angles are associated with the distal portions of the alluvial aprons, and the higher angles are associated with the proximal portion of the aprons. A histogram of slope frequency in the Harquahala Valley bolson plain is given in Figure 7. Sixty-one percent of the bolson plain has slopes less than 0.5°, and two and one-half percent of the bolson plain has slopes greater than 2°. The mean slope for the bolson plain is 0.5°.

The variation in slope angles distributed over the bolson plain is shown in Figure 8. Construction of this slope map is outlined in the section on Techniques of Investigation. In general, this map shows greater slope angles in the northern portion of the study area than in the southern portion.

The isopleths on the slope map follow the same general trends as the topographic contour lines because the slope map is a derivative of topographic maps. However, a slope map provides added insight by removing minor variations in slope produced by incised drainage. Continuous, alluvial apron surfaces are represented by slope isopleths convex toward the basin axis. The intersection of two major apron surfaces is indicated by isopleths convex toward the mountain front. The 'trough' in the isopleths produced by intersection apron surfaces has lower slope angles than the adjacent areas. These troughs are the location of major, active drainage lines where sediment is transported from the mountain interior to the center of the bolson plain. This relationship is apparent in Figure 8 when the major drainage lines are compared to the convexity of the isopleths.

The spacing between the isopleths indicates the rate of change of alluvial apron slope and can be expressed as dS/dL where S equals slope and

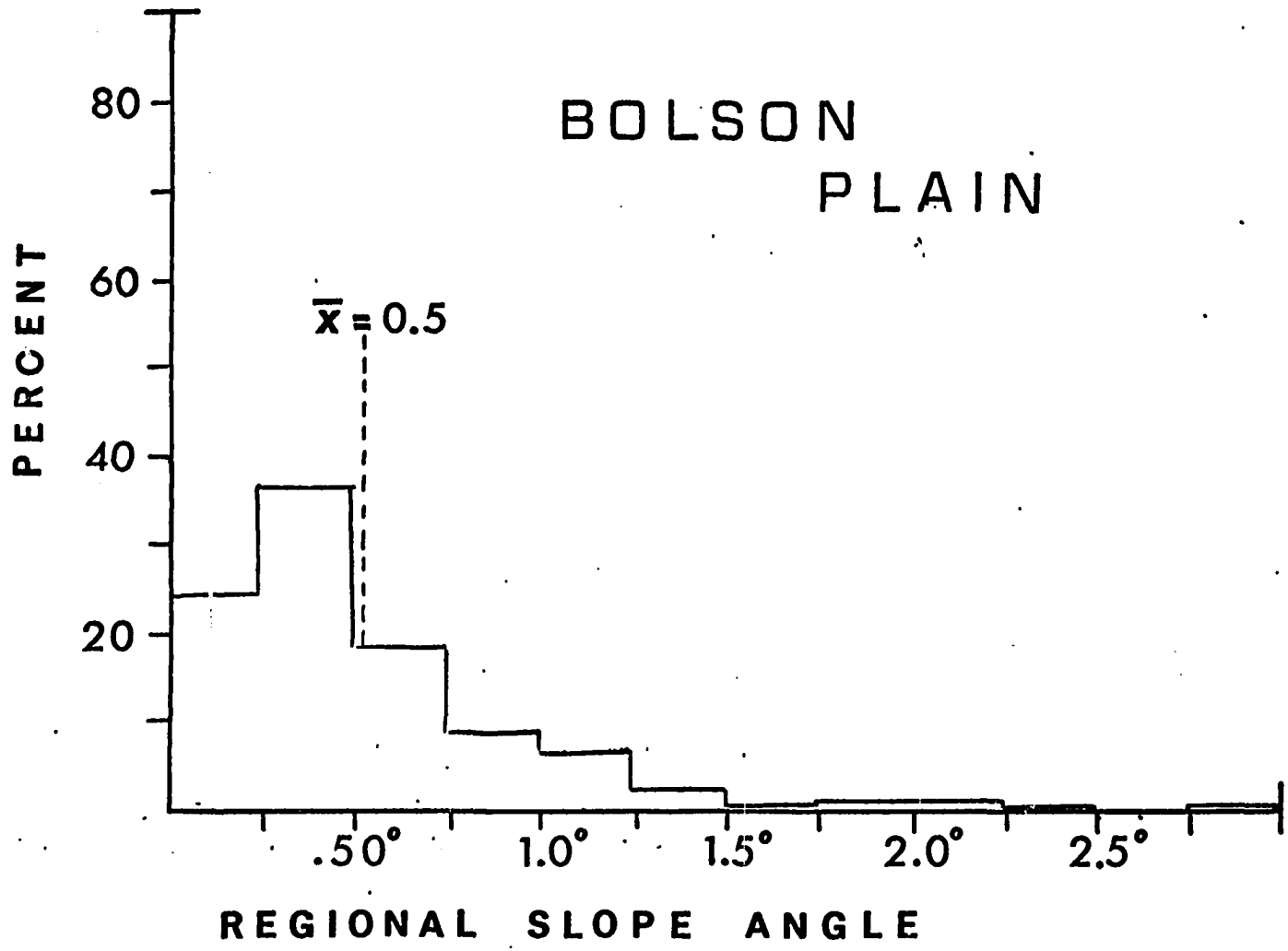

Figure 7. Histogram showing frequency of regional slope angles on the Harquahala Valley bolson plain; $\bar{X}$ = mean regional slope.

L equals any length of an apron orthogonal to the slope isopleths. The spacing between the isopleths increases away from the mountain front and indicates that dS/dL is greater in the proximal portion of the aprons. In addition, the spacing between the isopleths is not uniformly parallel to the apron-bedrock contact but varies considerably. Figure 8 illustrates this along the southwestern flank of the Big Horn Mountains. The spacing between the isopleths is less along the southern flank of the Big Horn Mountains apron; therefore, dS/dL is greater. Further north along the apron, the spacing increases and dS/dL is less. A comparison between these two regions on the slope map (Fig. 8, in pocket) and the geologic map (Fig. 2) indicates that two different rock types occur in the source areas. Andesites, and other associated extrusive igneous rocks, crop out in the southern Big Horn Mountains; whereas, granite and granitic gneisses are predominant further north in the mountain range. Results of a Mann-Whitney U test (Siegel, 1956) show that dS/dL values for aprons composed of andesite are significantly different than dS/dL values for aprons composed of granitic detritus at $\alpha = 0.05$ (Appendix I). Higher values of the dS/dL are associated with extrusive igneous rocks such as andesites.

Thus, the lithology of the detritus forming the alluvial aprons is related to the rate of change of slope down the aprons. Greater rates of change of slope are associated with fan composed of detritus derived from extrusive igneous rocks as compared to intrusive igneous rocks.

A third major geomorphic parameter of an arid basin is drainage texture. Drainage texture is a measure of the length and frequency of eroding drainage lines per unit area. Erosion of alluvial fans has been discussed by several investigators, and a summary of their results is given

by Cooke and Warren (1973).

Observations in the Harquahala Valley and examination of the topographic maps indicate that local erosion is not uniformly distributed on the alluvial aprons. A drainage texture map has been constructed to display the variation in amount of erosion and to illustrate its distribution over the bolson plain (Fig. 9). This map exhibits variations in local drainage erosion as compared to fan deposition by means of isopleths of equal drainage texture.

Approximately 68 percent of the bolson plain has less than two eroding drainage lines per km^2 (Fig. 10). The areas of higher local erosion are predominant in the mid and proximal portions of alluvial aprons (Fig. 9, in pocket). The highest degree of erosion does not occur adjacent to the apron-bedrock contact. Rather, the drainage network developed on the aprons show maximum drainage frequency and incision some distance away from the mountain front (Fig. 11).

Two portions of the study area show particularly high drainage texture values in the distal portions of the aprons. The center of the Harquahala Valley between the Eagletail and Big Horn mountains and between the Gila Bend and Saddle mountains has drainage texture values greater than 2 km of eroding drainage line per km^2; whereas, the majority of the distal aprons regions have values less than 2 km/km^2. Comparison of the slope map (Fig. 8) and the drainage texture map (Fig. 9) reveals that the anomalously high drainage texture values for the two areas in the center of the bolson plain occur with local higher slopes, or higher dS/dL. Also, the highly eroded area between the Gila Bend and Saddle Mountains occurs upstream from the point where the axial drainage has deeply incised into

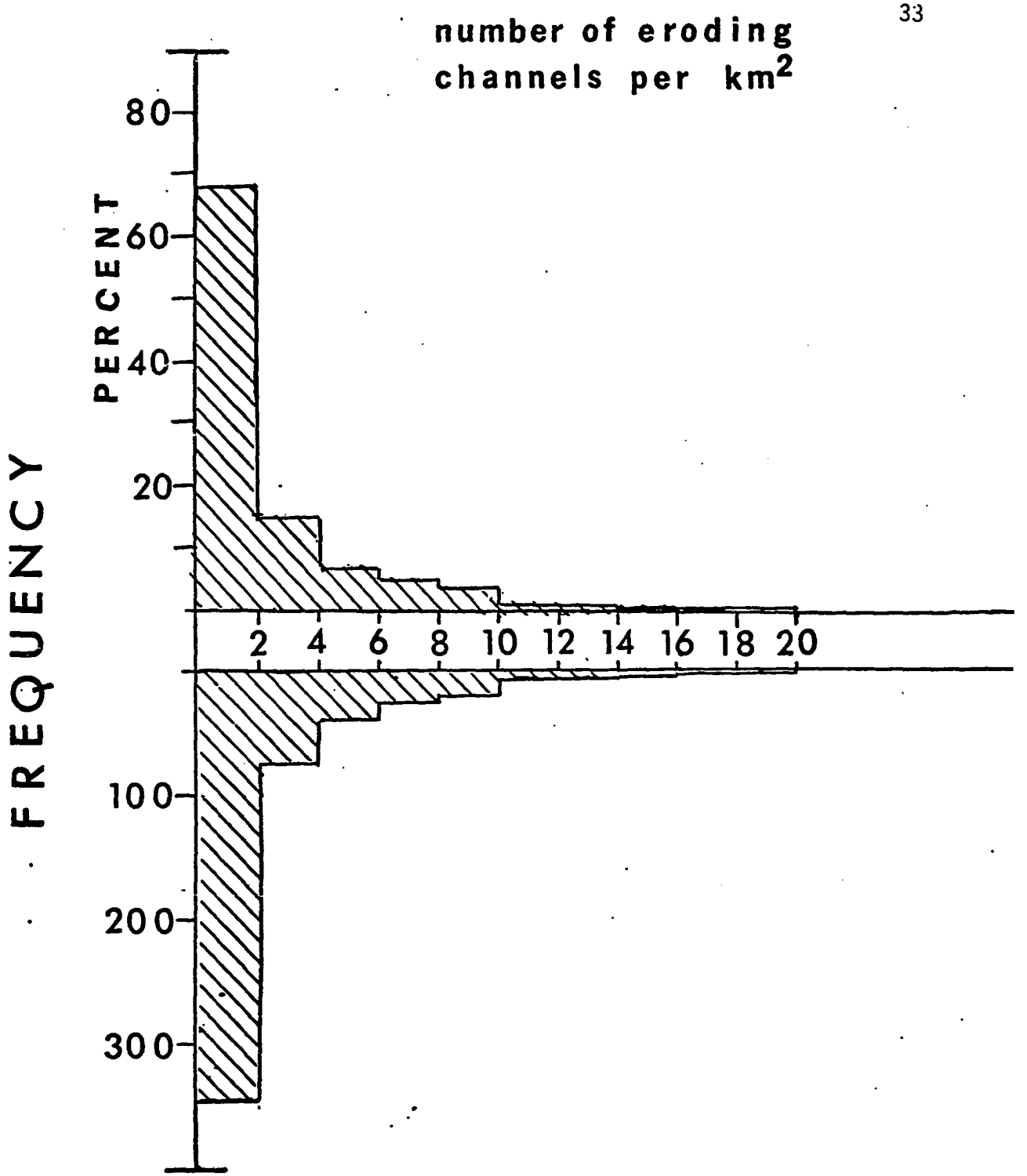

Figure 10. Histogram showing frequency of drainage texture values, measured in km of eroding channels per km^2.

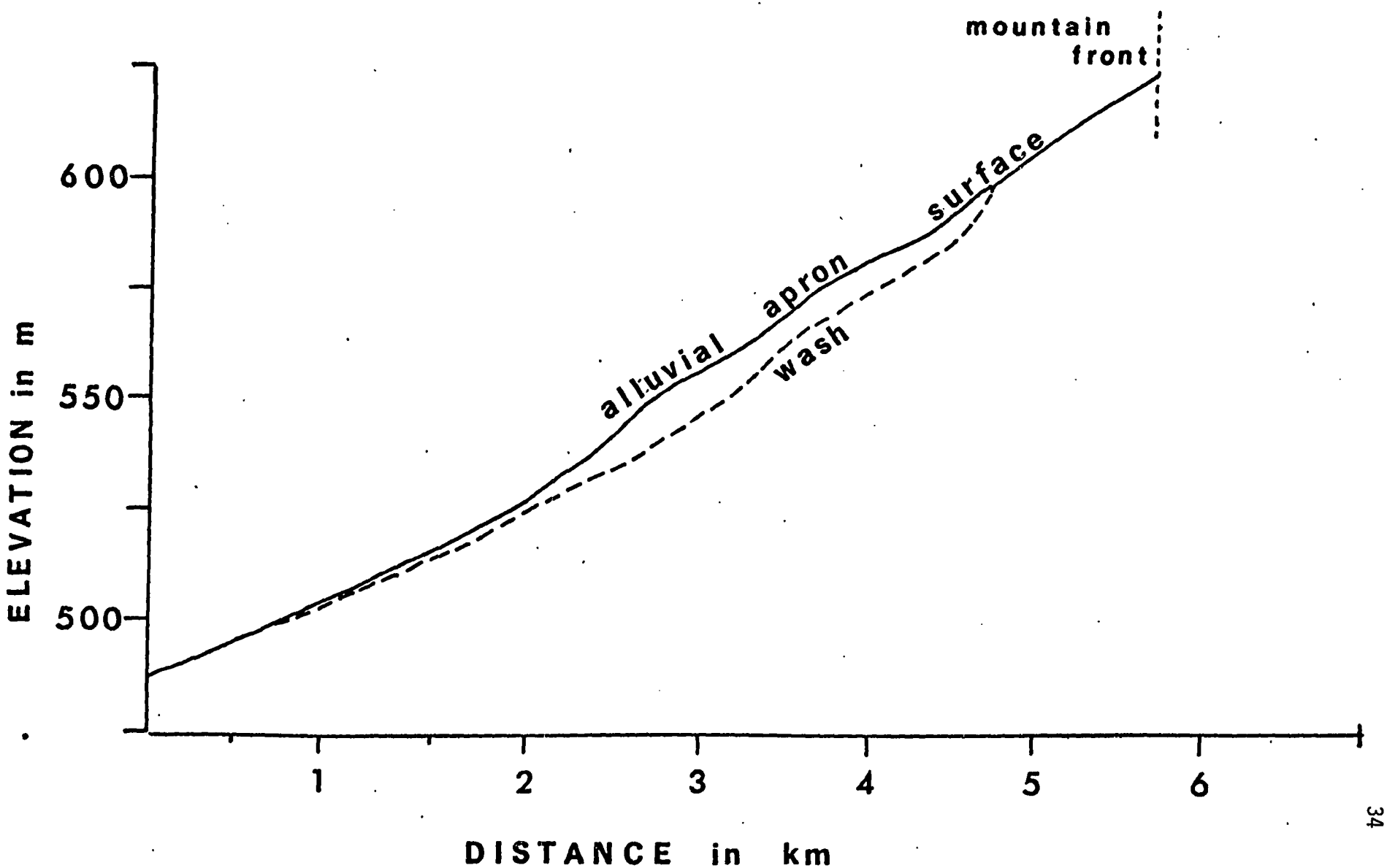

Figure 11. Longitudinal profile of fan surface and wash on Harquahala Mountain alluvial apron illustrating maximum incision of wash in mid apron region.

the valley floor (Fig. 9).

It is concluded that lowering of base level in the past caused an increase in the drainage texture in the axial portions of the bolson plain. Additionally, axial portions of the bolson plain, which have higher local slopes due to fan-building processes, have higher values of drainage texture, or more eroding drainage lines, than areas of lower local slopes.

In each alluvial apron, the highest texture value and the frequency of its occurrence is given in Table 2. The alluvial aprons are then ranked according to their highest value and frequency (Table 2).

The distribution of channel erosion across the bolson plain should, in part, be related to the distribution of the available potential energy in the basin. The total potential energy capable of eroding an alluvial apron should be directly related to the vertical distance from the top of a mountain range to the axial drainage. The Kendal coefficient of concordance (Siegel, 1956) is computed to test the relation among relief in the bedrock area, relief on the apron, and the drainage texture (Appendix I).

Alluvial Apron	Highest Drainage Texture Value (km/km^2)	Frequency	Rank
Saddle Mountain	8	2	3
Gila Bend Mountains	8	1	4
Eagletail Mountains	8	1	5
Big Horn Mountains	8	3	2
Little Harquahala Mountains	2	1	6
Harquahala Mountains	16	2	1

Table 2. Rank of flanking alluvial aprons according to their highest frequency and drainage texture value in the Harquahala Valley.

The computed coefficient, W, is 0.80, which is significant at $\alpha = 0.05$ for the three variables and six aprons and mountain ranges.

Alluvial aprons and mountain ranges of higher local relief and aprons which exhibit greater erosion occur together in the Harquahala Valley. The available potential energy thus appears to influence the distribution of the drainage texture over the bolson plain.

General Drainage Features

The axial drainage of the Harquahala Valley is the southeasterly flowing Centennial Wash (Fig. 1) which is tributary to the Gila River. Centennial Wash originates in McCullen Valley and flows through a gap between the Little Harquahala and Harquahala mountains entering the Harquahala Valley. This gap is known as the Harrisburg Valley (Fig. 4). Centennial Wash leaves the study area through a gap between the Gila Bend and Saddle mountains and joins the Gila River. Centennial Wash is deeply incised and contains coarse alluvium where it passes through these gaps. These two areas are the only places that the axial drainage is a distinct channel (Ross, 1923) (Fig. 6). In all other places, Centennial Wash is a very broad and shallow feature containing fine alluvium. It is ephemeral and very rarely carries discharge through the entire length of the wash.

Two other major ephemeral washes, which drain areas of considerable size, are Tiger (formerly Rogers) Wash and Burnt Mountain Wash (Fig. 4). Tiger Wash drains the southern Harquahala and northern Big Horn mountains, and Burnt Mountain Wash receives drainage from the southern and eastern portions of the Big Horn Mountains. Both join Centennial Wash in the southern portion of the Harquahala Valley.

The majority of smaller washes originate on the bolson plain, and only a few washes drain from the mountain interiors. Not all the flanking ephemeral washes reach Centennial Wash, but the majority are oriented orthogonally to the axial drainage. Those drainage lines associated with the Big Horn Mountains' alluvial apron are not orthogonal to Centennial Wash. Rather, they trend parallel to the axial drainage. The washes draining the Eagletail Mountains apron are orthogonal to Centennial Wash (Fig. 12). The mean direction of flow of the major drainage lines on the Eagletail Mountains apron is N34°E and on the Big Horn Mountains apron is S20°E (Fig. 12). The general trend of Centennial Wash is S55°E. The drainage lines which parallel the front of the Big Horn Mountains tend to receive more drainage from bedrock areas as compared to those drainage lines which are oriented perpendicular to the mountain front.

Two types of drainage patterns are discernible from color Skylab photography (S190B) at a scale of 1:125,000. Figure 47 is a map showing the areas of these drainage patterns in the Harquahala Valley as mapped from the Skylab photography. These patterns are: 1) deeply incised, tributary drainage systems developed on the upper apron surface and 2) broad, shallow anastomosing-distributary drainage systems developed on the lower apron (Fig. 13). The tributary drainage lines are incised from 1 to 25 m below the level of the bolson plain. The anastomosing-distributary drainage lines are incised about 0.5 m below the bolson plain. The boundary between these two drainage types is not sharp, but is transitional (Fig. 13B). The boundary marks the place where one drainage pattern type dominates over the other type.

The three major types of drainage channels described by Leopold

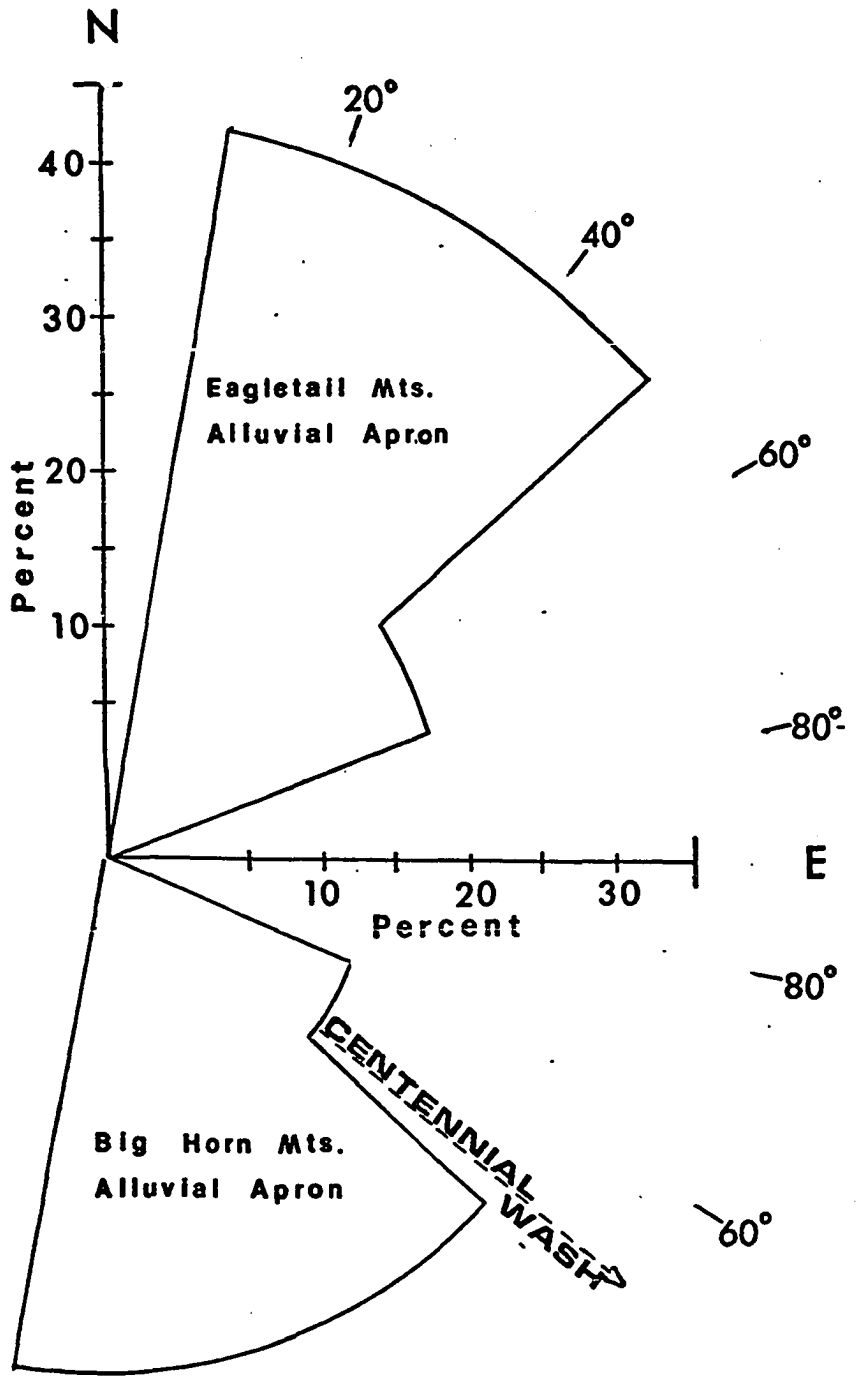

Figure 12. Rose diagram of frequency of major drainage line orientations on selected alluvial aprons in the study area, as compared to orientation of axial drainage.

A. Incised, tributary drainage systems in proximal alluvial apron region.

B. Transition from incised tributary drainage to anastomosing-distributary drainage in mid alluvial apron region.

C. Anastomosing-distributary drainage system in distal alluvial apron region.

Figure 13. General drainage patterns on alluvial aprons. Arrows indicate direction of regional slope.

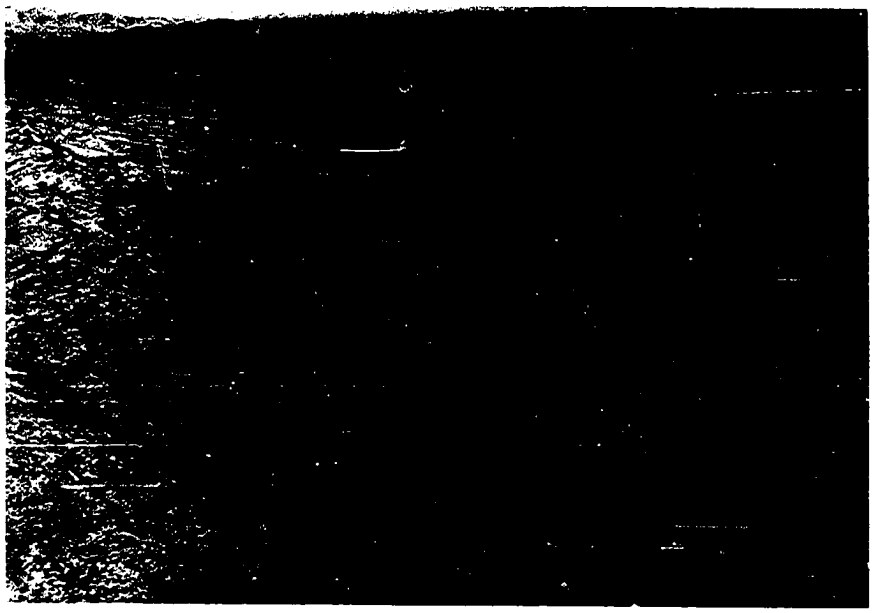

and others (1964) are meandering, braided, and straight. These types occur in both drainage patterns described above (Fig. 13).

GENERAL HYDROLOGY OF THE STUDY AREA

The purpose of this section is to describe the general characteristics of surface runoff and to determine the relationship between this runoff and precipitation. The ground-water conditions in the Harquahala Valley have been described by numerous investigators (Metzger, 1957a; Stulik, 1964; Denis, 1971) and have not been investigated during the present study.

Streamflow Characteristics of Centennial Wash and Other Ephemeral Washes

In the Harquahala Valley, the only source of runoff is derived from precipitation. All washes are ephemeral except during periods of rainfall, when intense flooding may occur. There are no base flow (ground-water) contributions to runoff; certain portions of Centennial Wash do receive a minimal amount of water from leakage in irrigation ditches.

A. U.S.G.S. gauging station has been installed on Centennial Wash near Arlington, Arizona since 1961, and discharge records are available (U.S.G.S. Water Supply Papers, 1970 and 1975; Wehro, 1967). The drainage area for this gauging station, which is outside the Harquahala Valley, is 4686 km^2. Selected hydrographs for stream discharge in Centennial Wash during 1970 are given in Figure 14. The flood pulses on these hydrographs are similar in form to those described by Keppel and Renard (1966). The highest discharge ever recorded at this station for a ten-year period is 410.5 m^3/sec. and the average discharge is 0.09 m^3/sec (U.S.G.S. Water

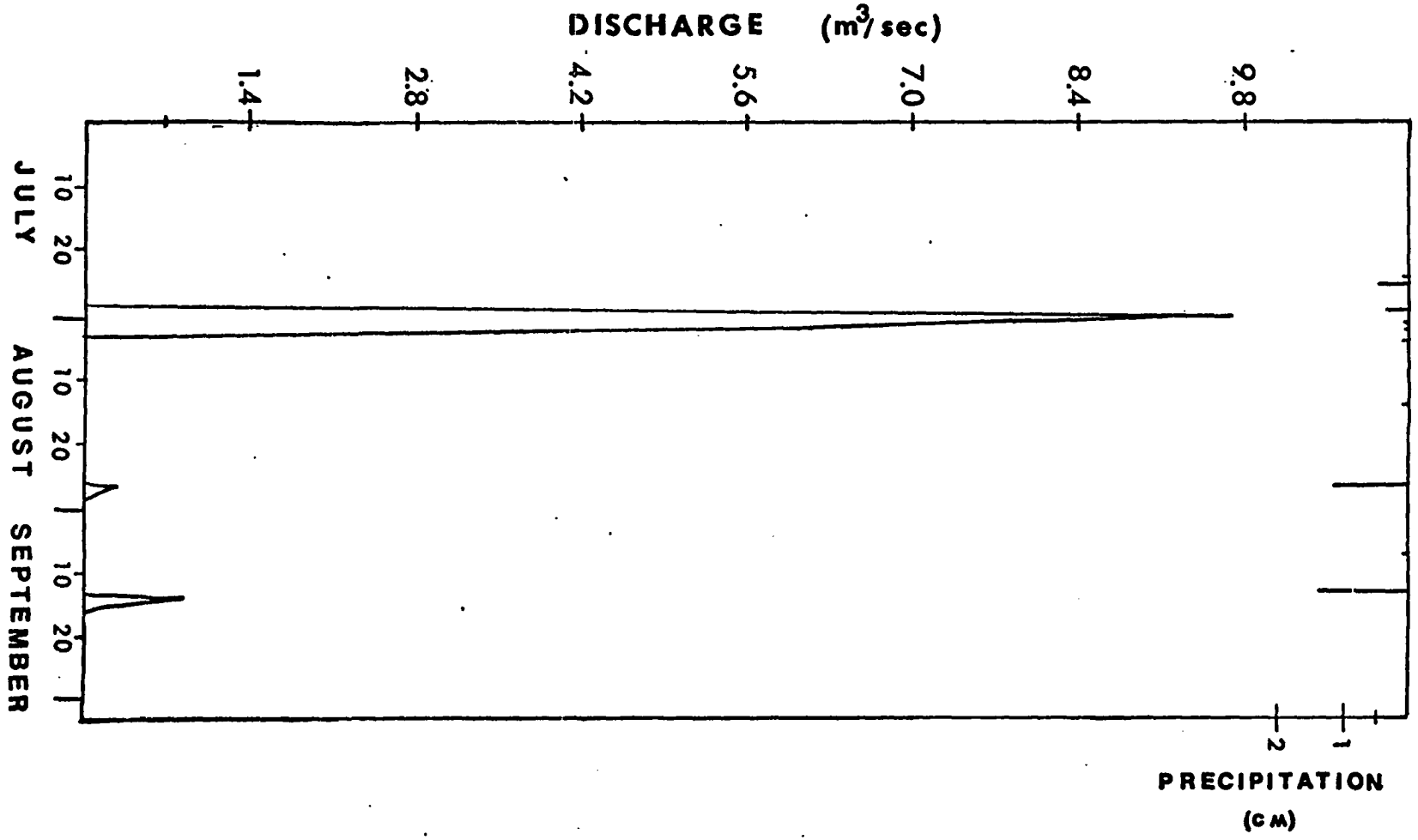

Figure 14. Discharge hydrograph for summer flood events on Centennial Wash, Arizona. Data based on U.S.G.S. Water Supply Papers (1970, 1975) and Wehro (1967).

Water Supply Papers 1970 and 1975). A cumulative frequency, or flow duration, curve for this gauging station is given in Figure 15. Flow in Centennial Wash occurs approximately 5 percent of the time, and the average discharge of 0.09 m^3/sec is equalled or exceeded only 2.9 percent of the time (Fig. 15). The frequency of yearly maximum peak discharge for Centennial Wash is shown by a plot of its recurrence interval (Fig. 16). A flood of 100 m^3/sec should reoccur on Centennial Wash every 2.2 years. The mean annual flood has a recurrence interval of 2.3 years.

Only one tributary to Centennial Wash in the Harquahala Valley has been successfully gauged for a period of three years (Wehro, 1967), It is in the northern portion of the basin and has a drainage area of 7.2 km^2. A flow duration curve for this tributary is given in Figure 15. Flow in this tributary occurs less than three percent of the time, and its maximum discharge for a three year period of 20 m^3/sec.

Regional flood-frequency studies provide a basis for estimating the magnitude and frequency of floods at ungauged washes. Although most of southern Arizona has established flood-frequency relations (Patterson and Sommers, 1966), the Sonoran Desert is not included. Therefore, the magnitude and frequency of floods in the Sonoran Desert can only be estimated from the flow duration curves given in Figure 15. In general, flow occurs 5 percent of the time in washes examined; discharges of 20 to 30 m^3/sec occur less than 0.05 percent of the time for basins less than 10 km^2. For basins greater than 350 km^2, discharges of 20 m^3/sec are equalled or exceeded 0.8 percent of the time.

In summary, Centennial Wash discharges less than 5 percent of the time yet has a mean annual flood of approximately 100 m^3/sec. That is,

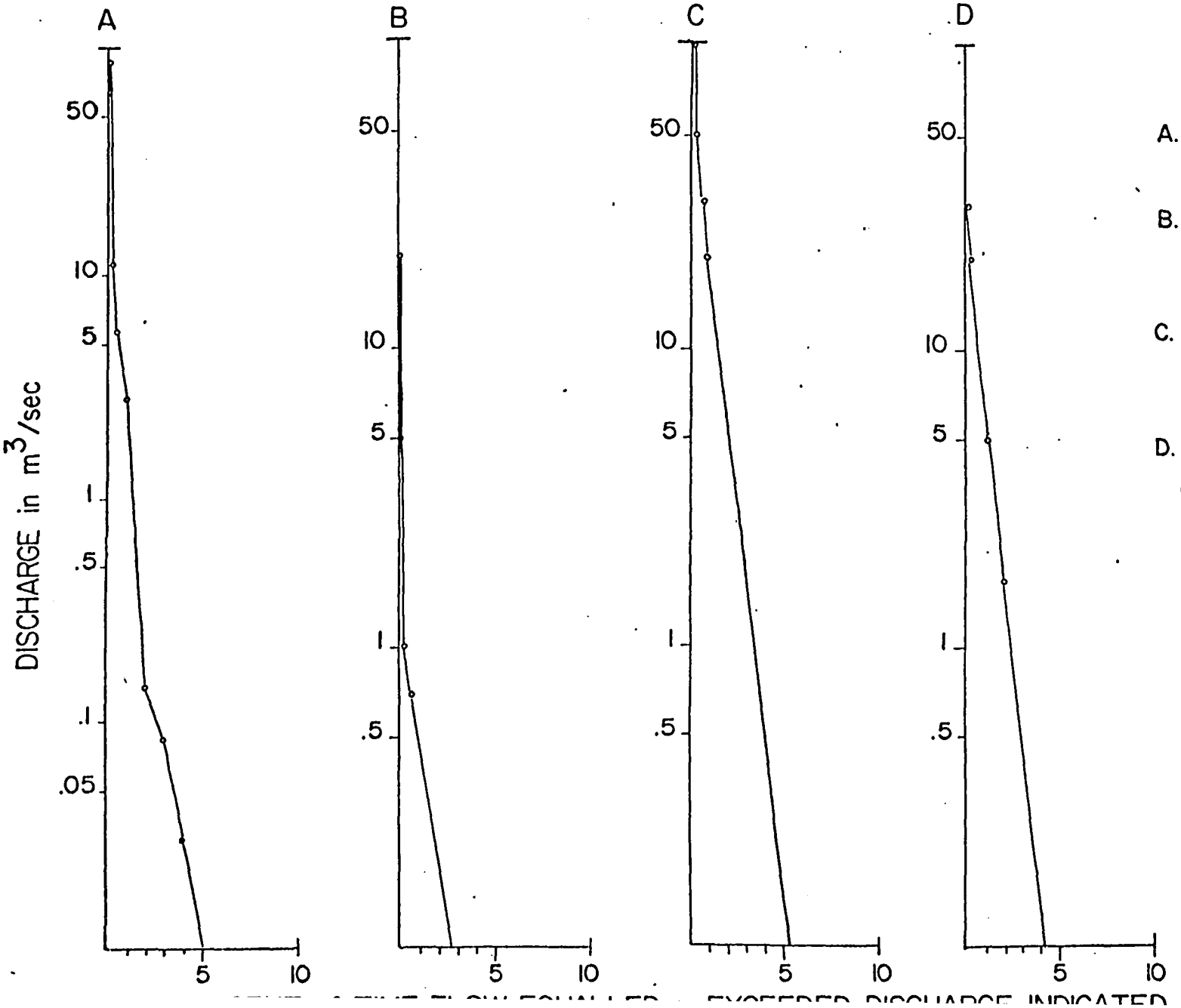

A. Centennial Wash, drainage area = 4686 km^2

B. Tributary to Centennial Wash near Salome, drainage area = 7.2 km^2

C. Jack Rabbit Wash near Burnt Mt., drainage area = 355 km^2

D. Rainbow Wash near Buckeye, drainage area = 8.9 km^2

Figure 15. Flow duration curves for selected washes in the Sonoran Desert. Data based on Wehro (1967).

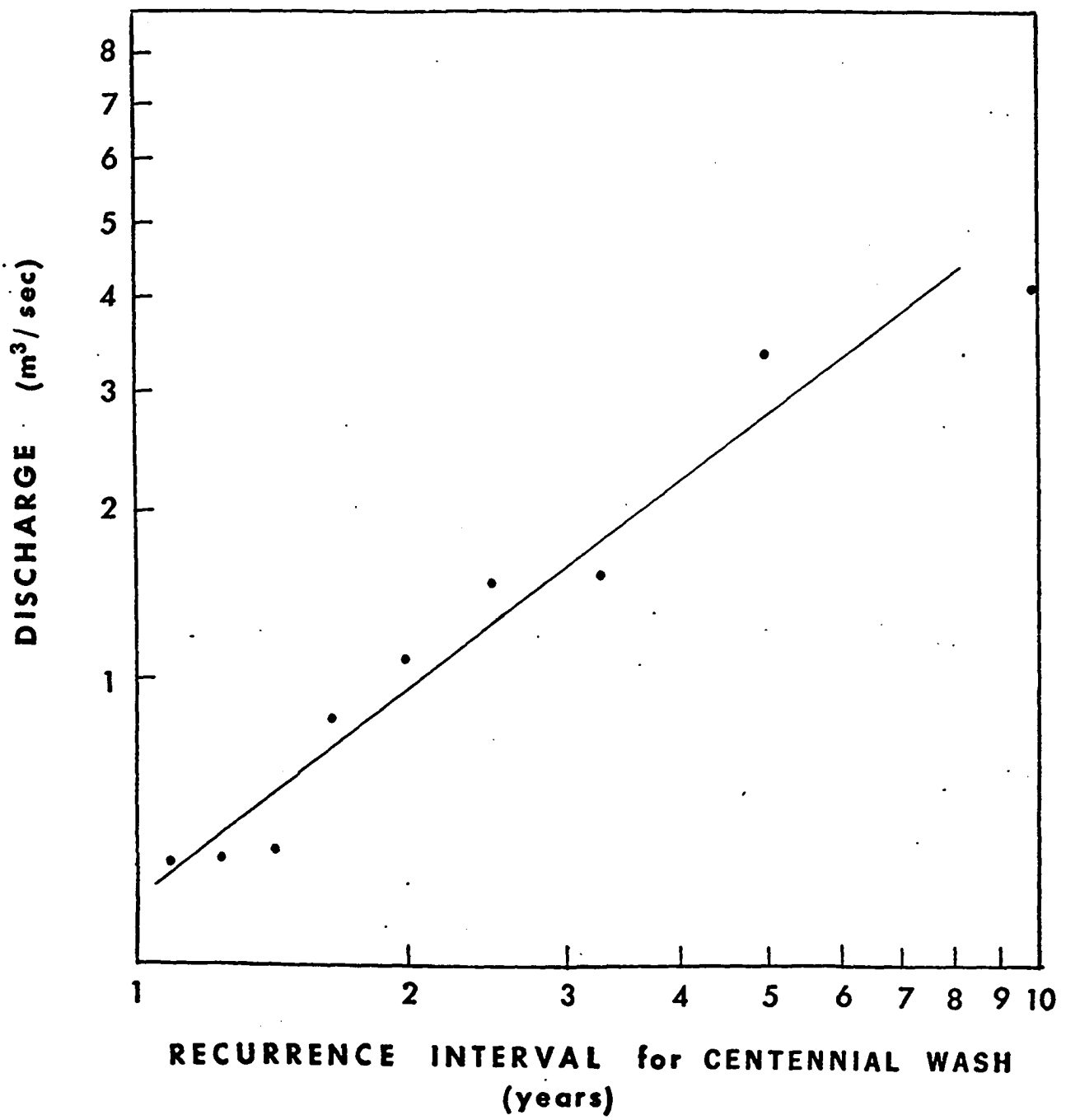

Figure 16. Recurrence interval for Centennial Wash, Arizona.

streamflow, which is an infrequent event, is high in magnitude. Floods on Centennial Wash occur as pulses which have the largest discharge at the beginning of the pulse.

Precipitation and Runoff Relationships

Two major factors affect surface runoff: climate and physiography (Chow, 1964). For an arid region such as Harquahala Valley, precipitation and evaporation are the most important climatic variables, and basin and channel characteristics are important physiographic variables.

Rainfall in the Sonoran Desert can be divided into two types (Dunbier, 1968). Precipitation during the winter months of November through April covers larger areas, is longer in duration per storm, and is not as intense as summer precipitation. In the summer months of May through October, the precipitation covers smaller areas and is of short duration and high intensity. Observations during winter and summer field work indicate that little runoff is produced by winter rainfall; whereas, high surface runoff in the form of flash floods is produced by summer storms. Runoff records at the gauging station on Centennial Wash and precipitation data from the study area are used to determine seasonal variations between precipitation and runoff. A logarithmic plot of runoff and precipitation during summer and winter seasons shows considerable scatter, but the two seasons can be distinguished (Fig. 17). Various factors influence surface runoff and precipitation correlation (Chow, 1964); therefore, the scatter in Figure 17 is predictable. The Spearman Rank correlation coefficient (r_S) for summer runoff and precipitation is 0.81 and is significant at $\alpha = 0.05$. The r_S for winter precipitation is 0.50 and is not significant

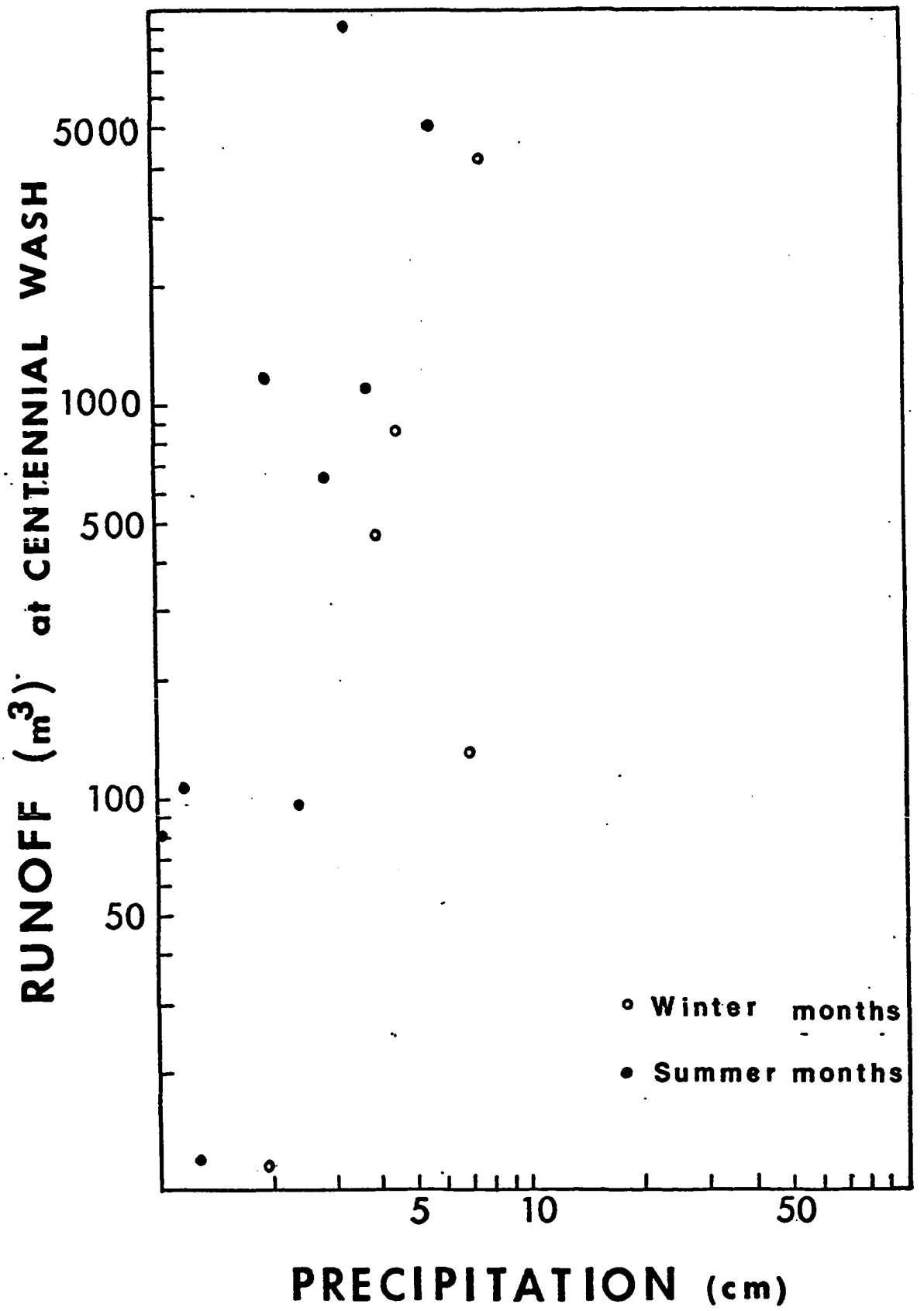

Figure 17. Logarithmic plot of runoff and precipitation during winter and summer months in the Harquahala Valley. Data based on U.S.G.S. Water Supply Papers (1970, 1975) and NOAA (1961-1970).

at $\alpha = 0.05$. Therefore, during summer months there is a positive correlation between rainfall and surface runoff in Centennial Wash.

Thus, field observations and statistical analyses indicate seasonal differences in runoff and precipitation relationships. In order to determine the magnitude and frequency of these differences, a comparison is made between the percentage of monthly rainfall and runoff averaged over a ten year period (Fig. 18). Fifty-four percent of the precipitation occurs during the winter months and produces only fourteen percent of the yearly runoff. In the summer months, 46 percent of the precipitation results in 86 percent of the surface runoff. It is concluded that, even though rainfall is distributed evenly between winter and summer seasons, over 80 percent of the runoff is associated with intense summer storms of short duration.

Comparison of the Study Area to a Semi-arid Basin near the Sonoran Desert

The results presented above concerning runoff and precipitation relationships are very different from those found by Thomsen and Schumann (1968) in a semi-arid basin approximately 200 km to the east of the Harquahala Valley. They studied the hydrologic behavior of the 500 km^2 Sycamore Creek basin which is composed of 15 percent unconsolidated fill and 85 percent hard, consolidated rocks. The Sycamore Creek basin receives 50.8 cm of rainfall per year, or nearly three times that of the Harquahala Valley. The Sycamore Creek basin produces 90 percent of the runoff in the winter months and only 10 percent in the summer months. Runoff is closely related to winter precipitation in semi-arid basin. Thomsen and Schumann attribute higher runoff in the winter to changes

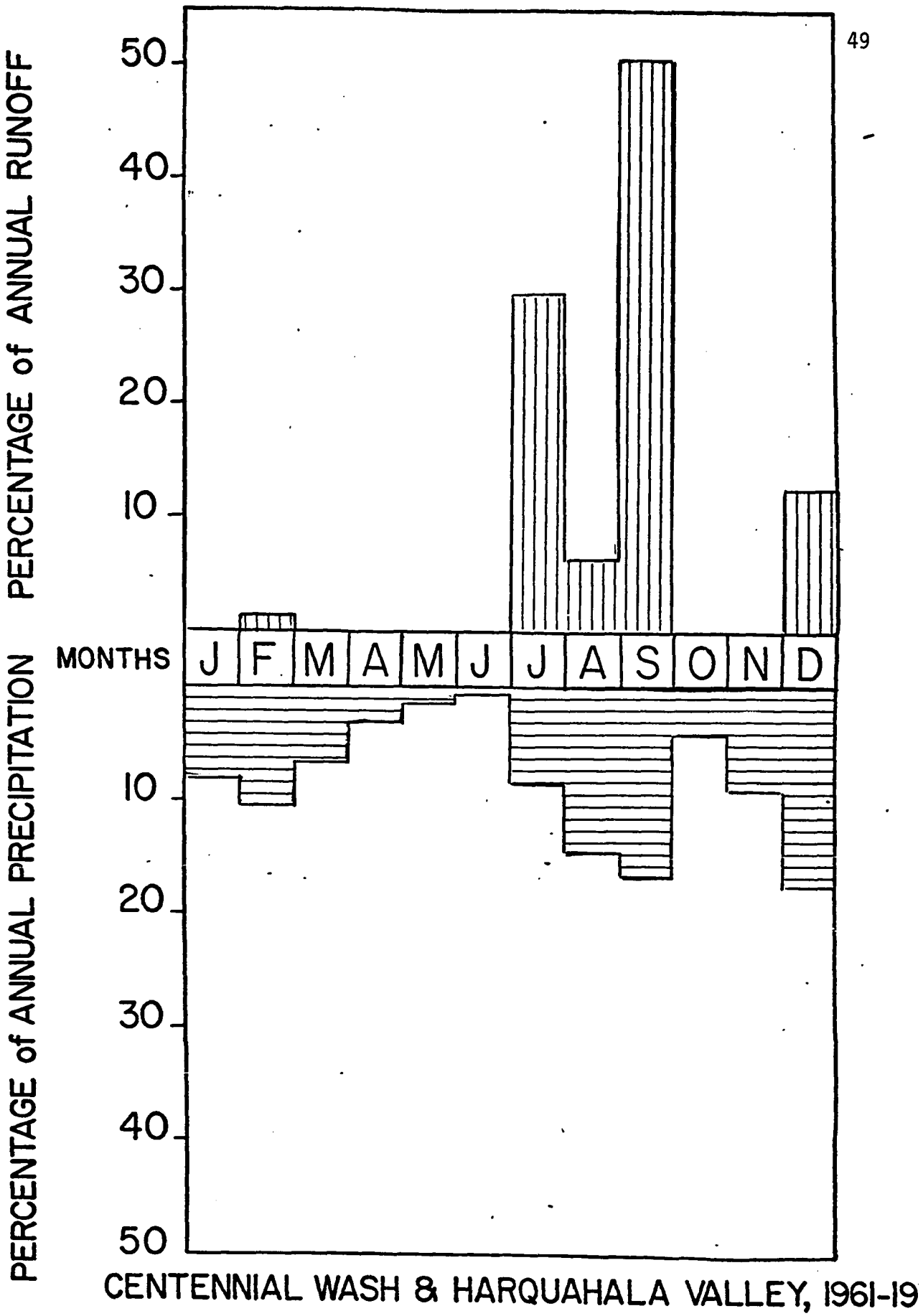

Figure 18. Percentage of annual runoff and precipitation for Centennial Wash and Harquahala Valley for the period of 1961 to 1970.

in soil moisture content and vegetation activity. In the Harquahala Valley, the opposite conditions exist, because of low soil moisture content and sparse vegetation (excluding cultivated areas), basin conditions remain fairly constant.

The short duration and high intensity rainfall of the summer months has more influence on runoff in the arid Harquahala Valley than in the nearly semi-arid basin. An alternative explanation for the hydrologic differences of these basins is that the Harquahala Valley is four times larger than the semi-arid basin. This explanation seems less likely because smaller basins are more sensitive to high intensity rainfalls of short duration (Chow, 1964).

QUATERNARY SURFICIAL DEPOSITS OF THE HARQUAHALA VALLEY

Several types of Quaternary surficial deposits are distributed throughout the Harquahala Valley. The surficial deposits are shown in the map in Figure 25. These deposits are not mapped in the conventional way because of the special purposes of this study. Rather, they are differentiated using parameters which affect runoff and infiltration. To meet the requirements of this study, two parameters are used: 1) particle size and distribution, and 2) degree of secondary deposition and weathering. Such secondary deposition, although in part related to lithology, is more significant than lithology in affecting hydraulic parameters. The resulting map is of greater geomorphic significance than a map based on lithology and particle size. These surficial deposits have been mapped on 1:60,000 vertical, black and white, aerial photographs as a base. Some additional mapping information has been obtained from LANDSAT imagery.

Mapping Units of the Surficial Deposits

The material covering the bolson plain ranges in size from boulders 2 m in diameter to clay-size particles. Almost all the map units are transitional with each other and also may include smaller areas of the other map units; therefore, the map units represent the dominant type of sediment and are not necessarily exclusive of the other types described below. Five map units are based on dominant particle size and three are based on secondary features. These deposits are described in order of decreasing areal extent:

1. Quaternary coarse grained fans (Qfc): Coarse gravels and sands with occasional silt and fine sand cover the alluvial apron surfaces (Fig. 25). Generally, two-thirds of this map unit has particles larger than 2 mm (-1ϕ) based on field observations and sieve analyses (Figures 19, 20). The thickness of the coarse grained alluvial fans is highly variable, with a minimum thickness of 1 m and a maximum observed thickness of 30 m. Cut and fill structures are common in these poorly stratified sediments. These sediments occur as abandoned wash deposits and as desert pavements. Weathering and desert varnish are present. Coarse grained alluvial fans are found on alluvial aprons steeper than 0.5°. This unit covers over 900 km^2, or 62 percent of the Harquahala Valley bolson plain (Fig. 21).

2. Quaternary fine grained alluvial fans (Qff): The deposits in this unit are mainly fine sands and silts, but include coarser sand and gravel as stringers or lag deposits. Forty percent of the particles of this map unit are less than 0.125 mm in diameter (3ϕ) (Figures 19, 20). Fine grained alluvial fans usually range in thickness from 1 to 2 m and occur as

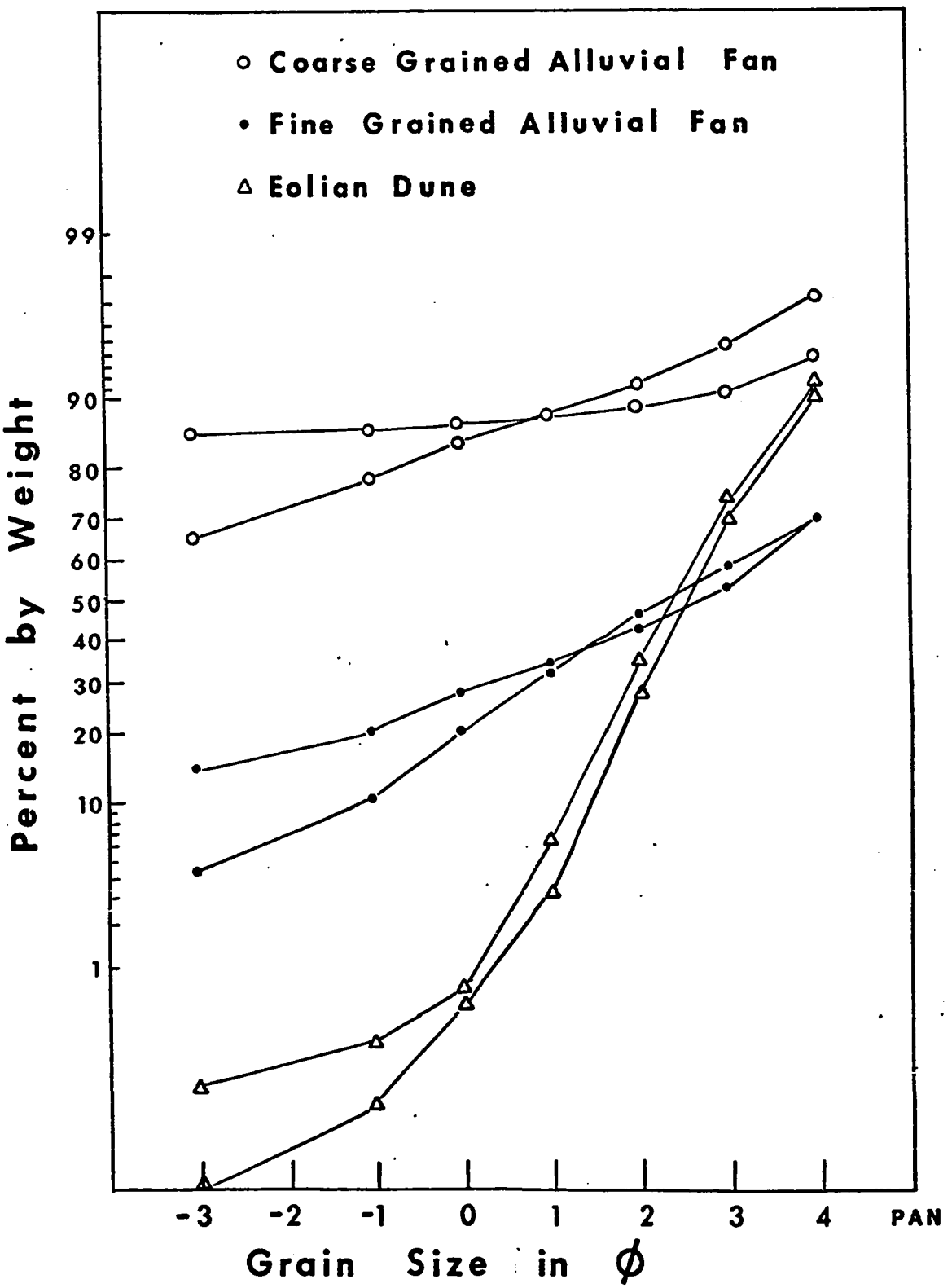

Figure 19. Cumulative curves of particle sizes for selected Quaternary deposits.

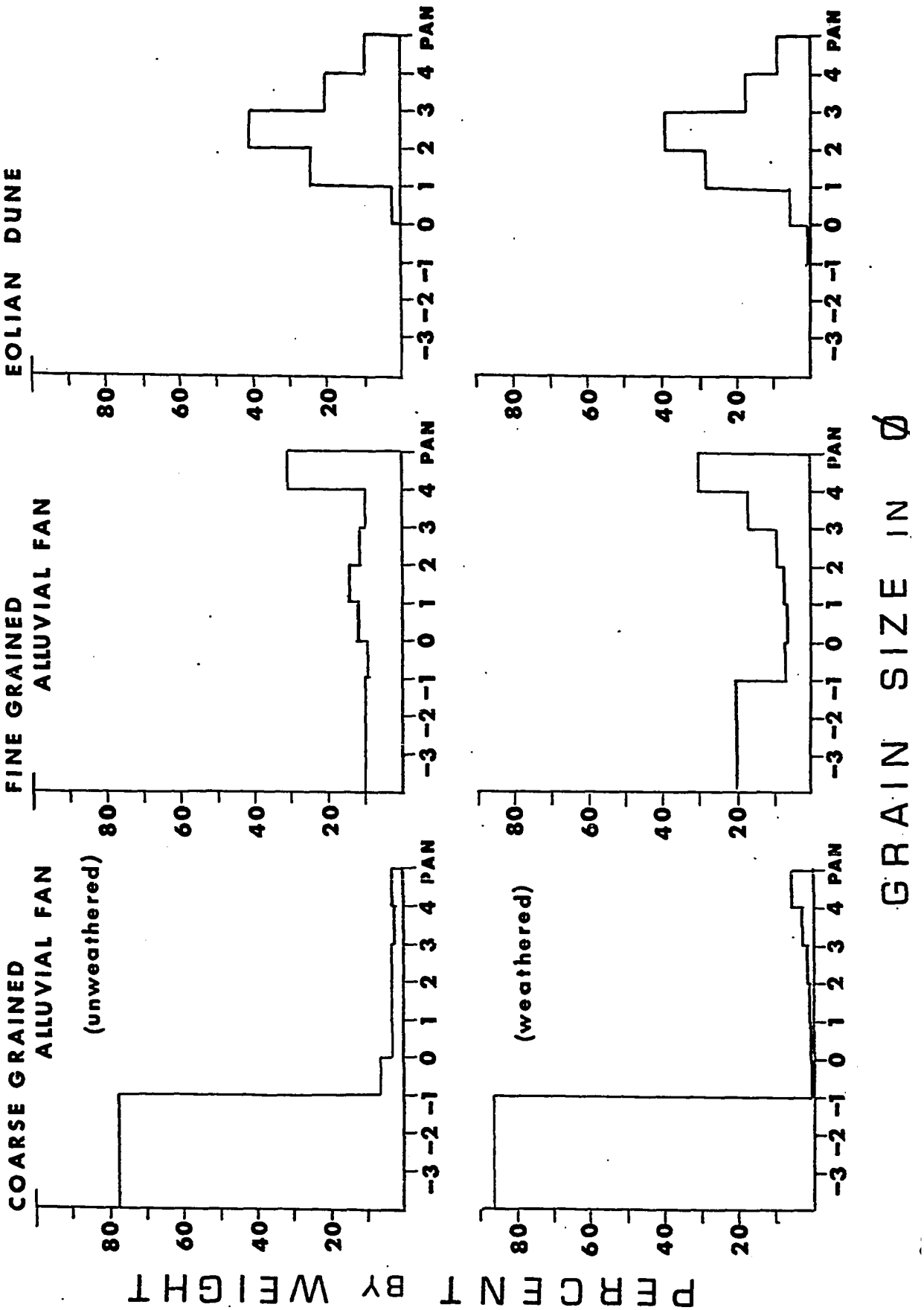

deposits of coalescing active washes. These deposits display no signs of desert pavement development (Fig. 22). The primary bedding of this deposit varies from a fine lamination to a thick massive bedding; however, bedding is often obscured by eolian reworking of the upper few centimeters. Fine grained alluvial fans occur on alluvial aprons that are usually less than 0.5° and cover nearly 250 km^2, or 16 percent of the bolson plain (Fig. 21).

3. Quaternary alluvial fans undifferentiated (Qfu): These are local coarse grained alluvial fans that have indistinguishable, or unmappable, smaller areas of varnished gravels and caliche rubble. The description of this unit is the same as the coarse grained fans (Qfc) except that the upper 1 m is composed of heavily varnished gravels and caliche rubble. Approximately 120 km^2, or 8 percent of the bolson plain has this sediment type (Fig. 21).

4. Eolian sand dune deposits (Qds): These deposits are medium to fine grained sands with some silt and coarse sands. Over seventy five percent of the weight of the eolian sand is between 0.5 and 0.62 mm in diameter (1 to 4 ϕ) (Figures 19,20). These deposits are found on slopes less than 0.33°, and cover nearly 80 km^2, or 5 percent of the bolson surface (Fig. 21).

The dune deposits have been extensively modified by man. Figure 25 illustrates the distribution of eolian dunes in 1953 as detectable from 1:50,000 vertical, black and white, aerial photographs. The majority of these dunes have been bulldozed into smooth surfaces and cultivated (Fig. 23); therefore, the areal extent of these dunes shown in Figures 25

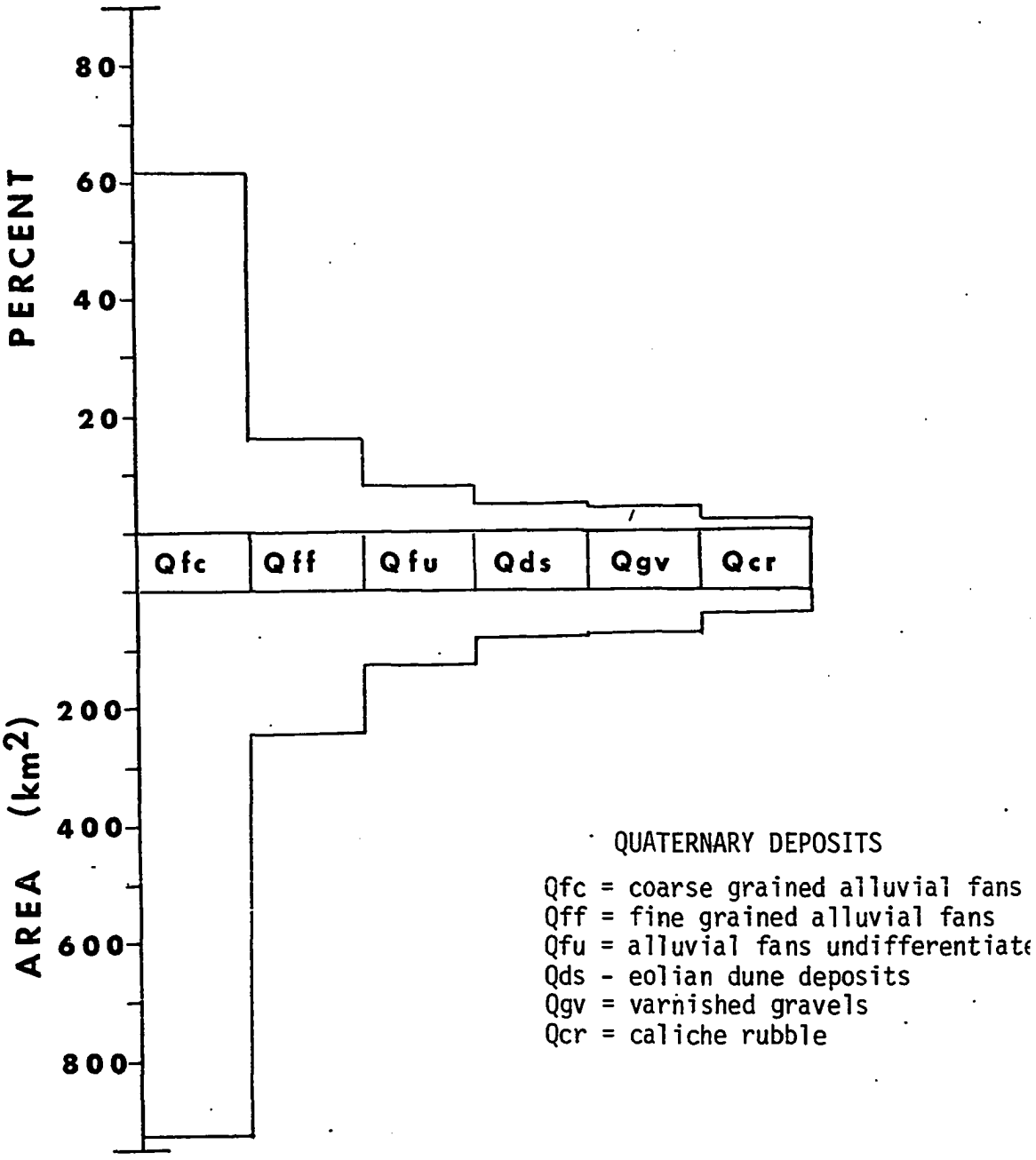

Figure 21. Histogram showing frequency of areal extent of Quaternary surficial deposits on the bolson plain of the Harquahala Valley.

A. Aerial view of fine grained alluvial fan (arrow indicates direction of regional slope).

B. Ground view of fine grained alluvial fan with coppice dunes (scale is in 0.1 m).

Figure 22

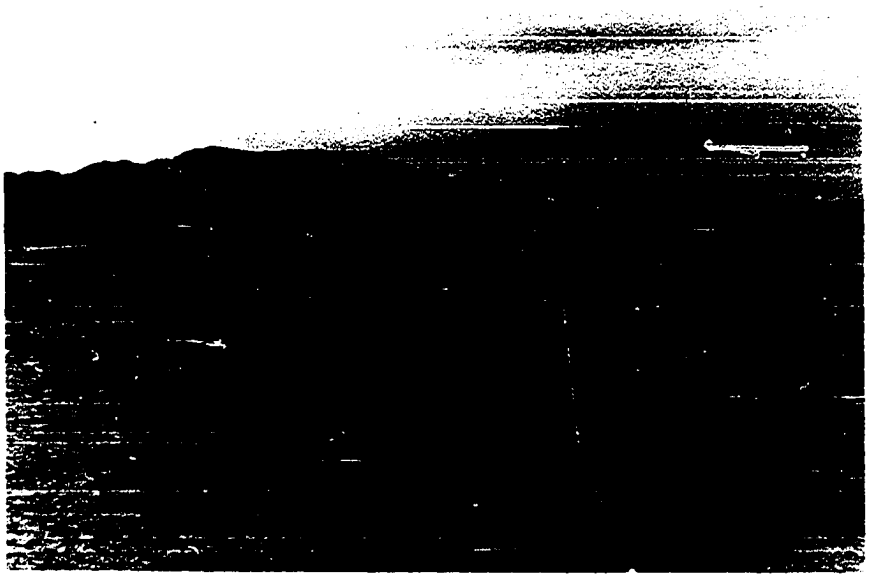

A. Aerial view of eolian dune deposits and their eradication by cultivation. These deposits were quite extensive in the southern Harquahala Valley prior to 1953, when extensive farming began.

B. Close-up aerial view of eolian dunes showing linquoid form.

Figure 23.

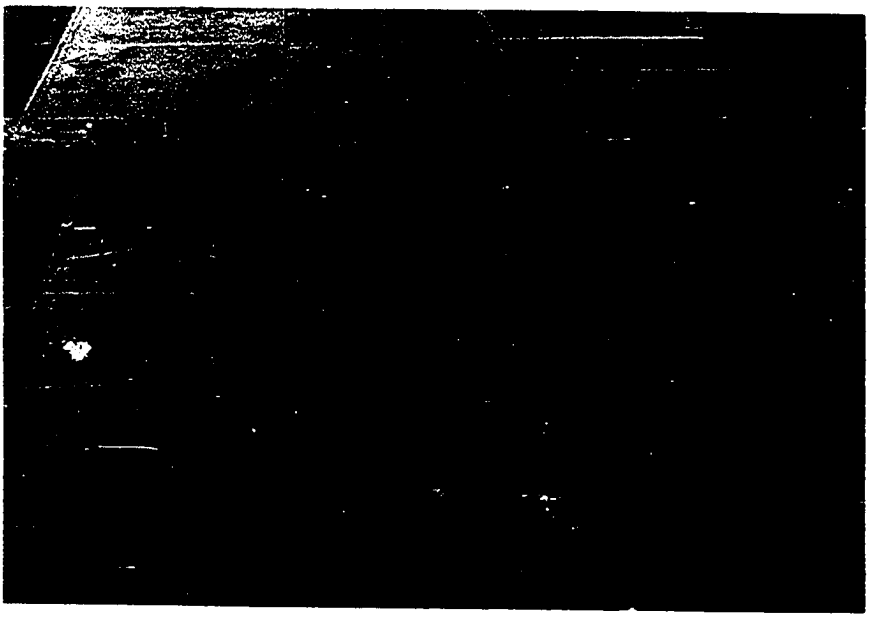

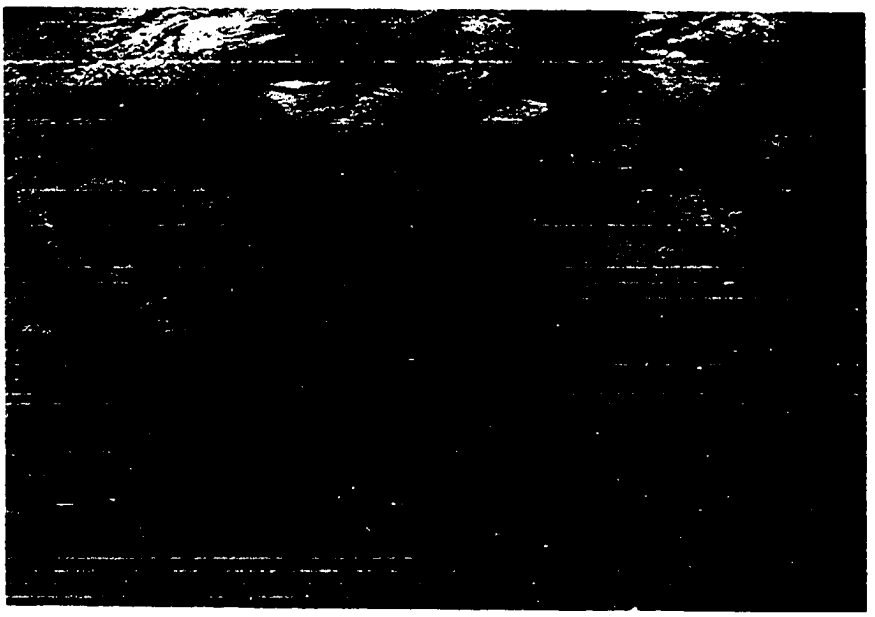

is based on 1953 aerial photographs. The description of the deposit is based on the few remaining dunes in the extreme southern Harquahala Valley.

Saline deposits (TQsa) form a sub-unit of the eolian deposits. These deposits may be either late Pliocene or early Pleistocene in age. This sub-unit is always associated with sand dunes and lies stratigraphically below them. Saline deposits are exposed in areas were dissection has occurred. These deposits are primarily composed of salty, clayey silts with included gypsum crystals. On fresh surfaces, the clayey silts range in color from drab olive green to brownish maroon. Weathered surfaces have a whitish to light tan colored crust 2 to 4 cm thick. These crusts are highly saline and form a protective surface over the silts. Field observations indicate that this crust can form in a matter of months. Additionally, these crusts have a 'popcorn' texture which is typical of expandable clays. Stringers, or lens, of highly weathered volcanic gravels are typical in this unit. The thickness of the saline deposits ranges from 0.4 to an observed maximum of 5 m. The actual areal extent cannot be determined due to cultivation and lack of exposures.

5. Quaternary varnished gravels (Qgv): Areas of heavily varnished gravels compose this mapping unit. These deposits occur in two forms: 1) as well developed desert pavements (Fig. 24), and 2) as water-worked colluvium on the slopes of deeply dissected, calcium carbonate-cemented, alluvial fans and pediments (Fig. 26). Varnished gravels in the form of desert pavements are the most common. A discussion on the composition

Figure 24. Trench in the Quaternary varnished gravels showing a few centimeters of thick desert payment and a mixed gravel and silt layer approximately 20 cm thick. Scale is 0.1 of meter.

A. Ripple train of caliche rubble and silt on interfluves of apron.

B. Deeply dissected apron surface covered with Quaternary caliche rubble. Note change in cord length of ripple-trains at center left. Arrow indicates regional slope. Varnished gravels line the banks of dissected washes.

Figure 26. Aerial view of alluvial apron flanking Saddle Mountain.

of this varnish is given by Cooke and Warren (1973). The varnished gravels which form well developed desert pavements are underlain by an orange-brown, vesicular silt which has been described by Denny (1965), Lattman (1971), and Cooke and Warren (1973) (Fig. 24). Both forms of varnished gravels occur on a wide range in slopes but are not present on slopes below 0.5°. This mapping unit covers approximately 70 km^2, or 4.5 percent of the Harquahala Valley bolson plain (Fig. 21).

6. Quaternary caliche rubble (Qcr): Intermixed silts and fragments of well-indurate secondary calcium carbonate form a caliche rubble (Lattman, 1973) (Fig. 26). These fragments range from 10 to 50 cm in diameter. The caliche rubble is derived from the mechanical break-up of extensive petrocalcic horizons (Lattman, 1973). Occasionally, the petrocalcic horizon is exposed at the surface, but it is usually buried up to 50 cm by rubble and silt. The petrocalcic horizons vary in thickness, reaching a maximum of 1 m. This mapping unit is found on slopes of the aprons greater than 1°. Caliche rubble covers 35 km^2, or 2.5 percent of the desert plain (Fig. 21).

7. Quaternary alluvium (Qal): This mapping unit consists of recent and unweathered alluvium in drainage lines on the bolson plain. Alluvium is found in all units. In the bolson plain where alluvium is areally extensive, it is separated from the other mapping units (Fig. 25, in pocket). The alluvium is highly variable in particle sizes and will be discussed in detail below.

8. Quaternary debris flows (Qdf): Heavily varnished and calcium carbonate-cemented debris flow levees are composed of very coarse detritus (Fig.

45). The size of the detritus forming the levees ranges up to a maximum of 3 m. Debris flows are restricted to hillslopes and proximal portions of alluvial aprons, which are composed of extrusive igneous rocks. The slopes where debris flows occur are greater than 5°.

Particle Size Analyses of the Surficial Deposits

Results of sieve analyses of samples from coarse and fine grained alluvial fans and eolian dune deposits are given in Figure 19. Cumulative frequency plots of percent by weight illustrate the three different sediment size populations. Figure 20 shows the particle size distribution for these deposits.

The weathered and unweathered coarse grained alluvial fans are differentiated by particle size distribution as well as weathering. Field observations and sieve analyses indicate that the weathered coarse grained alluvial fans have a bimodal distribution of particle sizes. These fans have extremely high percentages by weight of coarse gravels and smaller amounts of silt and clay size material. The coarse grained fans which show less weathering contain higher percentages by weight of sand size particles (less than 2 mm and greater than 0.125 mm in diameter).

Fine grained alluvial fans are composed of relatively unweathered detritus. Histograms in Figure 20 show changes in the relative amount of sand and gravel; whereas, the silt and clay size fractions remain fairly constant. Field observations and sieve analyses (Fig. 19) suggest that these deposits contain larger percentages by weight of coarse material near the proximal portions of the alluvial aprons, and in the distal portion of the aprons, there is less coarse material.

The sediment size distribution of the eolian sand dunes is given in Figure 20 and in the Harquahala Valley is distinctive and similar to those described by Warren (1971) and Folk (1971). The sediments are positively skewed and moderately to well sorted. There is a very sharp cut off of the sediment size distribution toward the coarse grains with a tail extending toward the fine material (Fig. 20).

Distribution and Form of the Surficial Deposits

The areal extent and distribution of the surficial deposits across the bolson plain are shown in the surficial sediment map (Fig. 25). The areal extent of these deposits is summarized in Figure 21.

The two most extensive surficial deposits, coarse and fine grained alluvial fans (Qfc, Qff), occur in different parts of the bolson plain. The coarse grained fans are associated with the upper alluvial apron regions, and the fine grained fans are located in the lower apron regions (Fig. 25). The fine grained deposits are usually associated with the troughs in the slope map (Fig. 8) and follow major drainage lines up the aprons to an apex (Fig. 25). The apex of the fine grained fans is often the location of the boundary between tributary and anastomosing-distributary drainage systems.

The eolian dune deposits (Qds) and associated saline deposits (Qsa) are restricted to the southern and central portions of the Harquahala Valley (Fig. 25). Broad, flat channels of alluvium associated with Centennial Wash divide the eolian dune deposits into isolated sections in the northern portion of this unit (Fig. 25). In the southern section of this unit, Centennial Wash is incised and the eolian dune deposits are

perched on the old valley floor. This surface now represents a terrace level (Fig. 25). The drainage lines in the region of the eolian dune fields are diverted around the boundary of this unit. However, south of Saddle Mountain, the drainage lines cut through the eolian dunes.

Caliche rubble is primarily found on aprons surrounding Saddle Mountain and occurs less extensively on the flanks of the Big Horn and Harquahala Mountains. The best developed surfaces containing caliche rubble are those which are deeply dissected around the southern portions of Saddle Mountain (Fig. 25). The deeply dissected caliche rubble surfaces of Saddle Mountain are located near a lowering base level in the Harquahala Valley. That is, Centennial Wash has incised into the bolson plain in this region (Fig. 6).

Another feature related to the caliche rubble on the southern flanks of Saddle Mountain is the large ripple-train texture, only apparent from aerial observation (Fig. 26). The general ripple morphology is similar to that of the giant ripple-trains described by Baker (1973). The variation in composition of the ripple-train feature accounts for the tonal variations seen in Figure 26. The alternating light and dark bands are composed of light caliche fragments and dark lichen-encrusted silts, respectively. Similar lichen crusts have been described by Cameron and Blank (1966) and have been found to be associated with "translucent or transparent" rocks in the soil. The fan material surrounding Saddle Mountain has abundant translucent chalcedony derived from secondary vein fillings in the volcanic rocks. The caliche rubble forms the topographic high, or ripple, and the lichen encrusted silts fill the troughs. The maximum height of the ripples is 25 cm, and an average cord length

(measured from trough center) is 85 m. The cord length varies over the caliche rubble surface (Fig. 26). The cord length decreases to 40 m or less in shallow rills developed on the interfluves in this map unit. Baker (1973) and Harms and Fahnestock (1965) have associated the smaller cord lengths on ripple-trains with lower flow velocities. Thus, the smaller ripple-train cord lengths in the active drainage lines may represent smaller flow velocities than the larger cord lengths on the interfluves. It is suggested that this feature may have been formed by sheet flow over the caliche rubble surface.

The ripple-trains are mapped in detail on Figure 27 and can be seen to occur only on the wide, flat interfluves capped with a thick petrocalcic horizon and caliche rubble. The extension of the caliche and ripple-trains to the edge of the interfluves (Fig. 27) suggests that the process which formed the ripple trains occurred prior to incision of the Saddle Mountain alluvial apron.

The varnished gravels of well developed desert pavements are always found within the coarse grained alluvial fans and are located on the mid to proximal regions of the aprons (Fig. 25). The proximal portions of these pavements are drained by shallow rills, and the distal portions are drained by incised, meandering gullies (Fig. 28). The desert pavement segments are usually oblong, being widest in the middle (Fig. 25). The maximum length and width of the pavement segments were measured from 1:60,000 aerial photographs and are given in Table 3. A linear regression analysis (Fig. 29) of the maximum length and width measurements in Table 3 indicates the following relationship: $W_{dp} = -.13 + .45\ L_{dp}$, where W_{dp} is the maximum width and L_{dp} is the maximum length of pavement segments.

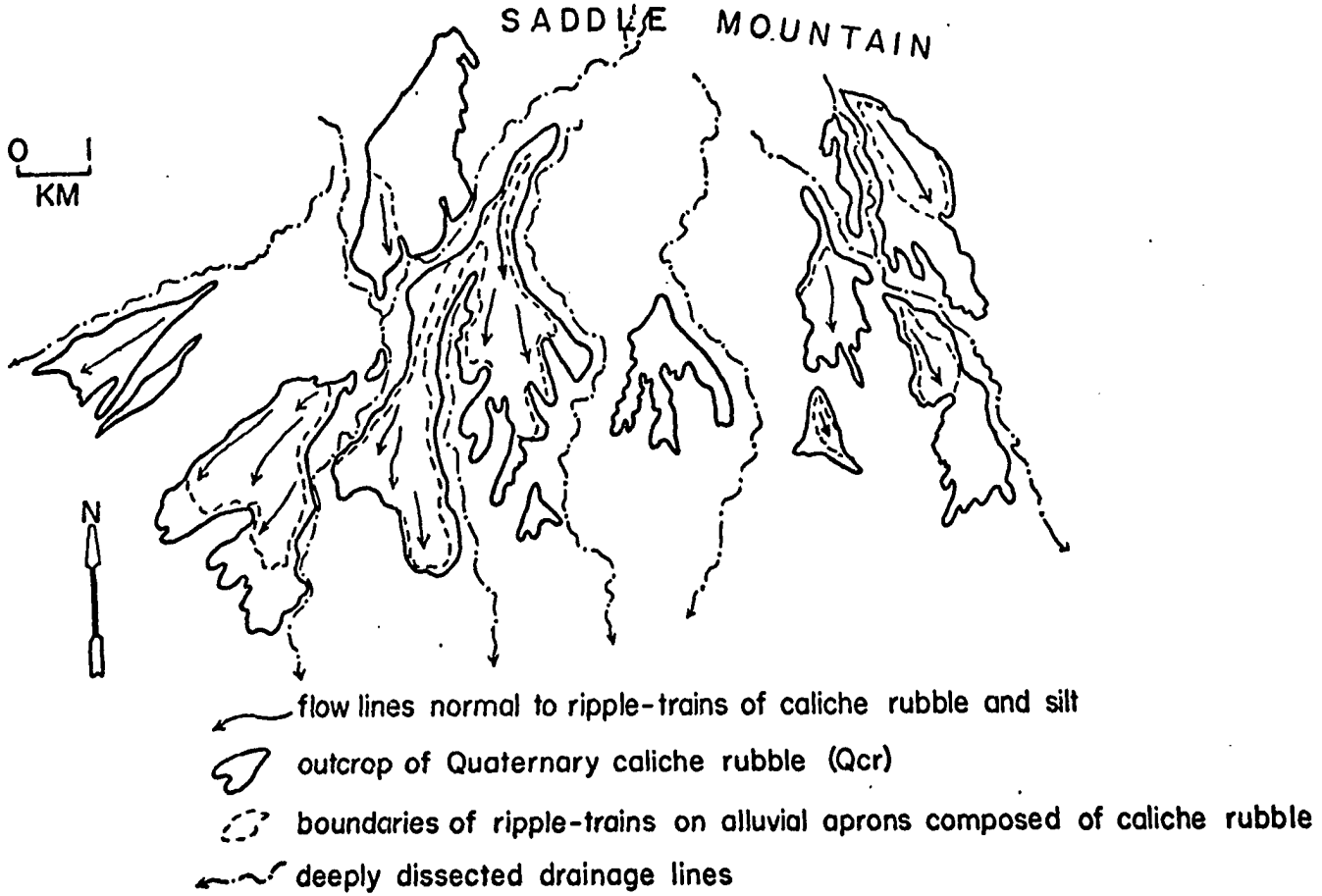

Figure 27. Areal extent of ripple-train phenomena on caliche rubble deposits of alluvial apron flanking Saddle Mountain.

A. Varnished desert pavement surface in mid apron region showing little dissection. Contact with fine grained alluvial fan shown in bottom of photograph.

B. Varnished desert pavement surface (Qgv) in proximal apron region showing dissection by meandering gullies. Arrows indicate regional slope.

Figure 28.

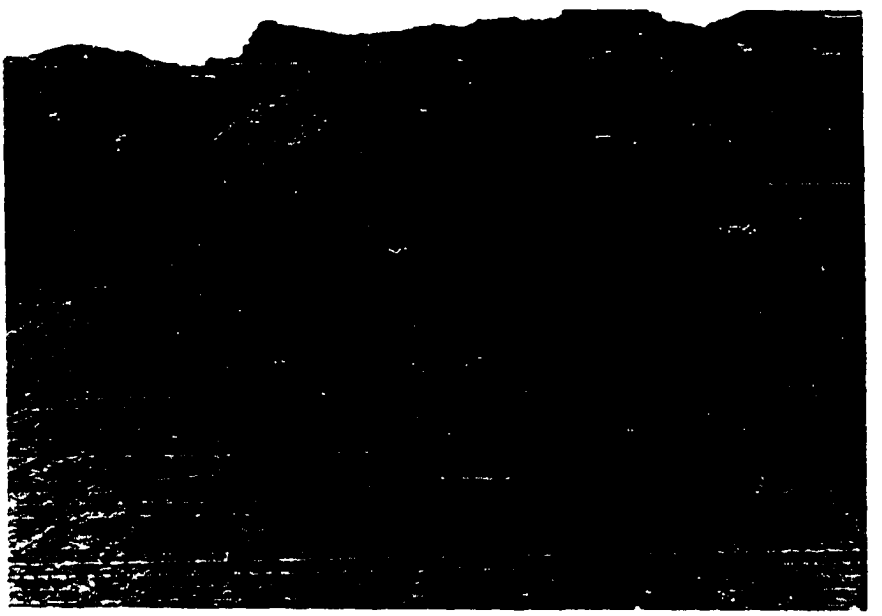

DESERT PAVEMENT SEDMENT	MAXIMUM WIDTH (km)	MAXIMUM LENGTH (km)	RATIO L/W
a	0.81	2.32	2.9
b	0.90	2.32	2.6
c	0.31	0.81	2.6
d	0.40	1.30	3.2
e	0.61	1.61	2.6
f	0.40	1.21	3.0
g	0.40	1.42	3.6
h	0.61	1.61	3.0
i	0.06	0.27	2.6
j	0.61	1.61	2.6
k	0.40	1.21	2.6
l	0.21	0.74	3.6
m	0.21	0.74	3.6
n	2.82	6.53	2.3

Range in ratios for maximum length to maximum width: 2.3 to 3.6

Mean ratio: 2.9

Table 3. Selected geometric parameters of well developed desert segments in the Harquahala Valley.

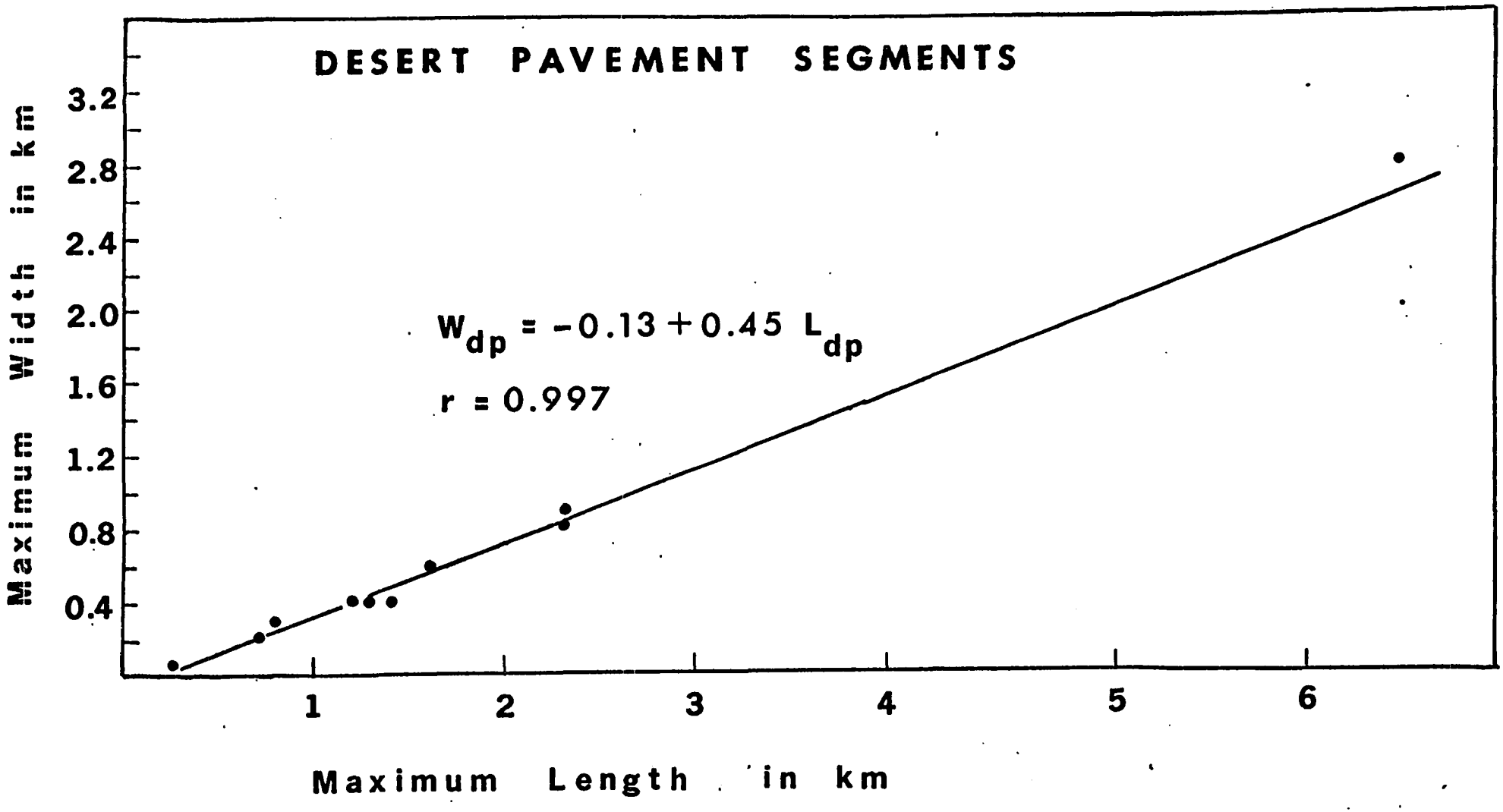

Figure 29. Relationship between maximum length and width of desert pavement segments in Harquahala Valley. Regression coefficient is given as r.

The regression coefficient for this relationship is 0.997. These results indicate that the maximum width and length of these segments maintain a ratio which is nearly constant, and this ratio between length and width ranges between 2.3 and 3.6 (Table 3). The mean ratio of the maximum length and width is approximately equal to 3.

Relationship of Surficial Deposits to Topography

Selected cross and longitudinal profiles are plotted with descriptions of the surficial deposits (Figures 30, 31, 32, 33, 34). Below is a list of important relationships between the surficial deposits and topography:

1. The banks of all incised drainage lines in the coarse grain alluvial fans (Qfc), varnished gravels (Qgv), and caliche rubble (Qcr) areas are covered with colluvium that shows reworking by water. Miniature terraces, described by Denny (1965) as being related to creep processes, are typical in this colluvium.

2. Micro-relief in coarse grained alluvial fans is related to the size of the particles which form ridge and swale topography. Ridge and swale topography is formed by abandoned channel bar deposits (Denny, 1965). Micro-relief in fine grained alluvial fans (Qff) is a function of eolian accumulation around creosote bushes (Larrea divaricata). These accumulations are known as coppic dunes (Gile, 1966). The transition between coarse grained and fine grained alluvial fans can be detected by the amount of relief on the coppice dunes. A logarithmic plot of amount of surface covered with gravels and maximum micro-relief produced by coppice

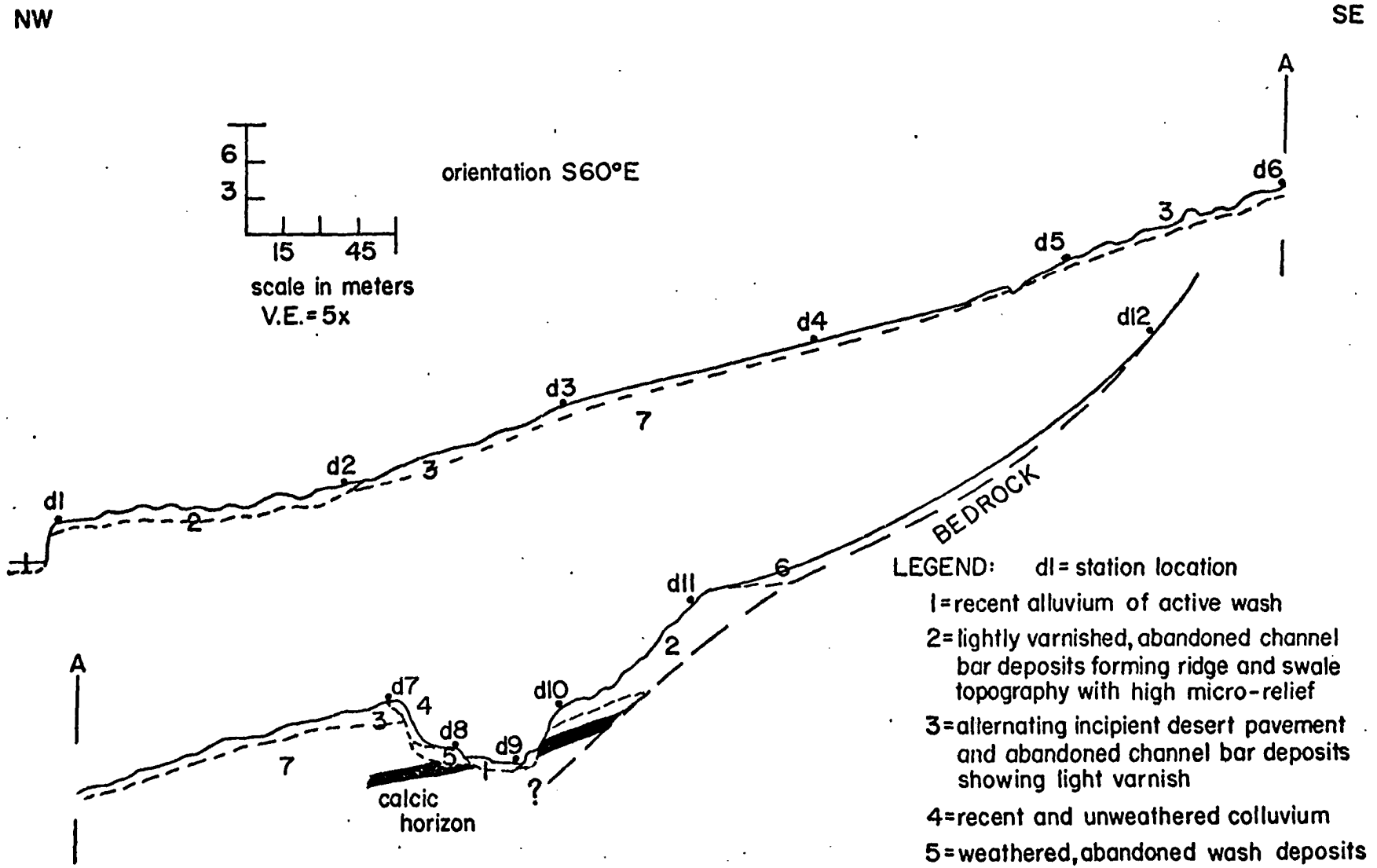

Figure 30. Detailed longitudinal profile (BHL-d) and description of surficial deposits on

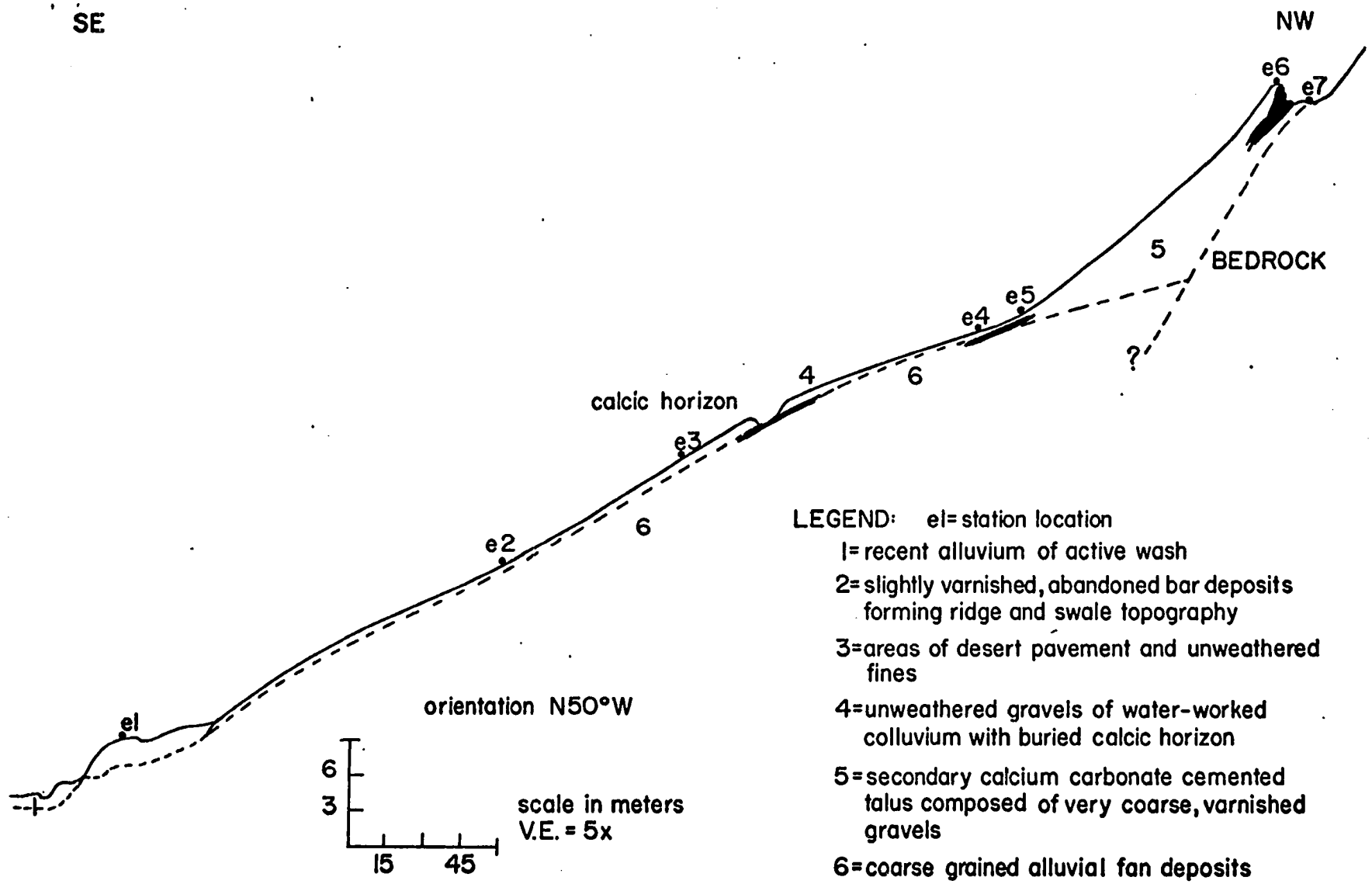

Figure 31. Detailed longitudinal profile (BHL-e) and description of surficial deposits on Big Horn Mountain alluvial apron.

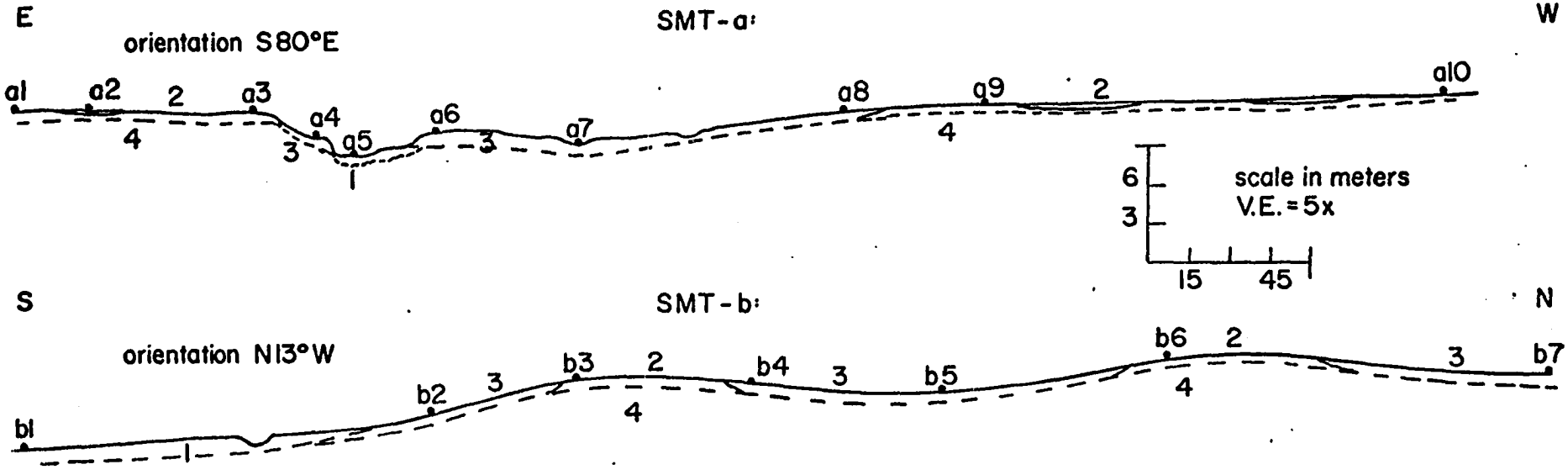

LEGEND for SMT-a: a1=station location

1= recent alluvium of active wash

2=caliche rubble with fine sand and silt; occasional varnished cobble; silts fill topographic lows; partially exhumed petrocalcic horizon approximately 1m thick

3=slightly weathered colluvium; barely cemented with secondary calcium carbonate

4=coarse grained alluvial fan deposits

LEGEND for SMT-b: b1=station location

1= fine sand and silt; slightly calcareous; unweathered; fine grained alluvial fan

2= desert pavement composed of varnished gravels and caliche rubble with buried calcic horizon

3=water worked colluvium of varnished gravels and caliche rubble

4=coarse grained alluvial fan deposits

Figure 32. Detailed topographic profiles (SMT-a and SMT-b) and descriptions of surficial deposits on Saddle Mountain alluvial apron.

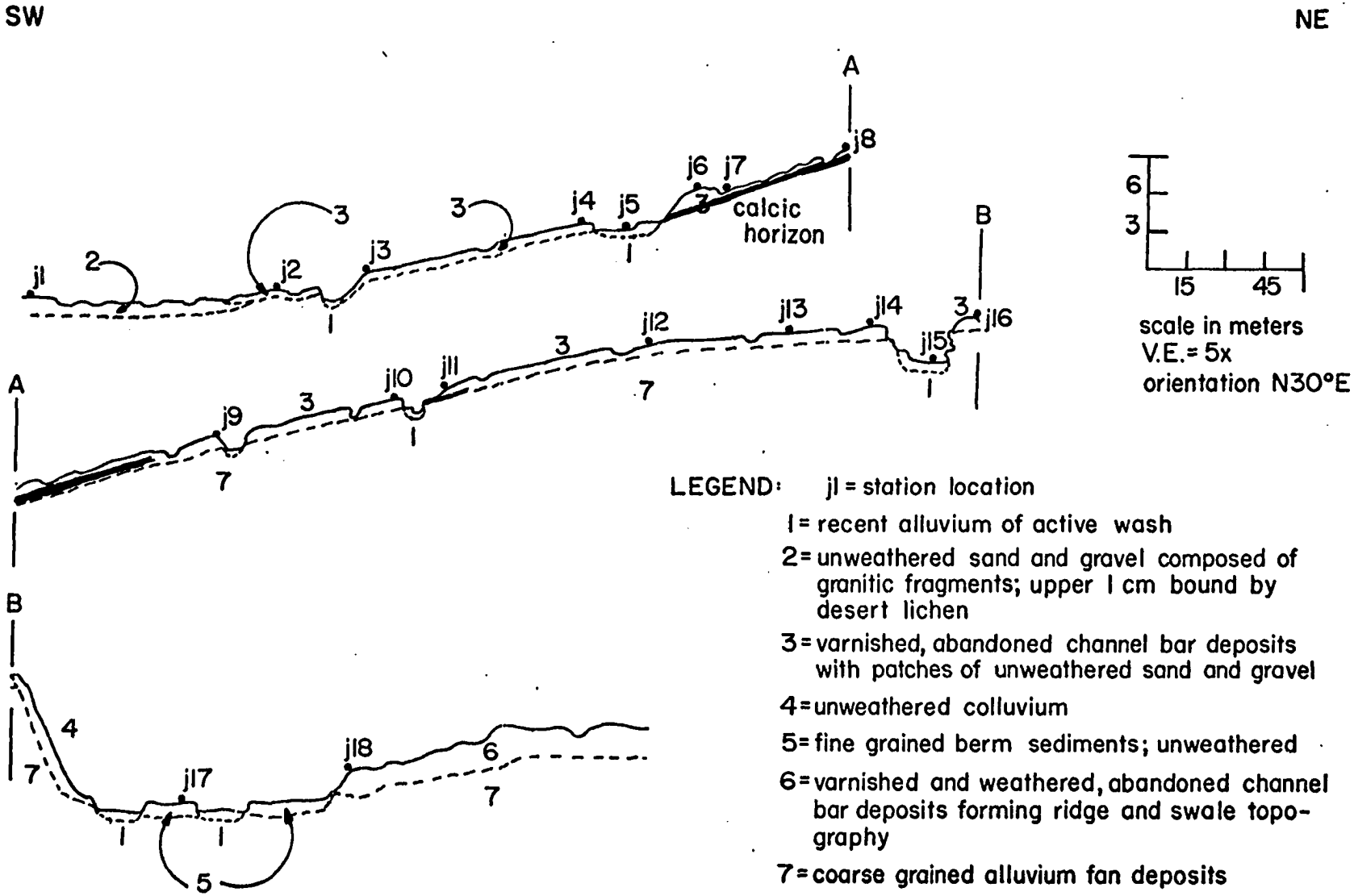

Figure 33. Detailed topographic profile (BHT-j) and description of surficial deposits on Big Horn Mountain alluvial apron.

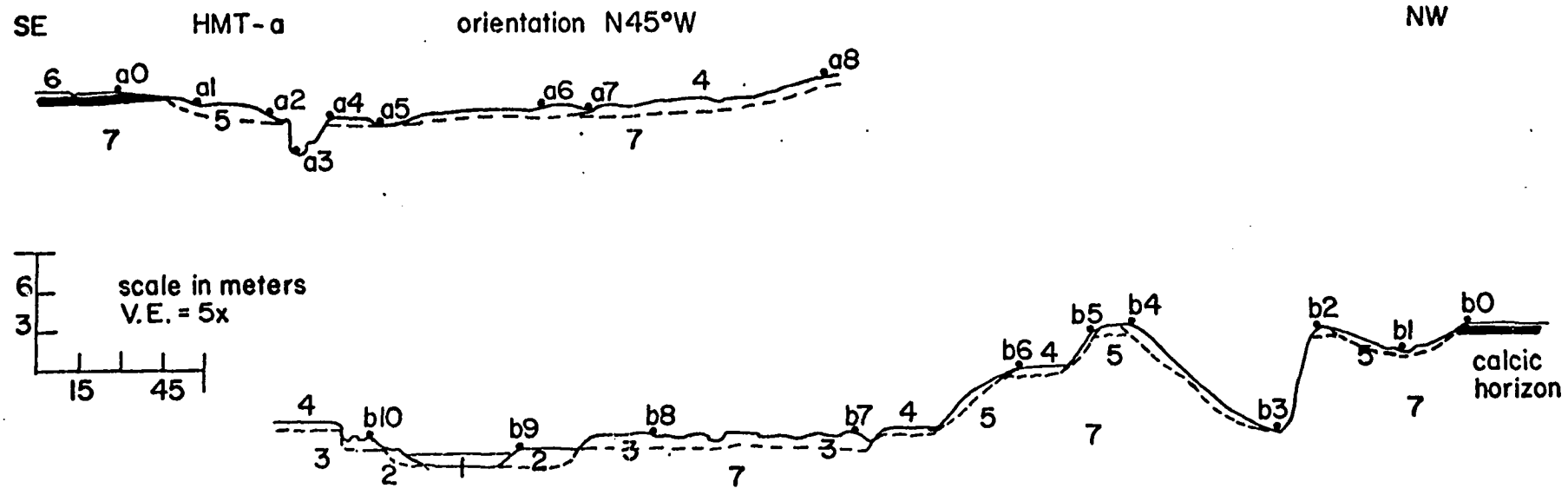

LEGEND: a1 and b1 = station

1 = recent alluvium of active wash

2 = fine grained sediments of berm

3 = varnished, abandoned channel bar deposits forming ridge and swale topography

4 = varnished gravels forming desert pavement covering thick silt layer

5 = weathered, water-worked colluvium

6 = varnished gravels and caliche rubble forming desert pavement and covering thick petrocalcic horizon

7 = coarse grained alluvial fan deposits

Figure 34. Detailed topographic profiles (HMT-a and HMT-b) and description of surficial deposits on Harquahala Mountains alluvial apron.

dunes shows an inverse relationship (Fig. 35). The fine grained alluvial fans have the most extensive and highest coppice dunes.

3. The proximal alluvial apron deposits, which include interfingering of water-worked colluvium and talus, are often characterized by a scarp facing toward the mountain front (Figures 30, 31). Between the scarp and the bedrock outcrop are drainage lines (Fig. 30). These deposits at the apron-bedrock contact are usually well indurated with calcium carbonate.

In areas not characterized by these scarps and on extrusive igneous rocks, the levees of debris flows (Qdf) are common. Debris flow levees are usually found below steep outcrops of bedrock. The levees are commonly devoid of any fine matrix, and it is concluded the eolian and water-related processes have removed the fines.

4. The interfluves developed on caliche rubble deposits (Qcr) are broad and flat, with little relief (Fig. 32). Shallow depressions containing silt occur between mounds of caliche rubble and have an average relief of 25 cm. A few centimeters of relief may occur between an exposed petrocalcic horizon and the surface on the interfluve.

The width of the interfluves in coarse grained alluvial fans is highly variable and is related to the drainage density. In areas of high dissection and low bank erosion, the cross-sectional profile of the interfluve is convex, not concave (Fig. 32). The convexity of these slopes is interpreted as being related to creep processes.

In fine grained alluvial fans, the interfluves and washes are difficult to distinquish due to the similarities in the particle sizes and low relief in these areas (Fig. 22).

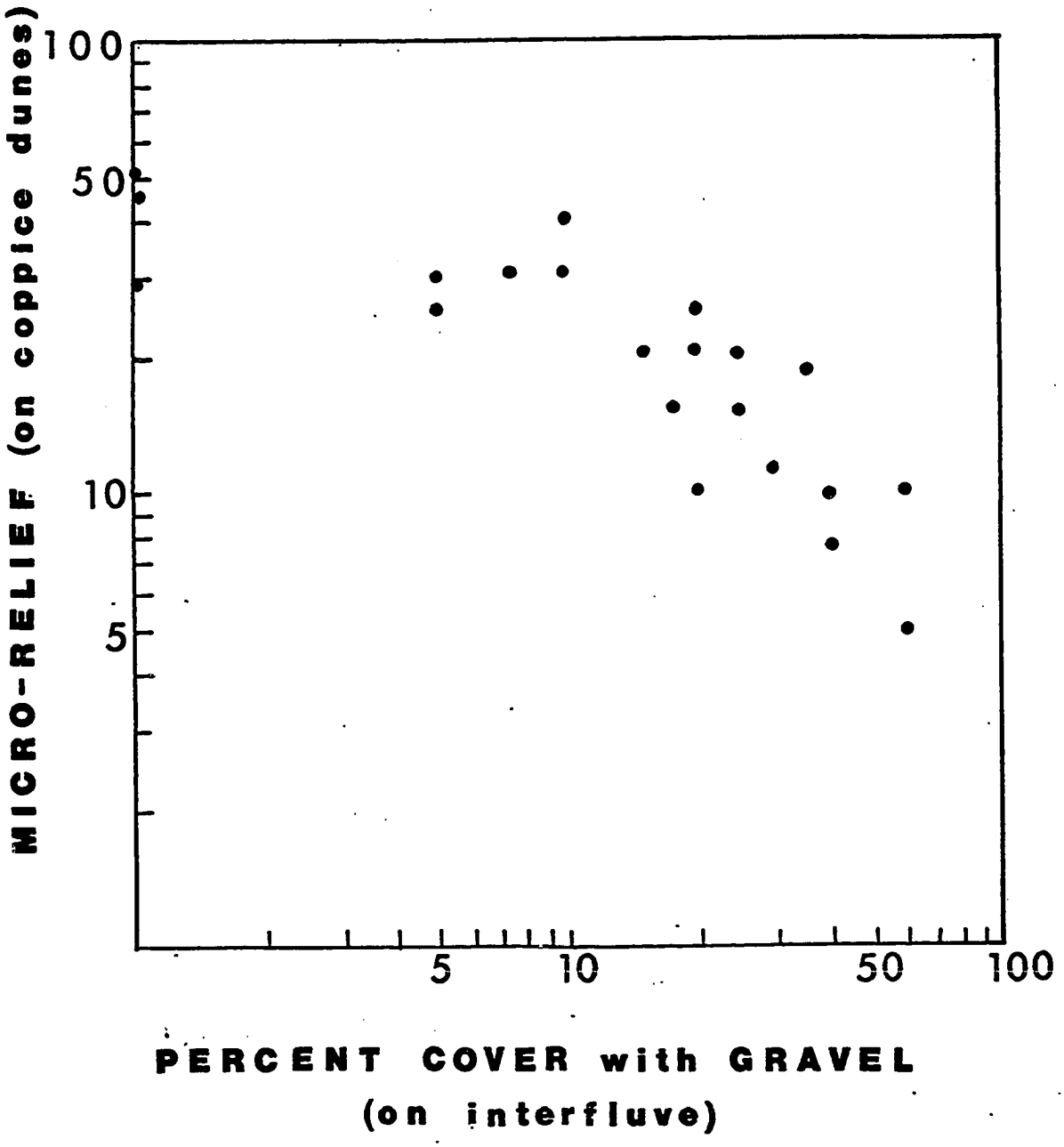

Figure 35. Logarithmic scatter plot showing relationship between micro-relief produced by coppice dunes and amount and concentration of gravels on surface of interfluves.

5. Slope angles on the interfluves of caliche rubble and coarse grained alluvial fans have the largest variation and mean slope values (Fig. 36). Interfluves of varnished gravels and fine grained alluvial fans have less variation and lower mean slope angles (Fig. 36).

6. The amount of local relief due to dissection decreases down the alluvial aprons, but the amount of micro-relief increases.

7. Coarse grained alluvial fans occur in isolated areas in the northern portion of the Harquahala Valley and are surrounded by fine grained alluvial fans (Fig. 25). Additionally, isolated segments of coarse valley fill can be seen in the Harquahala Mountains. In order to determine whether these isolated coarse gained deposits represent a single depositional unit, two longitudinal profiles are drawn from topographic maps which include isolated areas of coarse grained fans and coarse valley fill (Fig. 37). The longitudinal profiles of alluvial fans commonly have the form of curves which can be expressed as $Y = Ae^{BX}$, where Y equals elevation, X is distance, and A and B are constants for each profile (Lattman, 1973). The profiles connecting these deposits were drawn and fitted with the equation of this form (Fig. 37). Regression coefficients exceeded 0.960, indicating that isolated occurrences of coarse grained deposits in the mountain ranges and in the center of the basin are part of the same depositional unit.

Curves of exponential form were also fitted to the profiles of the modern drainage lines which parallel the longitudinal profiles. The results are given in Figure 37.

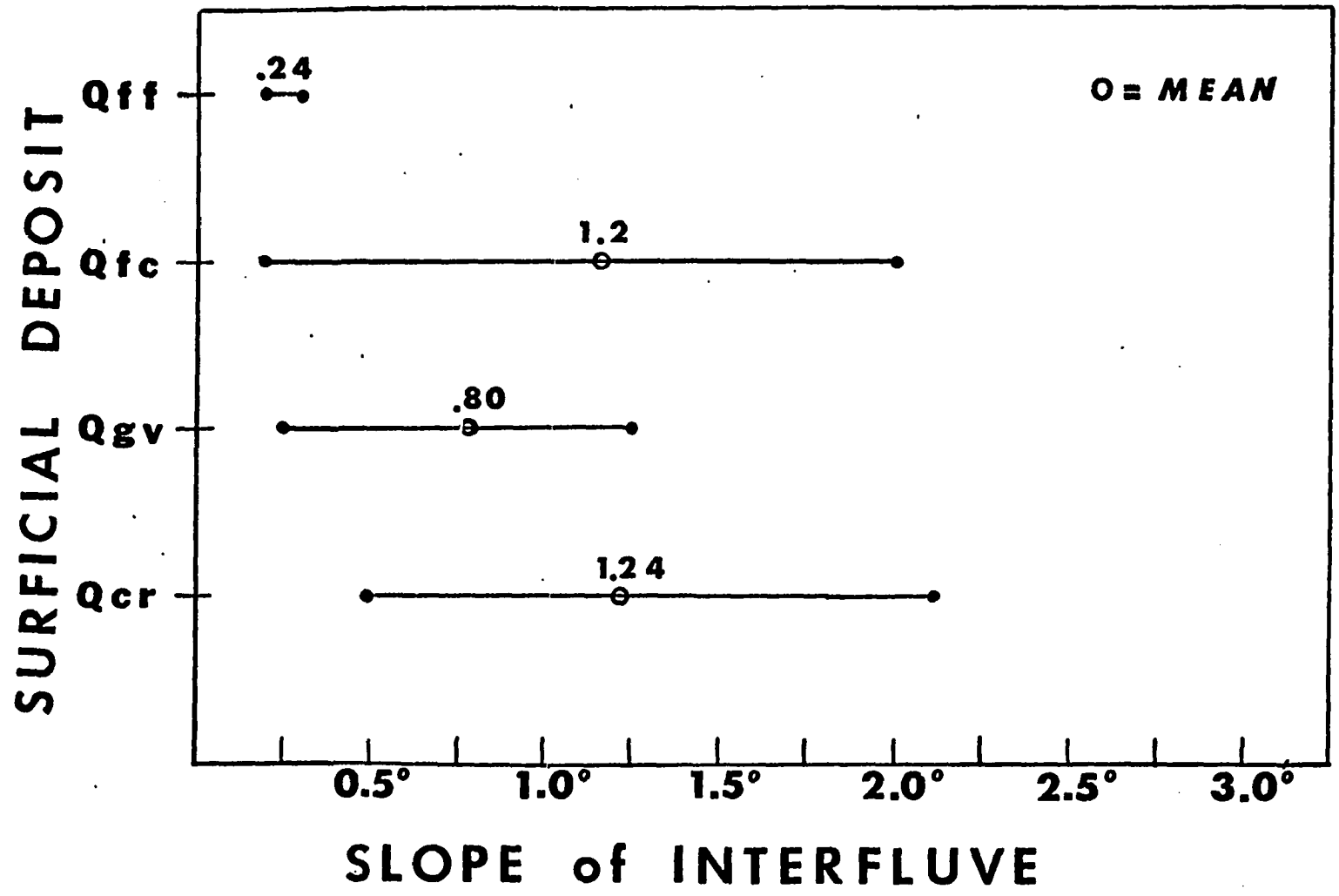

Figure 36. Bar graph showing range inslope angle on interfluves of different Quaternary deposits. Mean slope angle is denoted by $\overline{X}$.

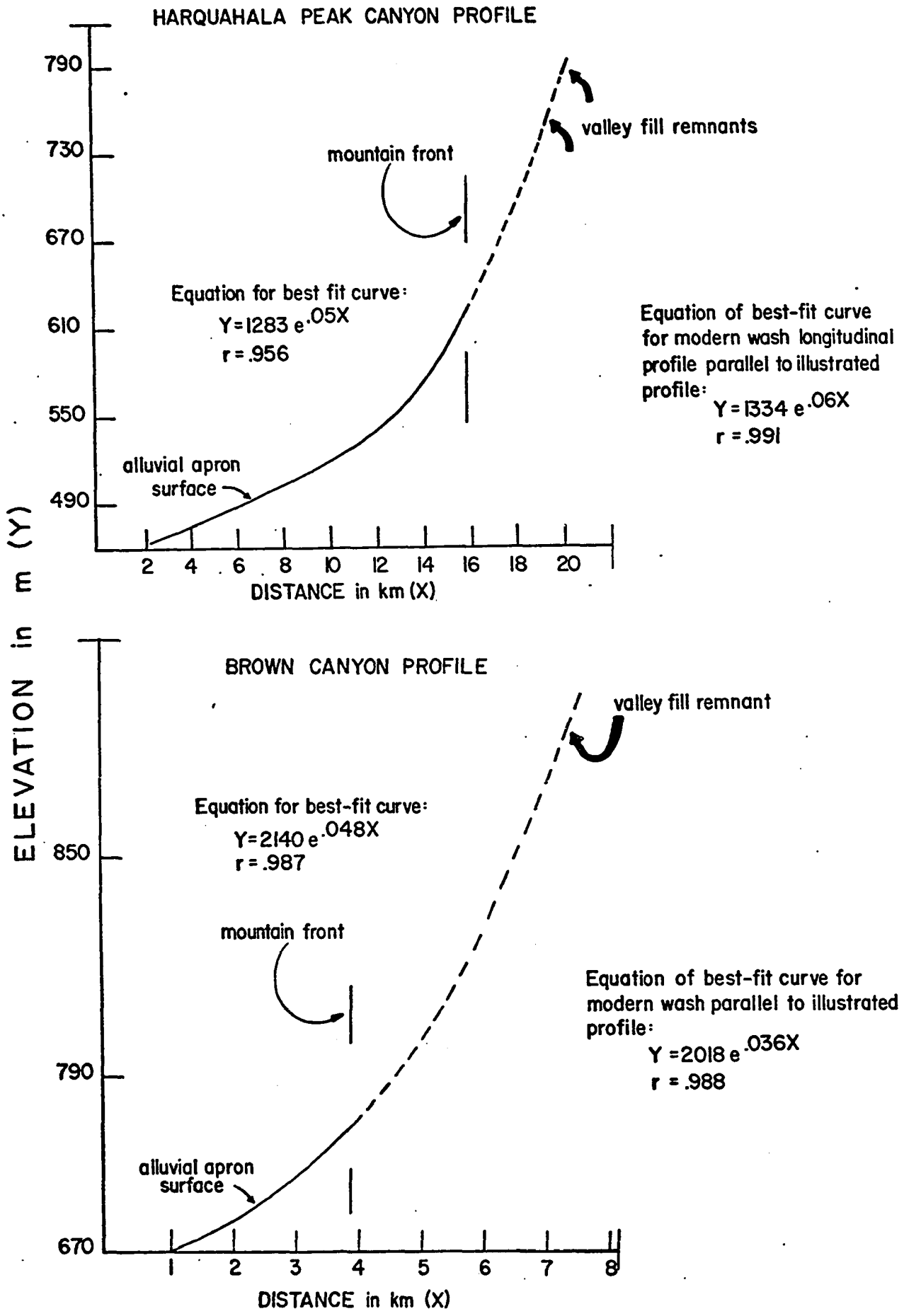

Figure 37. Curves fitted to longitudinal profiles of alluvial apron surfaces of Harquahala Mountains and valley fill remnants in canyons of Harquahala Mountains

SOILS OF THE HARQUAHALA VALLEY

Examination of soils developed on alluvial apron surfaces in arid basins is useful in understanding present and past pedogenic processes (Gile, 1974). A study of soils developed on the bolson plain of the Harquahala Valley was conducted to determine those processes which form the weathered mantle and to define any buried soil horizons which reflect previous weathering conditions.

Soils of the Harquahala Valley have been mapped by the Soil Conservation Service (Hartman, 1973; Chamberlin, in preparation). The areal distribution of these soils is given in Figure 38 and is a compilation of the soils maps for Yuma and Maricopa counties. There are two basic soil orders in the Harquahala Valley, the entisols and aridisols. These soils are divided into the following sub-groups: torrifluvents, haplargids, natrargids, calciorthids, and paleorthids. Five soil associations have been mapped by Hartman and Chamberlin in the study area. These soil associations reflect the topography and parent material on which they have developed. The calciorthids and paleorthids are common the proximal portion of coarse grained alluvial fans (Qfc). Torrifluvents are typical in the distal portion of the coarse grained fans and are associated with fine grained alluvial fans (Qff). Natrargids and haplargids are associated with eolian deposits (Qds), which have the saline deposits (Qsa).

In addition to the work of Hartman (1973) and Chamberlin (in preparation), soils were examined during the present study. Descriptions of the soil profiles at selected sights on the bolson plain deposits are given in Appendix IV. Qualitative estimates of the soils' physical

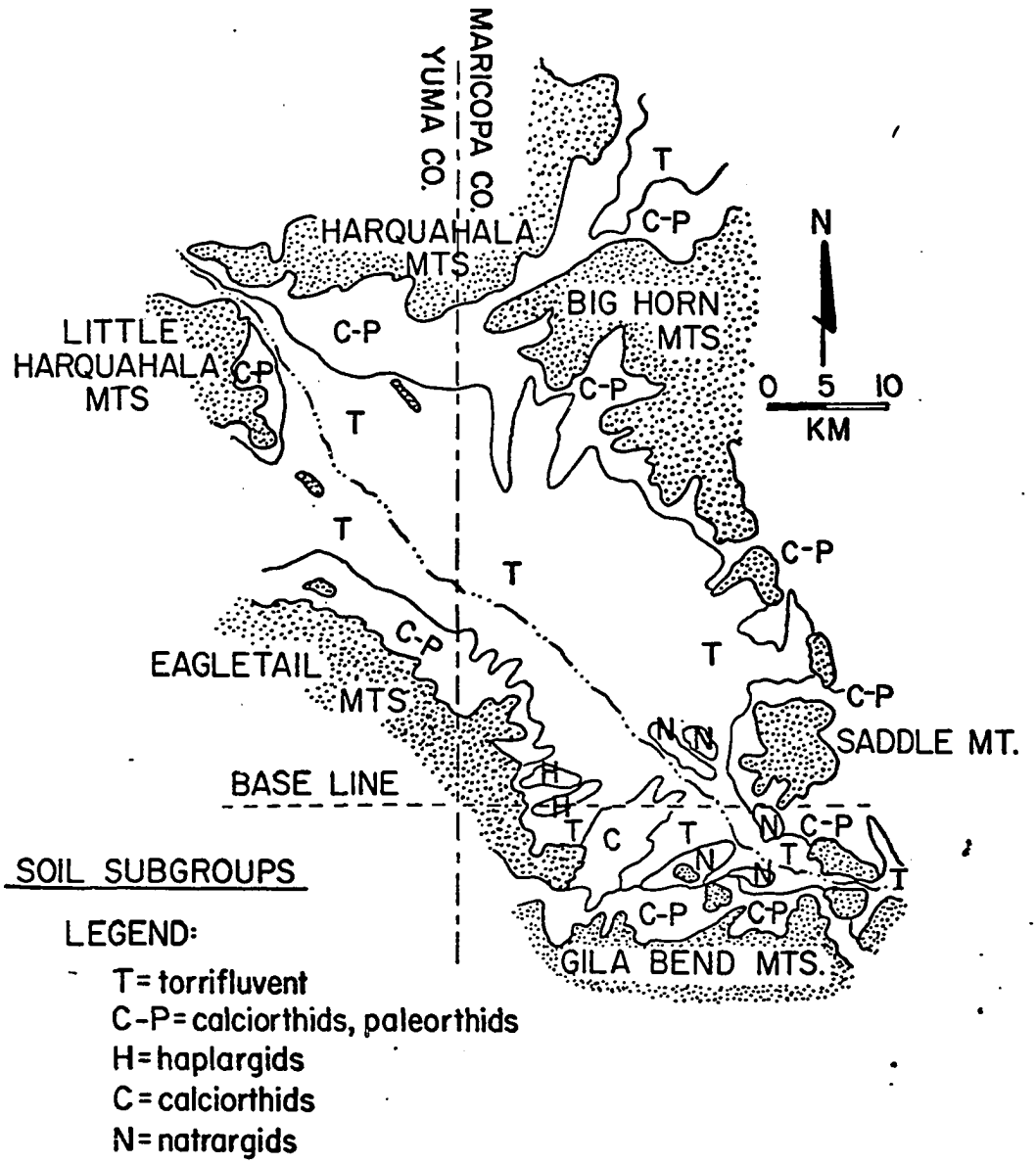

Figure 38. Generalized soils map of the Harquahala Valley bolson plain. Modified from Hartman (1973) and preliminary soils map of Yuma County, courtesy of Chamberlin.

properties were made in the field.

The following description of a soil profile is typical for coarse grained alluvial fans, which are the most abundant surficial deposit. The soil profile has a poorly developed (ochric) A horizon. The A horizon has more yellowish-red hues (5 to 10 YR) and lower chroma values (2). The B horizon increases in reddish hue (5 to 10 R), along with having an increase in the amount of clay and secondary calcium carbonate. The C horizon is the zone of maximum accumulation of calcium carbonate, Cca (Bertz and Horberg, 1949; Brown, 1956). In the Harquahala Valley, the Cca horizons range from poorly indurated to well indurated. Soil profiles in the mid and proximal portion of the alluvial apron typically have higher concentrations of calcium carbonate and are more indurated. Secondary calcium carbonate accumulations formed by pedogenic and non-pedogenic processes, which have been described by Lattman (1973), are found in the study area.

It is concluded that the upper portion of the alluvial aprons, which includes coarse grained fans (Qfc), varnished gravels (Qgv), and caliche rubble (Qcr), have had longer durations of weathering. The lower portions of the alluvial aprons, which include fine grained fans (Qff) and eolian dune deposits (Qds), have poorly developed soil horizons, which indicate shorter durations of weathering in these areas.

During the field work, a buried soil horizon (Bca ?) was commonly found in exposures of the mid and distal aprons (Fig. 39). This is a paleosol. The criteria for the recognition of a paleosol is given by Yaalon (1971) and is used in this study. The paleosol in the Harquahala Valley has the following characteristics: 1) darker red hues and higher chroma

Figure 39. Paleosol buried by fine grained alluvial fans (Qff) in the Harquahala Valley bolson plain. Scale is .5 meters.

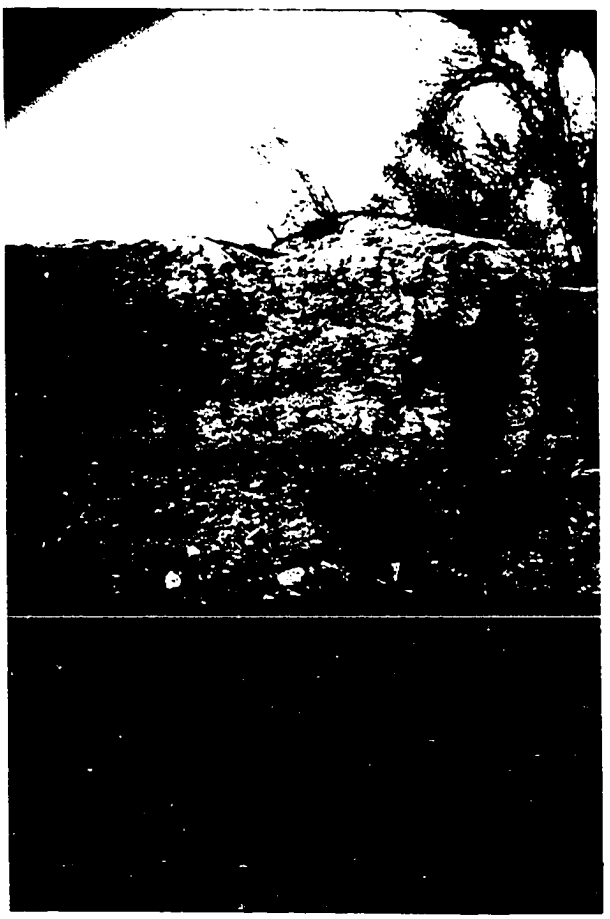

saturation (4 · 10R 4/6); 2) nodules and filaments of secondary calcium carbonate; 3) plastic and sticky textures with high clay content; and 4) blocky weathering appearance. These characteristics are interpreted as due to considerable weathering (Birkeland, 1974).

The paleosol described above can be traced laterally along certain reaches of the Big Horn Mountains alluvial apron in exposures of drainage diversion channels, abandoned irrigation ditches, and deeply incised channels (Fig. 39). The paleosol can be identified throughout the basin and is therefore useful as a time plane. The importance of the paleosol as a time plane will be discussed below.

STRATIGRAPHIC RELATIONSHIP OF BASIN FILL UNITS IN THE HARQUAHALA VALLEY

Subsurface Units

The stratigraphic relationships of the sedimentary and volcanic rocks within the fill of the Harquahala Valley have been briefly discussed by Metzger (1957) and Denis (1971). Subsurface records from water wells provide the only means by which general stratigraphic units may be delineated. These records show that the sub-surface lithologies possess complex lateral variations and discontinuities. It is the purpose of this section to use selected water well data and other published data to establish a generalized stratigraphic column of the major subsurface units in the Harquahala Valley.

The majority of water wells have been drilled in the cultivated regions in the southern bolson plain. Data obtained from these wells concerning the subsurface stratigraphy can be compared with detailed

stratigraphic sections of the basin fill near the southern portion of the study area. During preliminary site evaluations for a nuclear power plant, FUGRO (1974) drilled several wells and described the subsurface stratigraphy approximately 13 km eastward from Saddle Mountain. The stratigraphic column constructed by FUGRO provides reliable dates of the basin fill units, as dating was accomplished by potassium-argon dates on volcanic rocks and estimated from paleomagnetic studies on clays and silts. The general stratigraphic units and their age are given in Figure 40.

Records of selected water wells along the base line across the southern Harquahala Valley are given in Appendix IV, and Figure 41 is a schematic diagram of the major subsurface units based on this profile and FUGRO's section. The following stratigraphic sequence is derived from the water well data in the southern Harquahala Valley and FUGRO's dates on similar units.

The oldest units encountered are granite and volcanic rocks which form the basement rocks of the basin. No spatial relationship can be established between the granite and volcanic rocks in the subsurface section of the Harquahala Valley; however, observations of the relationship between volcanic rocks and granites in the mountain ranges of the study area indicate that the volcanic rocks either penetrate or overlie the granitic rocks. A similar relationship is shown in the section constructed by FUGRO (1974), in which granites are tentatively assigned a Pre-cambrian age and the volcanic sequence is early to mid Miocene. Overlying the volcanics is a well indurated conglomerate, which correlates with FUGRO's indurated fanglomerate of mid Miocene age, which rests on the volcanic sequence. These units may correlate with isolated outcrops of conglomerate

AGE	MAXIMUM THICKNESS (m)	DESCRIPTION
Holocene-Pleistocene	5	gravel in a silt matrix; poorly sorted and moderately stratified
Mid-Pliocene (3.2 m.y.)	60	slightly porphyritic olivine basalt flow
Mid to late Pliocene	15	brown, poorly consolidated silty, sand and gravel
Late Pliocene to Mid Miocene	120	brown, red-brown, silt and clayey silt with interbedded sand; silty and clayey poorly sorted sand and gravel
Mid Miocene	100	moderately to very well cemented fanglomerate composed of volcanic clasts from underlying bedrock
Early to Mid Miocene	600	volcanic bedrock sequence basalt, tuff, plugs, dikes, andesite, welded tuff
Precambrian		granite, granitic gneisses, metamorphic rocks

Figure 40. Generalized stratigraphic column of basin fill near Arlington, Arizona. Modified from FUGRO (1974).

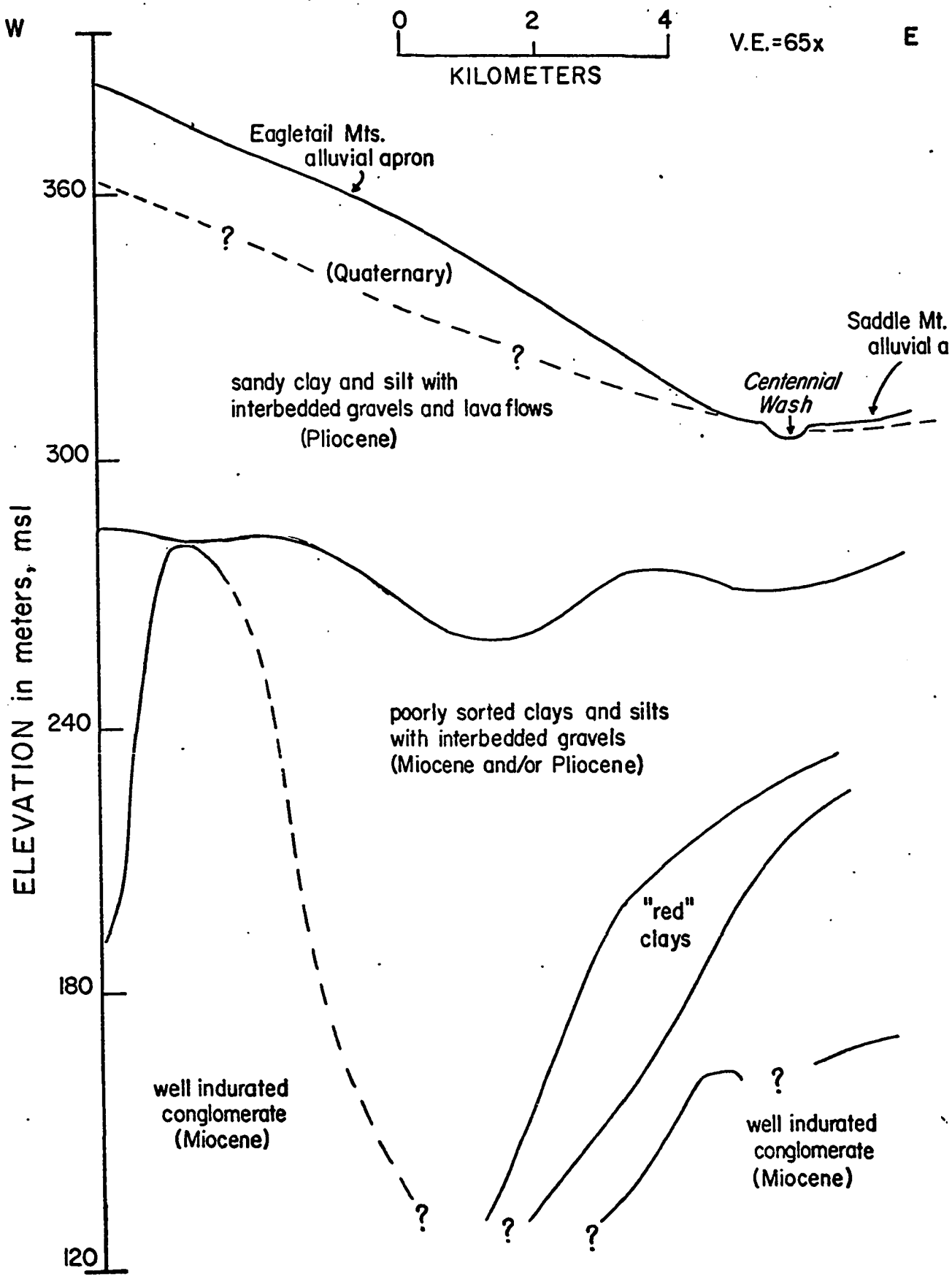

Figure.41. Subsurface units and their stratigraphic relationships in the Harquahala Valley.

in the mountain ranges of the Harquahala Valley basin (see Bedrock Geology section).

The next younger major unit consists of gravelly clays with interbedded "red" clays and is correlated with the red-brown clays and silts in the FUGRO section (Fig. 40). These sediments are tentatively assigned to the late Miocene to mid Pliocene. Resting on the gravelly clays in the Harquahala Valley is a unit consisting of sands and silts with interbedded "malpais", or lava beds. This unit corresponds to the "upper" sand and gravel unit of FUGRO's section and contains a 3.2 million year old basalt flow. The sediments above this unit are, therefore, late Pliocene and younger. These younger units are treated as surficial deposits, as they are exposed at the surface.

Surficial Deposits

The surficial deposits are tentatively assigned an age ranging from late Pliocene to Holocene. No detailed dating of these deposits has been conducted in the Harquahala Valley, and only relative ages can be established by stratigraphic relationships.

The following stratigraphic relationships are based on detailed field studies during geomorphic mapping of the bolson plain (Appendix IV). The general stratigraphic relationships of the late Tertiary and Quaternary surficial deposits are given in Figure 42, and a detailed example of a stratigraphic section along Centennial Wash is given in Figure 43.

The oldest surficial deposits are the saline, silt and clay (TQ_{sa}), which have limited exposures in the southern Harquahala Valley (Fig. 25). Overlying these deposits are the coarse grained alluvial fans (Qfc) (Fig. 43),

	AGE	SURFICIAL DEPOSIT
QUATERNARY	HOLOCENE ?	Alluvium (Qal)
		Fine grained alluvial fans (Qff)
		Eolian dune deposits (Qds)
		Debris flows deposits (Qdf)
	----------?	----------? ----------? ----------
	PLEISTOCENE	Varnished gravels (Qgv)
		Caliche rubble (Qcr)
		Corase grained alluvial fans (Qfc)
	Pliocene ?	Saline deposits - saline and gypsiferous clayey silts

Figure 42. Generalized stratigraphic column of surficial deposits of the Harquahala Valley.

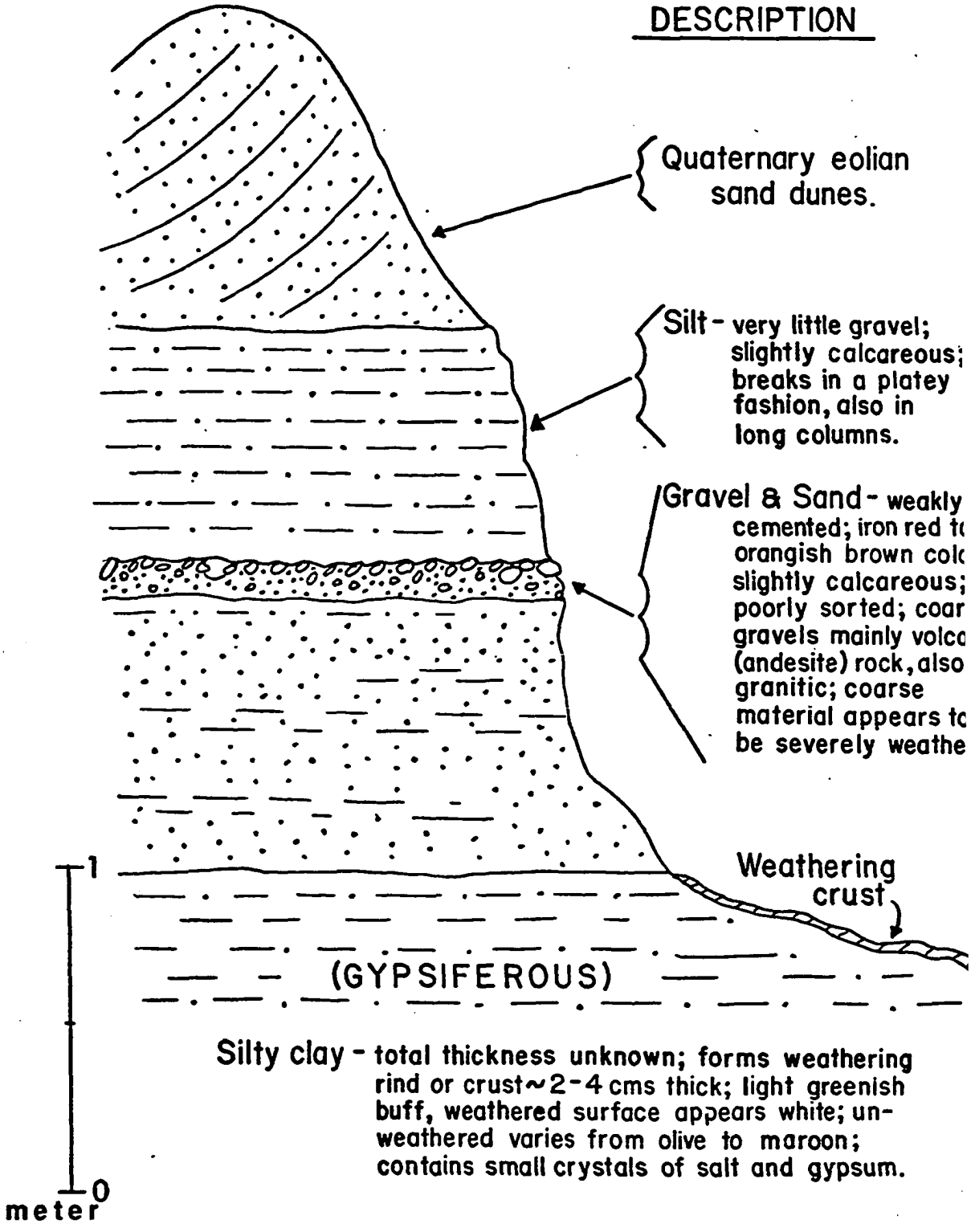

Figure 43. Detailed stratigraphic section along the banks of Centennial Wash south of Saddle Mountain.

which are, therefore, younger. The next youngest deposits are caliche rubble (Qcr), which are developed on the coarse grained fans. Varnished gravels (Qgv) occur on the caliche rubble deposits but are not incorporated in the petrocalcic horizon. Therefore, varnished gravels are younger than the petrocalcic horizon from which the caliche rubble is derived. Eolian dunes are younger than the varnished gravels in that these deposits are stratigraphically higher than the varnished gravels (Figure 43).

The paleosol is also stratigraphically lower than the eolian dune deposits and may be contemporaneous with the varnished gravels (Figure 44). Therefore, the varnished gravels and paleosol are older than the eolian dune deposits. The caliche rubble surfaces are buried below the varnished gravels in the distal regions of Saddle Mountain. The development of the petrocalcic horizon, which is weathered to rubble, occurred after the deposition of coarse grained alluvial fans and prior to the development of varnished gravels and eolian dune deposits.

The next younger deposits of the Harquahala Valley are the fine grained alluvial fans (Qff) (Fig. 42). These fine grained fans, which occur in the mid and distal protions of the aprons, are stratigraphically higher than the coarse grained fans. In addition, these fine grained fans overlie and cut into the eolian dune deposits. Other deposits, which overlie and are therefore younger than the coarse grained fans, are debris flows (Qdf). These flows occur in the proximal portion of the aprons (Fig. 45) and can be seen disturbing the varnished gravels. It is not known whether the debris flows formed before, after, or at the same time as the fine grained alluvial fans. Several debris flows show signs of induration by secondary calcium carbonate, which suggests a long duration

Figure 44. Paleosol buried by eolian dune deposits in southern Harquahala Valley.

A. Varnished gravels forming levees on flow.

B. Debris flows disturbing varnished gravels on hillslopes.

Figure 45. Quaternary debris flows (Qdf) on proximal portions of alluvial aprons (A) and on hillslopes (B). These usually form on detritus derived from extrusive igneous rocks.

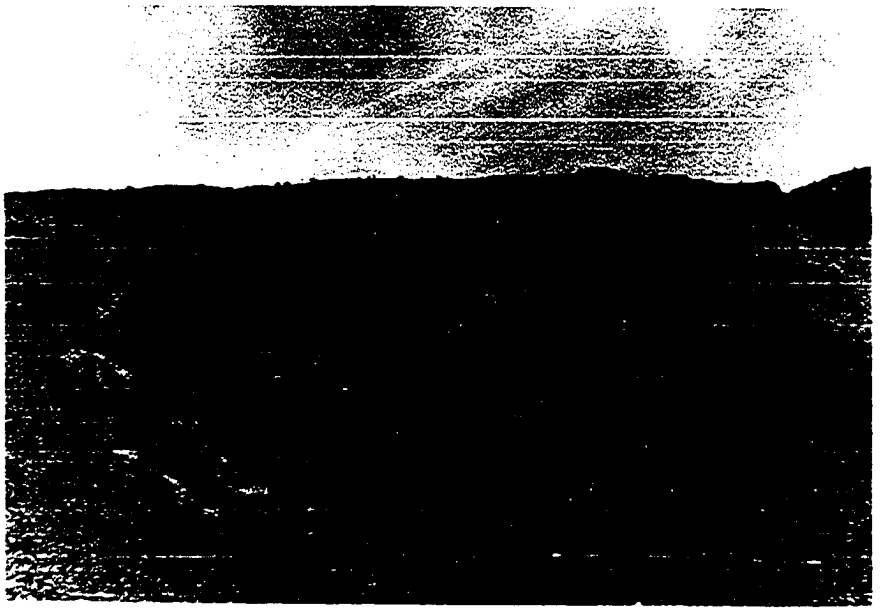

of weathering; whereas, the fine grained fans do not show this accumulation. Thus, the debris flows may be older than the fine grained fans. Alluvium along the drainage lines cuts through all the deposits above and is the youngest unit (Fig. 25).

ANALYSIS OF LANDSAT IMAGERY AND THE SURFICIAL DEPOSITS OF THE STUDY AREA

Recent desert studies of the southwestern United States have found aerial imagery to be a useful tool for identifying calichified fan surfaces in arid and semi-arid basins (Lattman, 1971; Lenhart, 1974). Two types of aerial imagery from LANDSAT (formerly ERTS) satellites have been analyzed in the present study to determine whether the surficial deposits of the bolson plain can be distinguished. These two types of imagery are: 1) black and white MSS Band 7 and 2) color infrared composites of Bands 4, 5, and 7.

Lenhart (1974) used two techniques, the ratio and contrast methods, to quantitatively evaluate the differences in the density of calichified and non-calichified fans. He found the contrast method to be the optimum technique to separate these fan surfaces, and his results are used in the present study.

MSS Band 7

The mechanics of imagery analysis are described in detail in the Techniques of Investigation. The density measurements for each major Quaternary surficial deposit are given in Appendix I. The results of these measurements are summarized in Figure 46. Three surficial deposits (fine grained fans, caliche rubble, and varnished gravels) appear to be drawn

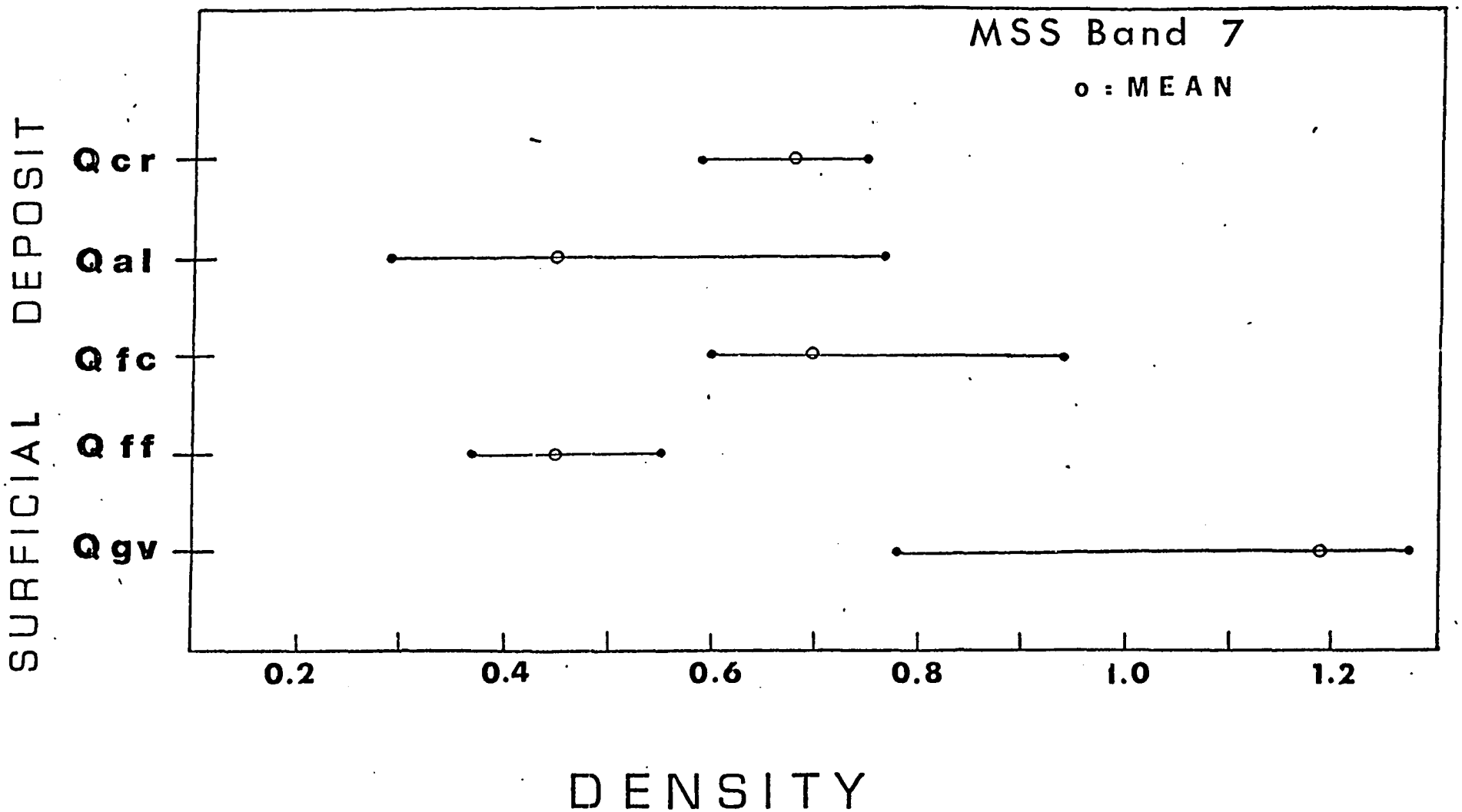

Figure 46. Bar graph illustrating range in densities and mean density for surficial deposits shown on LANDSAT imagery in the Harquahala Valley.

from different image density populations since their density ranges do not overlap (Fig. 46). Alluvium and varnished gravels display the greatest amount of variation in density, while fine grained fans and caliche rubble show the least amount.

The Mann-Whitney U (Siegel, 1956) is used to test the statistical significance of differences in density comparisons for the surficial deposits (Appendix I). The results of these statistical tests for each comparison are outlined below:

1. The null hypothesis is rejected for all three tests comparing densities of coarse and fine grained alluvial fans at $\alpha = 0.05$. The fine grained fans are less dense and reflect more light than the coarse grained fans. Thus, these two sediment types can be readily distinguished on MSS Band 7.

2. Varnished gravels are different from coarse grained fans. The null hypothesis is rejected for all three tests at $\alpha = 0.05$ (Appendix I), and the two deposits can be differentiated by density differences.

3. Calichified fans are not different from coarse grained fans, and the null hypothesis is accepted at $\alpha = 0.05$. Lenhart (1974) was able to separate these deposits on fan surfaces in Nevada.

4. Null hypothesis that image densities of alluvium (covered by low amounts of vegetation) and fine grained fans are the same is accepted for the three tests at $\alpha = 0.05$. The image density of alluvium is not significantly different than fine grained fans.

In summary, the two most extensive surficial deposits of the Harquahala Valley, fine and coarse grained alluvial fans can be differen-

tiated on MSS Band 7 imagery due to differences in image densities.

Color Composite Imagery

The density measurements given in Table 4 are based on color composites of MSS Bands 4, 5, and 7. As before, these densities are tested for a statistically significant difference by the Mann-Whitney U (Appendix I). A summary of the results is given below.

1. Fine and coarse grained fans have statistically different image densities at $\alpha = 0.05$; therefore, the null hypothesis is rejected (Appendix I).

2. The null hypothesis that varnished gravels and coarse grained fan deposits have indistinguishable densities on the color composite is rejected at $\alpha = 0.05$. The two types of Quaternary deposits can be distinguished on color composites.

3. The null hypothesis is accepted at $\alpha = 0.05$ for the comparison of caliche rubble surfaces and coarse grained alluvial fan surfaces, as well as fine grained alluvial fans and alluvium. The densities from color composites of Bands 4, 5, and 7 are not useful for discriminating among these units.

Summary

Satellite imagery analysis is useful for distinguishing the following sediment types of the Harquahala Valley: fine and coarse grained alluvial fans, and varnished gravels and coarse grained alluvial fans. Calichified fans and coarse grained alluvial fans cannot be distinguished, nor can alluvial and fine grained alluvial fans be separated. Density analysis

QUATERNARY SURFICIAL DEPOSIT	DENSITY MEASUREMENTS							
Varnished gravels (Qgv)	0.67	0.69	0.71	0.65	0.64	0.68	0.64	0.61
Fine grained fans (Qff)	0.43	0.39	0.40	0.34	0.37	0.38	0.38	0.31
Coarse grained fans (Qfc)	0.49	0.42	0.44	0.37	0.35	0.47	0.56	0.45
Alluvium (Qal)	0.19	0.27	0.30	0.43	0.30	0.48	0.30	0.28
Caliche rubble (Qcr)	0.45	0.50	0.34	0.33	0.35	0.33	0.37	0.63

Table 4. Density measurements from color composite transparencies of MSS Bands 4, 5, and 7 of LANDSAT imagery of the Harquahala Valley. LANDSAT imagery was taken on February 2, 1973.

by the contrast method gives similar results for MSS Band 7 and color composites of Bands 4, 5, and 7. Either type of LANDSAT imagery may be useful in studying some types of Quaternary deposits in arid regions.

GEOMORPHOLOGY OF LOW ORDER DRAINAGE BASINS IN THE HARQUAHALA VALLEY

Geomorphic, sedimentologic, and hydrologic paramenters of twelve low order drainage basins are investigated to elucidate those surficial processes which operate locally in the study area. Figure 47 is a map showing the location of these low order basins. Geomorphic parameters, which include drainage area, relief ratio, drainage density, and drainage frequency, are given for each low order drainage basin in Appendix VI. Hydrologic and sedimentologic parameters, which include maximum width of wash, maximum depth of flow, maximum discharge and velocity, and particle size distribution of wash sediments, are measured along selected stations on trunk washes in the low order drainage basins. These parameters are listed according to their associated low order basin in Appendix VI.

Geomorphic Parameters of Low Order Drainage Basins

Shape and Size:

The largest low order basins have drainage areas larger than 285 km^2, and the smallest low order basin has a drainage area of approximately 1 km^2. The average drainage area of all low order basins is 56 km^2. Figures 48, 50 through 59 illustrate the shape and size of the twelve low order basins. The majority of these basins are elongated and oriented approximately orthogonally to the axial drainage. These low order basins range in length, as measured parallel to the principal wash, from 2 to 35

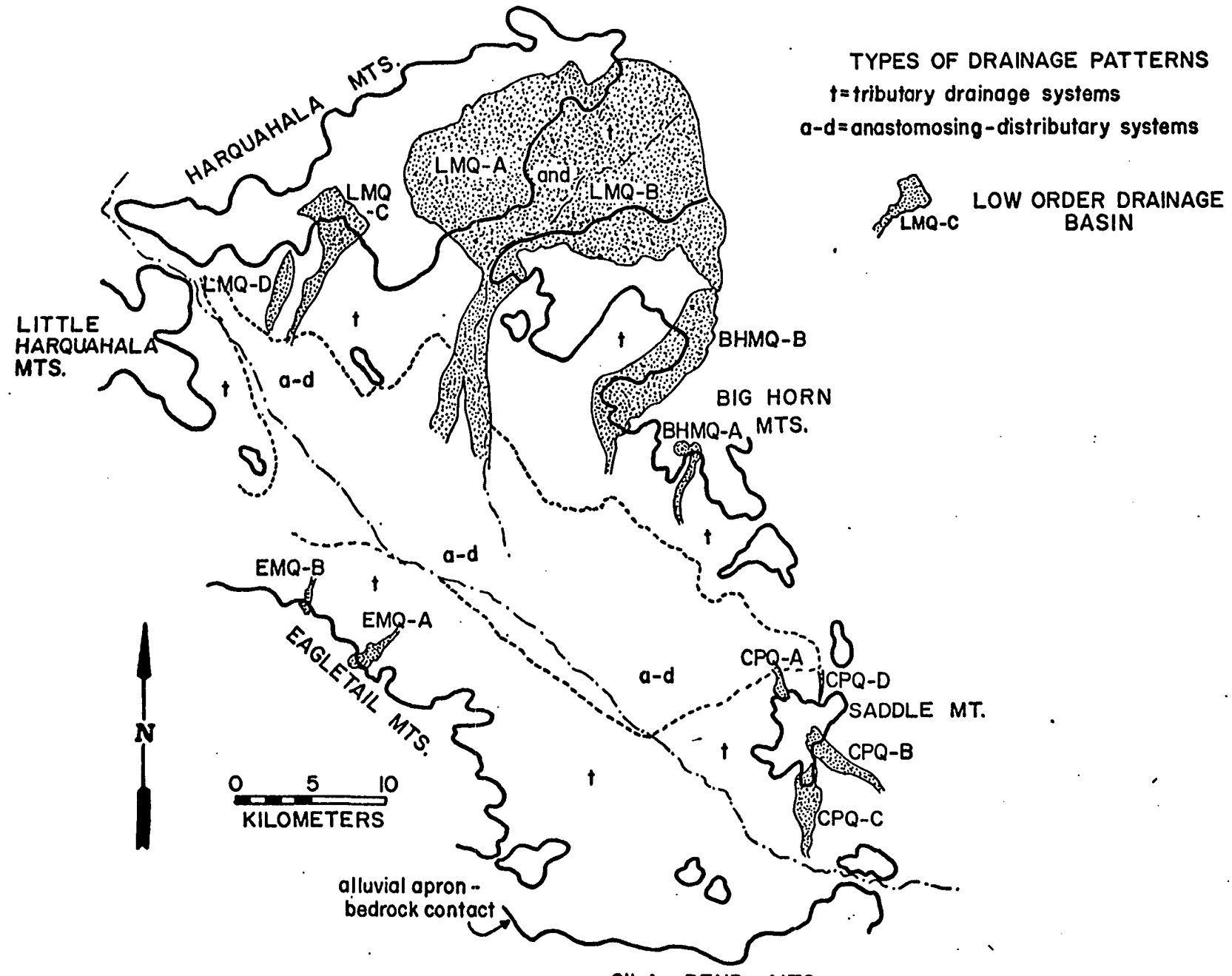

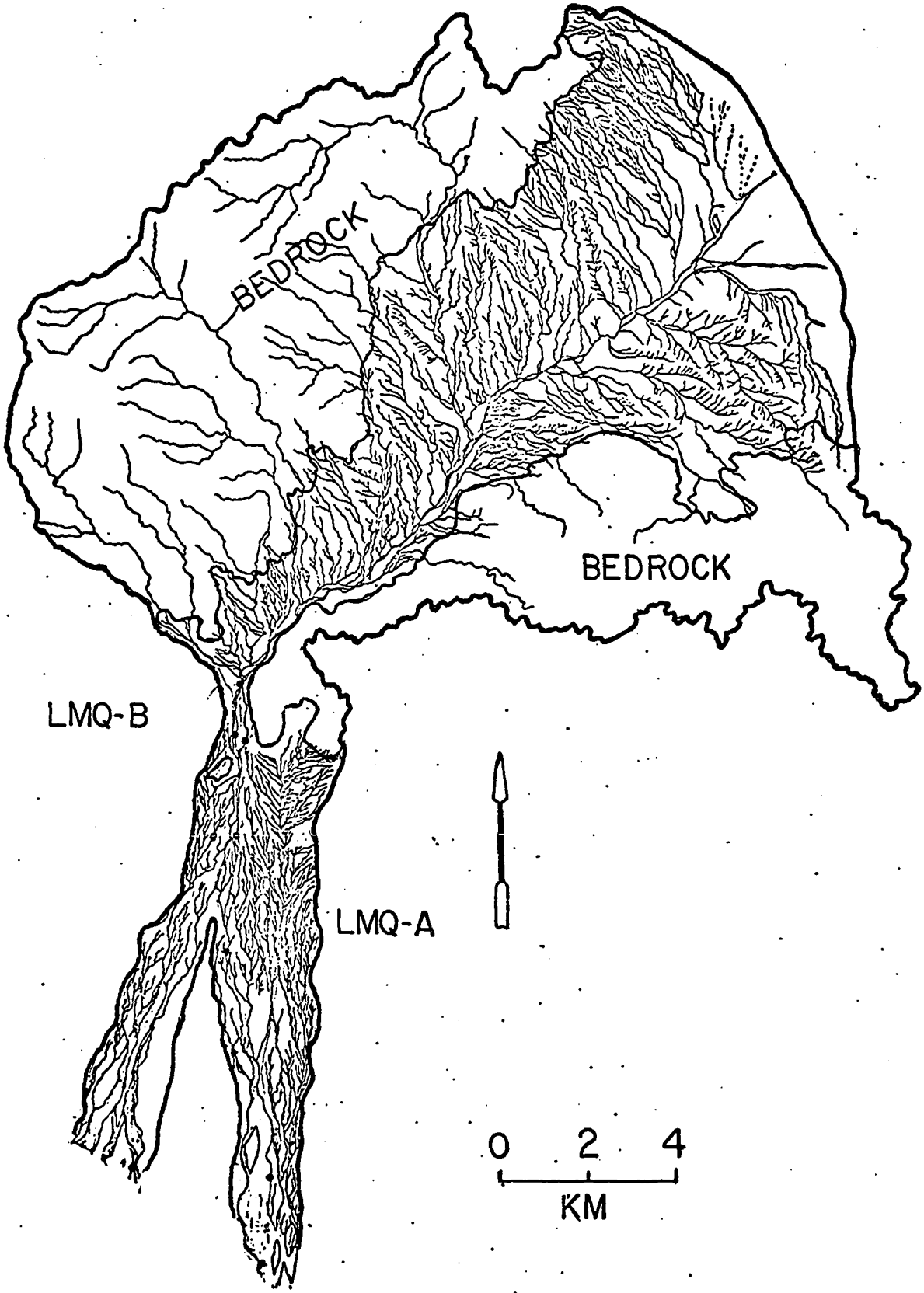

Figure 48. Map of the low order drainage basin LMQ-A and LMQ-B illustrating station locations (black dots) and drainage systems on the alluvial apron. These basins represent the Tiger Wash watershed.

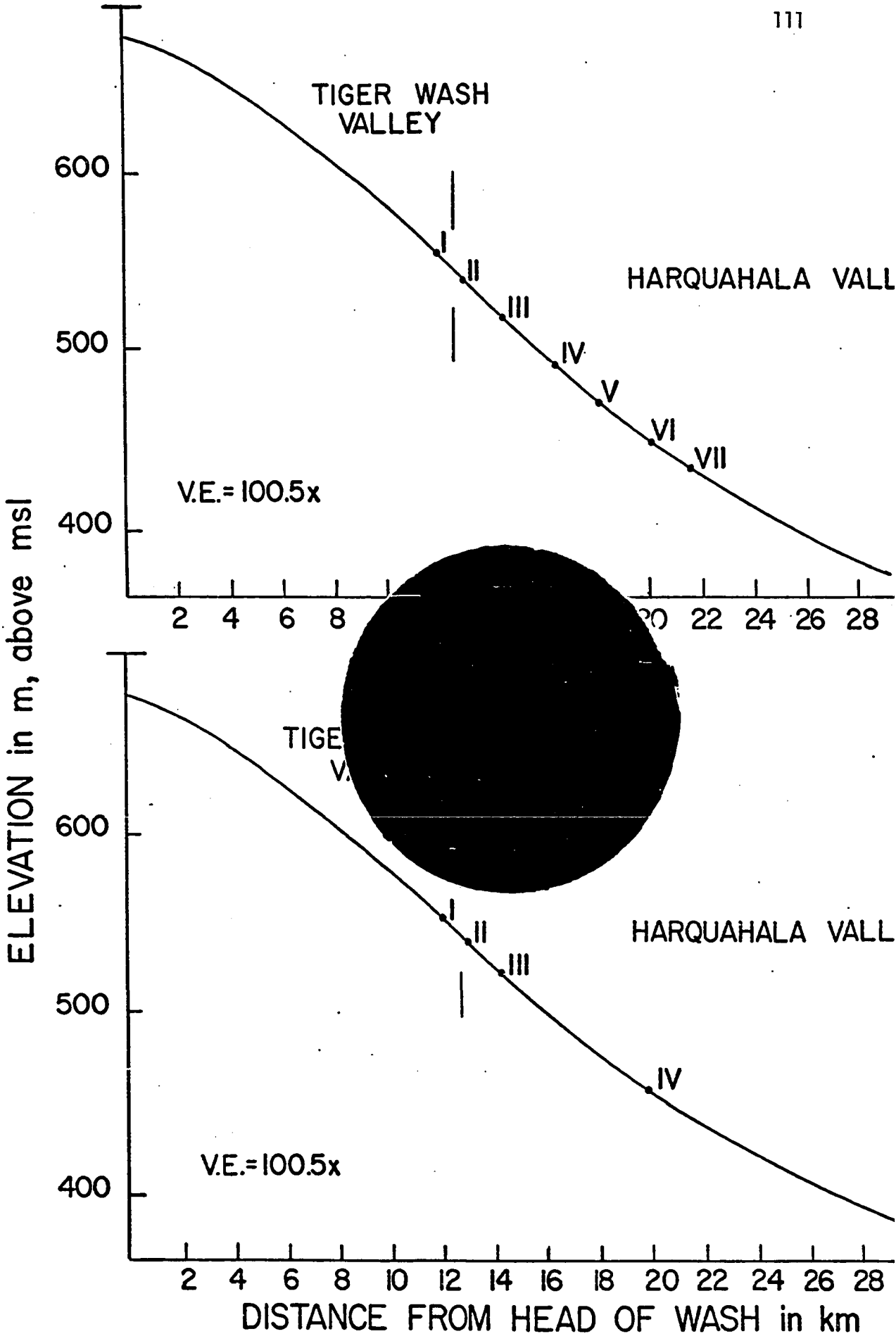

Figure 49. Longitudinal profiles of principal washes and station locations for low order drainage basins LMQ-A and LMQ-B.

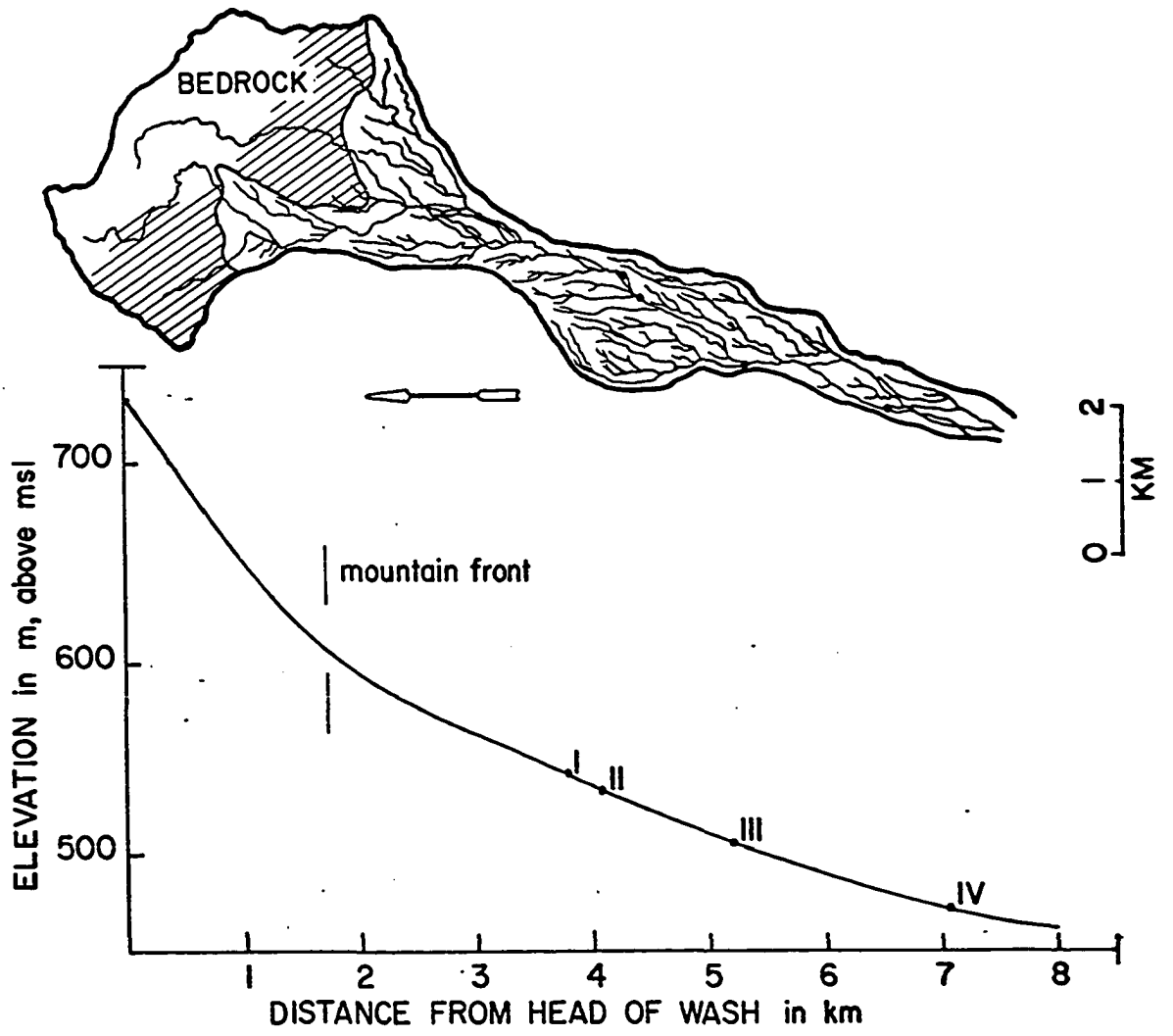

Figure 50. Map of low order drainage basin LMQ-C and longitudinal profile for principal wash draining basins. Station locations are given as black dots.

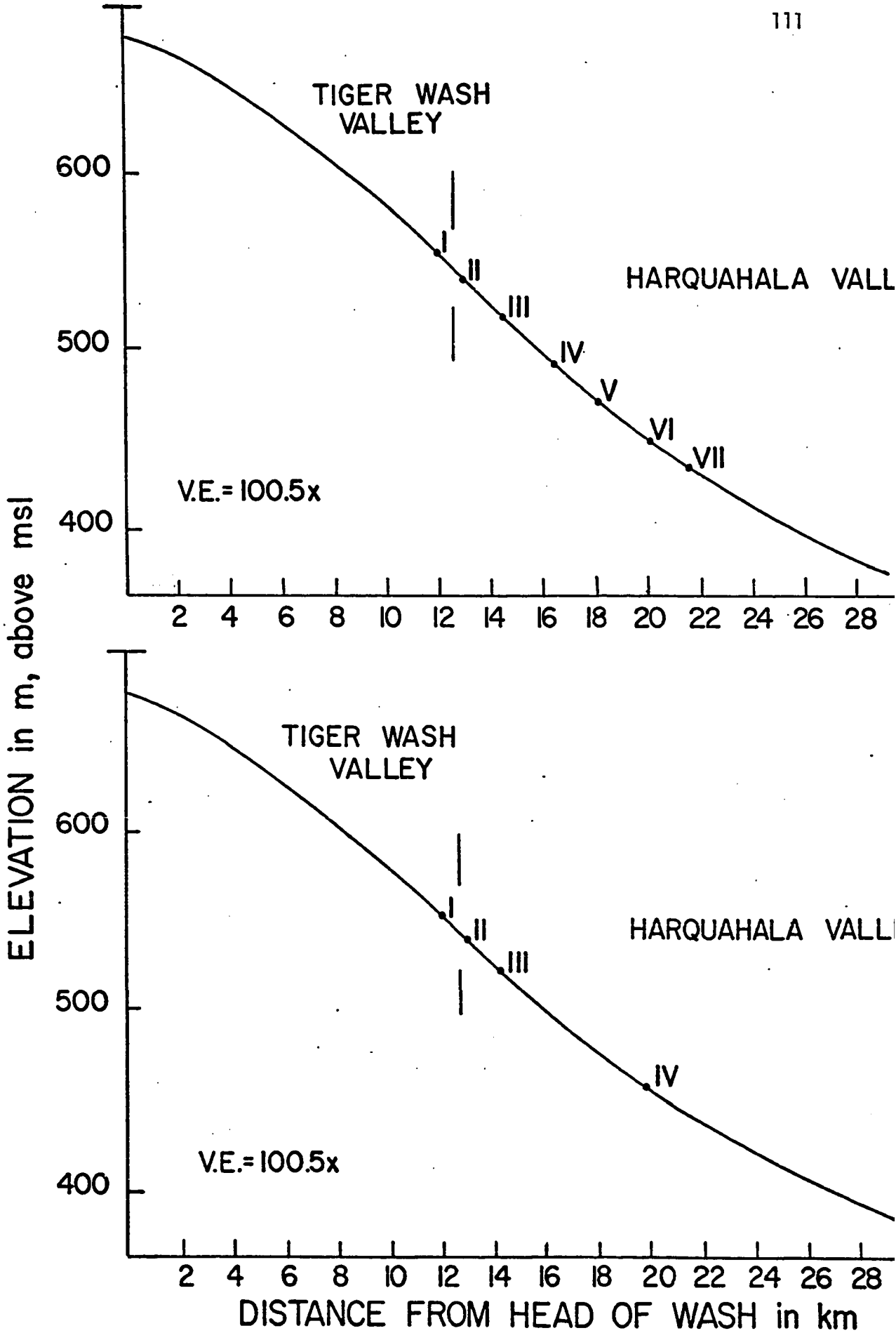

Figure 49. Longitudinal profiles of principal washes and station locations for low order drainage basins LMQ-A and LMQ-B.

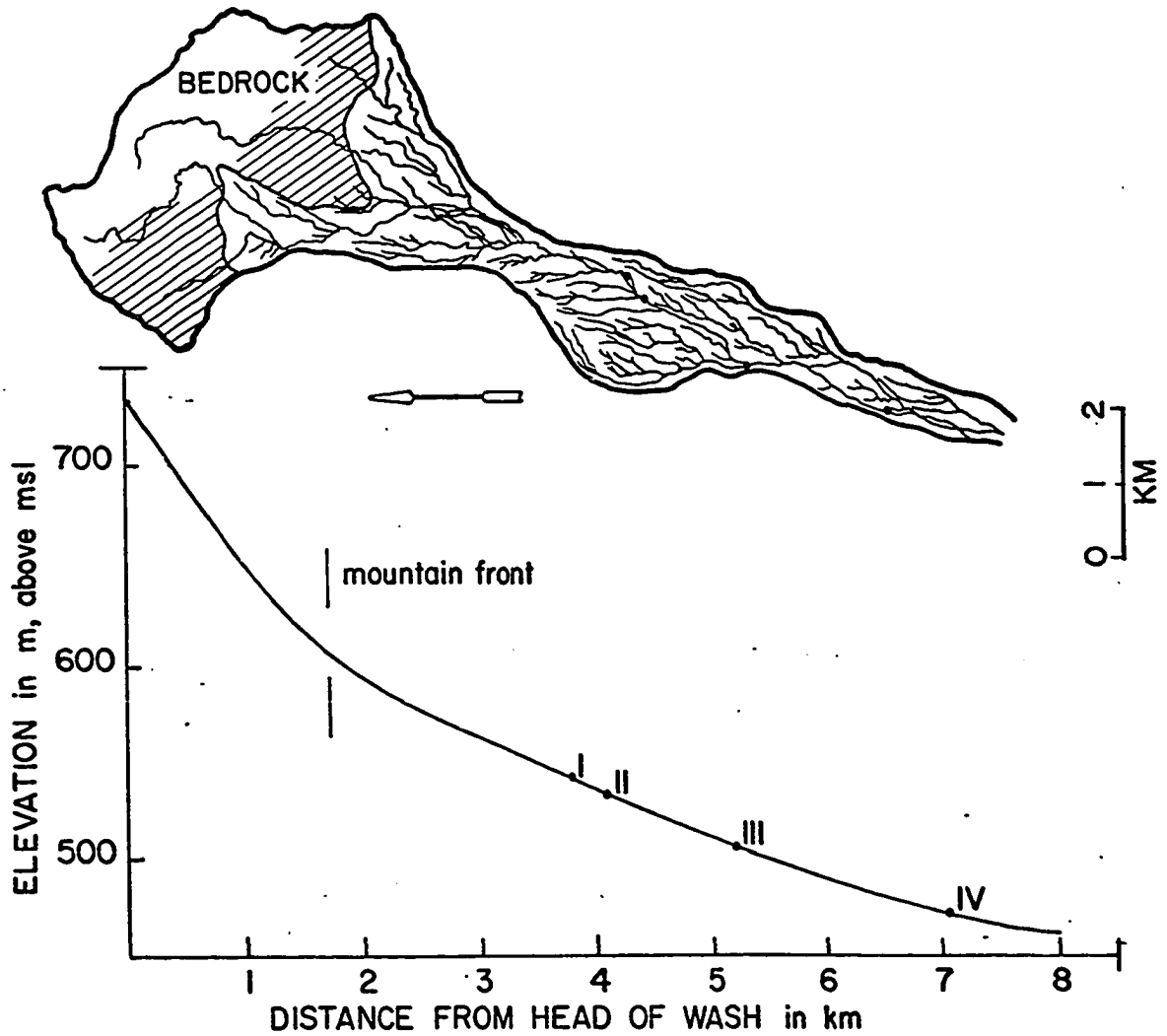

Figure 50. Map of low order drainage basin LMQ-C and longitudinal profile for principal wash draining basins. Station locations are given as black dots.

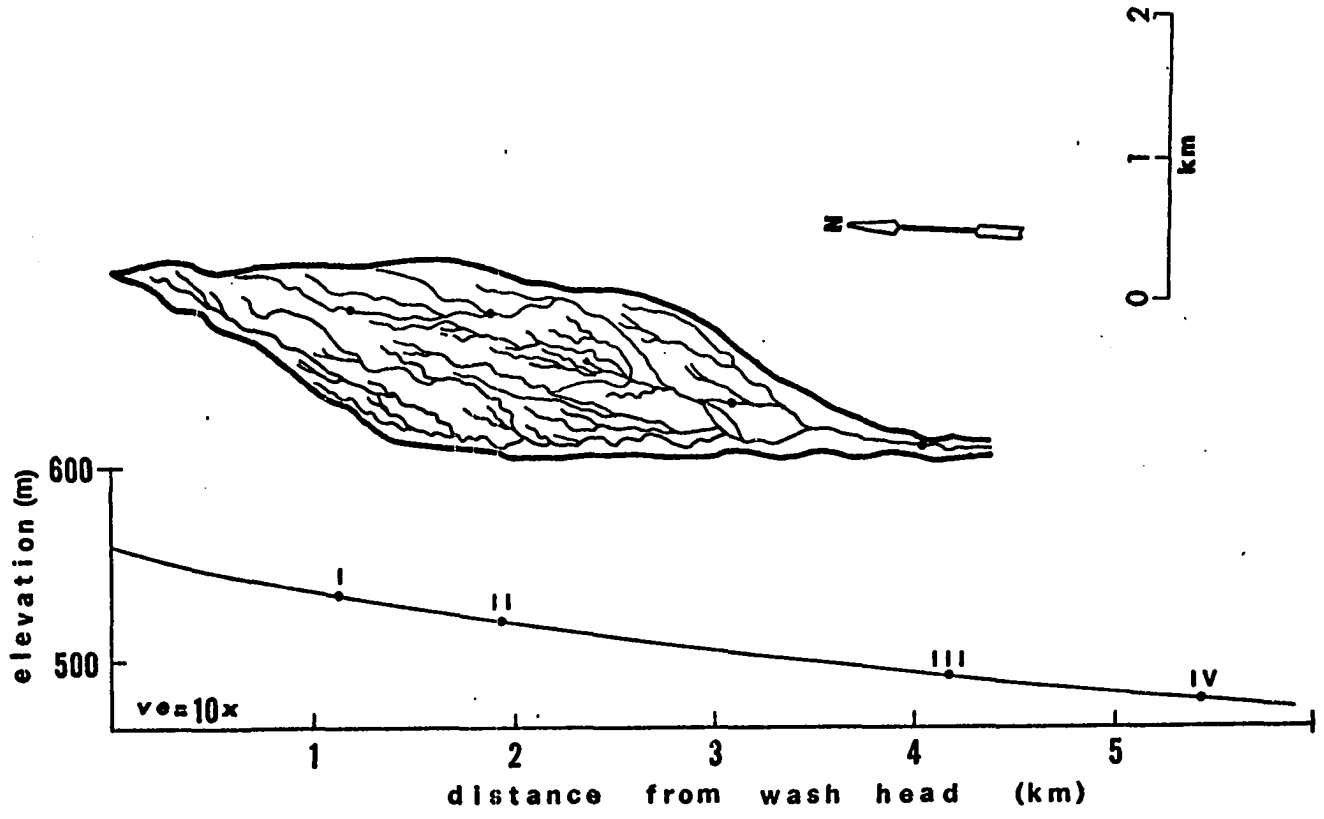

Figure 51. Map of low order drainage basin LMQ-D and longitudinal profile of principal wash draining basin. Station locations are given as black dots.

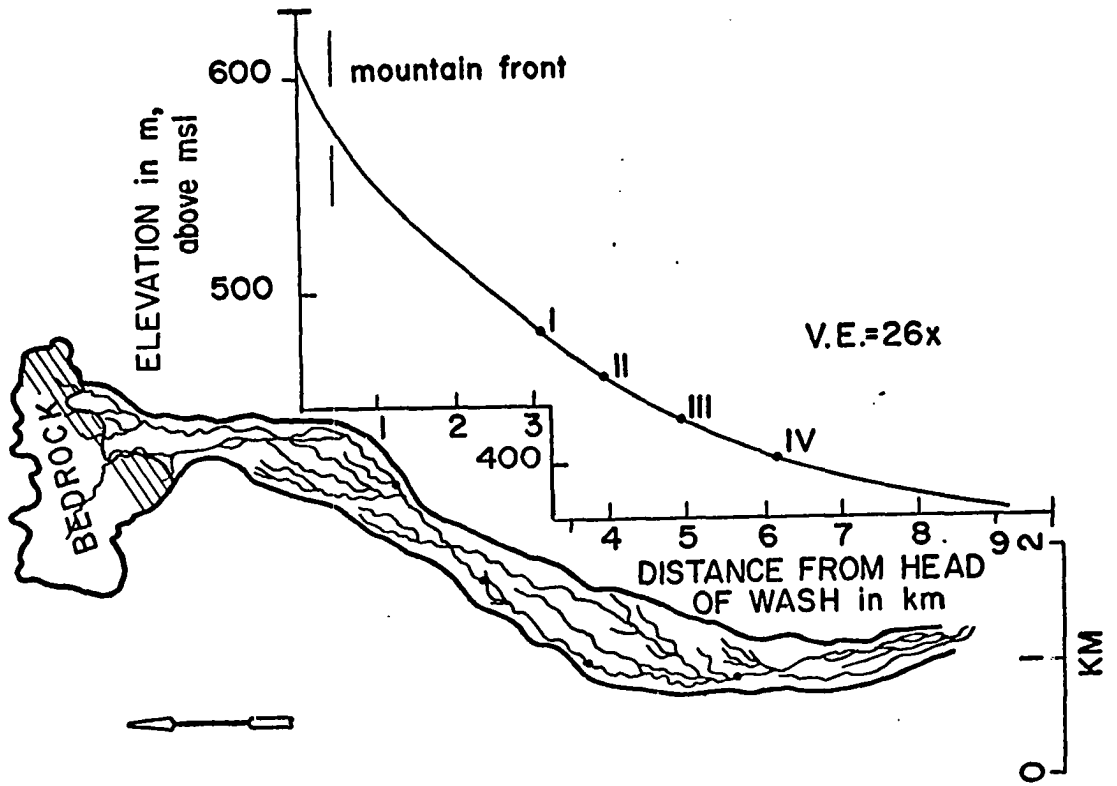

Figure 52. Map of low order drainage basin BHMQ-A and longitudinal profile of principal wash draining basin. Station locations are given as black dots.

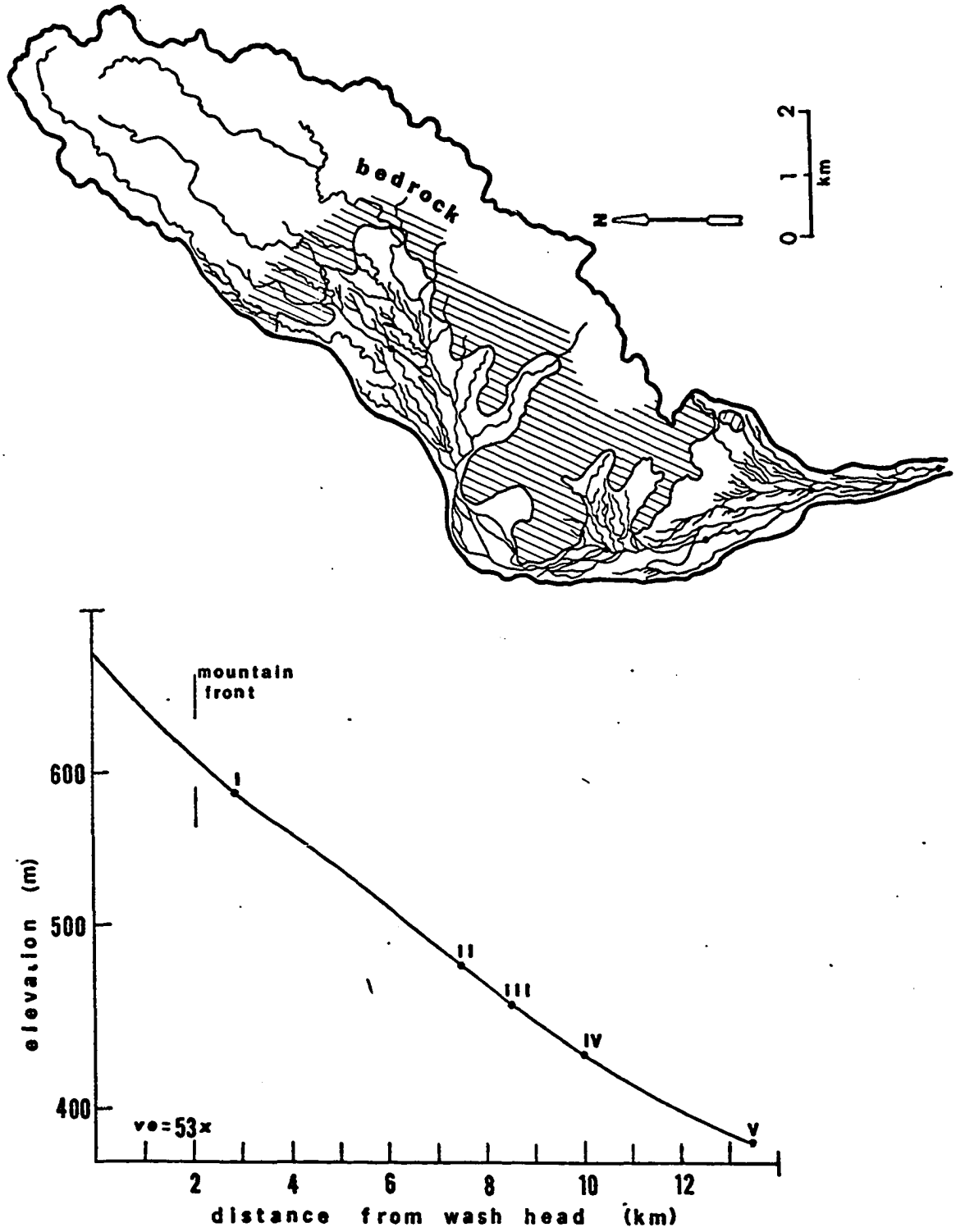

Figure 53. Map of low order drainage basin BHMQ-B and longitudinal profile of principal wash draining basin. Station locations are given as black dots.

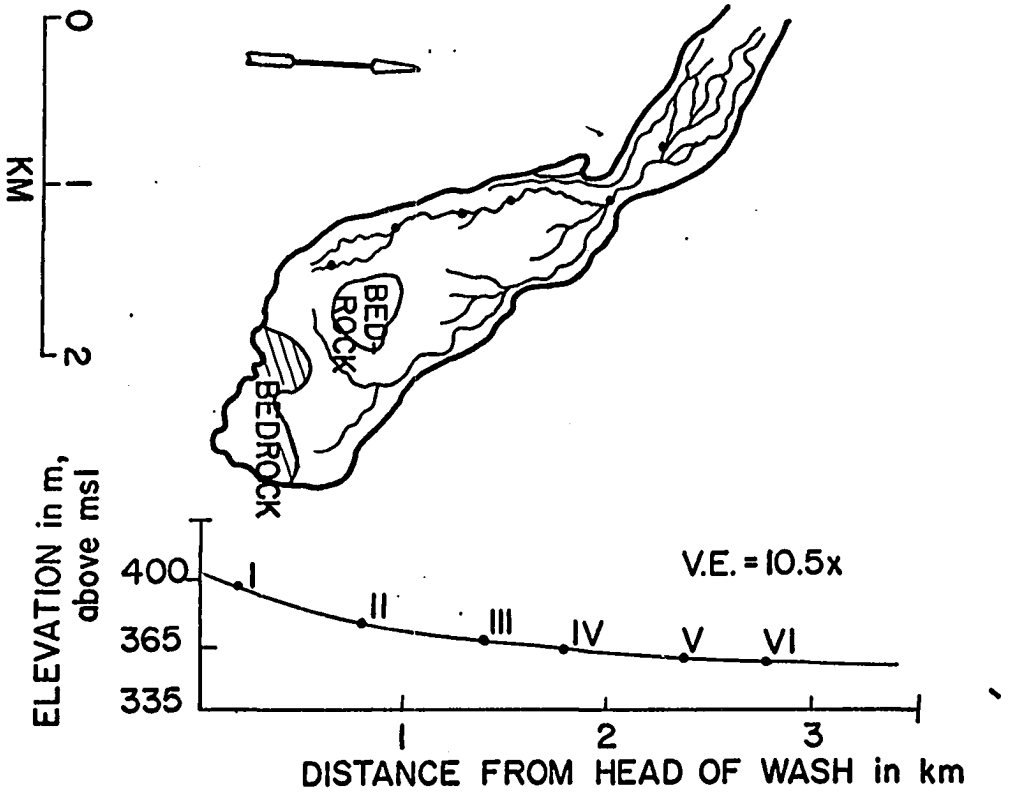

Figure 54. Map of low order drainage basin CPQ-A and longitudinal profile of principal wash draining basin. Station locations given as black dots.

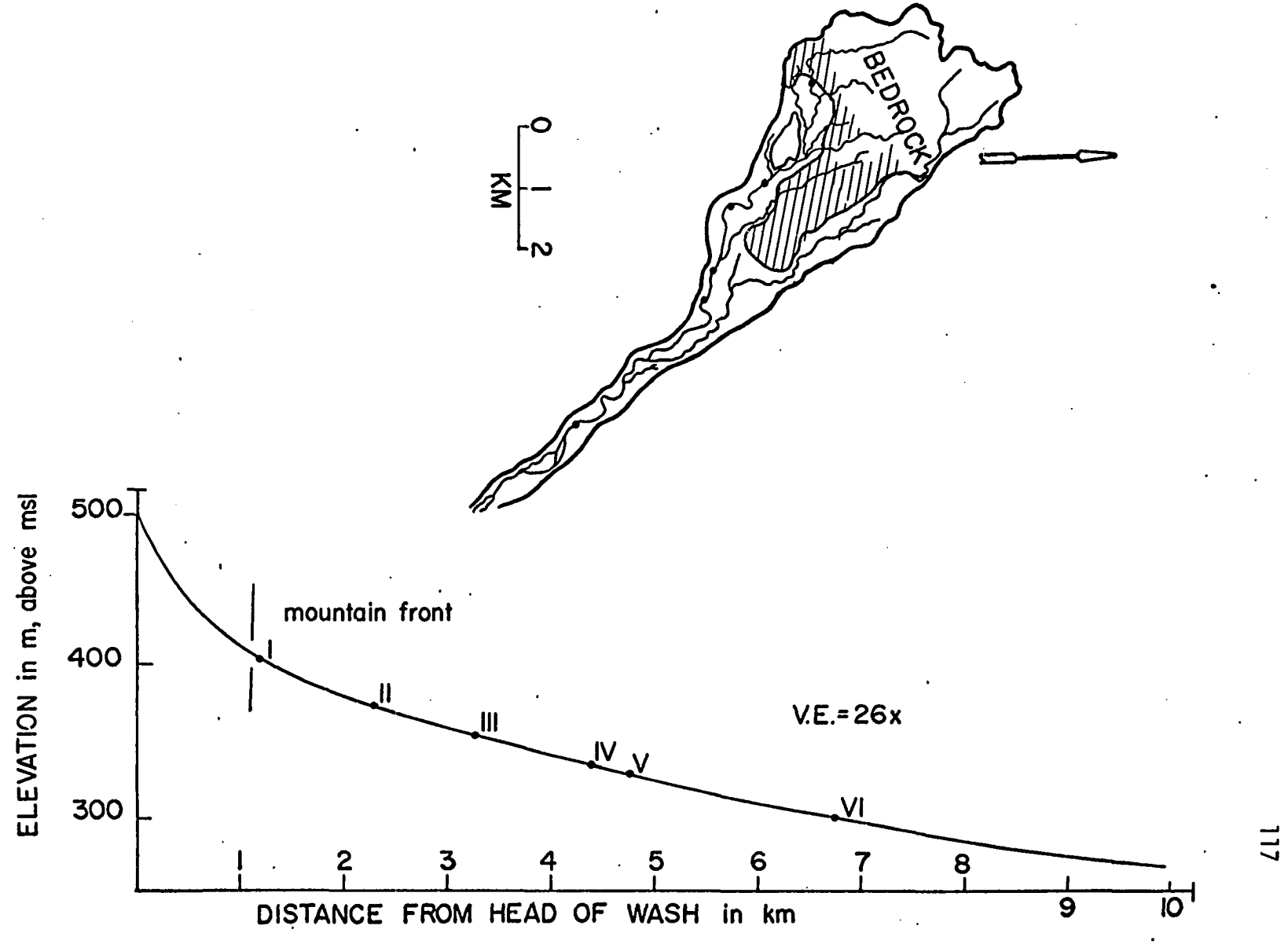

Figure 55. Map of low order drainage basin CPQ-B and longitudinal profile of principal wash draining basin.

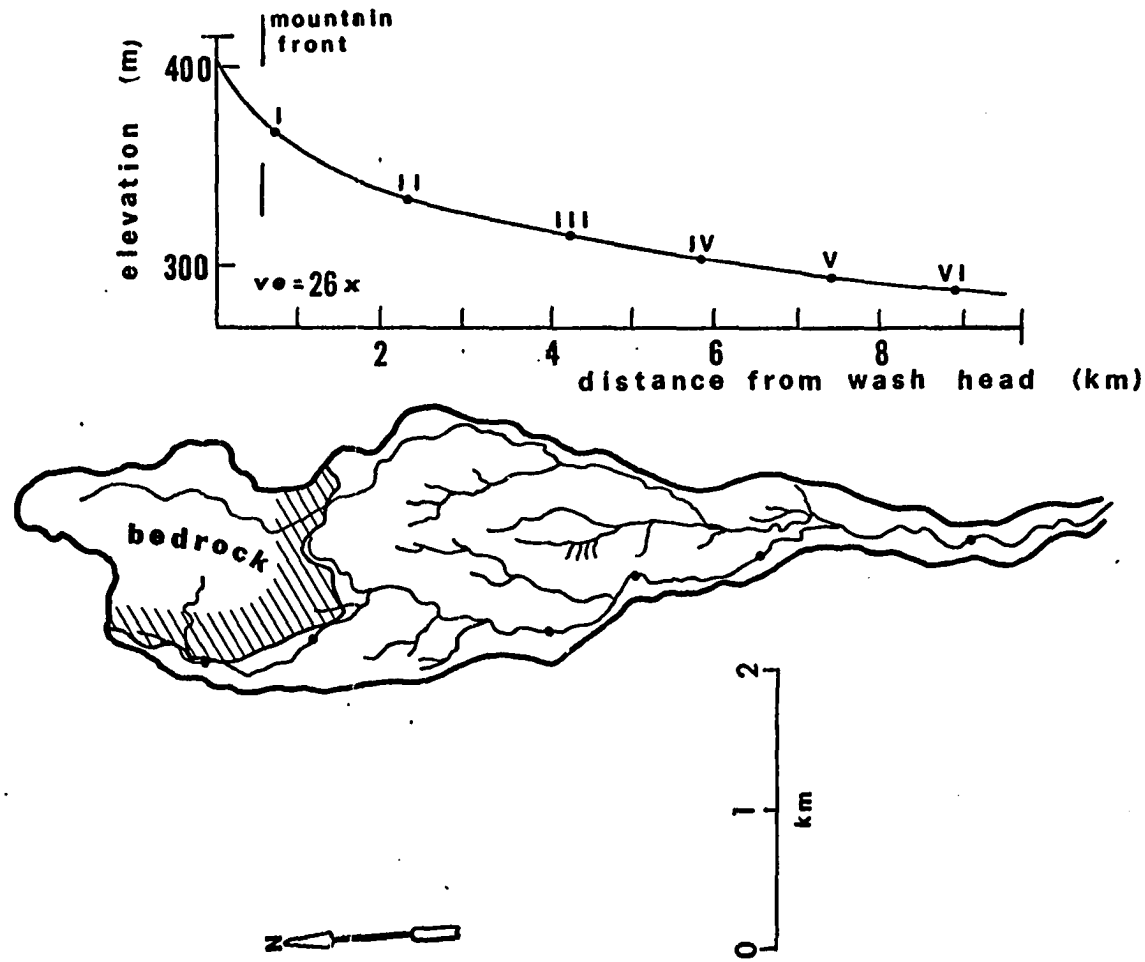

Figure 56. Map of low order drainage basin CPQ-C and longitudinal profile of principal wash draining basin. Station locations given as black dots.

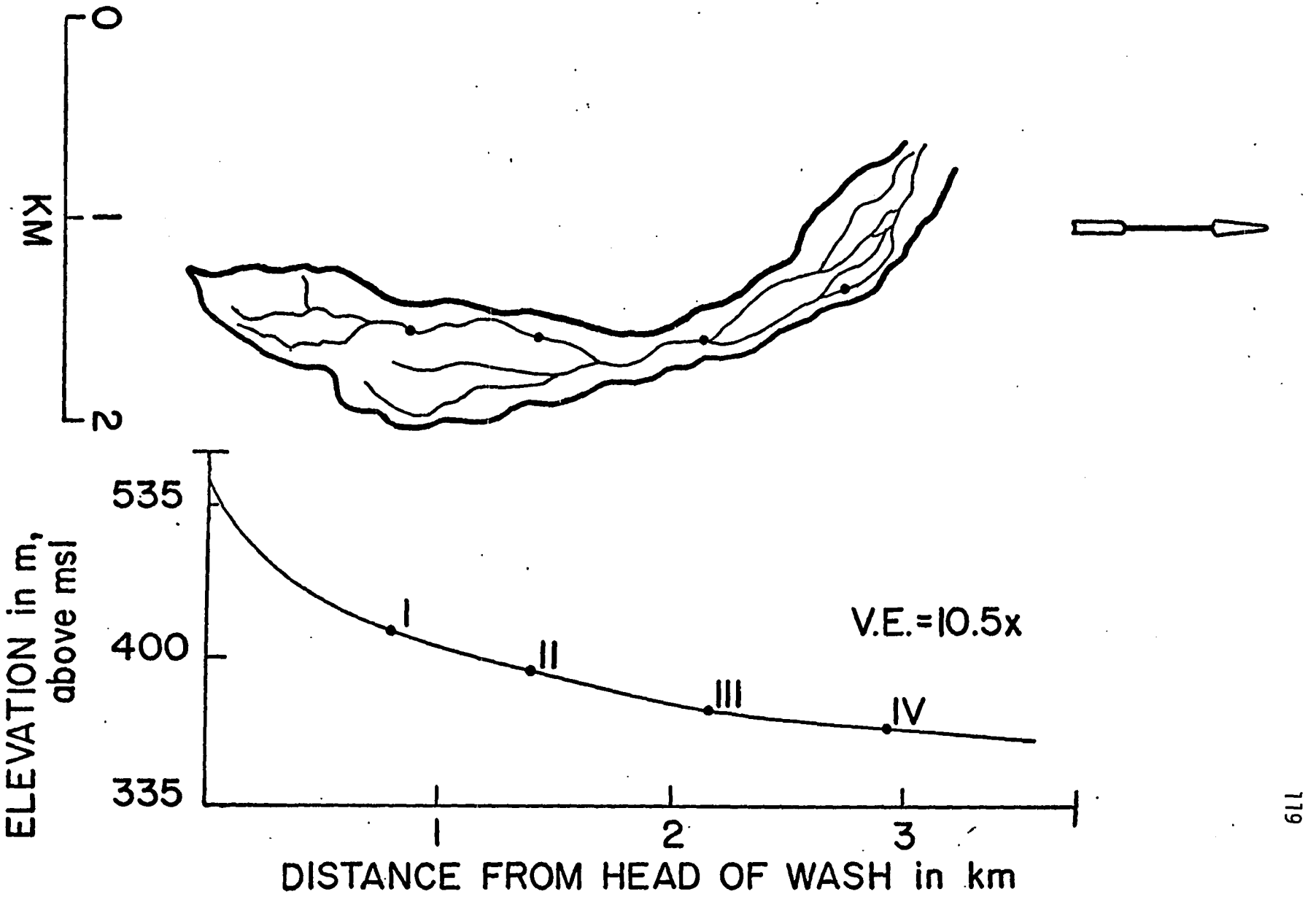

Figure 57. Map of low order drainage basin CPQ-D and longitudinal profile of principal wash draining [illegible] as black dots

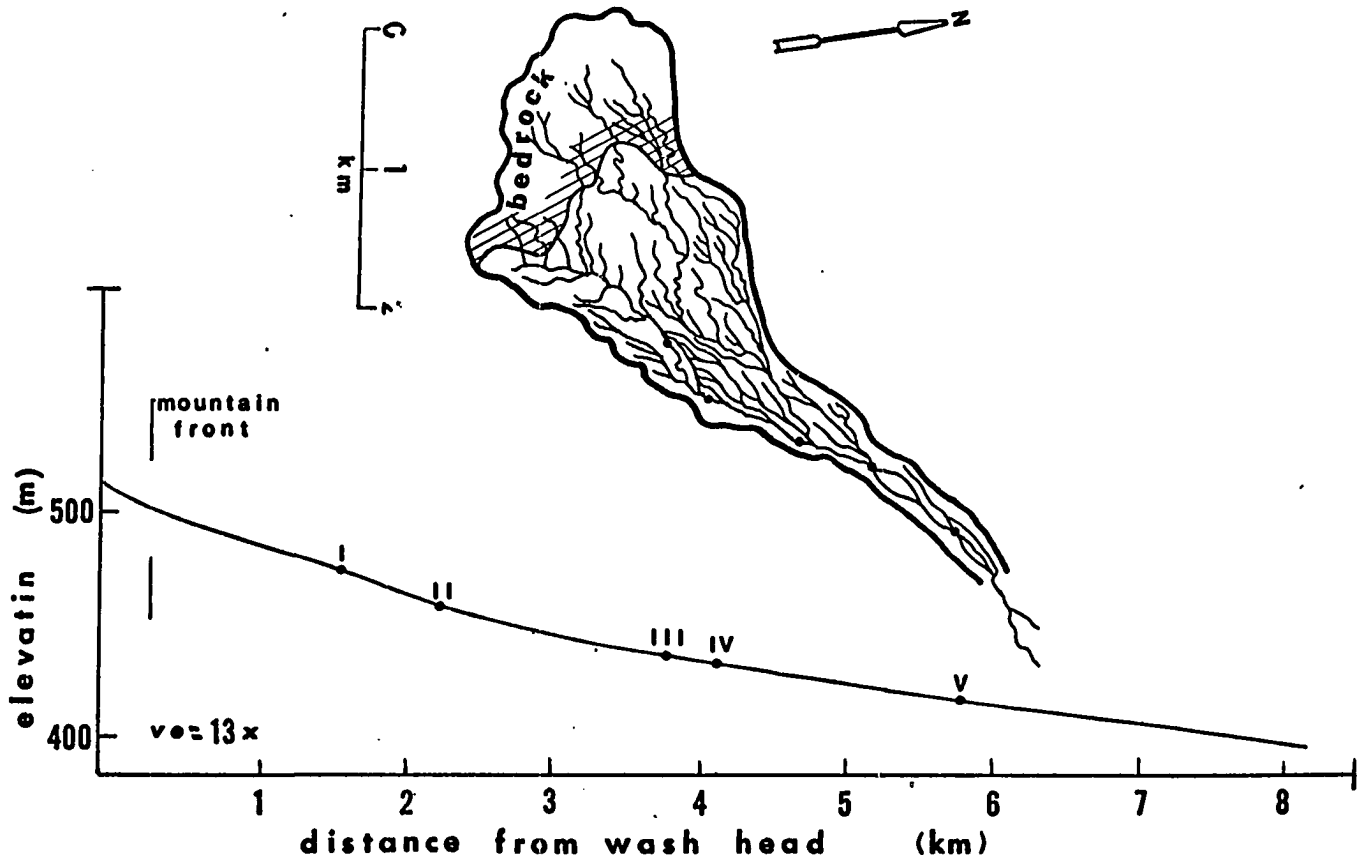

Figure 58. Map of low order drainage basin EMQ-A and longitudinal profile of principal wash draining basin. Station locations given as black dots.

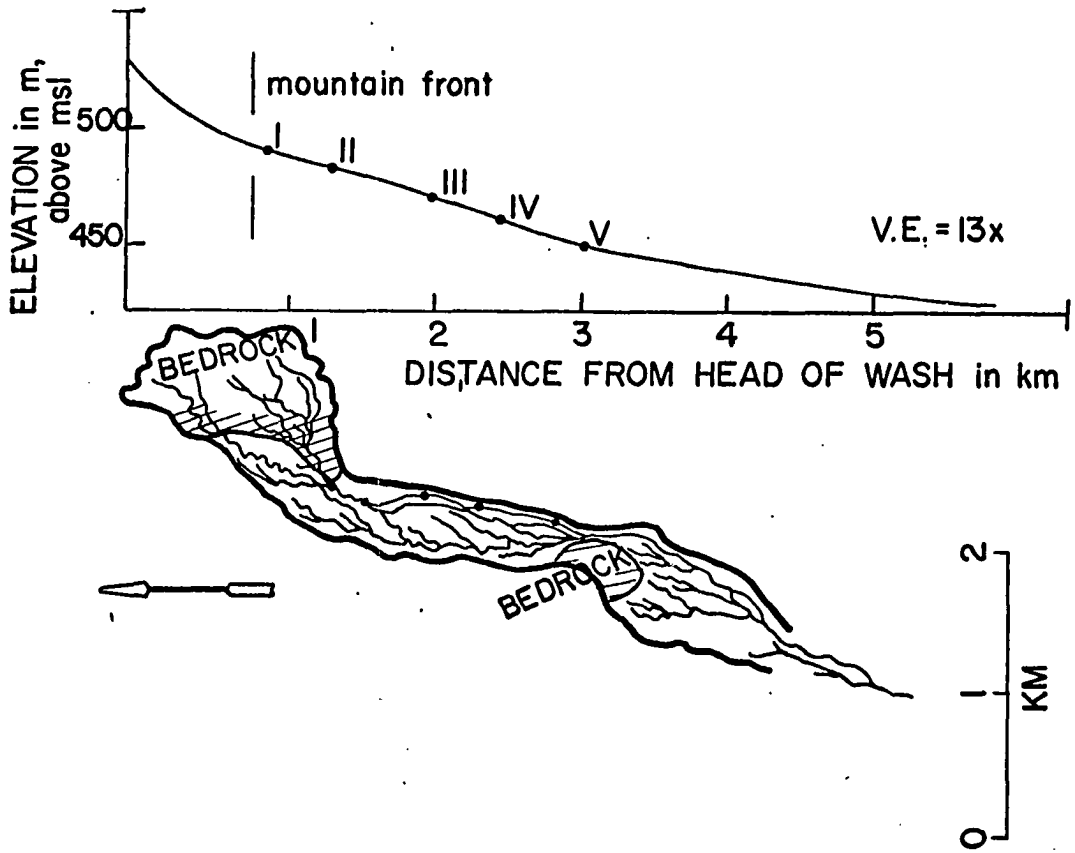

Figure 59. Map of low order drainage basin EMQ-B and longitudinal profile of principal wash draining basin. Station locations are given as black dots.

km (Appendix VI). The range in mean width for all twelve low order basins is .4 to 5.8 km, and an average mean width of these basins 2.2 km (Appendix VI).

All but two low order drainage basins have bedrock outcrops in their drainage areas. The ratio of alluvial apron area to bedrock area for each low order basin is given in Appendix VI. The range in this ratio is 3.5 to 0.4, and the average ratio is 1.2. The average low order basin has approximately equal amounts of bedrock and apron areas. The ratio of bedrock to apron area varies with distance down the fan and usually shows a net increase. However, at the junction of major tributaries with the trunk wash, the ratio may be reduced if the tributary is draining large areas of bedrock.

Relief and Relief Ratio:

The maximum relief, as measured from the highest point in the basin to the last station on the trunk wash, ranges from 100 to 1300 m for the low order drainage basins (Appendix VI). The highest maximum relief occurs in those low order basins, which include both bedock areas and alluvial aprons of the Harquahala Valley. The lowest maximum relief occurs in those basins which head on the alluvial aprons and not in the mountain ranges. Low order basins developed on mountain ranges and alluvial aprons composed of metamoprhic and sedimentary rocks have high maximum relief, but those basins draining extrusive and especially intrusive igenous rocks have lower maximum relief.

The lower relief in intrusive igneous rocks, such as granites, may be attributed to weathering of this lithology to a grus. Rahn (1965) and Cordiviola (1974) demonstrated how intrusive igneous rocks weather to a

grus, or sand size detritus. This size is optimum for fluvial transport (Sundborg, 1956); therefore, the weathered mantle can be easily removed from hillslopes. Thus, this material can be swept off the hillslopes during runoff more readily than other lithologies and may be lowered at a faster rate. Tuan (1959) postulated that this relationship between lithology and the weathered product on granites is the reason for the numerous pediments formed on igneous extrusive rocks in southeastern Arizona.

Drainage Density and Frequency:

The density and frequency of washes which form the drainage net in the low order drainage basins are given in Figure 48, 50 through 59 and summarized in Appendix VI. The drainage density of these basins ranges from 3 to 20 and has an average of 7.7. Drainage frequency ranges from 4 to 70 and has an average of 24 for the low order basins.

The drainage density of low order basins developed on alluvial aprons containing caliche rubble (Qcr) and petrocalcic horizons, such as those flanking Saddle Mountain, is compared to the drainage density of low order basins developed on aprons without caliche rubble, or calcic horizons. The Mann-Whitney U is used to test the difference between drainage densities of low order basins developed on fans with and without caliche rubble (Appendix I). The null hypothesis that drainage density of the low order basins with caliche rubble is the same as low order basins without caliche rubble is accepted at $\alpha = 0.05$. Therefore, there is no significant difference between drainage density in low order basins developed on these two types of Quaternary surficial deposits.

Drainage frequency of low order drainage basins with and without

caliche rubble is tested by the Mann-Whitney U (Appendix I). The null hypothesis that drainage frequency is the same for basins in both types of surficial deposits is not accepted at $\alpha = 0.05$. Thus, the frequency of drainage lines is different (less) in those basins developed on caliche rubble. This may be due to the impermeable caliche rubble and petrocalcic horizon reducing channel erosion and favoring sheetflow.

Sedimentology of Ephemeral Washes in Low Order Drainage Basins

The trunk washes in the low order drainage basins given in Appendix VI and in Figures 49 through 59 can be divided into two reaches based on differences in sedimentology and topography. The first reach, or channel, is characterized by coarse sediments, and the topographically higher second reach, or berm, is characterized by fine sediments (Fig. 60). Differences between channel and berm sediments are shown by means of sieve analysis (Appendix II) (Figures 61 through 65). The berm sediments typically have grains whose diameters are less than 0.125 mm. Channel sediments have grain sizes which are larger than 2 mm in diameter (Figures 61 through 65). The topographic relationship between these two reaches is shown in Figure 60 and is common to most ephemeral washes in the Harquahala Valley.

In all but one wash (Fig. 65), there is an obvious difference between the sediment sizes of the berm and channel (Figures 61 through 64). The similarity in the grain sizes of the berm and channel sediments in this wash is related to the lithology of the source area. The berm and channel are composed of granitic detritus, which is derived from the grus mantled hillslopes in the source area. Granite, which commonly weathers to a uniform sand size, obscures the difference in particle size typical

W_m = maximum width of flow

W_c = maximum width of channel

W_b = maximum width of berm

D_m = maximum depth of flow

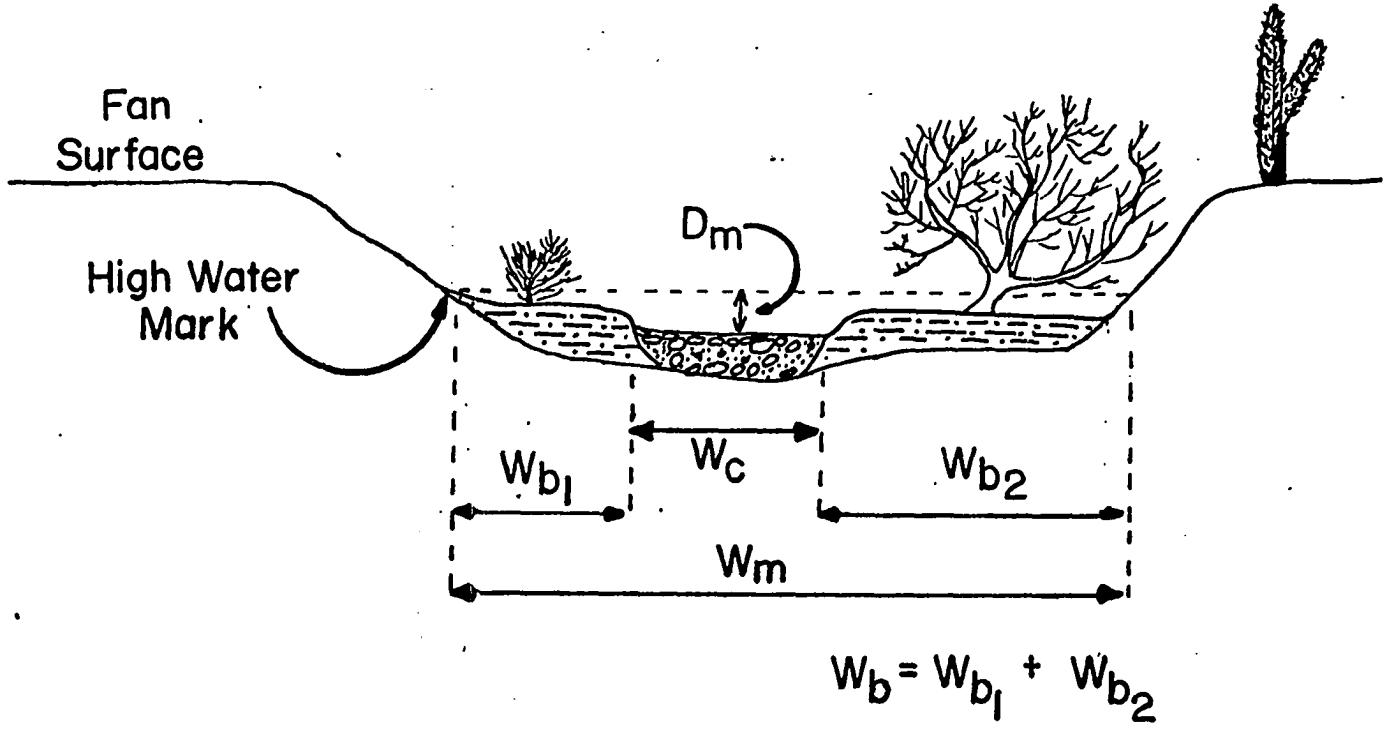

Figure 60. Idealized cross-section of ephemeral wash showing berm and channel in addition to hydraulic geometry of a wash based on high water marks from a previous flood.

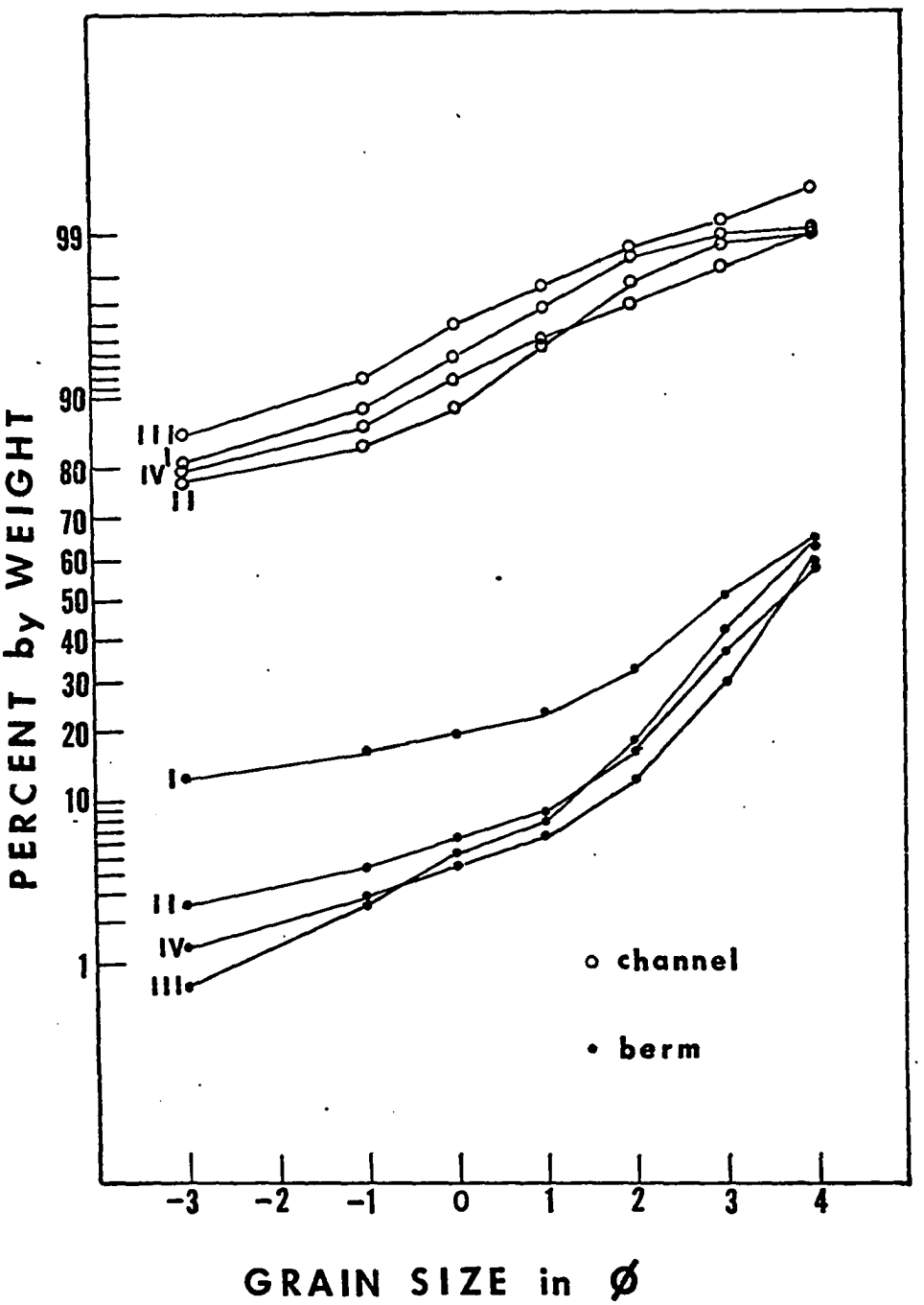

Figure 61. Cumulative curves for sediments at selected stations of principal wash draining low order drainage basin LMQ-D.

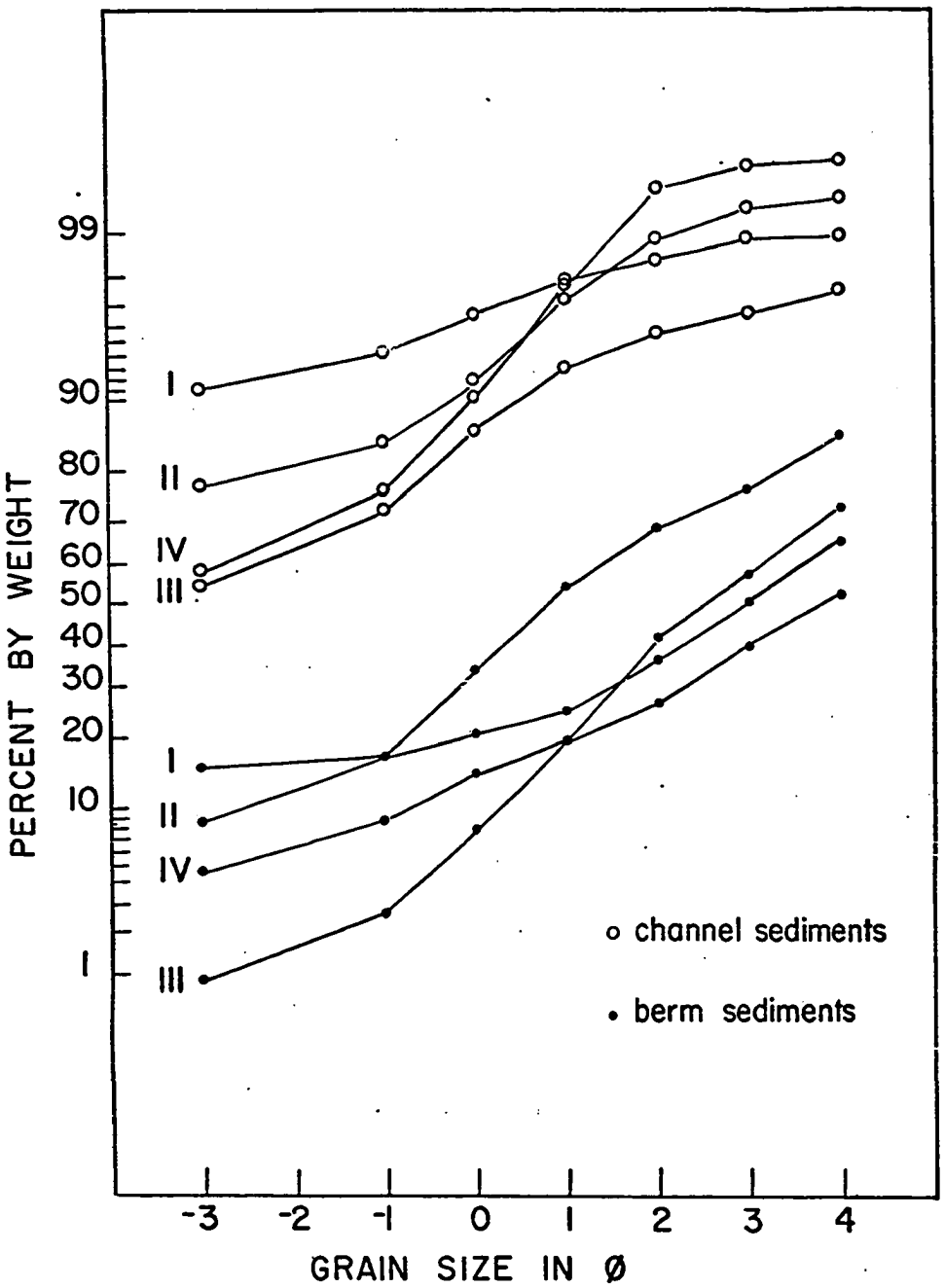

Figure 62. Cumulative curve for sediments at selected stations on principal wash draining low order drainage basin CPQ-C.

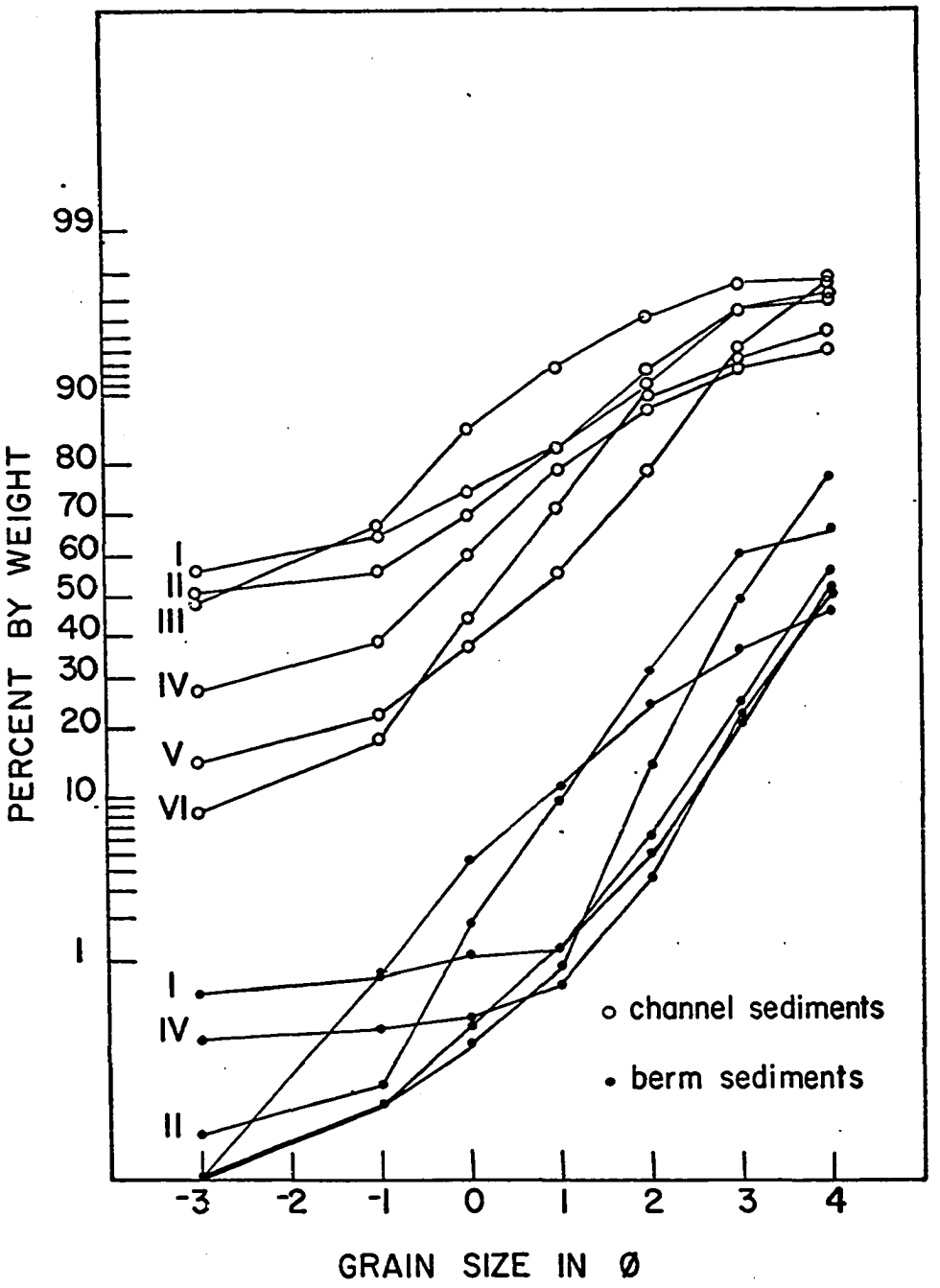

Figure 63. Cumulative curve for sediments at selected stations on principal wash draining low order drainage basin LMQ-A.

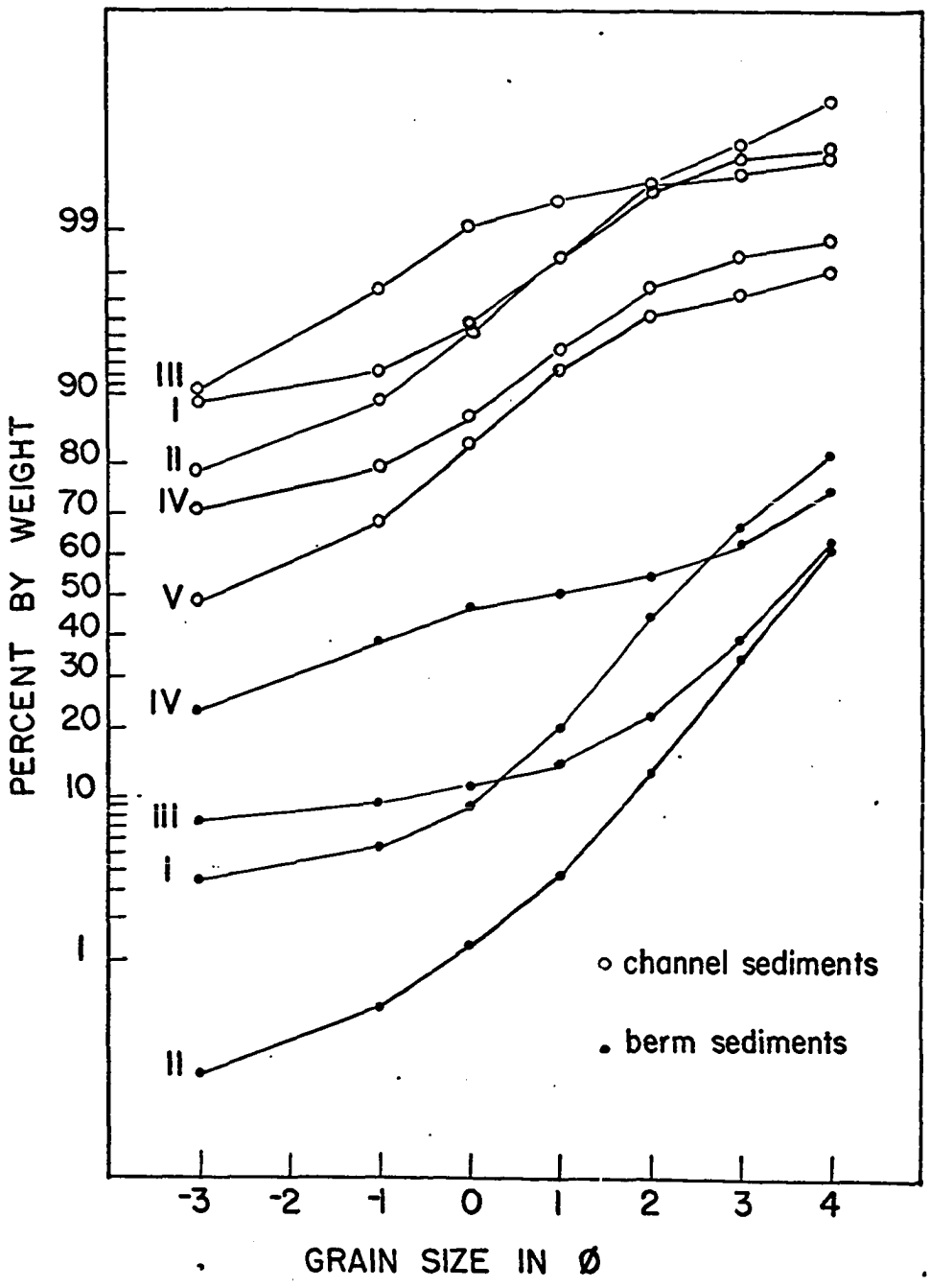

Figure 64. Cumulative curves for sediments at selected stations on principal wash draining low order basin CPQ-B.

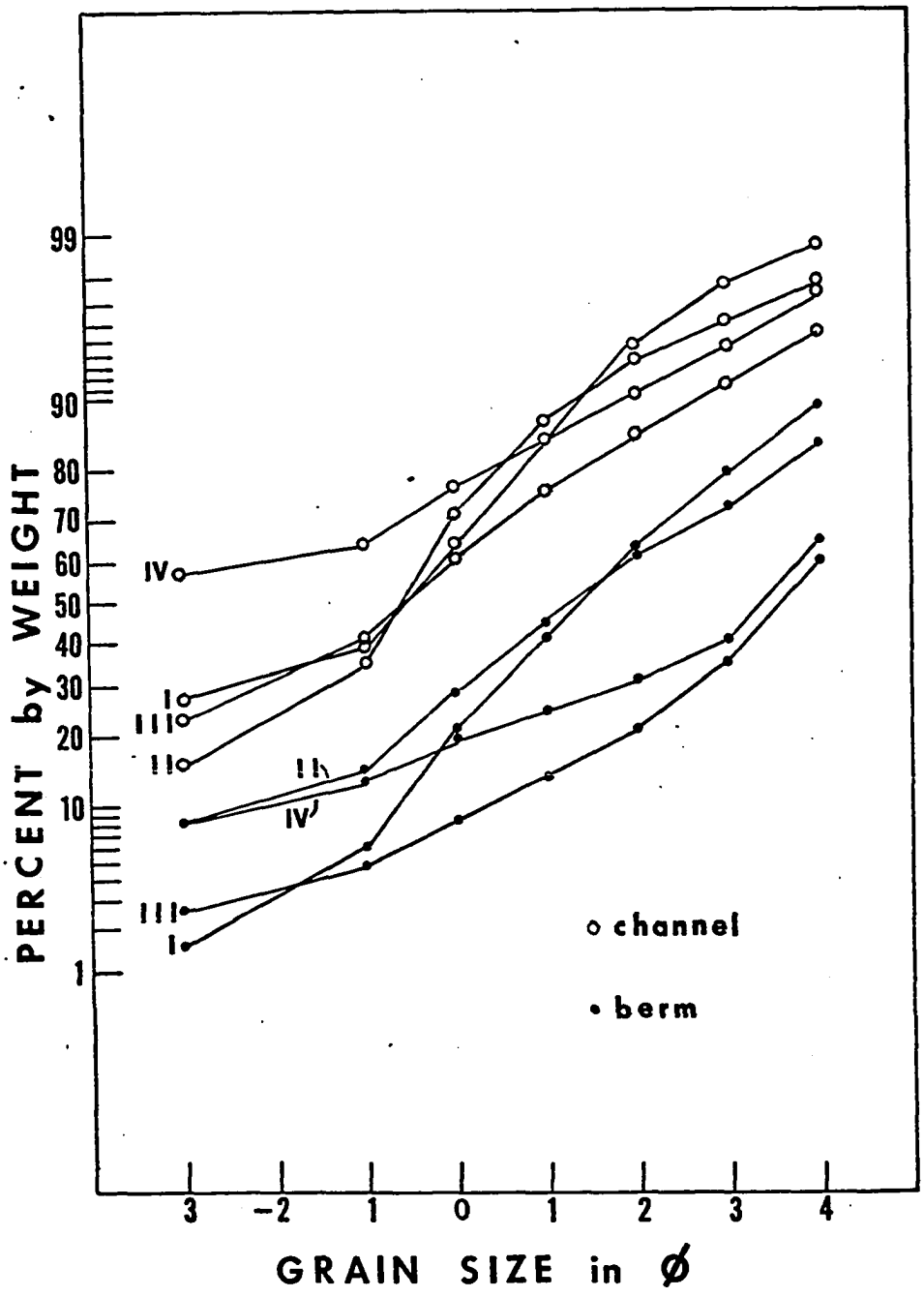

Figure 65. Cumulative curves for sediments at selected stations on principal wash draining low order basin BHMQ-B.

to berm and channel deposits composed of other lithologies.

The relationship between the lithology and size of the sediment in the berm and channel of ephemeral washes is illustrated in Figure 66. The difference between the two sediment size populations is obvious except for granitic sediments. Most berm deposits, composed of sedimentary, metamorphic, volcanic, and combinations of these detritus, contain approximately 60 percent fine sand and silt, but berms composed of granitic detritus have higher percentages of sand (Fig. 66). Channel deposits usually have a mixture of less than 30 percent sand and more than 70 percent gravels, which are derived from all lithologies except granite (Fig. 66). Changes in the particle size distribution of berm and channel sediments down wash may result from the influx of new lithologies by tributary washes draining other source areas. Figure 71 illustrates changes in the grain size distribution down an ephemeral wash when volcanic rocks are introduced by a major tributary in the lower reaches of the low order basin.

Variations at each station in the particle size distribution for berm and channel sediments on trunk washes are given in Figures 67 through 71. Three washes show a marked reduction in the percent weight of gravels and coarse sand (greater than -1ϕ) in the channel deposits; one wash shows little change and the other wash shows an increase in the percent weight of gravels and coarse sand. The percent weight of the grain sizes less than 4 ϕ remains fairly constant. Berm sediments typically increase the percent weight of grain sizes less than 3 ϕ.

In summary, the percent by weight of the fine grained berm sediments increases downwash as the percent by weight of coarse channel gravels

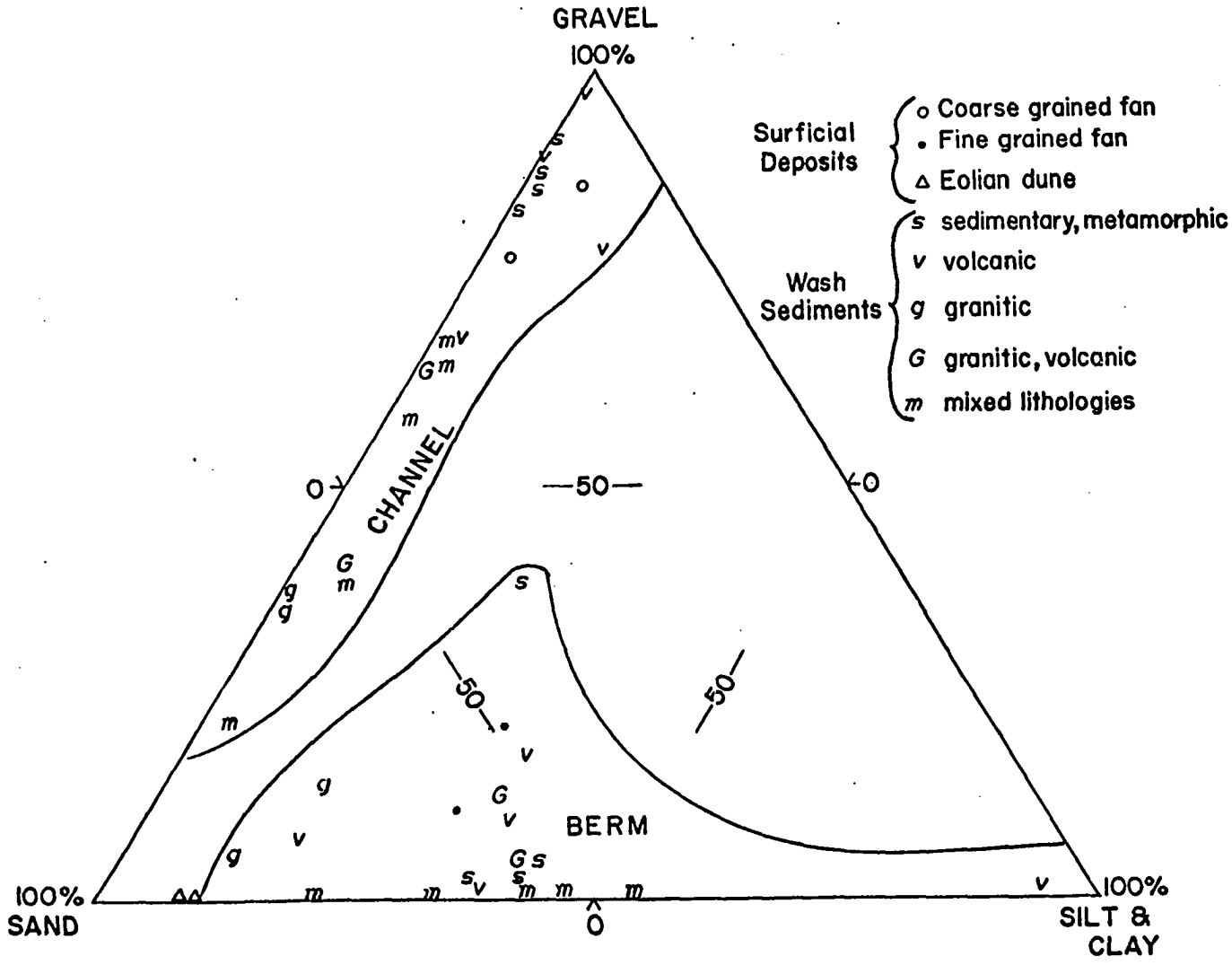

Figure 66. Relationship between particle size (expressed as percent by weight) and lithology of the clasts for wash sediments and surficial deposits in the Harquahala Valley.

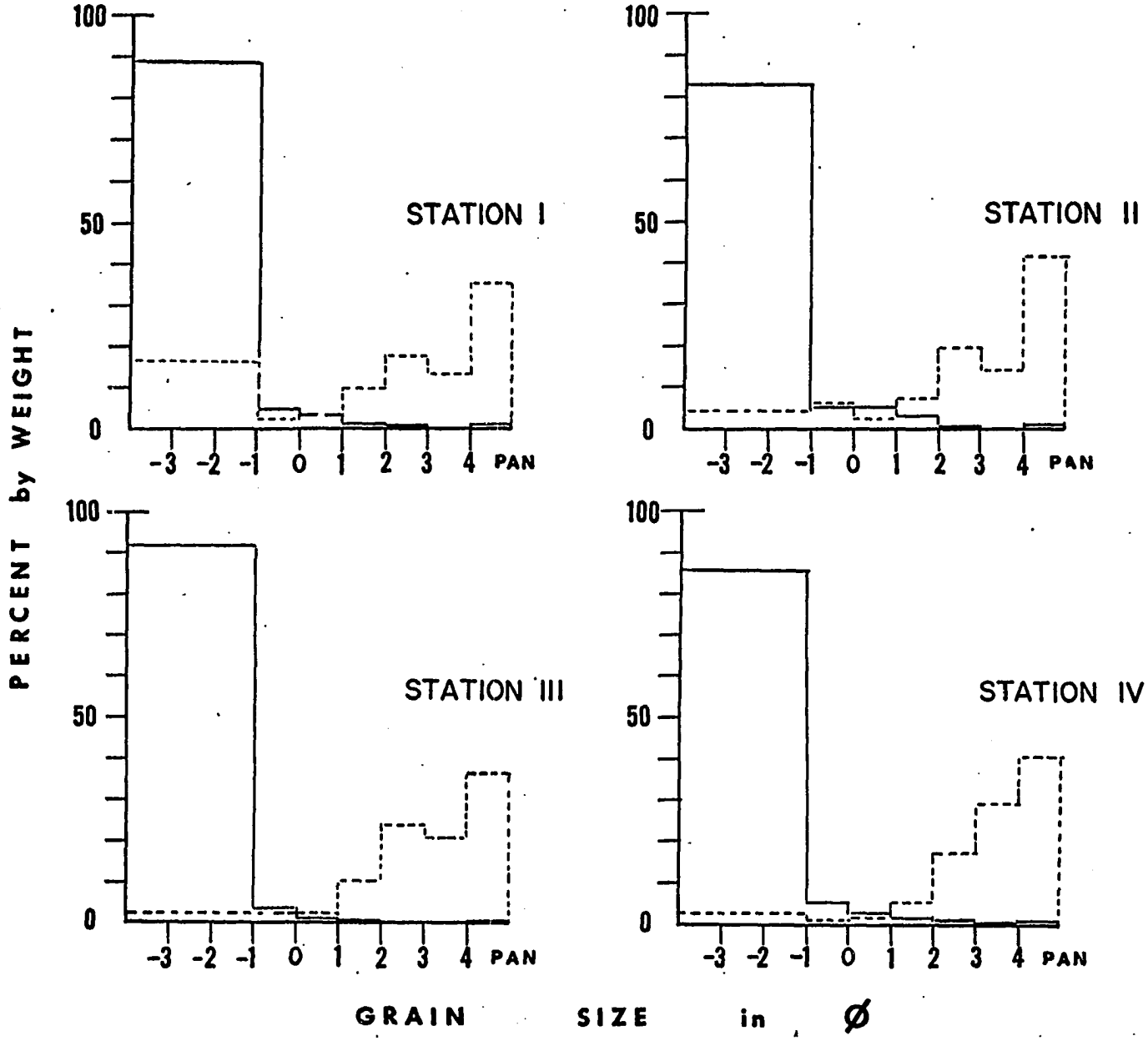

Figure 67. Histograms showing frequency of grain size in ϕ interval for channel (solid line) and berm (dashed line) sediments in the principal wash draining low order basin LMQ-D.

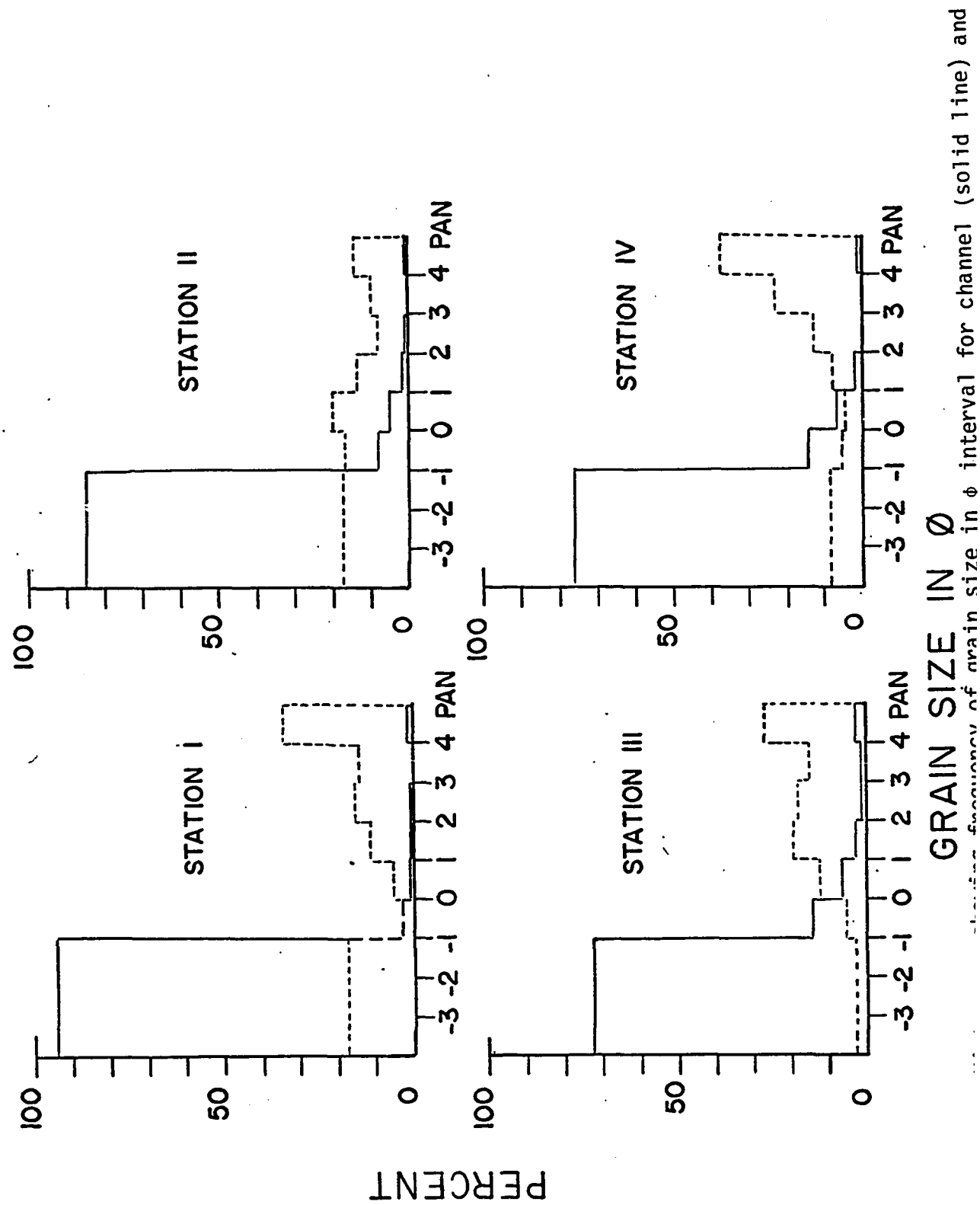

...frequency of grain size in ϕ interval for channel (solid line) and

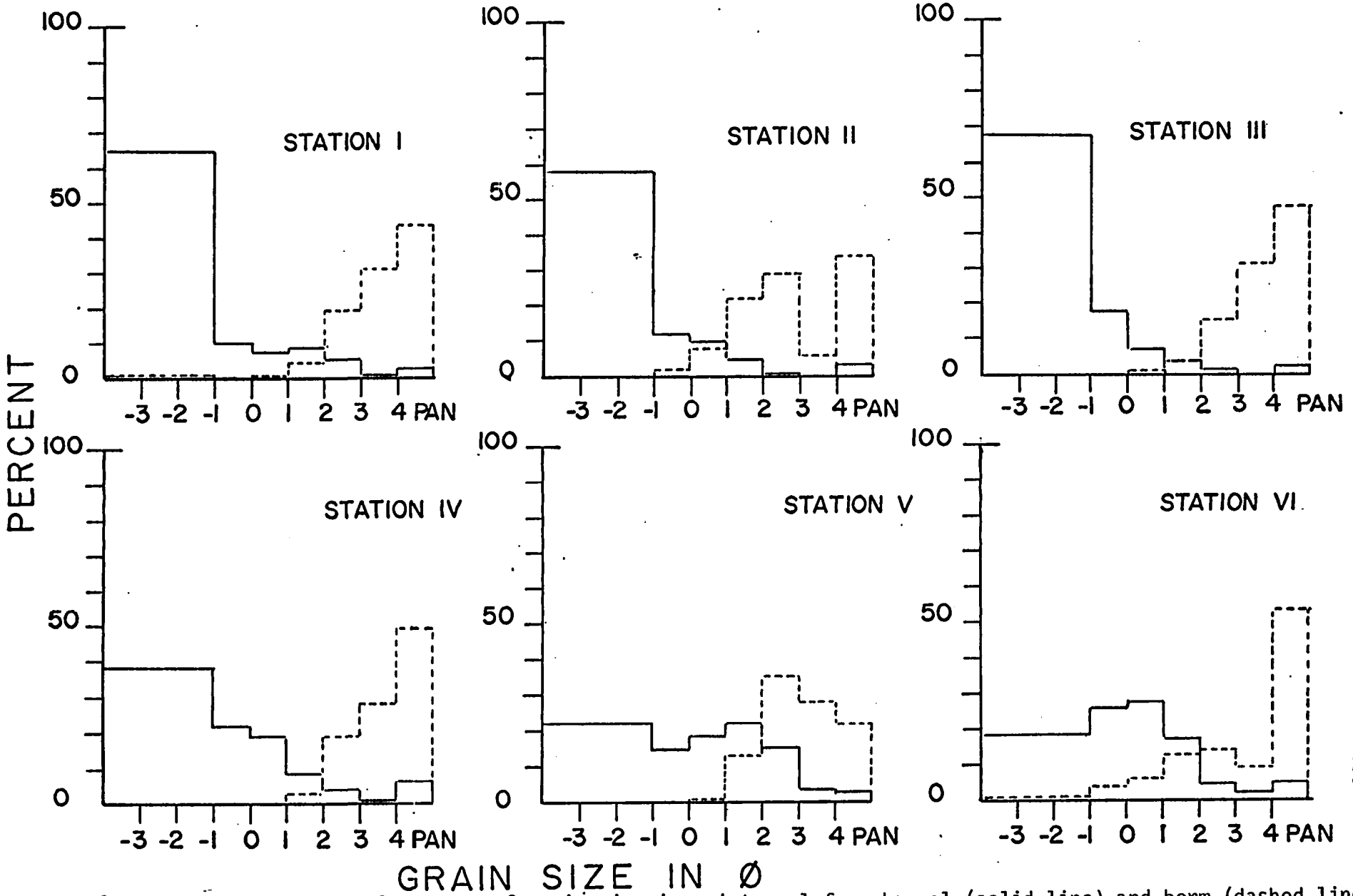

Figure 69 . Histograms showing frequency of grain size in ϕ interval for channel (solid line) and berm (dashed line)

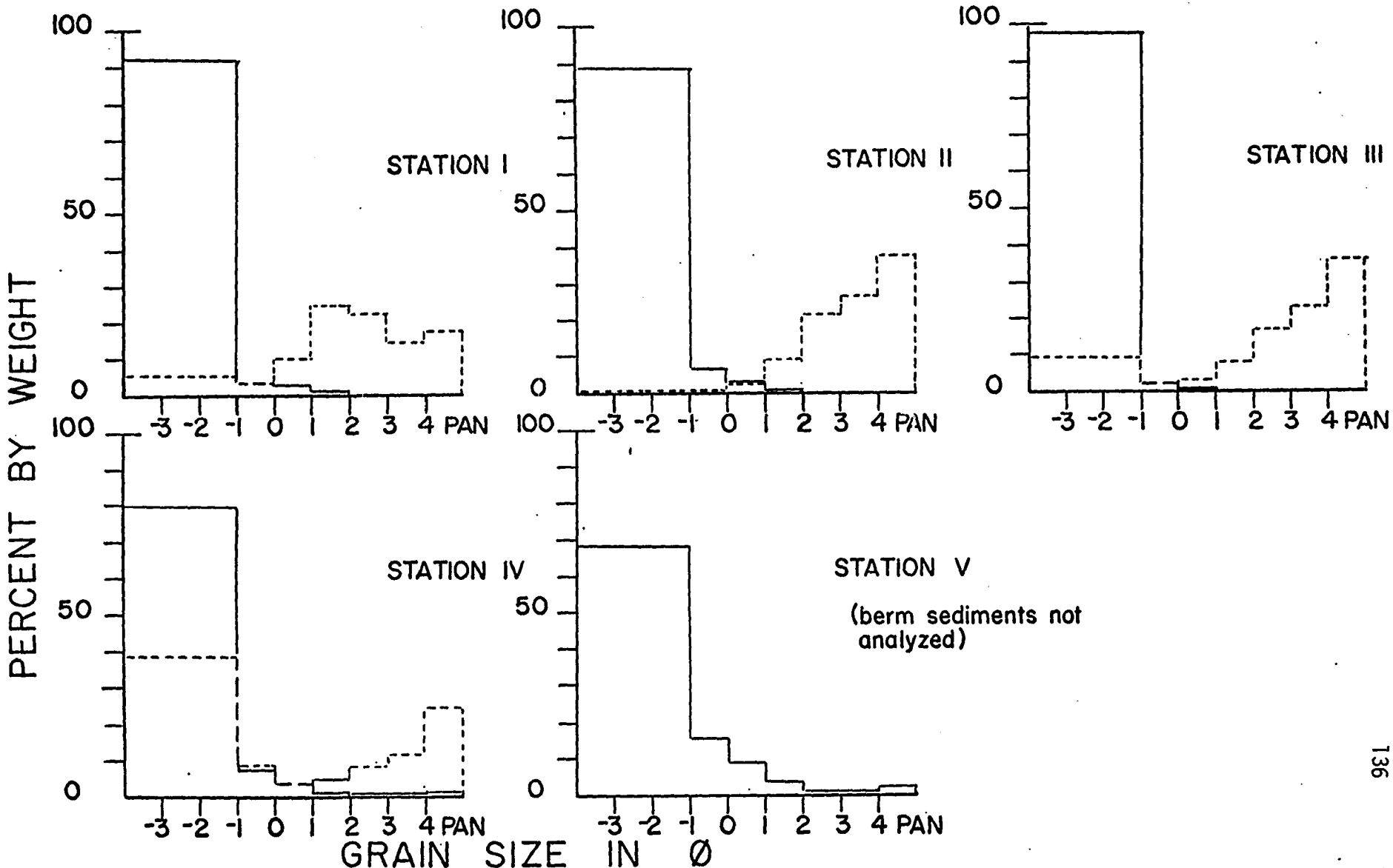

of grain size in ϕ interval for channel (solid line) and berm (dashed line)

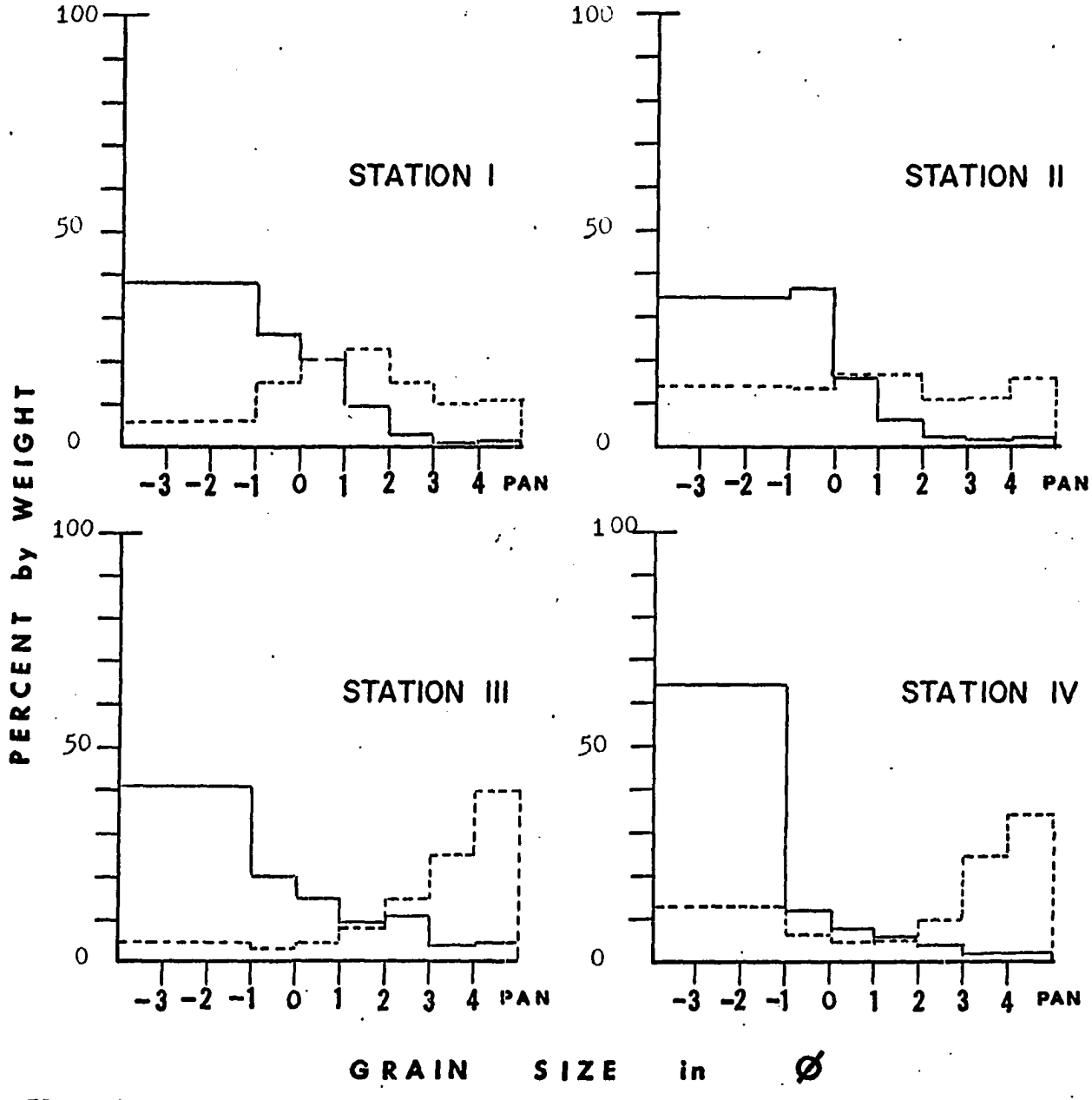

Figure 71. Histograms showing frequency of grain size in ϕ interval of channel (solid line) and berm (dashed line) sediments in principal wash draining low order drainage basin BHMQ-B.

decreases down wash. This relationship suggests a change in the competence of the floods down the alluvial apron. Table 5 is a list of the maximum particle sizes, measured along the largest diameter for selected trunk washes in the low order drainage basins. The maximum particle size decreases with distance from the divide in seven of the eight washes (compare Table 5 with stations in Appendix VI). The decrease in maximum particle size, as well as the relationship given above, suggests that the tractive forces (shear stresses) are decreasing down wash. The Spearman Rank correlation coefficient, r_S, is used to determine if a relationship exists between maximum particle size (Table 5) and the computed tractive forces (Appendix VI). The coefficient, r_S, is 0.67, which is significant at $\alpha = 0.05$ (Appendix I).

The maximum particle size and tractive forces are plotted in Figure 72 on logarithmic scale. Although considerable scatter occurs, the general trend suggests that with decreasing tractive forces, the maximum particle size decreases. An important feature is illustrated by the logarithmic plot and is seen in the sharp break in the lower tractive forces (Fig. 72). This well defined break suggests a minimum, or critical, tractive force necessary to move particles of that size.

Low correlation coefficients and considerable scatter on logarithmic plots may be attributed to changes in the floods' specific weights, which are assumed to be constant in the calculations, or they mean that the maximum particle size, which may be derived from older fan material, cannot be transported by modern flood events.

Low Order Drainage Basin	STATIONS						
	I	II	III	IV	V	VI	VII
LMQ-A	70	91	64	34	31	10	2
LMQ-D	34	27	24	12			
CPQ-A	50	60	75	23	34	20	
CPQ-B	40	37	51	52	42	45	
CPQ-C	46	38	23	35	30	19	
BHMQ-B	33	10	46	46	15		
EMQ-A	56	39	22	27	23		
EMQ-B	84	32	43	48	19		

Table 5. Maximum particle diameter in cm at selected stations on principal washes draining low order drainage basins.

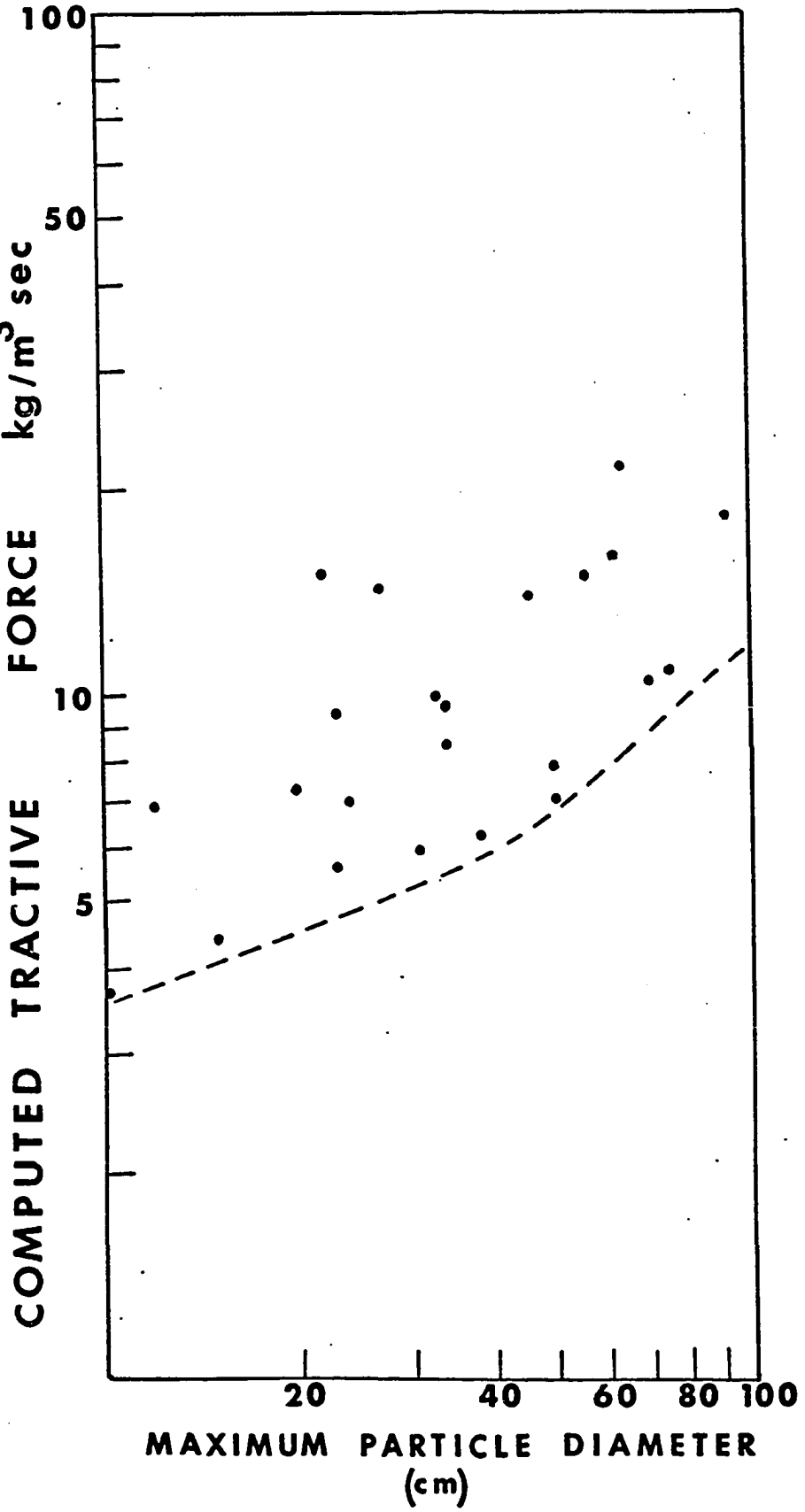

Figure 72. Logarithmic plot of maximum particle diameters and tractive forces for selected stations of principal washes in low order basins.

Hydraulic Geometry and Hydrology of Ephemeral Washes in Low Order Drainage Basins

The hydraulic geometry, as measured from residual high water marks of maximum flood events, is listed for selected stations along the trunk washes of low order basins in Appendix VI. Additionally, hydrologic parameters, such as discharge and velocity, are summarized for these stations in Appendix VI. A summary of the most important relationships of the hydraulic geometry and hydrologic parameters of these washes are given below:

1. The maximum width, width of berm, and width-depth ratio increase with distance from the head of the wash (Appendix VI).

2. The depth of flow and channel slope decrease with distance from the head of the wash for the majority of trunk washes (Appendix VI).

3. The maximum width, maximum depth of flow, and cross-sectional area show little net change down the trunk washes of the low order basins developed on the alluvial apron of the Eagletail Mountains (Appendix VI).

4. The width of the wash channel is larger than the width of the berm near the head of the ephemeral wash, but the berm gradually becomes wider than the channel with distance from the head of the wash (Appendix VI).

5. Width of the channel initially increases with distance from the divide, passes through a maximum, and then decreases (Appendix VI). That is, a point occurs on the majority of trunk washes where the channel is locally wide, and this point is here defined as the local maximum channel width. Aerial reconnaissance and other field observations show that this relation-

ship occurs on other washes not studied in detail (Fig. 82B).

6. The velocity computed at each station on the trunk washes is based on the average of the Mannings velocity and gravity wave velocity and is listed in Appendix VI. In this study, flow is assumed to be steady for the purpose of using these formulas. Renard and Keppel (1966) found that the average of these two computed velocities equalled the measured peak velocity of floods in ephemeral washes of southeastern Arizona and central New Mexico. The Mannings and gravity wave velocities computed from the hydraulic geometry of the washes in the present study show approximately similar values (Appendix VI). The averaged velocities from these two equations for the washes in low order basins of the study area are usually greater than 2 m/sec. According to the relationship between velocity, grain diameter, and state of sediment established by Sundborg (1956), the washes are transporting and eroding the beds of the washes during the maximum flood events. Additionally, the computed Froude number for each station supports this relationship for the upper reaches of the wash (Appendix VI); however, the Froude number drops below 1 at some point down the wash, and erosion may no longer occur with these velocities.

7. Maximum discharge computed from the hydraulic geometry of these washes is given in Appendix VI. Maximum discharge shows both net increases and decreases down the washes. The decrease in discharge down wash may result from infiltration into the alluvium covering the wash bed, and the increase may be due to isolated storm cells centering on the lower portions of the basins, which produce higher discharges in the distal regions.

8. Tractive forces are computed for the entire wetted perimeter of the ephemeral washes and are given in Appendix VI. Hydraulic radius is substituted for depth in the conventional equation, $T = \gamma DS$. In almost all washes, the tractive forces show a net decrease with distance down the wash.

Sources of errors in computations of those hydrologic parameters listed in Appendix VI may be attributed to: a) use of channel slopes instead of water surface slope in the Mannings equation; b) assuming steady state flow conditions during flood events; c) using maximum depth of a flood event rather than several depths across the cross-section of the wash to compute the discharge; and d) assuming the specific weight to be constant in the tractive force equation.

Geomorphic Relationships in Low Order Drainage Basins

The major relationships between geomorphic, hydrologic, and sedimentologic parameters and the hydraulic geometry of trunk washes are described below:

1. Spearman Rank correlation coefficient, r_s, is computed for the local maximum channel width and its distance from the head of the wash for the low order basins (Appendix I). The value of r_s is 0.88 and is significant at $\alpha = 0.05$. This indicates that the length of the channel above the maximum channel width is related to the local maximum width of the channel. That is, with longer channel length, the channel will be wider at the local maximum. A logarithmic plot of local maximum channel width and channel length to that point is given in Figure 73, which supports a

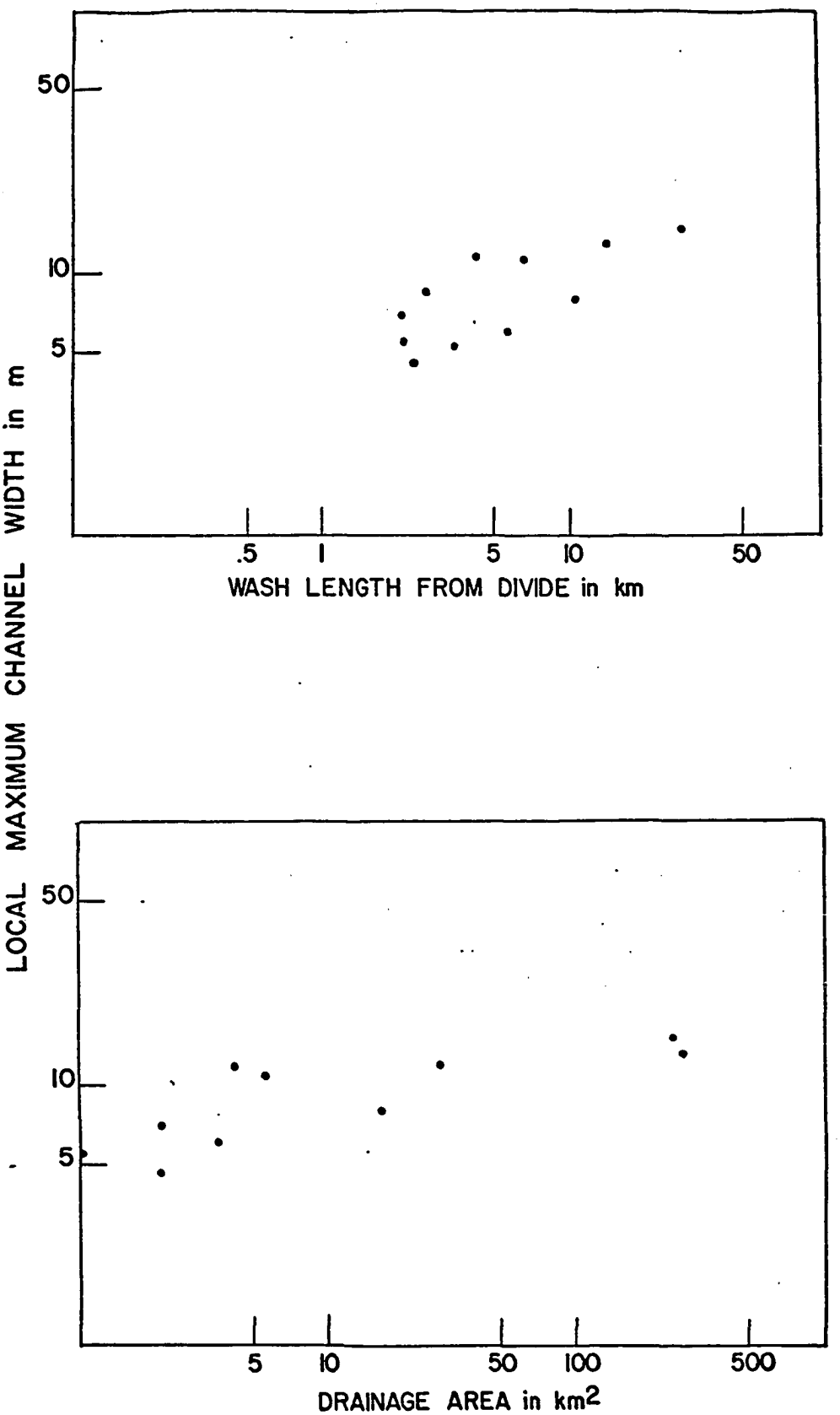

Figure 73. Logarithmic plots of local maximum channel width and length of wash and drainage area above the maximum width for principal washes in low order drainage basins.

positive relationship between these two variables.

2. The relationship between local maximum channel width and the drainage area above that maximum is tested by the Spearman Rank correlation coefficient (Appendix I). The correlation coefficient is 0.82, which is significant $\alpha = 0.05$. A logarithmic plot of the local maximum width of the channel and the drainage area above that point shows a positive relationship between drainage area and maximum width of the channel (Fig. 73).

3. The local maximum width of the channel in 80 percent of these basins is shown to be proportional to both channel length and drainage area above the local maximum. The relationship between the length of the channel and drainage area of these low order basins at the local maximum channel width r_s is equal to 0.988, which is significant at $\alpha = 0.05$.

A power function regression equation is used to analyze the relationship between channel length and drainage areas above the maximum, since these variables show a linear relationship on logarithmic plots (Fig. 73). The regression equation for the relationship is: $A_d = 2.5^{1.1} L_c$, where A_d is the drainage area and L_c is the channel length above the local maximum channel width. The regression coefficient for this power function regression is 0.923. A plot of these variables is given in Figure 74. Hack (1957) found the relationship between channel length and drainage area along any point on a stream in northeastern United States to be a power function in the form of $L_c = 1.4 A_d^{0.6}$. The relationship between drainage area and channel length in low order basins of the Harquahala Valley can be expressed in a similar form as Hack's equation and is illus-

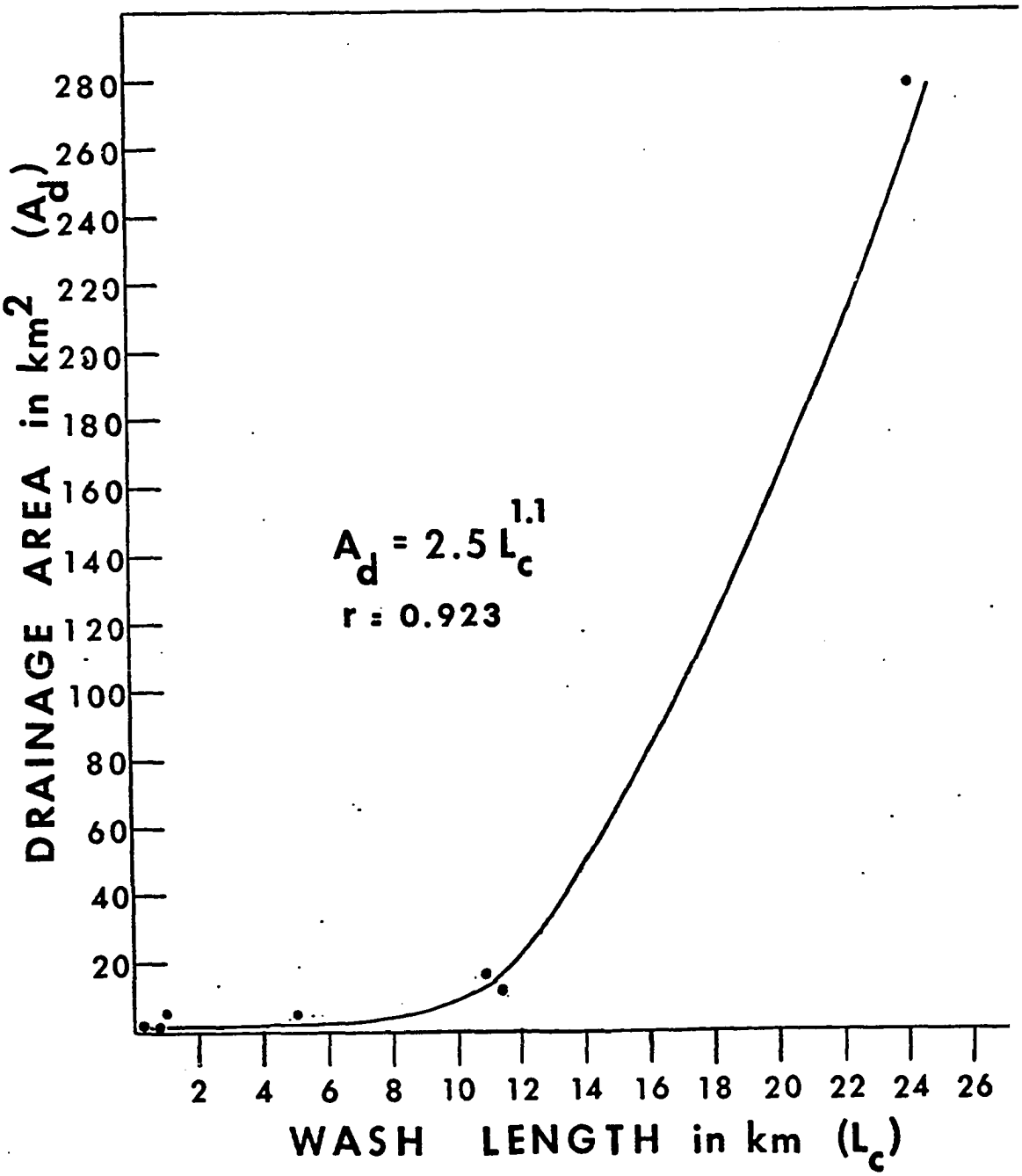

Figure 74. Relationship between wash length and drainage area above local maximum channel width for principal washes in low order drainage basins. Regression coefficient is expressed as 'r'.

trated in Figure 75. This relationship is $L_c = 0.60\ A_d^{0.75}$ at the point of maximum channel width.

These two equations relating channel length and drainage area for ephemeral washes in the low order basins can be rewritten as a dimensionless ratio, as follows:

Assume drainage area, A_d, is equal to the mean basin width, $\bar{b}$, times the channel length, L_c: $A_d = \bar{b}\ L_c$. Then, the equation, $A_d = 2.5\ L_c$, is expressed as $\bar{b}\ l_c = 2.5\ L_c$, or $\bar{b} = 2.5$, assuming exponent 1.1, to be 1. The mean widths of the low order drainage basins (Appendix VI) are averaged and are equal to 2.4, which supports the dimensionless ratio given above.

It is concluded that mean width of low order drainage basins and channel lengths, or the basin geometry, influence the position of the local maximum channel width. Since the basin geometry influences the discharge (Chow, 1964), the discharge of maximum flood events in low order drainage basins in the Harquahala Valley may influence the point of maximum channel widening.

4. In addition to the basin geometry, the local maximum channel width is related to thresholds in the tractive forces along the wash bed. Table 6 gives the tractive force for each low order basin, as well as the major variables of tractive force. These variables are depth, or in this case hydraulic radius, and slope of channel. Maximum channel widening occurs when tractive forces are less than 12 Kg/m^3sec^2, depth of flows is less than 1 m (or hydraulic radii less than 0.900) and slopes are less than 1.4°.

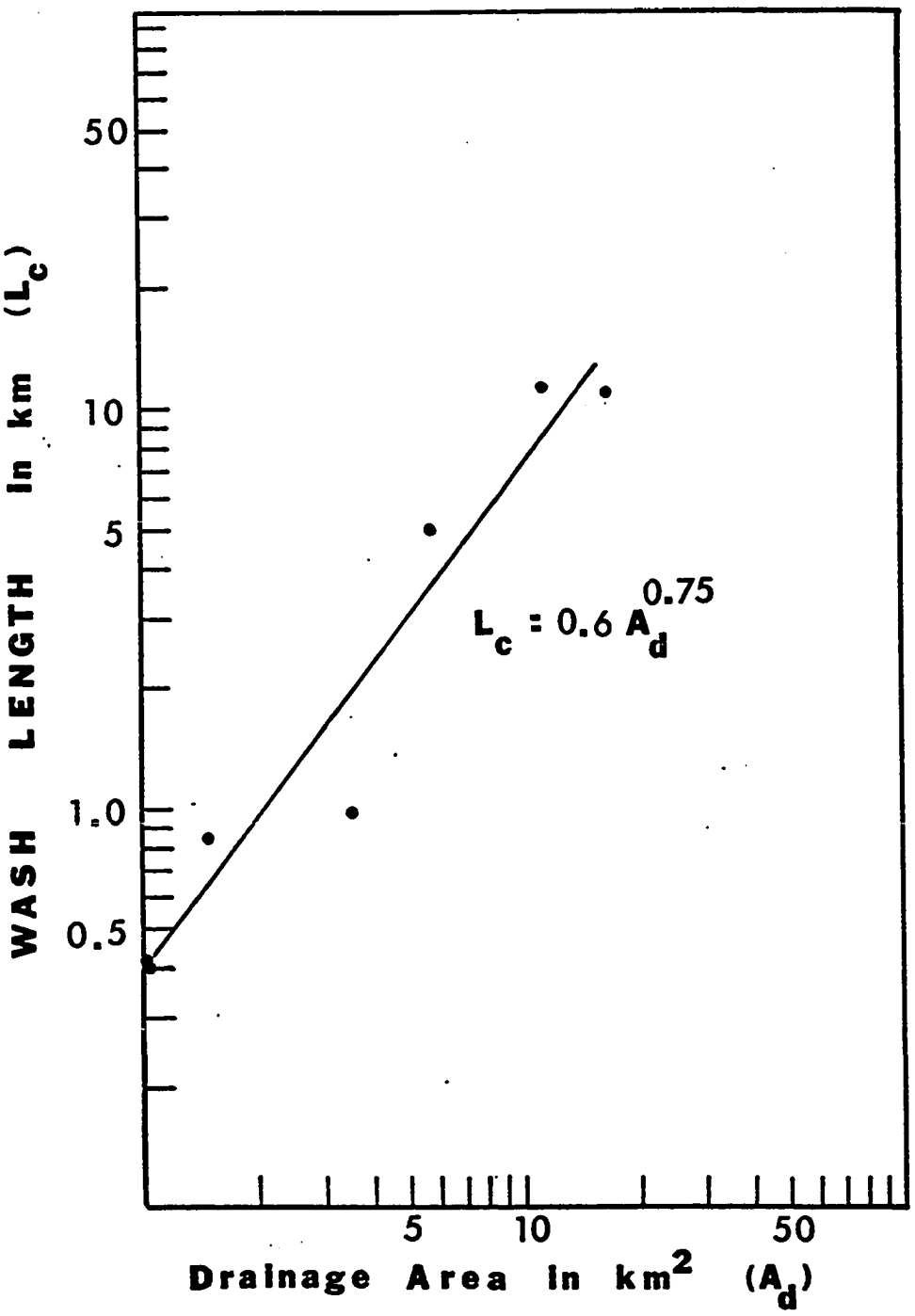

Figure 75. Logarithmic plot of drainage area and length of wash above local maximum channel width of principal washes in low order drainage basins. Regression coefficient given as 'r'.

LOW ORDER BASIN	MAXIMUM DEPTH (m)	HYDRAULIC RADIUS	SLOPE (degrees)	TRACTIVE FORCE (Kg/m^3sec^2)
LMQ-A	.70	.697	.5	5.9
LMQ-C	.81	.760	.75	11.4
LMQ-D	.66	.638	.60	7.0
BHMQ-A	.48	.460	1.00	7.8
BHMQ-B	.76	.708	.75	9.9
CPQ-A	.53	.612	1.30	10.8
CPQ-B	.51	.501	.30	3.0
CPQ-C	.51	.473	.25	2.4
CPQ-D	1.07	.887	.60	9.8
EMQ-A	.51	.487	1.20	10.2
EMQ-B	.34	.400	1.40	10.8

Table 6. Selected hydraulic geometry parameters and tractive forces for principal washes draining low order drainage basins in study area.

A Sign Test (Siegel, 1956) is used to determine changes in computed tractive force down ephemeral washes for selected alluvial aprons in the study area (Appendix I). This test indicates that there are more washes in the alluvial aprons whose tractive forces at the local maximum channel width are less than the computed tractive forces at the preceeding (upwash) station. That is, there are a significant number of washes which show a reduction in tractive force at the local maximum channel width. This relationship suggests that decreases in tractive forces may be related to the maximum channel width.

5. The computed discharge at the maximum channel width is plotted against the drainage area above that local maximum for low order drainage basins with and without caliche rubble (Qcr) in Figure 76. These variables are related to each other by a power function for low order basins with different surficial deposits. Power function regression equations are used to determine the equations for these functions, and they are:

a) $Q_c = 10.4\ A_d^{.72}$ for low order basins without caliche rubble, and where Q_c is the computed discharge at the local maximum channel width and A_d is the drainage area above that point. The regression coefficient is 0.990.

b) $Q_c = 25\ A_d^{.36}$ for low order basins with caliche rubble at the maximum channel width. The regression coefficient for this equation is 0.983.

The logarithmic plots of these variables and the regression equations indicate that low order basins with caliche rubble have higher computed discharges at the local maximum channel width than those basins

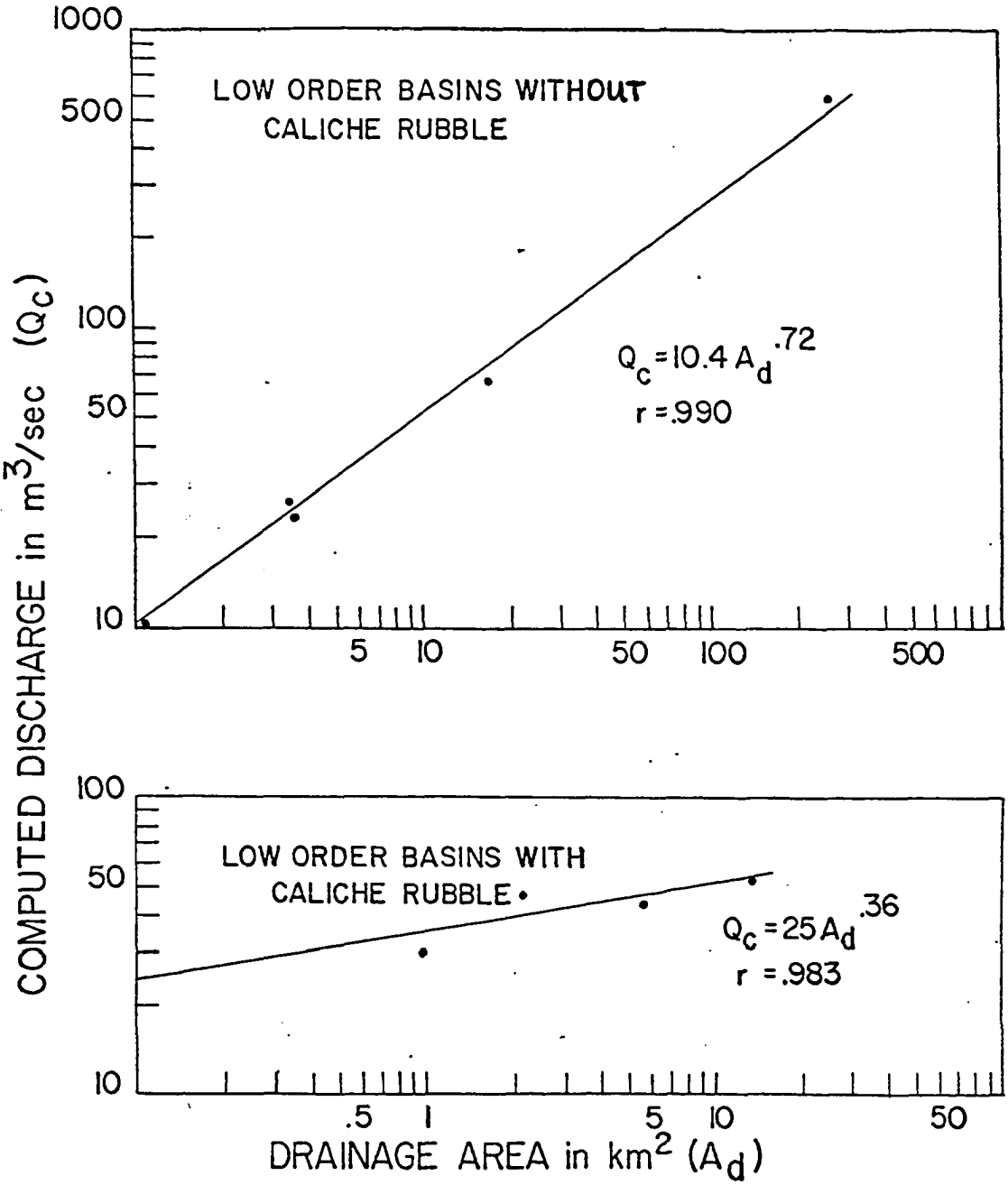

Figure 76. Logarithmic plots and regression analyses of computed maximum discharge and drainage area at the local maximum channel width in low order basins with and without caliche rubble (Qcr).

without the caliche rubble. This is expected since infiltration is low on caliche rubble surfaces and runoff is higher (Cooley et al., 1973). The lower slope of the line on the logarithmic plot of discharge and area in basins with caliche rubble indicates that basins larger than 10 km^2 would have lower discharges than basins without caliche rubble. An explanation of this relationship is that low order basins with caliche rubble are not larger than 10 km^2 in the Harquahala Valley; therefore basins above this size follow the relationship: $Q_c = 10.4\ A_d^{.72}$.

6. As the channel decreases in width after the local maximum, the berm increases rapidly in width (Appendix VI). Observations during the field work, plus these results, indicate a change in the mode of sediment transport down the alluvial apron. Figure 77 illustrates the results of sediment transportation during a summer thunderstorm in the Harquahala Valley. The wash is the same in each picture of Figure 77, but part A is in the mid apron region and part B is in the distal portion of the apron. Only fine grained sediments, which are carried as suspended load, are found in the distal alluvial apron. Coarser sediments are dropped further up the alluvial apron slope. Additionally, the width-depth ratio increases rapidly between these two points.

The increase in berm width is illustrated by the rapid increase in the width-depth ratios for the trunk washes in the low order basins (Appendix VI). A plot of width-depth ratio with distance down the wash is given in Figure 78. The point at which a rapid increase in the width-depth ratio occurs can be seen as an inflection point on the curves. The inflection point falls within a range of width-depth ratios equal to

A. Mid portion of alluvial apron has coarse sediment deposited.

B. Distal region of the same apron and wash has fine sediments deposited; Burnt Mountain in background. Arrow indicates flow direction.

Figure 77. Flood deposits resulting from a summer thunderstorm on Big Horn Mountain alluvial apron.

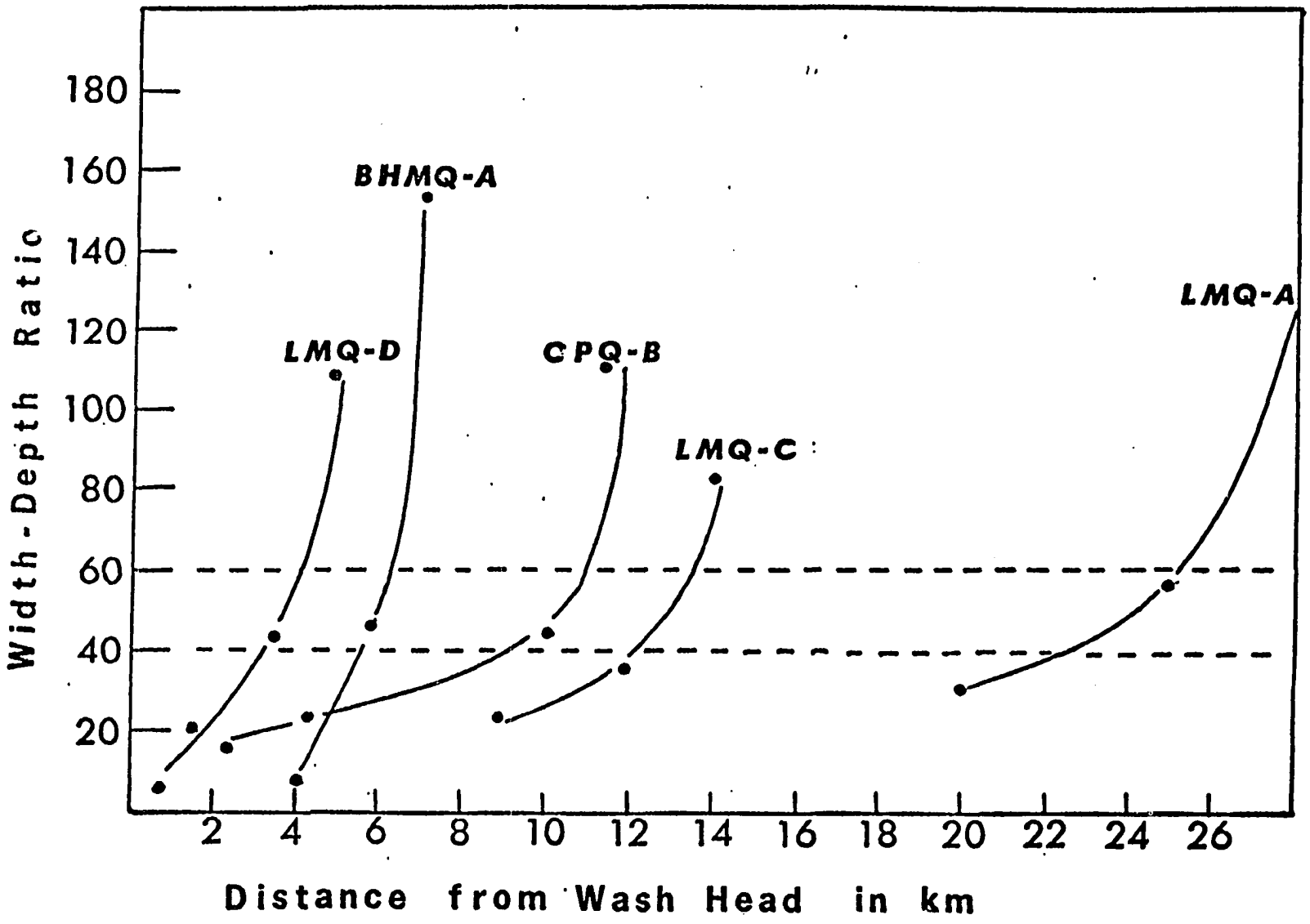

Figure 78. Relationship between width-depth ratio and distance from head of principal wash for selected low order drainage basins. Inflection point where width-depth ratio increases

40 to 60. The mean width depth ratio for this inflection point is 50.

The drainage area and channel length above the width-depth ratio inflection point is plotted on a logarithmic scale in Figure 79. A power function regression is used to determine the relationship between drainage area and wash length above the inflection point on width-depth ratios, or where the width depth ratio has a sudden increase. The power function regression equation is $A_d = .138\ L_c^2$ and has a regression coefficient of 0.960.

This equation can be rewritten as a dimensionless ratio. Assume $A_d = L_c\ \bar{b}$ (where $\bar{b}$ is the mean basin width), then $\bar{b}\ L_c = .138\ L_c^2$. This can be expressed as $\bar{b} = .38\ L_c$, $\bar{b}/L_c = .138$, or $L_c/\bar{b} = 7.4$. The average ratio of channel length to mean basin width averaged for all the low order basins is equal to 7.1. This supports the computed ratio given by the power function relationship above.

Thus, the point along an ephemeral wash in the Harquahala Valley where the width of the berm increases rapidly occurs typically when the width-depth ratio is greater than 50. This increase in berm width is directly proportional to the ratio of mean basin width and channel length above this point in low order drainage basins.

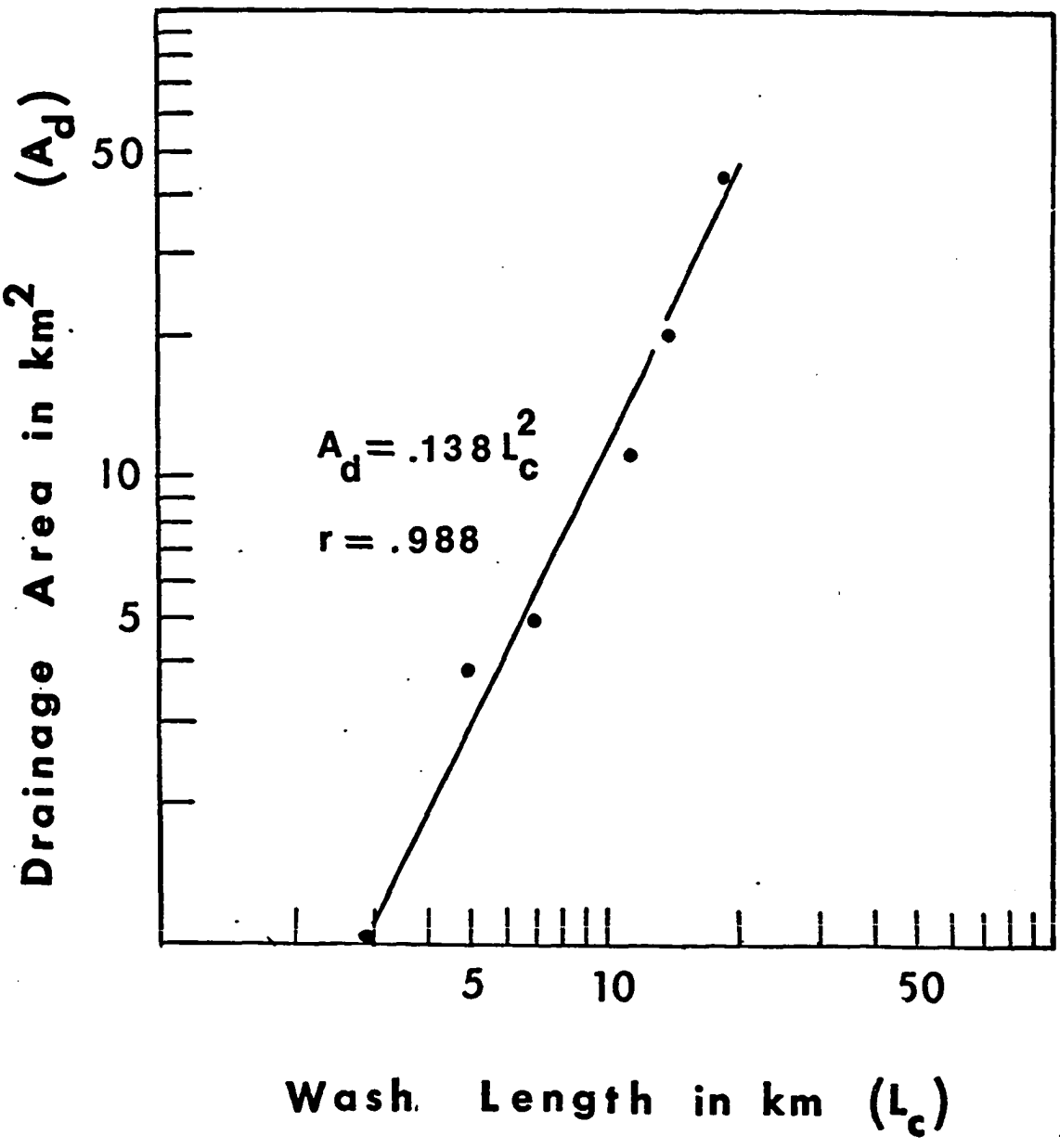

Figure 79. Logarithmic plot and regression analysis of wash length and drainage area above that point on the wash where the width-depth ratio increases rapidly. Width-depth ratios are typically greater than 50 for this relationship. Regression coefficient is given as 'r'.

DISCUSSION OF THE RESULTS

SURFICIAL PROCESSES IN LOW ORDER DRAINAGE BASINS OF THE HARQUAHALA VALLEY

Hydrologic Behavior of Ephemeral Washes

The hydraulic geometry measured during field studies is based on the peak, or maximum, flood event recorded at each station. The discussion of the hydrologic behavior of ephemeral washes is therefore based on flow during maximum discharges.

In the Harquahala Valley, the short, intense rainfall from July to August produces flash floods with the highest runoff (Fig. 18). Dubief (1953) noted similar relationships in the Saharan Desert, where low rainfall with high intensity in the summer produces more runoff than a larger amount of less intensity in the winter.

The hydrographs of summer flood events on Centennial Wash have steeply rising limbs, very peaked curves, and less steep, falling limbs (Fig. 14). These hydrographs are interpreted as having very short durations of peak flow, which follows very closely to the front of the flood pulse. The steep, rising limbs on the hydrographs indicate a short rise time. These flood events produce a large amount of discharge in a short amount of time near the beginning of the pulse, therefore, the discharge appears as a "wall of water" during the flash flood. Renard and Keppel (1966) have analyzed the hydrographs of ephemeral streams in southeastern Arizona and central New Mexico. They have found that the short, intense rainfall of summer storms causes the largest amount of

runoff, and that the processes by which this runoff is transmitted from portions of the basins to a given channel cross-section are reflected in the hydrographs. Hydrographs from runoff in the southern desert of Israel (Schick, 1970) show steep, rising limbs similar to those found in this study and by Renard and Keppel. These investigators have related the short rise time on these hydrographs to transmission losses into the beds of washes. Additionally, Renard and Keppel have related the shortened rise time on hydrographs to abrupt, translatory waves of water moving off of the interfluves. The similarity of the hydrographs on Centennial Wash and those constructed by Schick, Renard, and Keppel suggests that transmission losses are important processes affecting flood events in the study area.

Measurement of transmission losses in the eastern Sonoran Desert range from 23 to 80 percent (Babcock and Cushing, 1942). Transmission losses cannot be evaluated on Centennial Wash since there is only one gauging station. The New River, 50 km east of the study area, has approximately 70 percent reduction in peak discharge over a 30 km reach during a summer thunderstorm (Fig. 80). The actual volume of water, or runoff, lost by infiltration into the wash is probably much higher. Transmission losses in the Harquahala Valley must be equally as high as those described by Babcock and Cushing (1942). Field observations indicate that a summer storm in 1974, which produced approximately 1 cm of rainfall in a two hour period, did not yield enough runoff to reach the axial drainage and exit the Harquahala Valley. Thus, transmission losses, combined with evaporation, effect 100 percent reduction in runoff in the bolson plain.

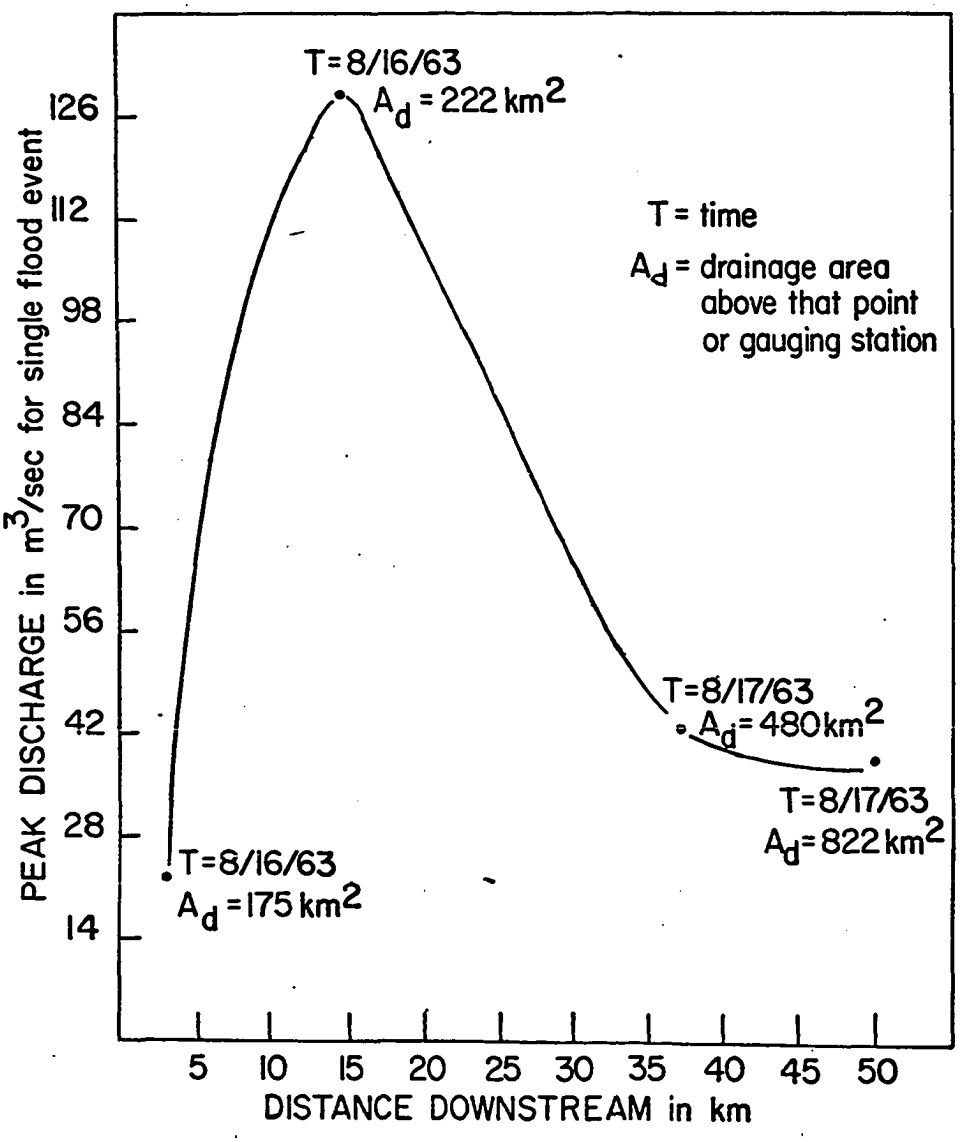

Figure 80. Relationship between peak discharge and distance down channel for a single flood event on New River, Arizona. Data based on Wehro (1967).

Transmission losses appear to be the most rapid and highest in the upper portion of the alluvial apron. Little runoff reaches the center of the bolson plain unless rain falls directly on this area. Personal communications with inhabitants of the Harquahala Valley indicate that after heavy rainfall on the center of the bolson plain, water may pond to a depth of nearly 0.3 m. Babcock and Cushing (1942) found that transmission losses in desert washes of Pinal County, Arizona are highest in coarse gravels and lowest in fine silts and clays. That is, the rate of infiltration is inversely related to the fine sediment content in a flood pulse and in a wash bed. Observations during the field season of 1974 indicate similar relationships to those described by Babcock and Cushing. Several borrow pits, where gravel was taken for the construction of the Interstate highway, are lined with fine silts and clay in the deepest portions. Water has been observed standing in the deepest part of these borrow pits for several days after rainfall. Infiltration is reduced by the silt and clay covering, and evaporation may further reduce the volume of water.

Coarse gravels and sands, where water is readily transmitted into the alluvium, occur in the mid to proximal portions of the alluvial aprons in the Harquahala Valley (Fig. 25). The fine sediments, which reduce rapid infiltration, are most extensive in the lower or distal portion of the alluvial aprons (Fig. 25). Infiltration should be the most rapid and highest in the channels of the washes in the upper apron regions of the Harquahala Valley, since the silt and clay content and extent increases in the washes down apron (Figures 69 and 71).

Appendix VI illustrates that the width-depth ratio increases with

distance from the head of the wash as the fine grained berm sediments increase in width. The increase of width-depth ratio at an exponential rate down the wash implies a rapid change from channelized flow to unchannelized flow with distance down the aprons. Additionally, observations of the recent results of a flood in the study area indicate that the width increases as the depth decreases (Fig. 77). Rahn (1967) observed streamflood, or channelized flow, in the upper apron, and sheetflow in the lower apron of the Harquahala Valley. Blissenback (1954) related the occurrence of sheetfloods and streamfloods to the amount of dissection on alluvial fan surfaces. The greater the drainage density and the deeper the incision below the level of the fan surface, the less opportunity for washes to overflow and form unchannelized flow.

The drainage texture map exhibits the regional dissection in the Harquahala Valley (Fig. 9). Since the sheetflow is inversely proportional to the degree of dissection, the Harquahala Valley has primarily channelized flow in 30 percent of the area and sheetflow in 70 percent, assuming maximum discharge events.

The change from channelized to unchannelized flow across the alluvial aprons increases with distance from the divide. Based on the change in width-depth ratios, this change in flow conditions may be exponential with distance. The relationship of width-depth ratio and length of wash from the divide is exponential and is expressed as power function curves (Fig. 78). The results of these regression analyses are given in Table 7. The general relationship between width-depth ratio and wash length from the divide can be described by an equation of the form: $W/D = k\ L_c^{\ j}$ where W/D is width-depth ratio, L_c is the length of the wash

LOW ORDER DRAINAGE BASIN	REGRESSION EQUATION	REGRESSION COEFFICIENT
LMQ-A	$W/D = 0.1\ L_c^{6.7}$	0.934
LMQ-C	$W/D = 0.06\ L_c^{2.7}$	0.990
LMQ-D	$W/D = 8.1\ L_c^{1.6}$	0.980
BHMQ-A	$W/D = 0.01\ L_c^{5.7}$	0.954

Table 7. Regression equation and coefficients for relationship between width-depth ratio and length of wash from divide in selected low order drainage basins.

from the divide, k is a coefficient which varies from 0.01 to 8, and j is an exponent which ranges from 1.5 to 6.7. The increase of the width-depth ratio with increasing wash length depends on transmission losses which reduce the discharge of a flood event and the depth of incision of the wash below the apron surface. The exponent, j, is greater than unity, which indicates that the width-depth increases faster than the length of the wash. This is reasonable since channelized flow occurs in a limited area in the proximal apron regions and transmission losses are most rapid in this area due to the larger amounts of coarse sediment lining the washes.

Channel Forming Events and Aggradation in Low Order Drainage Basins

The ephemeral washes of low order drainage basins in the Harquahala Valley have two components which are differentiated by topography and sedimentology (Fig. 60). These two components are the channel, containing coarse gravel, and the berm, containing fine silts and sands. The channel gravels are primarily moved by traction, as bed load. The finer sediments of the berm are moved primarily in suspension. These modes of transportation are supported by plotting mean grain diameter (d_{50}) of the berm sediments and the grain diameter at the 75 percentile for sediments on Sundborg's (1956) chart, which relates grain size, velocity, and the state of the sediment (Fig. 81).

The berm sediments are topographically higher than the channel gravels, which implies that with increasing discharge at a station, the amount of suspended sediment increases. The relationship between discharge and suspended load at a station in ephemeral washes of New Mexico has been described by Leopold and Miller (1956). They found that suspended

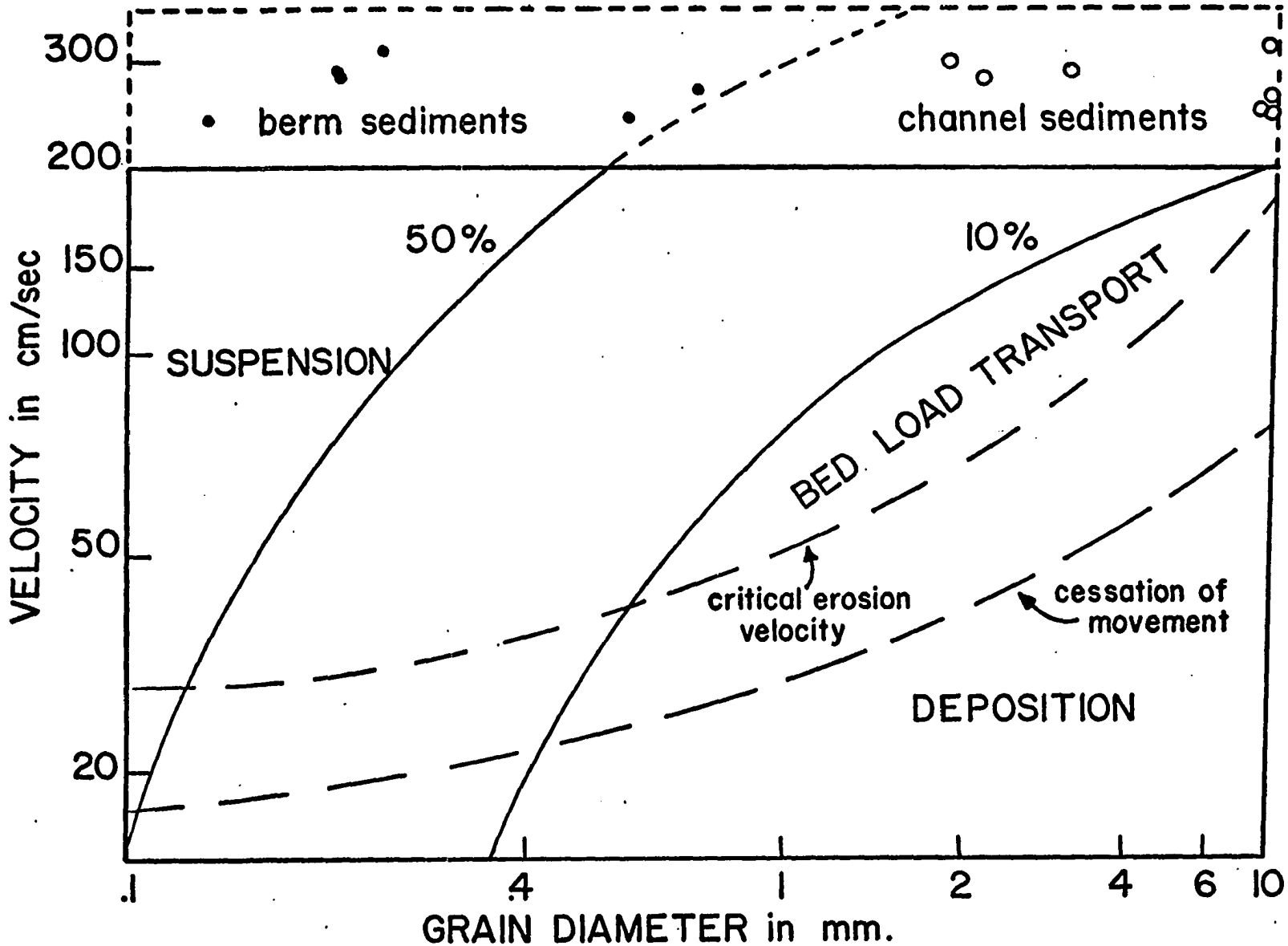

Figure 81. Relationship between computed velocity, grain diameter of berm sediments (d_{50}) and channel sediments (d_{75}), and state of sediment. Modified from Sundborg (1956).

load increases with increasing discharge at a cross-section along an ephemeral wash. The form of the washes in the Harquahala Valley therefore indicates a similar relationship between discharge and suspended load.

The width of fine grained berm sediments and the width-depth ratio increase down the alluvial apron exponentially (Fig. 78; Table 7). These results suggest that the amount of suspended sediment carried down the wash increases with distance from the divide. Particle size distributions for the washes in Figures 69 and 71 show an increase in the weight percent of fine sand and silt, which supports the concept that suspended load increases down the alluvial apron. Leopold and Miller (1956) calculated that the suspended load increases faster than the amount of discharge down ephemeral washes of New Mexico, as $S_1 = m\ Q^n$ where S_1 is suspended load, Q is discharge, m is a constant, and n is an exponent which is greater than unity (1.3 is the average value of n computed by Leopold and Miller). In the study area, the width-depth ratio is influenced by the width of the berm and increases down the wash exponentially (Fig. 78). The exponents in the equations in Table 7 are also greater than unity; therefore, those processes which related the suspended load to discharge in ephemeral washes in New Mexico appear to apply to the ephemeral washes in the Sonoran Desert. Leopold and Miller (1956), Chow (1964), and Schick (1970) attribute the greater increase in suspended load to discharge down ephemeral washes to transmission losses which reduce the volume of water. The suspended load-discharge ratios in the washes of low order drainage basins in the study area are interpreted as increasing with distance from the divide due to infiltration into coarser sediments.

Observations reveal that sheetfloods typically have high concentrations of fine suspended sediment (McGee, 1897, Joly, 1952; Blissenback, 1954). The width of the berm, width-depth ratio, and sheet flow increase down wash, indicating that the berms are expanded laterally by unchannelized flow. General aggradation in the Harquahala Valley by lateral expansion of berm sediments over interfluves can be seen as buried palo verde tree trunks and buried desert pavement surfaces (Fig. 83B). It is believed that the primary mode of ephemeral wash aggradation is by lateral extension of berm sediments in the low order drainage basins.

Another type of wash aggradation occurs at the local maximum channel width. In plan view, the maximum width of the channel appears as an accumulation of gravel (Fig. 82B). Inspection of this point on the surface indicates that it is often a deposit of coarser material which has been deposited over the finer berm materials (Fig. 82A). The maximum width of the channel is proportional to the drainage area above this point (Figure 75) and is related to exceeding a threshold tractive force (Table 6). The point of maximum channel aggradation usually precedes the point at which sheet flow (overbank) occurs. It is concluded that channel aggradation occurs by streamflood (channelized flow) and not sheetflood in low order drainage basins.

During flood events in ephemeral washes in the Sonoran Desert, a maximum discharge occurs at some point along the reach of the wash (Fig. 80). The depth of flow increases prior to this maximum discharge, and with increasing depth the shear stresses, or tractive forces, increase. After the maximum discharge, the depth of flow and tractive forces are decreasing. It follows that aggradation of the channel and

A. Coarse sediment deposited over fine grained sediment of berm; scale is .5 m.

B. Local maximum channel width produced by aggradation. Note large slump blocks from caving of banks.

Figure 82. Channel aggradation in ephemeral washes.

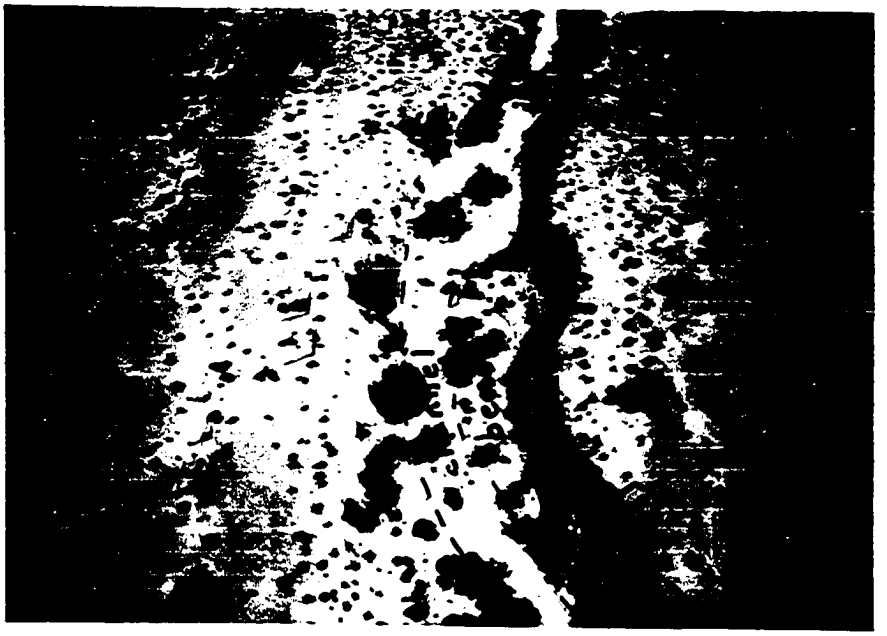

A. Big Horn Mountains alluvial apron.

B. Both photographs illustrate the burying of desert pavement by fine grained sediments.

Figure 83. Berm aggradation in distal portion of Harquahala Mountains alluvial apron.

development of the local maximum channel width must occur after the maximum discharge of an ephemeral wash.

Berm aggradation and channel aggradation occur during the late stage of a flood event, and both types of aggradation are related to transmission losses. Berm aggradation results from increasing suspended load-discharge ratios, and channel aggradation occurs when critical tractive forces are attained.

These aggradational processes primarily affect beds of washes rather than banks of washes. Observations by Leopold and Miller (1956) lead them to believe that bank erosion occurs primarily from caving after a flood event rather than during the flood. Field observations in the Harquahala Valley support this idea. Figure 86 illustrates the large blocks of debris which have caved in and are resting on the berm. These features and similar ones in the study area show no covering with flood sediments or alterations by floods. Since these blocks are resting on the berm which forms during maximum flood events and indicate no sign of modification, the banks of washes collapsed after the maximum flood and not during the event.

An exception to the post flood bank-failure process occurs in areas where secondary calcium carbonate has cemented the banks of the washes. Van Arsdale (1974) has shown that undercutting of the calcic horizon and collapse of the bank is effective as an erosional process in the Sonoran Desert.

Thus, the events that shape washes in the bolson plain of the Harquahala Valley occur during the summer months when rainfall causes

nearly 90 percent of the runoff. Rainfall during these months produces flash floods. The magnitude and frequency of these wash-modifying events are different from those events which modify channels in humid climates (Wolman and Miller, 1960). The computed discharges for the point of maximum channel width and incipient berm aggradation in their associated low order drainage basins are given in Appendix VI. Comparison of the values of discharge in Appendix VI and the flow duration curves for washes in the Sonoran Desert (Fig. 15) suggests that wash-modifying events have discharges that occur less than 0.05 percent of the time. Thus, such events that shape the channel and berm are infrequent and large in magnitude.

Relationship Between Wash Processes and Geomorphic Parameters of Low Order Drainage Basins

If width-depth ratios equal or exceed 50, berm aggradation occurs by sheet flow. The length of the wash and drainage area above the point of incipient berm aggradation are related by the expression: $A_d = .138\ L_c^2$ (Fig. 79). This expression can be rewritten as a dimensionless ratio of mean low order basin width to channel length, and this ratio is equal to 0.138. The calculated ratio is obtained by averaging the mean width to channel length ratio for all the low order basins and this is equal to 0.141. The difference between the computed and calculated ratio is 0.003. This suggests that the drainage area above incipient aggradation is equal to the mean basin width ($\bar{b}$) times the channel length (L_c). The range in the $\bar{b}/L_c$ values extends from 0.222 to 0.109. However, for those low order basins with width-depth ratios greater than 50, the values for

for the ratio of mean basin width and channel length cluster around a value of 0.140. Aggradation of ephemeral wash berms occurs if the mean low order basin width to channel length ratio approaches 0.140. The major washes of EMQ-A and CPA-C do not have width-depth ratios greater than 50 and do not show signs of berm aggradation. The values for this ratio of these basins are 0.115 for EMQ-A and 0.111 for CPA-C. In low order basins LMQ-D and LMQ-C, the width depth ratios are greater than 50 and berm aggradation is occurring. The values for the ratio of mean basin width to channel length are 0.143 for LMQ-D and 0.125 for LMQ-C.

Schumm (1956) defined the reciprocal of drainage density as the constant of channel maintenance. This constant is a measure of a basin's drainage texture, or the distance between channels, and is the area needed to maintain a unit length of drainage line (Schumm, 1956). Additionally, Strahler (1956) related the drainage area and channel length by this constant in the expression, $A_d = C\ L_c$ where C is the constant of channel maintenance. In the present study, the relationship between drainage area and channel length above incipient berm aggradation is expressed as $A_d = 0.138\ L_c^2$, where 0.138 is Strahler's constant C. The reciprocal of the mean drainage density on the alluvial aprons of the low order drainage basins is equal to 0.130. The difference between the theoretical and computed values of $1/D_d$ (D_d is drainage density on the alluvial apron of a low order basin) is 0.008. The equation can now be rewritten as $A_d = L^2/D_d$, which is rational assuming $\bar{b} \alpha L_c$ and $A_d \alpha \bar{b} L_c$, then $A_d \alpha L^2$. The inverse of the drainage density is, therefore, the constant relating drainage area to channel length.

The physical meaning of the low order basins' geomorphic parameters

of drainage area, channel length, and the inverse of drainage density (as measured on the alluvial apron) compared to berm aggradation is discussed below:

Aggradation of fine berm sediments is related to an increasing suspended load-discharge ratio (S_l/Q) with distance down the wash. The discharge is decreasing from infiltration into the channel (transmission losses). The source of suspended sediment is primarily from sheet erosion operating on the interfluves of basins drained by ephemeral washes (Leopold et al., 1966). The length of overland flow necessary to cause sheet erosion and pick up fine sediment therefore influences the sediment yield. Channel erosion has been shown to be relatively unimportant with respect to sediment yield for aggradation (Leopold et al., 1966).

In the present study, the geomorphic parameters of low order drainage basins are related to berm aggradation by the expression $A_d = L_c^2/D_d$. The constant, or inverse of drainage density, is equal to the distance between two drainage lines, and one half this distance is equal to the length of overland flow (Leopold et al., 1964). Thus, the length of overland flow is incorporated in the expression given above and represents a measure of the length across an interfluve necessary for runoff to erode fine sediments. The fine sediments eroded from the interfluves aggrading by sheet flow and cuase berms to extend laterally.

The length of overland flow defined by the expression, $A_d = L_c^2/D_d$, is 0.5 times $1/D_d$, or 0.5 times 0.138, which is equal to approximately 0.07 km, or 70 m. The mean length of overland flow for the low order drainage basins is computed by taking the reciprocal of drainage density on the alluvial aprons given in Appendix VI times 0.5, and these values

for each basin are averaged. This computed value is equal to 0.09 km, or 90 m, and is close to the theoretical value.

With increasing drainage density and decreasing overland flow, the fine sediments produced by sheet erosion should decrease according to the relationships defined above. The suspended load-discharge ratio is lowered with decreasing supply of fine sediments, and aggradation of the berm cannot occur. For example, low order drainage basins, EMQ-B and CPQ-C, have computed lengths of overland flow equal to approximately 0.05 km, since they have high drainage densities on their alluvial aprons (Appendix VI). These low order drainage basins do not have width depth ratios over 50 or show signs of berm aggradation. In low order drainage basins, CPQ-D and BHMQ-A, the length of overland flow computed from data in Appendix VI is equal to 0.08 km, or 80 m. These latter low order basins have width-depth ratios greater than 50 and show signs of major berm aggradation.

The length of overland flow necessary to supply fine grained sediments for berm aggradation for all low order drainage basins is approximately equal to 70 or 90 m. Berm aggradation does not occur if the length of overland flow is much larger or much less than this mean value. Additionally, the length of overland flow is a time independent variable since it is the inverse of drainage density. A measure of steady state conditions in landscape is to determine whether time independent variables cluster around a mean (Lattman, 1972, personal communication). It is concluded that the variation of the time independent variable, length of overland flow, around a mean value implies that berm aggradation is approaching a steady state condition in the Harquahala Valley for low order

drainage basins. Since all the computed length of overland flows vary about a mean value of 70 m, but do not all equal this value, it is interpreted that steady state conditions have not been attained.

Conceptual Model for Ephemeral Wash Aggradation

A conceptual model of washes in low order drainage basins of the Harquahala Valley is constructed to predict the spatial distribution of wash sediments, wash morphology, and wash hydrology during a flood event. The model is derived from the relationships among the previously discussed factors which influence wash aggradation. In addition, the model is based on a hypothetical series of flood hydrographs which are given in Figure 84. These hydrographs illustrate the behavior of a flood pulse as it moves down a major ephemeral wash and are based on general results found by Renard and Keppel (1966) and the behavior of a flood event on New River, Arizona (Fig. 80).

The conceptual model for aggradation and runoff during a flood pulse is as follows:

1. Runoff resulting from intense, short, and rather infrequent summer precipitation is transmitted down a wash. Recharge in the wash results from overland flow moving off the interfluves and into the drainage lines. Transmission losses occur in the channel gravels and produce steep, rising limbs on the hydrographs shown in Figure 84. When the transmission losses are greater than the recharge from overland flow, the runoff decreases in peak flow as well as volume. The decrease in volume can be seen as a decrease in area below the curves on the hydrographs

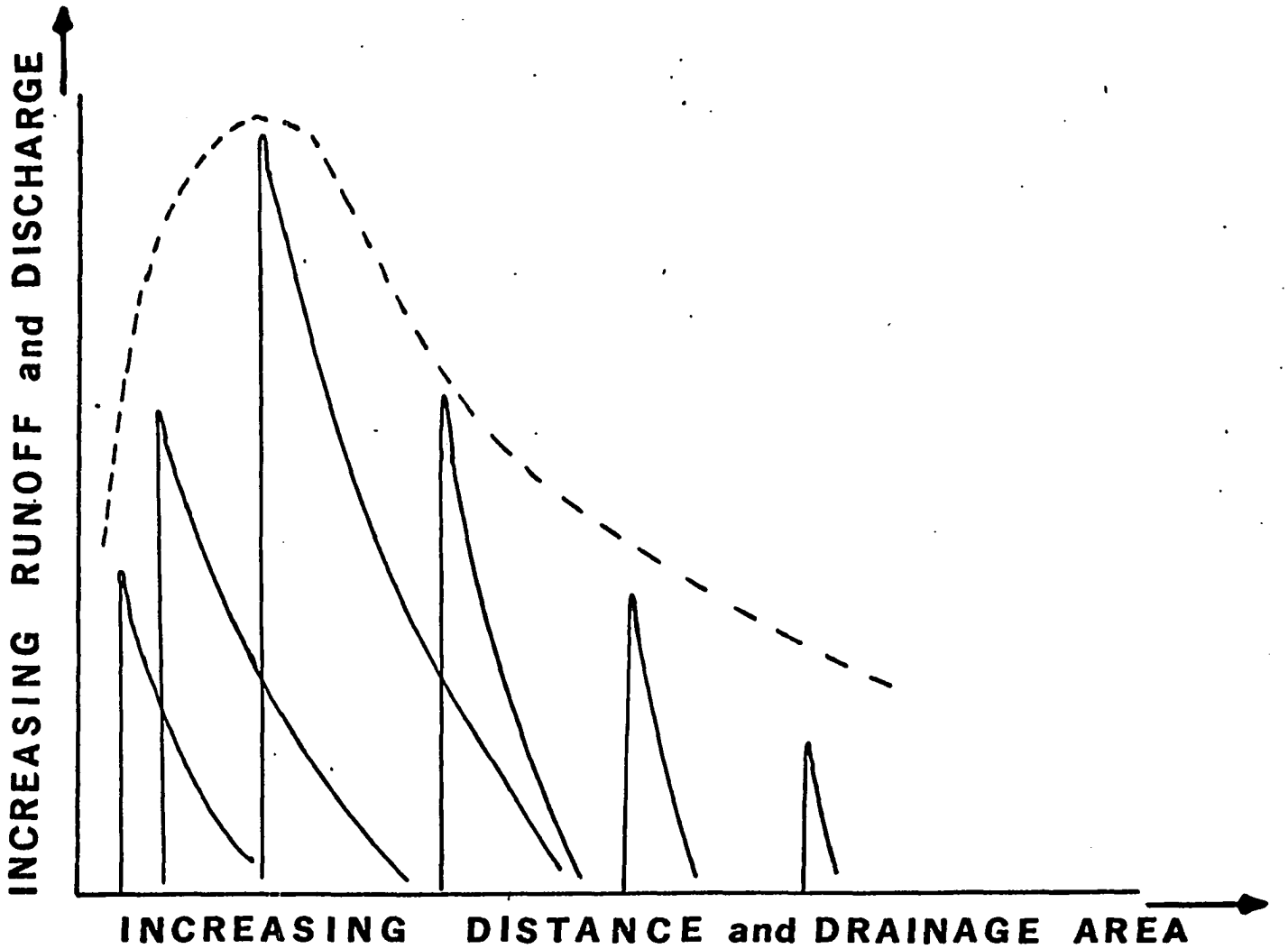

Figure 84. Hypothetical series of hydrographs on an ephemeral wash in the Sonoran Desert. Based on flood event on New River (Fig. 80) and data from Renard and Keppel (1966).

(Fig. 84).

2. Depth of flow attains a maximum with the peak discharge at some point along the wash (Fig. 84). As the runoff decreases, the depth of flow also decreases. Channel slope decreases with distance down the wash (Appendix VI). When the depth of the flow decreases to approximately 1 m, and channel slope reduces to approximately 1.5°, the tractive forces approach a critical, or threshold value. That is, the tractive forces are reduced to the point where bed load transportation cannot be maintained. The coarse sediments are deposited and spread laterally over the berm (Fig. 83). This produces a local maximum width in the channel of the wash. The mean width of the drainage basin is typically less than 2.5 km where channel aggradation occurs.

3. During the overland flow on the interfluves, fine grained sediments are eroded by sheet wash. These sediments are carried off the interfluves into small tributaries and eventually flow to the major wash of the low order drainage basin. The amount of sediment eroded from the interfluves and introduced into the washes influences the suspended load-discharge ratio.

4. After the maximum discharge passes, runoff is reduced, resulting in an increase of the suspended load-discharge ratio. As the mean length of overland flow in the low order drainage basin approaches 70 to 90 m, or as the mean basin width to channel length approaches a value of 0.138, the flood becomes overloaded with fine sediment.

5. On slopes less than 1° and areas of low dissection, the flood, which is overcharged with fine sediment, spreads laterally over the shallow interfluves. Sheet flow dominates during this portion of the flood event and is depositional, not erosional. The suspended load is deposited with decreasing velocity and extends the berm sediments laterally over the interfluves. The width-depth ratio of the wash increases rapidly with distance from the divide, and aggradation of the berm occurs when the width-depth ratio approaches 50. Berm aggradation is areally more extensive than channel aggradation.

6. All of these relationships are illustrated in Figure 85. The same flood pulse shown in Figure 84 is plotted in Figure 85 with new coordinates of slope, depth of flow, length of overland flow, ratio of mean basin width to wash length, and increasing drainage area and distance from divide. Data from the low order drainage basins are plotted on these diagrams, and the areas of channel and berm aggradation are delineated. This diagram may be useful for predicting aggradation during flood events in the Harquahala Valley.

Processes on Interfluves of Low Order Drainage Basins

Detailed topographic transects and longitudinal profiles illustrate the difference in the morphology and sedimentology of interfluves (Figs. 30 through 34). The interfluves of the most extensive Quaternary surficial deposit, coarse grained alluvial fans (Qfc), and on varnished gravels (Qgv), show varying degrees of desert pavement development. The concentration of coarse gravels at the surface of alluvial fan interfluves

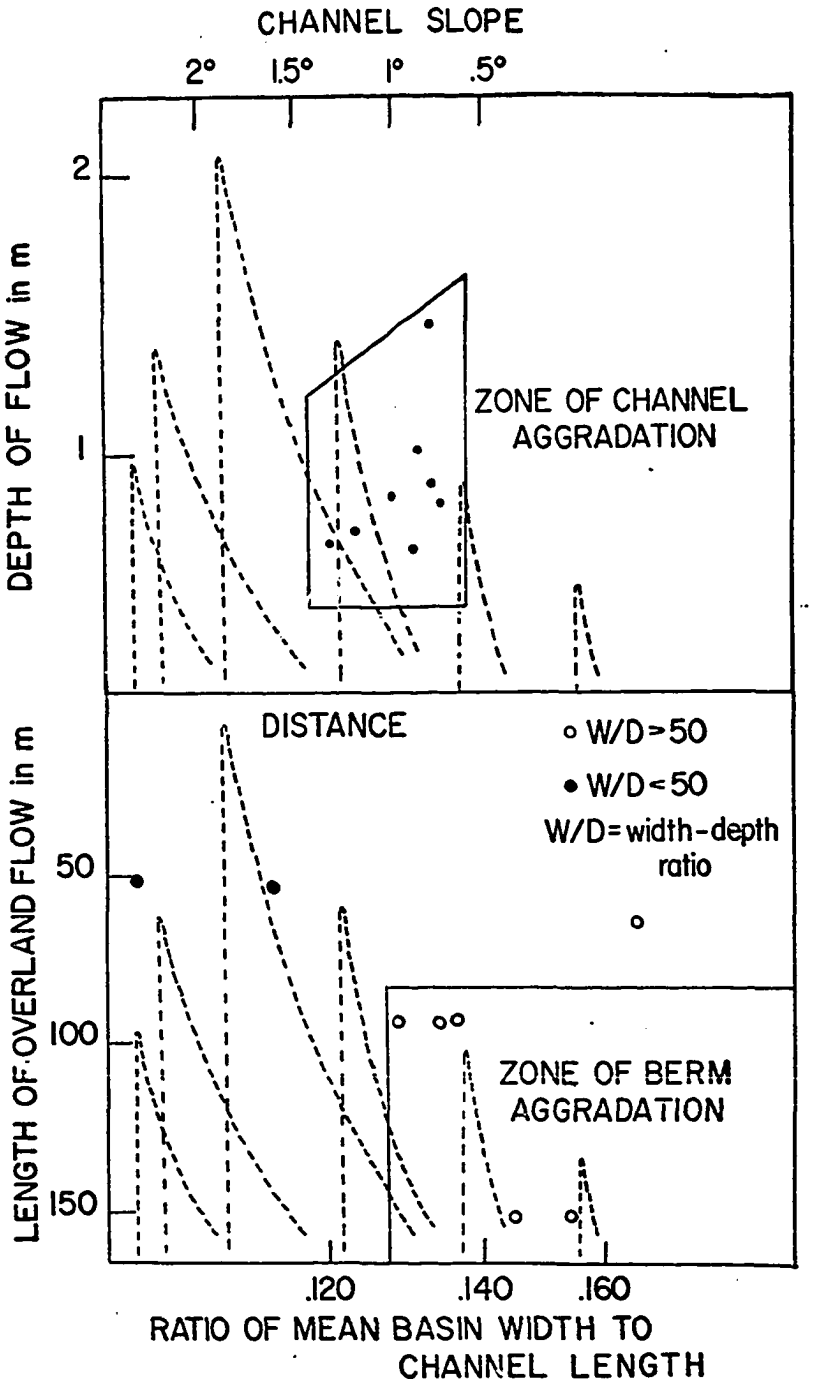

Figure 85. Relationship of geomorphic parameters which influence channel and berm aggradation in washes of low order drainage basins in the Harquahala Valley.

has been attributed to wind deflation (Gilbert, 1875; Moulden, 1905; Clements, et al., 1957; Symmons and Hemming, 1968), upward migration due to cycles of freezing and thawing (Mabbutt, 1965; Cooke, 1970), combinations of the former processes (Lattman, 1971), or removal of fines by slope, or sheet wash (Sharon, 1962). Denny attributed desert pavement development to flowage processes similar to creep. Cooke (1970) suggested that all the processes mentioned above have been important during the history of the pavement.

The following observations on desert pavements indicate a variety of conditions, or stages, of pavement development in the Harquahala Valley. In the mid and distal portions of the alluvial aprons, desert pavements are poorly developed. That is, the degree of concentration and area covered by coarse gravels is relatively small. In the proximal regions of the alluvial aprons, desert pavements have higher concentrations of gravels per unit area and cover larger areas (Fig. 35). The "development" of desert pavement is a measure of the concentration of gravels per unit area and the area covered with the gravels. The thickness of patina, or desert varnish, varies with the development of a desert pavement; less varnish occurs on poorly developed payments, and more varnish occurs on well developed pavements.

Field observations indicate that well developed pavements have a greater percentage of coarse gravels and silt-clay fractions. These pavements have a paucity of sand size material. Sieve analyses support the field observations (Appendix II). Well developed pavement has over 80 percent by weight gravels and over 6 percent by weight silt and clay fractions; whereas, less developed pavements have 65 percent by weight

gravel and less than 3 percent by weight silt and clay fractions (based on similar rock types). Nearly one half the weight percent of sand is removed from the well developed pavements. The grain size of these sands range from 0.125 to 2 mm in diameter. This is an optimum particle size for both suspended and bed load transport (Sundborg, 1956). Thus, the extent of desert pavements in the study area includes the removal of the sand size fraction by sheet wash on the interfluves.

Lowdermilk and Sundling (1950) and Sharon (1962) observed pavement formation resulting from surface runoff. The rate of removal of fine sediments by runoff is proportional to the slope of the surface (Lowdermilk and Sundling, 1950). These observations, together with the sieve and field analyses in the study area and the distribution of pavement development on the bolson plain, provide evidence for the importance of surface runoff in the form of sheet wash, forming pavements. The higher slopes of the proximal alluvial aprons are the location for the best developed pavement, and the lower slopes of the distal pavement are the location for the least developed pavement.

Under the present climatic conditions, freezing and thawing may be another process for concentrating gravels at the surface of interfluves and forming the thick silt layer beneath the pavement. For a 20 year average, 48 days have tempeatures below freezing (0°C), or, on the average, one sixth of the year has temperatures that drop below freezing. Thirty of the forty-eight days are in December and January, which combined, have 25 percent of the annual precipitation and only 12 percent of the annual runoff. There is a large amount of soil moisture during these months due to the low runoff, and this moisture can be used to form frost

which laterally and vertically displaces the fine sediments. Lattman (1971) demonstrated that frost-heaving from freezing and thawing cycles develops pavement in the desert near Las Vegas, Nevada.

Processes which appear to be actively destroying the desert pavement are either accelerated flowage of the silt and gravels during high soil moisture conditions toward the drainage lines or burial by fine grained sediments (Fig. 86). The drainage density and amount of relief produced by drainage lines incising into the alluvial apron are inversely proportional to the area of desert pavement. Channel erosion appears to accelerate the lateral flowage of the surface material and to "break up" the gravel armor and reduce the area covered by pavement. Additionally, in areas of low relief, the pavement may be buried beneath fine sediment deposited during sheetflood. These processes which destroy desert pavement occur in different locations on the alluvial apron. Accelerated 'creep' due to channel erosion is dominant in the upper regions of the apron, and deposition over the pavement is dominant in the lower alluvial apron regions.

Denny (1967) suggested that desert pavements are examples of steady state conditions in the desert of southern California, and that a balance between processes which develop and destroy pavements exists. In the study area of the Sonoran Desert, the maximum length and maximum width of well developed desert pavements are related by the expression: $W_{dp} = -.13 + .45\ L_{dp}$. The ratio of maximum length and width of the pavement segments is approximately equal to 3. The mean value for the computed ratios is 2.9 (Table 3), and the ratios have a maximum deviation of 0.6 from the mean. These data suggest that the area of desert pavement

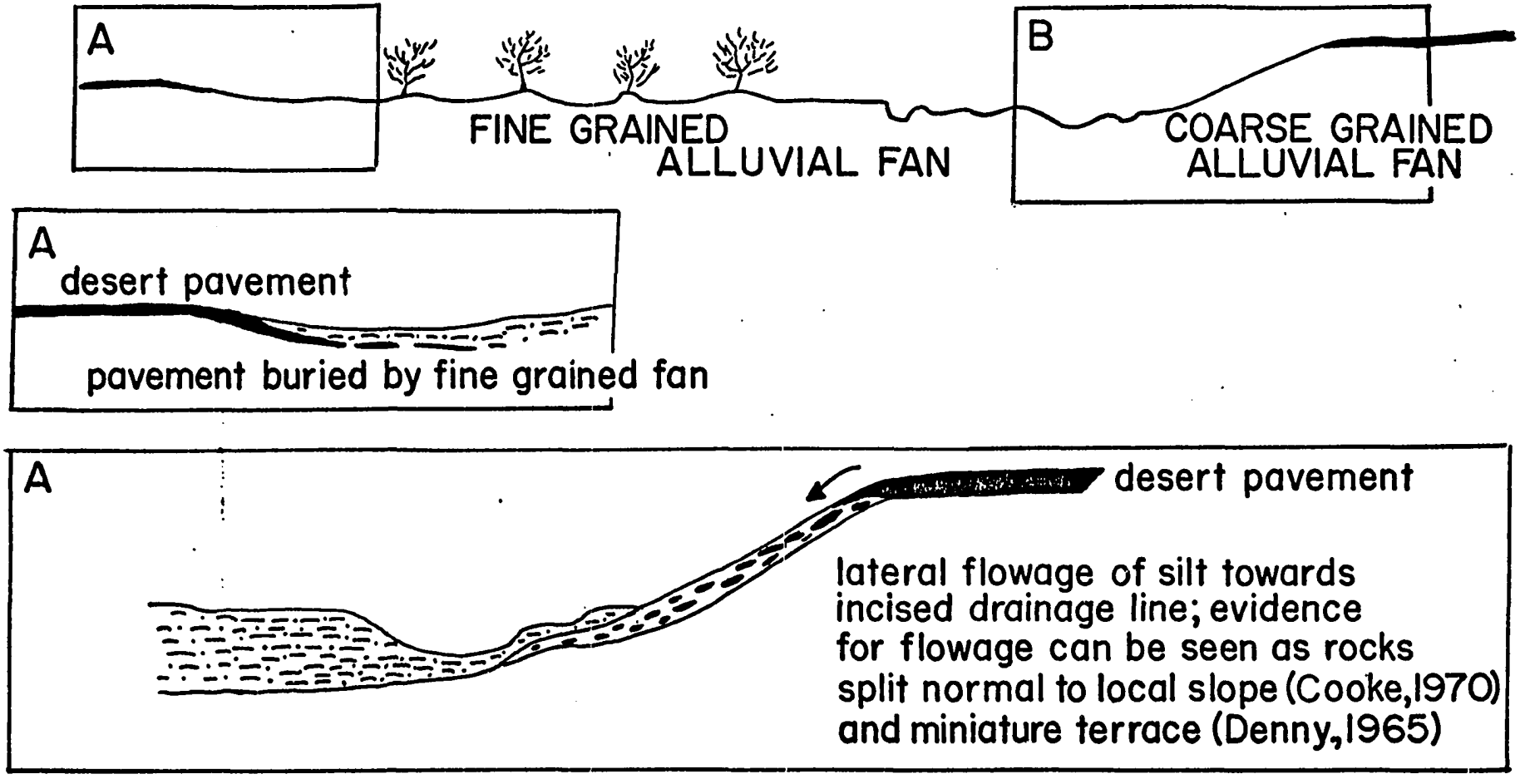

Figure 86. Idealized sketches illustrating processes which destroy desert pavement surfaces in the Harquahala Valley.

segments approaches a steady state condition in the Harquahala Valley. That is, those processes which form and destroy the pavement must be approaching a balance such that a constant geometry of the segment is maintained. These data support the idea given by Denny (1967) for the alluvial fans in Death Valley, California.

Eolian activity has been criticized by Cooke (1970; and Warren, 1973) as a pavement forming process. He notes that fine material is not typically loose for transport by wind, but, rather, is bound by a crust. No measurements were taken to analyze the effect of wind as a pavement-forming process in the study area; however, field observations across the study area indicate that a crust commonly occurs on fine grained material. This crust is formed by lichen and algae.

Eolian processes do have an important effect on the micro-relief on fine grained alluvial fans (Qff). Coppice dunes form around creosote bushes and accumulate up to 60 cm. high.

PROCESS GEOMORPHOLOGY OF THE HARQUAHALA VALLEY BOLSON PLAIN

Erosional and aggradational processes operating in the Harquahala Valley approach a steady state condition within individual low order drainage basins. The low order drainage basins taken together provide a basis for drawing conclusions about geomorphic processes over the bolson plain of the entire Harquahala Valley. The areal distribution of the dominant surficial processes and their relationship to major physiographic features of the Harquahala Valley are described below.

The majority of low order drainage basins are aggrading in the distal reaches of their washes by lateral extension of berm sediments.

Sheet flow causes this type of aggradation. These areas are fine grained alluvial fans (Qff of Figure 25). Approximately 16 percent of the Harquahala Valley is covered by fine grained alluvial fans. The particle size distributions of these fan sediments are nearly identical to particle size distribution of berm sediments (compare Figs. 20, 67 through 71). In the field, the aggrading berms are seen to coalesce to form a smooth, low relief surface (Fig. 22). Individual berm sediments can be traced to their apices up the washes (Fig. 25). Above the apices, the drainage patterns are tributary and are incised into the bolson plain. Below the apices, the patterns are anastomosing-distributary and are at the surface of the bolson plain. The regional drainage pattern above fine grained allvuial fans is an incised tributary system, and on the fine grained alluvial fans themselves is a non-incised, anastomosing-distributary system. Thus, the regional pattern is an analogue of the individual fan apron patterns.

Fine grained alluvial fans are interpreted as coalescing berm sediments which have spread laterally over the shallow interfluves of the lower alluvial aprons. The runoff in this area is by sheet flow, which has a high suspended load to discharge ratio. The fine grained fans represent areas of net aggradation in the Harquahala Valley and over approximately 16 percent. The contact between the fine grained and coarse grained alluvial fans is transitional (Fig. 13), but in general, the contact represents the lateral zero edge of alluviation on the bolson plain.

A widespread paleosol exists below the most recent fine grained alluvial fans and generally shows the same degree of development. This

suggests that the most recent building of the fine grained alluvial fans in the lower apron began throughout the Harquahala Valley at about the same time and followed a period of non-deposition or very slow erosion or deposition.

The sediment source for the fine grained fans is the fine sediment derived by sheet wash erosion from the coarse grained alluvial fans of the upper alluvial apron region, and to a lesser extent, the colluvium mantled bedrock slopes of the mountain ranges. The position of the zero edge of alluviation in the study area is controlled by the amount of sediment swept from the source. The present ratio of aggrading to eroding bolson plain is 1:5, and the ratio of aggrading areas to the total source area (including the bedrock) is 1:7.

Fine grained fans are not evenly distributed over the center of the bolson plain (Fig. 25). For example, the fine grained alluvial fans of the apron flanking the Eagletail Mountains have small areal extent as compared to those of the Big Horn Mountains, which have the most extensive areas of aggradation (Fig. 25). The drainage density on the alluvial aprons of these low order drainage basins flanking the Eagletail Mountains are greater than 10 and the mean basin width to wash length ratio is less than 6. This results in less overland flow and more channelized flow, resulting in more efficient removal of sediment from the apron. The Big Horn Mountains' alluvial apron has a low drainage density and higher mean basin width to channel length ratio in the low order drainage basins. Major physiographic differences between these areas are: 1) the Big Horn Mountains have larger bedrock source areas and a correspondingly higher mean apron length than the Eagletail Mountains, and 2) Centennial Wash

is closer to the Eagletail Mountains than the Big Horn Mountains. Both differences are related to the history of the bolson plain, but in general, the Big Horn Mountains have a higher sediment yield, which probably diverted the axial drainage towards the Eagletail Mountains, which have had a lower sediment yield. In addition to reducing apron length, the impingement of Centennial Wash on the Eagletail Mountains' apron has increased the drainage density. Both factors reduce the condition which promotes berm aggradation, reduce overland flow, and increase the mean basin width to channel length ratio above the steady state conditions.

Fine grained alluvial fans are developed below areas on the upper apron which have drainage texture values greater than 2 km/km^2 (compare Figs. 9 and 25). Nearly 32 percent of the bolson plain has drainage texture values greater than 2 km/km^2. The remaining 68 percent of the bolson plain are areas where fine grained alluvial fans occur. This relationship illustrates that erosion of the upper apron yields fine sediment, which is deposited in the lower apron regions.

Fine grained alluvial fans have regional slopes of less than 0.5°, and coarse grained alluvial fans have slopes typically above 0.5°. The parts of the bolson plain with the lower slopes are aggrading, and those with the higher slopes are eroding. Fine grained alluvial fans are located in the troughs shown on the slope map (Fig. 8). This implies that sediment derived from the mountains is carried by major drainage lines to areas of lower slopes in the center of the bolson plain. These sediments may be deposited as fine grained fans.

One anomalous occurrence of fine grained alluvial fan deposits is

in the headwaters of the Tiger Wash watershed between the Harquahala and Big Horn Mountains (Fig. 25). Evidence indicates that this area may have undergone a drainage reversal by stream piracy, and the spatial arrangements of these deposits are related to past events. (The anomaly will be discussed below in the Geomorphic History section).

Caliche rubble deposits (Qcr) in the Harquahala Valley are susceptible to intense runoff either as sheet flow on the interfluves or as channelized flow in the confined washes. Eolian deposits (Qds), where adjacent to caliche rubble, exhibit local increased incision from the higher runoff (Fig. 25). The eolian dune fields south of the caliche rubble deposits flanking the southern Saddle Mountain are deeply incised and have integrated drainage systems. This is atypical of eolian dune fields, where drainage lines are commonly diverted around the dune fields and are not incised into them.

In addition to caliche rubble, the varnished gravels (Qgv) forming well developed desert pavements produce intense runoff. The pavement serves as an armor, and the underlying silts have low infiltration rates (Lattman, 1971). These factors promote runoff and also deter sediment pickup. As a result, a low, suspended sediment concentration exists in the runoff of these areas and erosion is increased. Denny (1967) and Sharon (1962) have emphasized that dissection and pavement forming processes occur simultaneously. The intense runoff from pavement surfaces has a high capacity to erode channels developed on the pavements. This process may be the reason that pavements and dissection occur simultaneously.

GEOMORPHIC HISTORY OF THE HARQUAHALA VALLEY

Quaternary History

The late Tertiary (Pliocene)-Quaternary deposits of the Harquahala Valley range in thickness from 0 to 50 m. There are no detailed dates available on the various Quaternary stratigraphic units; only a relative sequence of events can be established based on stratigraphic relationships.

The history revealed here consisted of the bolson plain center being filled by coarse grained alluvial fan deposits, then a period of little or no erosion, followed by deposition resulting in a regional soil development. Subsequently, the soil was buried by renewed deposition consisting of the fine grained alluvial fan deposits.

The oldest and most extensive surficial deposits in the Harquahala Valley are the coarse grained alluvial fans (excluding the saline deposits). These deposits show extensive weathering and erosion and are exposed in the mid and proximal portions of the alluvial aprons. Thick accumulations of calcium carbonate and heavy varnish on the gravels are developed on these sediments. Exposures in the coarse grained alluvial fans on the upper aprons show no signs of a major unconformity, and therefore, the filling of the valley by these coarse sediments is interpreted as a continuous event. This interpretation is in agreement with the findings of Kottlowski and others (1965), that sedimentation was continuous in the early Quaternary in southern Arizona.

Alluvial filling of the mountain valleys is interpreted as being spatially continuous with deposition of the coarse alluvial fans. That is, the tops of the remnants of valley alluvium in the mountains and the tops

of the coarse grained alluvial fans were continuous prior to later incision. This is substantiated by the curves fit to the present coarse grained alluvial fan surfaces and the valley fill remnants in the Harquahala Mountains (Fig. 37). These surfaces have been shown to be fitted with exponential curves of the form, $Y = Ae^{BX}$. The regression coefficients for these curves are greater than 0.955. These results indicate that the Harquahala Mountains and surrounding apron were once aggraded to the highest level preserved today, if not higher. Similar relationships between remnants of valley filling in the other mountain ranges of the study area and the level of the coarse grained alluvial fans are interpreted as being due to similar history to that of the Harquahala Mountains.

During filling by alluvial fan building processes local erosional surfaces in the proximal portion of the alluvial aprons were developed. Modern alluvial fans show the development of such surfaces at their head during fan building. In the Harquahala Valley, these erosional surfaces can be seen buried below a weathered mantle (Fig. 87).

Other erosional events in the Harquahala Valley during this part of the Quaternary are piracies of drainage from adjoining basins. The mountains which surround the study area are discontinuous, and the Harquahala Valley has not been a physically closed system. Ross (1923) suggested that piracy of Centennial Wash drainage into the Harquahala Valley occurred in the Harrisburg Valley (Fig. 4) between the Little Harquahala and the Harquahala mountains. According to Ross, progressive headward erosion of drainage lines in the Harquahala Valley captured the drainage which was originally flowing into the McCullen Valley to the north.

A. Local erosion surface on coarse grained alluvial fan deposits (Qfc) of Harquahala Mts.' alluvial apron.

B. Local erosion surface of coarse grained alluvial fan deposits (Qfc) on alluvial apron south of Sallde Mountain.

Note weathered mantle covering erosional surfaces on both alluvial aprons.

Figure 87.

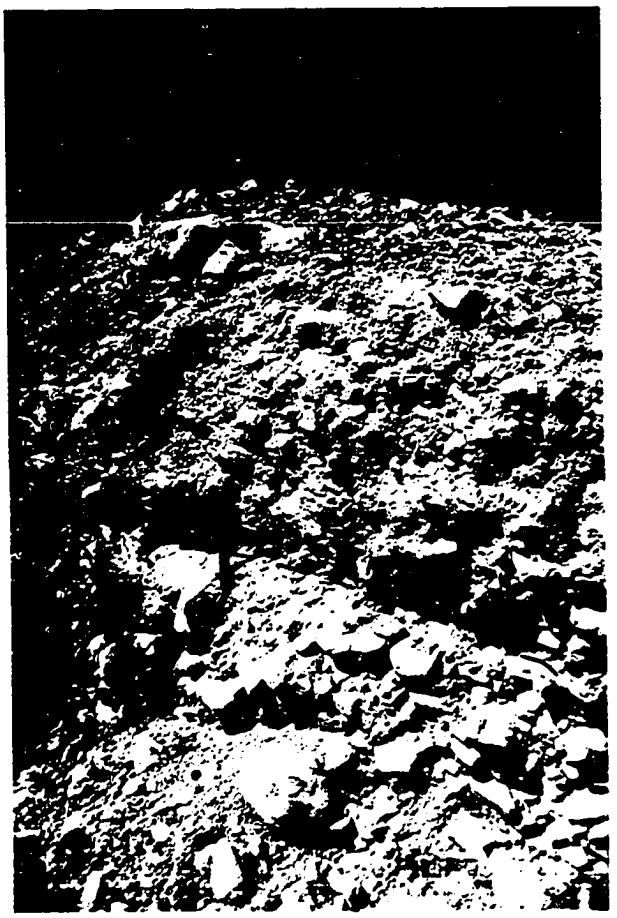

This erosion theory is supported by the extrapolation of the curves fit to the apron surface of the Harquahala Mountains, which indicated nearly 7 m of downcutting.

Additional capture of the original McCullen Valley (Fig. 4) drainage occurred in headwater region of Tiger Wash. The shape of this watershed suggests a northeastward direction of flow to McCullen Valley prior to capture. Additionally, the soils and surficial deposits associated with later lower apron processes occur in the present-day headwaters, and the profile of Tiger Wash (Fig. 49) is concave and not convex, as are those of other ephemeral washes (Figs. 50 through 59). Extrapolation of the curve fit to the original level of fill on the south side of the Harquahala Mountains and in the Tiger Wash watershed indicates that the entire upper Tiger Wash valley was aggraded to a level 100 m higher than the present level (Fig. 37). Headward migration of drainage lines captured this portion of the ancestral McMullen Valley, as the Harquahala Valley provided a lower base level. Headward migration and integration of this drainage appear to have been slow, since sediments resulting from later geomorphic conditions occur in the headwater region. That is, recent geomorphic processes, which are typical of lower apron processes, occurred in the headwaters of Tiger Wash, as the entire drainage system was not integrated to Harquahala Valley.

Both captures of McMullen drainage apparently caused subsequent aggradation of the bolson plain in the northern Harquahala Valley by fan-building processes. Aggradation in these regions diverted the ancestral Centennial Wash to a more westward position and diverted the drainage of the Big Horn Mountains to a more southward position. This event would

would explain the present orientation of drainage lines on the bolson plain (Fig. 12).

The southern porition of the Harquahala Valley appears to have been more stable than the northern areas. The southern and central portions of the bolson plain were characterized by internal drainage during piracy of the northern regions. The deposition of fine grained sediments, with large concentrations of gypsum and very low angle of slope (less than 0.33°), suggests that this area may have been a playa. Metzger (1957) interpreted this portion of the Harquahala Valley as once being covered with an extensive lake during damming of the Gila River by volcanic flows. However, dates on these flows (FUGRO, 1974) indicate an age of Pliocene, not Pleistocene, as suggested by Metzger. Internal drainage may have resulted from "overloading" this portion of the valley with sediment derived from pirated basins surrounding the Harquahala Valley.

Aggradation in the southern portion of the Harquahala Valley and degradation in the northern portions were less extensive for a major period of time. The playa dried up and the sediments became subaerial. Depositional, as well as erosional, processes on the interfluves of the aprons were less operative. During this time a regional soil developed over the bolson plain on the interfluves, as well as across the playa deposits. This soil is the paleosol seen in the exposures in the bolson plain today.

The next major event to occur in the southern portion of the Harquahala Valley was the development of extensive eolian dunes on the playa deposits (Fig. 25). Previous investigators in the southwestern United States (Bryan, 1940; Hack, 1941) reveal a major period of eolian sediment deposition during the Altithermal period (3000-7000 BP). These

dunes buried the soil horizon which developed on the ancient playa deposits (Fig. 44).

Following the development of dune fields, the axial drainage of the Harquahala Valley was integrated in the northern portion of the bolson plain. Prior to this time, the major drainage lines may have exited the valley through the pass between the Little Harquahala Mountains and the Eagletail Mountains. The axial drainage extended laterally through the eolian deposits and also incised into the valley fill south of Saddle Mountain (Fig. 25). This incision cut into eolian dunes, forming a terrace. The axial drainage then extended laterally between the Eagletail and Saddle mountains and was integrated with Gila River.

Assuming that incision of the drainage lines surrounding Saddle Mountain were related to this incision of the axial drainage, the ripple-train features on the apron surfaces formed prior to this integration and dissection.

Isolated relict geomorphic features of the Harquahala Valley are numerous debris flows, which dominate the slopes of volcanic bedrock and aprons composed of volcanic detritus (Fig. 25). The age of these features is later than the deposition of the coarse grained alluvial fans and before the incision of the upper apron regions. Again, assuming this incision is related to the incision of the axial drainage in the southern portion of the valley, the debris flows may be contemporaneous with the ripple-train features of Saddle Mountain.

The final geomorphic event in the Harquahala Valley is the development of fine grained alluvial fans in the lower portions of the aprons. These fans cover the well developed soils on the interfluves of ancient

coarse grained alluvial fans (Fig. 39). The development of these fine grained alluvial fans is given above.

Paleoclimatic and Paleohydrologic Considerations

The historical variations of Quaternary sedimentary types recorded above may reflect changes in climate, tectonism, vegetation, or other factors. Climatic and tectonic influences on arid basin processes and forms have been under considerable debate. Cooke and Warren (1973) summarize the different viewpoints on this topic.

Present field observation reveals no deformation of the Quaternary deposits in the Harquahala Valley. In addition, the ubiquity of basin fill and associated valley fill remnants in the mountain ranges surrounding the bolson plain suggest a similar regional history for the bolson plain. These results favor the idea that climatic changes have caused episodes of alluviation and degradation in the Harquahala Valley. It is less likely that tectonism could have produced similar features distributed over the entire Sonoran Desert.

The three major types of sediments deposited in the Harquahala Valley during the Quaternary are coarse grained and fine grained alluvial fans and eolian sand dunes. All three reflect different modes and energies of transportation and are presumed to be related to climatic variations. Eolian deposits reflect a drier period during the past when sand dunes were not stablized by vegetation. The coarse grained alluvial fans imply a time of higher rates of precipitation, resulting in higher rates of erosion and higher values of the tractive forces, or competence. The fine grained alluvial fans reflect the present conditions of runoff and

erosion and result from processes operating on deposits formed under different climatic conditions than the present.

Melton (1965) emphasized that changes to cooler temperatures in southern Arizona increased the sediment size in the Pleisotcene basin fills. Cooler temperatures would produce more freezing and thawing and result in larger fragments of sediment for transport. An increase in runoff above that of the present climate would be needed to transport the coarse grained alluvial fan material to the center of the bolson plain in the Harquahala Valley (Fig. 25). That is, the climate of the Harquahala Valley may have been closer to a semi-arid condition during the Pleistocene.

Schumm (1965) determined the relationships between mean annual sediment yield, mean annual precipitation, and mean annual temperature. Schumm's guidelines are used here to compare the semi-arid, Sycamore Creek basin of southern Arizona to the arid Harquahala Valley. Sycamore Creek basin receives 30 cm more rainfall and is about 10°C cooler per year than the Harquahala Valley. Maximum runoff (approximately 90 percent) in the semi-arid basin is related to 60 percent of the precipitation during the winter months. In the Harquahala Valley, approximately 90 percent of the runoff is related to 50 percent of the rainfall during the summer months. Vegetation in a semi-arid basin influences the runoff, but in an arid basin there is little vegetation, and the runoff is not so influenced. Thus, a change from the arid conditions to semi-arid conditions would result in changes in the seasonal runoff with increases in vegetation.

For the Harquahala Valley with a constant mean annual precipitation, a decrease in temperature would increase the mean annual runoff (Langbein et al, 1949). In order to produce the identical runoff in the Harquahala

Valley as in a semi-arid basin, the mean annual temperature would have to be depressed by 7°C (Fig. 88). However, if the mean annual rainfall in the study area was tripled, the temperature would only have to be depressed 4°C for the same amount of runoff as in a semi-arid basin of southern Arizona. General temperature and precipitation changes between the glacial and interglacial periods of the Pleistocene are estimated about 6°C and 25 cm in nonglaciated regions (Schumm, 1965). A climatic change approaching this magnitude in the Sonoran Desert would tend to increase runoff in the winter and reduce summer runoff. The berm aggradation associated with the present type of runoff in the Harquahala Valley would not occur. Coarser materials would be swept farther down the alluvial aprons.

It is concluded that moister and cooler conditions existed during the past in the Sonoran Desert, because coarser sediments of the early Pleistocene occur near the center of the bolson plain. Presently, fine grained alluvial fans are forming in these regions. Changes in vegetation associated with increasing moisture caused changes in the seasonal runoff from winter to summer.

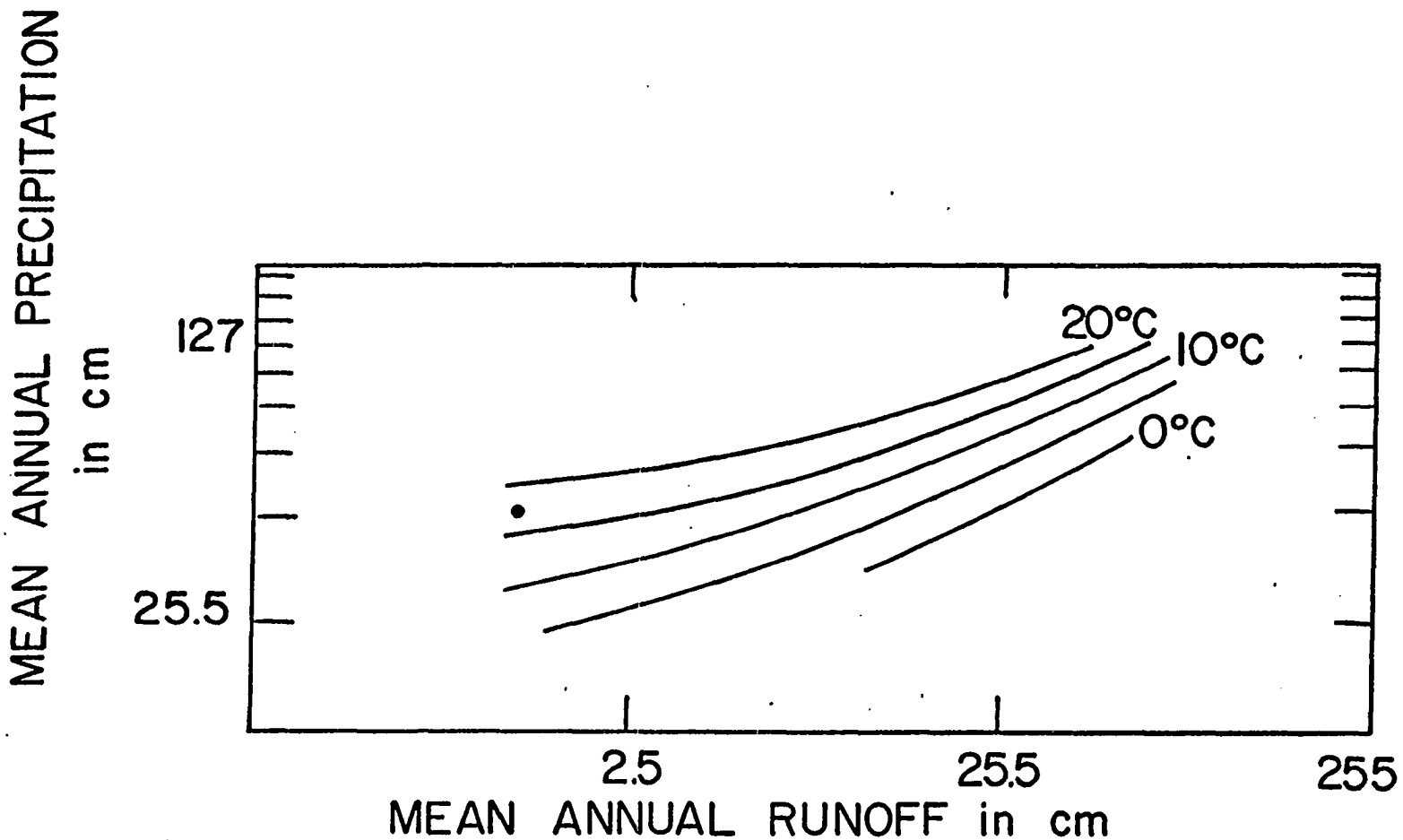

Figure 88. Relationship of mean annual runoff and precipitation for semi-arid Sycamore Creek basin near Sonoran Desert. Modified from Langbien and others (1949).

CONCLUSIONS AND SUMMARY

LANDFORMS AND SURFICIAL DEPOSITS OF HARQUAHALA VALLEY

The bolson plain of the Harquahala Valley is composed of coalescing alluvial aprons, which comprise two thirds of the basin area. A positive correlation exists between mean apron (fan) length and size of contributing bedrock area. Mean down-apron slope for the entire bolson plain is 0.5° and the maximum apron slopes are usually less than 4°. The rate of change of slope down the apron (dS/dL) is higher on those aprons composed of extrusive igneous rock detritus than on those composed of intrusive igneous rock detritus. The slope of the apron is, therefore, influenced by the type of material composing the fill.

Nearly 70 percent of the bolson plain has low drainage texture values, and the highest texture values are on aprons associated with the mountain ranges having the greatest maximum relief. The potential energy (maximum elevation difference between the mountains and aprons) has the ability to produce more channel erosion on the alluvial aprons.

The position of the axial drainage, Centennial Wash, in the Harquahala Valley is controlled by the amount of sediment from the mountain ranges flanking the bolson plain. The larger the bedrock areas, the more sediment and the longer the alluvial apron, and the axial drainage line is diverted away from these areas to areas with less sediment yield. Centennial Wash is aggrading by fan-building processes in two parts of the bolson plain where capture of drainage peripheral to the Harquahala Valley basin occurred in the past. Elsewhere, it is cutting down in the

lower, or southern, portion of the bolson plain and has left a terrace approximately 15 m above the present base level. The ephemeral washes that drain to Centennial Wash are incised tributary systems on the upper apron and aggrading anastomosing-distributary systems on the lower apron.

The Quaternary surficial deposits of the Harquahala Valley can be differentiated on the basis of particle size and alterations by weathering. The types of deposits mapped on the bolson plain are: 1) coarse grained alluvial fans (Qfc), 2) fine grained alluvial fans (Qff), 3) eolian dune deposits (Qds), 4) saline deposits (TQsa), 5) varnished gravels (Qgv), and 6) caliche rubble (Qcr). Coarse grained alluvial fans are primarily composed of particles greater than 2 mm in diameter, and fine grained fans are composed of grain sizes less than .25 mm in diameter. Coarse and fine grained alluvial fans are the most extensive features, covering 62 and 16 percent of the bolson plain, respectively. Eolian deposits overlie 5 percent of the bolson plain, varnished gravels cover slightly less than 5 percent, and caliche rubble superimposes 2.5 percent of the valley. The remaining area, 8 percent, is undifferentiated fan material, which includes combinations of coarse grained alluvial fans, varnished gravels, and caliche rubble deposits. Alluvium of modern washes is included in all the mapping units. Coarse grained alluvial fans occur on steeper slopes of the upper apron, and fine grained fans occur on the gentle slopes of the lower apron.

Desert soils, which have formed on these surficial deposits, are aridisols and entisols. Aridisols have developed on the coarse grained alluvial fans, and entisols have developed on the fine grained fans. The coarse grained fans are, therefore, older and have been subject to

longer durations of weathering than the fine grained fans.

LANDSAT imagery is useful for distinguishing fine and coarse grained alluvial fans. The tonal density difference of the surficial deposits on transparencies of MSS Band 7 and color composites of Bands 4, 5 and 7 can be determined by statistical analyses.

DYNAMICS OF SURFACE RUNOFF IN AN ARID BASIN

Summer precipitation associated with short, intense storms produces ninety percent of the runoff on Centennial Wash. Surface runoff during these storms usually takes the form of flash floods. The peak discharge of a flash flood is short in duration and close to the front of the flood pulse. This produces the 'wall of water' phenomenon during runoff. Excessive transmission losses into gravel-covered wash floors cause the shortened rise time of a flood hydrograph. Transmission losses are primarily most rapid in the upper apron regions where the coarse alluvium lines the washes. The excessive silt and clay fractions in the lower apron regions reduce the rate of infiltration of the runoff. Ground-water recharge in the Harquahala Valley is most frequent in the upper apron regions, since the lower rate of infiltration in the lower apron regions would allow evaporation to reduce the volume of water.

Runoff is channelized in the upper apron regions where drainage lines are well below the level of the interfluves. Sheet flow, which occurs on these interfluves, is mainly erosional. Fine grained sediments ranging from 0.125 to 2 mm in diameter are eroded by this sheet wash.

Surface runoff is unchannelized, or sheet flow, in the lower apron

regions of the Harquahala Valley. The lower relief between the interfluves and drainage lines, due to less dissection, results in the coalescing of washes, which form anastomosing-distributary systems on the interfluves. The uniform slope and smooth appearance of the center of the bolson plain result from the distribution of fine grained sediments across the interfluves. Sheet flow in the lower apron region is generally aggradational rather than erosional.

A flood pulse moving down the apron passes through a maximum discharge, with recharge from overland flow. Decreasing recharge and increasing transmission losses reduce the volume of water down a wash. This decreasing runoff results in an increase in the suspended load-discharge ratio. These flood pulses leave traces of high water marks along the washes in the study area. These high water marks tend to be preserved due to the low frequency of maximum flood events. Estimates of the hydraulic geometry and discharge at a cross-section can be made by using these high water marks.

FACTORS CONTROLLING EPHEMERAL WASH AGGRADATION

Aggradation of ephemeral washes occurs by channelized and sheet flow. Channel sediments, typically larger than 2 mm in diameter, occur in the talweg of the wash and are moved as bed load by floods. Tractive forces on the wash floor decrease after the maximum discharge with increasing distance from the head of the wash. Decreasing slope of the channel and depth of flow reduce the tractive forces. Aggradation of channels occurs when threshold values of slope (1.5°) and depth of flow (1 m) are attained. This aggradation occurs when the tractive forces are

no longer competent to move the sediments as bed load. Maximum channel widening is associated with this aggradation, and this local maximum channel width is proportional the distance from the divide and area above the point. The relationship between area and channel length during aggradation is expressed by $A_d = 2.5\ L_c^{1.1}$, or a mean width of a low order drainage basin equal to 2.5.

Aggradation by sheet flow is related to the deposition of berm sediments. Fine grained berm sediments are primarily transported by suspended load. The suspended load increases faster than the discharge with distance from the divide of ephemeral washes, as the discharge is lost by infiltration into the coarse sediments. Aggradation by sheet flow occurs as the washes extend over the interfluves of the lower apron regions and coalesce. The width of the berm and the width-depth ratio of the washes increase exponentially down the apron. Width-depth ratios are typically larger than 50 when berm aggradation takes place on the washes.

A specific drainage area and wash length are related to berm aggradation by the following expression: $A_d = 0.138\ L_c^2$. That is, the area and length of wash above the incipient berm aggradation are related as a power function. This expression can be rewritten as a dimensionless ratio of mean basin width to wash length, which equals 0.138. Berm aggradation results when the ratio of basin width to wash length approaches 0.138. This constant represents the distance between two channels; therefore, the length of overland flow is equal to one half this constant, or approximately 70 m. The length of overland flow controls berm aggradation as sheet erosion on the interfluves and produces fine grained

sediment, which forms the berm. The longer the overland flow, or the less the drainage density, the more the sediments are produced by sheet erosion.

Berm aggradation in the Harquahala Valley appears to be close to a steady state condition. The clustering of the lengths of overland flow around a value necessary to produce berm aggradation suggests a quasi-equilibrium condition. Aggradation caused by deposition of channel sediments is not related to a steady state condition. Rather, it is related to the exceeding of thresholds in slope and depth of flow.

FACTORS INFLUENCING DESERT PAVEMENT DEVELOPMENT

Well developed desert pavements in the Harquahala Valley have a paucity of sand size particles and have a bimodal distribution of coarse gravels and silt. Apron surfaces that show incipient pavement development have higher concentrations of sand size material. Sheet wash on the interfluves of the apron surfaces erodes the sand size material and carries it into the channels, as this size is the optimum for transportation. The amount of slope on the apron surface thus affects the degree of pavement development. Higher slopes in the upper alluvial apron exhibit better developed pavements than the lower slopes of the lower apron regions.

Freezing and thawing of soil moisture in the bolson plain may be another factor which influences the concentration of coarse gravels near the surface. An average of one sixth of the year in the study area is characterized by freezing temperatures, and this period coincides with the lowest period of runoff, or highest infiltration.

Maximum width and length of the desert pavement segments in the Harquahala Valley are related by the expression: $W_{dp} = -.13 + .45\ L_{dp}$. The ratios of the maximum length to width of these segments vary about a mean of 3. The processes which tend to build desert pavements are balanced by accelerated dissection and lateral flowage towards drainage lines of the weathered mantle. These destructional processes are proportional to the drainage density and depth of incision. These pavement segments are close to a steady state condition, which was first suggested by Denny (1965, 1967) for the pavements in southern California.

QUATERNARY GEOMORPHIC HISTORY OF THE HARQUAHALA VALLEY

Differences in the type and distribution of Quaternary deposits in the Harquahala Valley indicate changes in the rates and types of denudational and aggradational processes during the recent geomorphic history. Basin filling during the Quaternary was not continuous. Rather, periods of time reflect dominance by erosional or aggradational processes, which are not considered to be exclusive of each other.

Basin filling was primarily with coarse grained alluvial fans and was fairly continuous during the early Quaternary. Development of local erosional surfaces, which includes pediments, occurred with fan building processes and was limited to the proximal portions of the alluvial aprons. Headward eroding channels related to this local erosion may have cut through the alluvium filling the gaps between the major mountain ranges and captured additional drainage which was flowing north to a higher base level. The ancestral Harquahala Valley provided a lower base level, which further accelerated this piracy. Piracy through Harrisburg Valley

was either prior to the capture in the headwaters of the Tiger Wash valley, or rates of drainage integration were faster, since the headward migration of eroding channels is farther up the McMullen Valley than in the Tiger Wash Valley. The increase in source area resulted in an increase in sediment yield, which caused fan-building processes in the center of the bolson plain in the northern portions of the Harquahala Valley. These fan-building processes shifted the drainage lines in the center of the bolson plain to their present southwestern position.

The geomorphic events that followed were the development of a playa lake in the southern Harquahala Valley, which was associated with closed, or internal, drainage. This was followed by a relatively stable time with respect to rates of erosion and aggradation, which is reflected in a well developed, regional paleosol. Prior to the soil development, the lake in the southern Harquahala Valley dried up, and after the soil development, more aridity ensued, with the development of eolian dunes.

After the eolian dune development, Centennial Wash became integrated across the Harquahala Valley to its present position. This integration was accompanied with incision in the area between Saddle and Gila Bend mountains. This incision resulted in the development of a terrace along the axial drainage in this region and caused the headward migration of eroding channels up the alluvial aprons. Prior to this incision, debris flows and ripple-train features were developed.

The final and most recent geomorphic event was the development of fine grained alluvial fans in the lower portions of the bolson plain. This process moved the zero edge of alluviation up the apron slope and buried the soil developed on the interfluves.

Climatic changes appear to be the major factor which caused the changes in the types of processes and their associated deposits during the Quaternary. Changes in the type and amount of precipitation, as well as the temperature, affected the behavior of runoff across the Harquahala Valley. Sediments with large grain diameters were transported farther across the bolson plain, which indicates a more competent runoff in the center of the Harquahala during the past than the present. Cooler temperatures may have enhanced freezing and thawing processes on hillslopes, which supplied coarser particle sizes. The arid climate of the study area was probably shifted towards a semi-arid climate in the past.

Relicts from previous climates are preserved in the Harquahala Valley, and in some cases, influence the present day processes. Van Arsdale (1974) and Lattman (1974) have illustrated how caliche from a relict climate affects the channel geometries of washes in the Sonoran Desert. Likewise, the caliche cemented hillslope material, which reduces infiltration and erosion of the colluvium and talus, acts as a caprock. The hillslopes in the Harquahala Valley are typified by scarps of secondary calcium carbonate-cemented colluvium facing the mountain front. As the surface runoff from the bedrock erodes at the bedrock-apron contact, the scarps retreat down slope. Thus, slope processes are influenced by deposits from an ancient climate.

The coarse grained fans, which were formed during the early Quaternary, represent lag deposits of a different climate, which are undergoing erosion in the present climate. These sediments provide the fine silts for berm aggradation, and control the zero edge of alluviation through these sediment supplies in the present climate.

APPLICATIONS TO LAND USE AND PRACTICAL PROBLEMS IN THE SONORAN DESERT

Results from this study provide a framework for delineating optimum conditions for land use in the Harquahala Valley and other basins of the Sonoran Desert. Areas of erosion by sheet flow and deposition by channelized flow can be distinguished from areas of aggradation by sheet flow and extensive sheetflooding. Caliche rubble deposits and desert pavement surfaces cause intensive runoff due to low infiltration capacities of these deposits. Areas including these types of deposits or adjoining them may suffer from extensive flooding.

Areas for optimum ground-water recharge in the Harquahala Valley are along the coarse alluvium-covered washes on the upper apron slopes. High, or rapid, transmission losses in these regions add to the ground-water supply. The surficial deposit map provides a base for delineating these recharge areas. The fine grained alluvial fans, caliche rubble, and varnished gravels have low infiltration rates; therefore, the area of most rapid recharge lies below the caliche rubble-varnished gravel deposits on the upper apron and above the fine grained fan deposits of the lower apron surfaces.

Use of LANDSAT imagery to define the surficial deposits and their associated surficial processes permits regional delineation of these processes in the Sonoran Desert. Areas susceptible to practical problems, which are related to desert processes, can be distinguished prior to land use, and therefore provide optimum land management in arid basins of southwestern Arizona.

Additionally, LANDSAT imagery is useful for distinguishing

deposits whose related processes are approaching steady state conditions. In these regions, man may have a detrimental effect by disturbing the steady state conditions. Changes in these conditions may result in changes in the behavior of surface runoff. For example, borrow pits dug near the point of incipient fine grained fan deposition may lead to accelerated erosion (Fig. 89). Such erosion may capture major drainage lines and inhibit fine grained alluvial fan deposition.

Figure 89. Accelerated erosion and capture of major drainage lines as a result of lowering base level by excavating a borrow pit. This is in the zone of incipient fine grained alluvial deposition, which is disturbed by increase in drainage density and channelized flow.

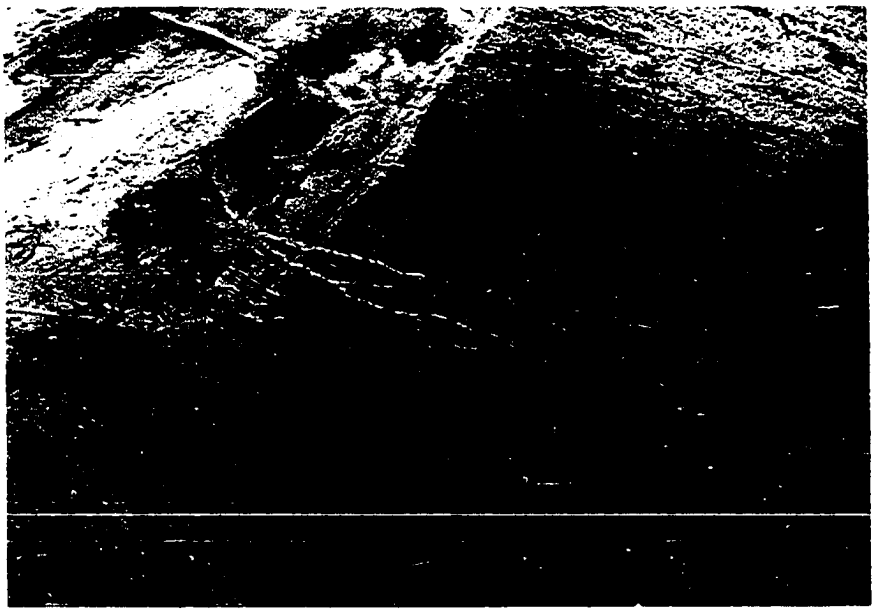

REFERENCES

Babcock, H. M. and Cushing, E. M., 1942. Recharge to ground-water from floods in a typical desert wash, Pinal County, Arizona. Am. Geophysical Union Trans. 23, p. 49-56.

Baker, V. R., 1973, Palehydrology and Sedimentology of Lake Missorila Flooding in Eastern Washington. Geol. Soc. Am. Spec. Paper 144, 79 pp.

Benson, M. A. and Dalrymple, T., 1967. General Field and Office Procedures for Indirect Discharge Measurements, U.S.G.S. Tech. of Water-Res. Invest., Chapter A1, Book 3, 30 pp.

Birkeland, P. W., 1974. Pedology, Weathering, and Geomorphological Research, Oxford Univ. Press, New York, 285 pp.

Blissenback, E., 1954 Geology of Alluvial Fans in Semi-Arid Regions. Geol Soc. Am. Bull., v. 65, p. 175-511.

Bretz, J. H. and Horberg, L., 1949, Caliche in Southeastern New Mexico. Jour. Geol., v. 57, p. 491-511.

Brown, C. N., 1956, The Origin of Caliche on the Northeastern Llano Estacado, Texas. Jour. Geol., v. 64, p. 1-5.

Bryan, K., 1925, The Papago Country. U.S.G.S. Water Supply Paper, 499, 435 pp.

Bryan, K., 1940. Erosion in the Valleys of the Southeast. New Mexico Quart., v. 10, p. 227-232.

Cameron, R. E. and Blank, G. B., 1966, Desert Algae: Soil Crusts and Diaphanous Substrata as Algal Habitats. NASA Tech. Rept. no. 32-971, 41 pp.

Carson, M. A. and Kirkby, M. J., 1971. Hillslope Form and Process, Cambridge, 475 pp.

Chamberlin, T., in preparation, General Soil Map-Yuma County Arizona. Soil Conservation Service.

Chorley, R. J., 1962, Geomorphology and General Systems Theory: U.S.G.S. Prof. Paper 500-B, 10 pp.

Chow, V. T. (ed.), 1964. Handbook of Applied Hydrology: a compendium of water-resources technology. McGraw Hill Book Co., New York.

Clancey, P. A. and Harmsen, L., 1975. A Hydrologic Assessment of the September 14, 1974 Flood in the Eldorado Canyon, Nevada. U.S.G.S. Prof. Paper 500-B, 10 pp.

Clements, T. et al., 1957. A Study of Desert Surface Conditions. Headmaster Research and Development Command, Environ. Prot. Res. Div., Tech. Rept. EP53, 110 pp.

Cooke, R. U., 1970. Stone pavements in deserts. Ann. Assoc. Am. Geog., v. 60, p. 560-77.

Cooke, R. U. and Warren, A., 1973. Geomorphology in Deserts. Univ. Calif. Press, Los Angeles, 374 pp.

Cooley, R. L. et al., 1973. Influence on Surface and Near Surface Caliche Distribution on Infiltration Characteristics and Flooding. Las Vegas, Nevada, Center for Water Resources Res., DRI, U. of Nevada, Sept., 41 pp.

Cordiviola, S., 1974. Hillslope Process in Southwestern Arizona. Unpublished M.S. thesis, Univ. of Cincinnati, 69 pp.

Dalrymple, T., 1960. Flood Frequency Analyses. U.S.G.S. Water Supply Paper 1543-A, 80 pp.

Darton, N. H., 1925. A resume of Arizona geology. Ariz. Bur. Mines Bull. 119, p. 221-223.

Denis, E. E., 1971. Groundwater conditions in the Harquahala Plains, Maricopa and Yuma Counties, Arizona, 44 pp.

Denny, C. S., 1965. Alluvial fans in the Death Valley Region, California and Nevada. U.S.G.S. Prof. Paper 466, 62 pp.

Denny, C. S., 1967. Fans and Pediments. Am. Journ. Sci., v. 265, p. 81-105.

Dubief, J., 1953, Les vents de sable dans le Sahara francais, in Actions Eoliennes, Cent. Nat. de Rech. Sci. Paris, Coll. Int., 35, p. 45-70.

Dunbier, R., 1968. The Sonoran Desert, University of Arizona Press, Tuscon, 426 pp.

Fenneman, N. M., 1931. Physiography of Western United States. New York, McGraw Hill Book Co., Inc.

Folk, R. L., 1971. Longitudinal Dunes of the northeastern edge of the Simpson Desert, North Territory, Australia, 1, Geomorphology and grain size relationships. Sedimentology, v. 16, p. 5-54.

FUGRO, 1974. Preliminary Site Review Report - Palo Verde Nuclear Generating Station, 52 pp.

Gilbert, G. K., 1875. Report on the geology of portions of Nevada, Utah, California, and Arizona, Part 1. and Surveys West of the 100th Meridian, 3, p. 21-187.

Gile, L. H., 1966. Coppice dunes and the Rotura Soil. Proc. Soil Sci. Soc. Am., v. 30, p. 657-660.

Gile, L. H., 1974. Holocene Soils and Soil-geomorphic Relations in an Arid Region of Southern New Mexico (abst.). Am. Quat. Assoc. 3rd Biannual Meeting, Wisc., p. 30-39.

Hack, J. T., 1941. Dunes of the Western Navajo Country. Geogr. Rev., v. 31, p. 240-263.

Hack, J. T., 1957. Studies of Longitudinal Stream Profiles in Virginia and Maryland. U.S.G.S. Prof. Paper 294-B, 53 pp.

Harms, J. C. and Fahnestock, R. K., 1965. Stratification, bedforms, and flow phenomena (with an example from the Rio Grande). Soc. Econ. Paleontologists and Mineralogists, Spec. Pub. 12, p. 84-115.

Hartman, G. W., 1973. General Soil Map, Maricopa County, Arizona. Soil Conservation Service, 49 pp.

Ingram, R. L., 1971. Sieve Analysis, in R. E. Carver (ed.) Procedures in Sedimentary Petrology, John Wiley and Sons, Inc., New York, p. 49-68.

Joly, F., 1953. Quelques phenomemes d'ecoulement sur la bordure du Sahara dans les Confins Algero-Marocains et leurs Consequences Morphologiques, Compt. Rend. XIX Congres Geol. Intern., Algiers 1952, pt. VII, Deserts actuels et anciens, p. 135-146.

Kam, W., 1961. Geology and ground-water resources of the McMullen Valley, Maricopa, Yavapai, and Yuma Counties, Arizona, 72 pp.

Kottlowski, F. E., Cooley, M. E., and Ruhe, R. U., 1965. Quaternary Geology of the Southwest, in H. E. Wright and D. G. Frey, The Quaternary of the United States, Princeton Univ. Press, Princeton, p. 287-298.

Langbein, W. B. et al., 1949. Annual Runoff in the United States, U.S.G.S. Circ. 52, 14 pp.

Lattman, L. H., 1971. Geomorphology of the east flank of the Spring Mountains, Nevada: Air Force Cambridge Research Laboratories, Rept. AFCRL-71-0326, 89 pp.

Lattman, L. H., 1973, Calcium Carbonate Cementation of Alluvial Fans in Southern Nevada. Geol. Soc. Am. Bull., v. 84, p. 3013-3028.

Lattman, L. H., 1974. Possible Influence of Secondary and Relict Climatically Controlled Features on Fluvial Systems (abst.). Am. Quat. Assoc. 3rd Biennial Meeting, Wisc., p. 66.

Lattman, L. H. and Ray, R. G., 1965. Aerial Photographs in Field Geology. New Yor, Holt, Rinehart, and Winston, 211 pp.

Lenhart, R., 1974. An evaluation of ERTS Imagery for Remote Sensing of Alluvial Fans in Nevada. Unpublished M.S. thesis, Univ. of Cincinnati, 69 pp.

Leopold, L. B. and Maddock, T., 1953. The hydraulic geometry of stream channels and some physiographic implications. U.S.G.S. Prof. Paper 252, 56 pp.

Leopold, L. B., Emmett, W. W., and Myrick, R. W., 1966. Channel and Hillslope Processes in a Semi-Arid Area, New Mexico. U.S.G.S. Prof. Paper 352-G.

Leopold, L. B. and Miller, J. P., 1956. Ephemeral streams-hydraulic factors and their relation to the drainage net. U.S.G.S. Prof. Paper 282-A, 37 pp.

Leopold, L. B., Wolman, M. G., and Miller, J. P., 1964. Fluvial Processes in Geomorphology. Freeman Press, San Francisco, 522 pp.

Lewis, 1963. Desert floods - a report on southern Arizona floods of September 1962, 13 pp.

Lowdermilk, W. C. and Sundling, H. L., 1950. Erosion pavement, its formation and significance. Trans. Am. Geophy. Union, 31, p. 96-100.

Mabbutt, J. A., 1965. Stone distribution in a Stony Tableland Soil. Austr. J. Soil Res., 3, p. 131-142.

McGee, W. J., 1897. Sheetflood erosion. Geol. Soc. Am. Bull., v. 8, p. 87-112.

McKee, E. D., 1947. Paleozoic seaways in western Arizona. Am. Assoc. Petroleum Geologists Bull., v. 31, no. 2, p. 282-292.

Melton, M. A., 1965. The geomorphic and paleoclimatic significance of alluvial deposits in southern Arizona. J. Geol., v. 73, p. 1-38.

Metzger, D. G., 1957. Geology and ground-water resources of the Harquahala Plains area, Maricopa and Yuma Counties, Arizona, 40 pp.

Moulden, J. C., 1905. Origin of pebble-covered plains in desert regions. Trans. Am. Inst. Min. Eng., 35, p. 963-964.

National Oceanographic and Atmospheric Administration 1961-1970. Records on Arizona Climate.

Patterson, J. L. and Sommers, W. P., 1966. Magnitude and Frequency of floods in the United States, pt. 9, Colorado River Basin. U.S.G.S. Water Supply Paper 1683, 475 pp.

Peterson, H. V., 1950. The problem of gullying in Western Valleys, in Applied Sedimentation. P. D. Trash (ed.), New York, p. 412-436.

Rahn, P. H., 1965. The Inselbergs of Southwestern Arizona. Unpublished Ph.D. Dissertation, Pennsylvania State University, 140 pp.

Rahn, P. H., 1967. Sheetfloods, streamfloods, and the formation of pediments. Ann. Assoc. Am. Geographers, v. 57, p. 593-604.

Renard, K. G. and Keppel, R. V., 1966. Hydrographs of Ephemeral Streams in the Southwest. Am. Soc. Civil Eng., no. HY2, Proc. Paper 4710, p. 33-52.

Roeske, R. H., 1971. Floods of September 1970 in Arizona, Utah and Colorado, 20 pp.

Ross, C. P., 1923. The Lower Gila Region, Arizona, U.S.G.S. Water Supply Paper 498, 237 pp.

Ruhe, R. V., 1967. Geomorphic Surfaces and Surficial Deposits in Southern New Mexico, New Mexico Bureau of Mines and Mineral Resources, Memoir 18.

Schick, A. P., 1970. Desert floods: interim results of observations in the Nahal Yael Research Watershed, southern Israel, 1965-1970. ISAH-UNESCO Symp. Res. on Rep. and Exp. Basins, New Zealand, p. 478-93.

Schumm, S. A., 1956. The evolution of drainage systems and slopes in badlands at Perth Amboy, New Jersey. Geol. Soc. Am. Bull., v. 67, p. 597-646.

Schumm, S. A., 1965. Quaternary Paleohydrology in: H. E. Wright and D. G. Frey (eds.) The Quaternary of the United States, Princeton, p. 783-794.

Sellers, W. D. and Hill, R. H., 1973. Arizona Climate. Univ. of Arizona Press, Tuscon, 616 pp.

Sharon, D., 1962. On the nature of hamadas in Israel. Zeit. fur. Geom., 6, p. 129-47.

Siegel, Sidney, 1956. Nonparametric Statistics for the Behavioral Sciences: McGraw-Hill Book Co., New York, 312 pp.

Strahler, A. N., 1956. Quantitative slope analysis. Bull. Geol. Soc. Am., v. 67, p. 571-96.

Stulik, R. S., 1964. Effects of ground-water withdrawal, 1954-63, in the lower Harquahala Plains, Maricopa County, Arizona, 8 pp.

Sundborg, A., 1956. The River Dlaralven, a study of fluvial processes. Geografiska Annaler, v. 38, p. 127-316.

Symmons, P. M. and Hemming, C. F., 1968. A note on wind-stable stone-mantles in the southern Sahara. Geog. Journal, v. 125, p. 60-64.

Thomsen, B. W. and Schumann, H. H., 1968. Water Resources of the Sycamore Creek Watershed, Maricopa County, Arizona. U.S.G.S. Water Supply Paper 1861, 53 pp.

Tight, W. G., 1905. Bolson plains of the southwest. Am. Geologists, v. 36, p. 271-284.

Tolman, C. F. 1909. Erosion and deposition in the Southern Arizona bolson region. Jour. of Geology, v. 17, p. 136-163.

Tuan, Y. F., 1959. Pediments in Southeastern Arizona. Univ. of Calif. Publications in Geography, 13, 140 pp.

U. S. Geological Survey, 1975. Surface Water Supply of the U.S., 1966-1970. Water Supply Paper 1926, p5. 9, Colorado River Basin, p. 681.

U. S. Geological Survey, 1970, Surface Water Supply of the U. S., 1961-1965. Water Supply Paper 1926, Colorado River Basin, 571 pp.

Van Arsdale, R., 1974. The Influence of Caliche on the Geometry of Arroyas Near Buckeye, Arizona. Unblished M.S. thesis, Univ. of Cincinnati, 69 pp.

Warren, A., 1971. Dunes in the Tenere Desert. Geog. Journal, v. 137, p. 458-461.

Werho, L. L., 1967. Compilation of flood data for Maricopa County, Arizona, through September 1965, 36 pp.

Wilson, E. D., 1933. Geology and mineral deposits of southern Yuma County, Ariz. Ariz. Bur. Mines Bull. 134, p. 28, 30 and 80.

Wilson, E. D., 1960. Geologic Map of Yuma Co., Arizona. Arizona Bur. of Mines and U. of Arizona.

Wolman, M. G. and Miller, J. P., 1960. Magnitude and frequency of forces in geomorphic processes. J. of Geology, v. 68, p. 54-67.

Yaalon, D. H., 1971. Paleopedology. Papers of the Symposium on Age of Parent Material and Soils, Amsterdam, Netherlands, 350 pp.

APPENDIX I

STATISTICS

(These are standard statistical tests, and their use is explained in Siegel (1956).)

Spearman Rank Correlation Coefficient for Relationship
Between Mean Alluvial Apron Length and Bedrock Area

Mountain Range and Associated Apron	$\bar{L}$ Mean Apron Length (km)	A Bedrock Area (km^2)	Rank L	Rank A	d_i	d_i^2
Eagletail Mts.	8	49	3	3	0	0
Big Horn Mts.	16.7	171	6	6	0	0
Harquahala Mts.	11.5	148	4	5	-1	1
Little Harquahala Mts.	4.8	40	1	2	-1	1
Saddle Mt.	5.2	38	2	1	1	1
Gila Bend Mts.	13.4	56	5	4	1	1

$$r_S = 1 - \frac{6\Sigma d_i^2}{N^3 - N} = 1 - \frac{6(4)}{(6)^3 - 6} = 0.89$$

$\alpha = 0.05$ table value = 0.829 therefore reject H_o

Value of r_S indicates significant positive correlation between $\bar{L}$ and A.

Spearman Rank Correlation Coefficient for Relationship
Between Mean Alluvial Apron Length and Maximum Bedrock Relief

Mountain Range and Associated Apron	$\bar{L}$ Mean Apron Length (km)	H Max. Bedrock Relief (m)	Rank $\bar{L}$	Rank H	d_i	d_i^2
Eagletail Mts.	8	420	3	4	-1	1
Big Horn Mts.	16.7	510	5	5	0	0
Harquahala Mts.	11.5	1060	4	6	-2	4
Little Harquahala Mts.	4.8	280	1	3	-2	4
Saddle Mt.	5.2	255	2	2	0	0
Gila Bend Mts.	13.4	220	6	1	5	25

$$r_S = 1 - \frac{6\Sigma d_i^2}{N^3 - N} = 1 - \frac{6(34)}{6^3 - 6} = 0.03$$

$\alpha = 0.05$ table value = .829 therefore accept H_o

Value of r_S indicates no correlation between $\bar{L}$ and H

Spearman Rank Correlation Coefficient for Relationship
Between Mean Alluvial Apron Relief and Maximum Bedrock Relief

Mountain Range and Associated Apron	$\bar{h}$ Mean Apron Relief (m)	H Max. Bedrock Relief (m)	Rank $\bar{h}$	Rank H	d_i	d_i^2
Eagletail Mts.	86	420	3	4	-1	1
Big Horn Mts.	210	510	6	5	1	1
Harquahala Mts.	200	1060	5	6	-1	1
Little Harquahala Mts.	18	280	2	3	-1	1
Saddle Mt.	91.5	255	4	2	2	4
Gila Bend Mts.	15	220	1	1	0	0

$$r_S = 1 - \frac{6\,d_i}{N^3 - N} = 1 - \frac{6(8)}{6^3 - 6} = 0.77$$

$\alpha = 0.05$ table value = 0.829 therefore accept H_o

Value of r_S indicates no significant correlation between H and $\bar{h}$.

Mann-Whitney U Test for Relationship of dS/dL (rate of change of slope) on Alluvial Aprons of Extrusive and Intrusive Igneous Rocks

E Extrusive Igneous Rocks dS/dL	I Intrusive Igneous Rocks dS/dL
.00375	.00036
.00400	.00065
.00152	.00033
.00167	.00143
.00233	.00079

*slope is expressed as tangent

.00033	.00036	.00065	.00079	.00143	.00152	.00167	.00233	.00375	.00400
I	I	I	I	I	E	E	E	E	E

$n_1 = 5$

$n_2 = 5$

$= 0.05$

$U = 0$

reject H_o (therefore two different samples)

Kendall Coefficient of Concordance (W) for Drainage Texture, Maximum Alluvial Apron Length, and Maximum Bedrock Relief

Geomorphic Parameters	Mountain Ranges and Associated Aprons (N)						
(k)	GBM	SM	EM	BHM	LHM	HM	
Drainage Texture	4	3	5	2	6	1	
Max. Bedrock Relief	6	3	4	1	5	2	$\bar{R}_j = 10.5$
Max. Apron Relief	6	5	3	2	4	1	
$R_j - \bar{R}_j$	5.5	0.5	1.5	-5.5	4.5	-6.5	
$(R_j - \bar{R}_j)^2$	30.3	0.25	2.3	30.3	20.3	42.3	

$$S = \Sigma (R_j - \bar{R}_j)^2 = 125.8$$

$$W = \frac{S}{1/12\ k^2 (N^3-N)} = \frac{125.8}{1/12\ (3)^2 (6^3-6)} = 0.800$$

$\alpha = 0.05$ $S = 125.8$ $k = 3$ $N = 6$ $W = 0.800$

dritical table value = 103.9

S greater than 103.9, therefore reject H_o (there is a positive, significant association among drainage texture, maximum apron relief, and maximum bedrock relief).

Spearman Rank Correlation Coefficient for Relationship between Seasonal Precipitation and Runoff at Centennial Wash and the Harquahala Valley

SUMMER MONTHS:

Precipitation P in cm	Runoff R in m^3	Rank P	Rank R	d_i	d_i^2
0.46	17,270	1	2	-1	1
0.46	86,353	2	4	-2	4
1.12	81,419	3	3	0	0
1.22	109,792	4	6	-2	4
1.25	11,966	5	1	4	16
2.18	1,167,004	6	11	-5	25
2.52	97,456	7	5	2	4
2.85	643,949	8	7	-1	1
3.40	9,252,144	9	13	-4	16
3.81	1,139,864	10	9	1	1
4.67	870,935	11	8	3	9
5.38	1,144,799	12	10	2	4
5.77	4,909,804	13	12	1	1
11.81	10,720,151	14	14	0	0

$$r_S = 1 - \frac{6\Sigma d_i^2}{N^3 - N} = 1 - \frac{6(86)}{6^3-6} = 0.81$$

$\alpha = 0.05$ table value = 0.456 therefore reject H_o

Value of r_S indicates a significant positive correlation between precipitation and runoff in summer months.

WINTER MONTHS:

Precipitation P in cm	Runoff R in m^3	Rank P	Rank R	d_i	d_i^2
4.00	494	3	1	2	4
1.96	11,719	1	2	-1	1
7.09	131,997	4	3	1	1
4.12	465,074	2	4	-2	4
7.77	4,157,297	5	5	0	0

$$r_S = 1 - \frac{6\Sigma d_i^2}{N^3 - N} = 1 - \frac{6(10)}{5^3 - 5} = 0.50$$

$\alpha = 0.05$ table value = 0.900 therefore accept H_o

Value of r_S indicates no evidence to support a correlation between runoff and precipitation in winter months.

Mann-Whitney U Test for Relationship of Drainage Density and Drainage Frequency of Low Order Drainage Basins with and without caliche rubble (Qcr)

Low Order Drainage Basin	Drainage Density	Drainage Frequency
LMQ-C	5.35	16.14
LMQ-D	8.01	23.35
CPQ-A	4.57	11.11
CPQ-B	3.40	4.16
CPQ-C	9.00	23.30
CPQ-D	6.25	11.54
BHMQ-A	6.27	16.72
BHMQ-B	3.17	16.10
EMQ-A	11.57	50.23
EMQ-B	19.33	69.57

low order basin with caliche rubble deposits = C

low order basin without caliche rubble deposits = N

Drainage Density Test:

3.17	3.40	4.57	5.35	6.25	6.27	8.01	9.00	11.57	19.33
N	C	C	N	C	N	N	C	N	N

n_2 = C = 4 U = 8

n_1 = N = 6 α = 0.05 table value - 3, therefore accept H_o.

U value inidcated drainage densities same in basins of different surficial deposits

---

Drainage Frequency Test:

4.16	11.11	11.54	16.10	16.14	16.72	23.30	23.35	50.23	69.57
C	C	C	N	N	N	C	N	N	N

n_2 = C = 4 U = 8

n_1 = N = 6 α = 0.05 table value - 3, therefore reject H_o.

U value indicates drainage frequency different in basins of different surficial deposits.

Spearman Rank Correlation Coefficient for Relationship Between Computed Tractive Force and Maximum Particle Diameter

Maximum Particle Diameter (m)	Tractive Force	Rank mpd	Rank TF	d_i	d_i^2
.02	2.6	1	1	0	0
.10	3.7	2	2	0	0
.10	9.0	3	13	-10	100
.15	4.5	4	3	1	1
.19	6.2	5	6	-1	1
.20	7.7	6	9	-3	9
.22	16.3	7	24	-17	289
.23	6.4	8	7	1	1
.23	9.8	9	15	-6	36
.27	10.7	10	19	-9	82
.31	5.9	11	5	6	36
.32	9.0	12	14	-2	4
.33	10.6	13	18	-5	25
.34	9.9	14	16	-2	4
.34	10.2	15	17	-2	4
.39	6.8	16	8	8	64
.43	8.2	17	10	7	49
.46	5.8	18	4	14	196
.46	17.6	19	25	6	36
.48	8.2	20	11	9	81
.50	8.6	21	12	9	81
.56	15.9	22	23	-1	1
.60	19.6	23	26	-3	9
.64	22.9	24	28	-4	16
.70	11.1	25	20	5	25
.75	12.0	26	21	5	25
.84	14.3	27	22	5	25
.91	19.6	28	27	1	1

Spearman Rank Correlation Coefficient for Relationship
Between Computed Tractive Force and Max. Particle Diameter
(continued)

$$r_S = \frac{6\Sigma d_i^2}{N^3 - N} = 1 - \frac{6(1191)}{28^3 - 28} = 0.67$$

$\alpha = 0.05$ table value = 0.317 therefore reject H_o

Value of r_S indicates significant positive correlation between computed tractive force and maximum particle diameter.

Spearman Rank Correlation Coefficient for Relationship Between Local Maximum Channel Width, Channel Length, and Drainage Area

DRAINAGE AREA:

A_d Drainage Area (km^2)	W_c Max. Channel Width (m)	Rank A_d	Rank W_c	d_i	d_i^2
1.0	5.5	1	2	-1	1
2.2	2.6	2	1	1	1
2.2	7.0	3	5	-2	4
3.6	6.0	4	3	1	1
4.3	11.8	5	7	-2	4
5.7	11.5	6	6	0	0
17.0	8.0	7	4	3	9
279.0	13.2	9	8	1	1
261.0	15.3	8	9	-1	1

$$r_S = 1 - \frac{6\Sigma d_i^2}{N^3 - N} = 1 - \frac{6(22)}{9^3 - 9} = 0.82$$

$\alpha = 0.05$ table value = 0.600 therefore rejct H_o

Value of r_S indicates a significant positive correlation between drainage area above the local max. channel width and the amount of width.

CHANNEL LENGTH:

L_c Channel Length (km)	W_c Max. Channel Width (m)	Rank L_c	Rank W_c	d_i	d_i^2
2.1	4.6	1	1	0	0
2.2	5.5	2	2	0	0
2.2	7.0	3	4	-1	1
3.7	6.0	4	3	1	1
4.3	11.8	5	7	-2	4
6.8	11.5	6	6	0	0
10.9	8.0	7	5	2	4
24.3	13.2	8	8	0	0

$$r_S = 1 - \frac{6\Sigma d_i^2}{N^3 - N} = 1 - \frac{6(10)}{8^3 - 8} = 0.88$$

$= 0.05$ table value = .643 therefore reject H_o

Value of r_S indicates a significant positive correlation between length of channel above the local maximum channel width and amount of channel width.

Spearman Rank Correlation Ceofficient for Relationship Between Channel Length and Drainage Area above Local Maximum Channel Width

Drainage Area (km^2)	Channel Length (km)	Rank A_d	Rank L_c	d_i	d_i^2
.98	.39	1	1	0	0
1.11	.42	2	2	0	0
1.50	.85	3	3	0	0
3.60	.98	4	4	0	0
4.30	1.00	5	5	0	0
5.70	5.00	6	6	0	0
11.40	11.40	7	7	0	0
17.00	10.90	8	8	0	0
261.00	29.90	9	10	-1	1
279.00	24.30	10	9	1	1

$$r_S = 1 - \frac{6\Sigma d_i^2}{N^3 - N} = 1 - \frac{6(2)}{10^3 - 10} = 0.988$$

$\alpha = 0.05$ table value - therefore reject H_o

Value of r_S indicates a significant positive correlation between area and length of channel above the local maximum channel width.

Sign Test for Differences in Computed Tractive Force Down Ephemeral Washes of Selected Alluvial Aprons in the Study Area

Alluvial Apron	A T_1 greater than T_2	B T_1 less than T_2	Direction of Difference	Sign
Harquahala Mts.	3	2	A > B	+
Saddle Mountain	4	2	A > B	+
Big Horn Mts.	1	0	A > B	+
Eagletail Mts.	2	0	A > B	+

T_1 = computed travite force for station which preceeds station with maximum channel width

T_2 = computed tractive force at station with local maximum channel width

X = number of fewer signs - 0

N = number of signs that show difference = 4

$\alpha = 0.05$ table value less than 0.031 therefore reject H_o.

Sign Test indicates that there are more washes on the alluvial aprons whose T_1 is greater than T_2, or a reduction in tractive force at the station with the local maximum channel width.

Spearman Rank Correlation Coefficient for Relationship Between Computed Discharge and Drainage Area at the Maximum Channel Width in Basins with and without Caliche Rubble Deposits

BASINS WITHOUT CALICHE RUBBLE DEPOSITS (Qcr):

A_d Drainage Area at Max. W_c (km^2)	Q_c Discharge at Max. W_c (m^3/sec.)	Rank A_d	Rank Q_c	d_i	d_i^2
1.11	10.0	1	1	0	0
3.40	36.2	2	3	-1	1
3.60	23.3	3	2	1	1
17.00	67.0	4	4	0	0
261.00	583.0	5	5	0	0

$$r_S = 1 - \frac{6\Sigma d_i^2}{N^3 - N} = 1 - \frac{6(2)}{5^3 - 5} = 0.90$$

$\alpha = 0.05$ table value = 0.9000 therefore reject H_o

Value of r_S indicates a significant positive correlation between computed discharge and drainage area at the local maximum channel width in low order basins without caliche rubble deposits.

BASINS WITH CALICHE RUBBLE DEPOSITS (Qcr):

Drainage Area at Max. W_c (km^2)	Discharge at Max. W_c (m^3/sec)	Rank A_d	Rank Q_c	d_i	d_i^2
.31	12	1	1	0	0
.98	30.6	2	2	0	0
2.21	47.8	3	4	-1	1
5.70	43.9	4	3	1	1
13.40	51.8	5	5	0	0

$$r_S = 1 - \frac{6\Sigma d_i^2}{N^3 - N} = 1 - \frac{6(2)}{5^3 - 5} = 0.90$$

$\alpha = 0.05$ table value = 0.90 therefore reject H_o

Value of r_S indicates a significant positive correlation between computed discharge and drainage area for the local maximum channel width in low order drainage basins with caliche rubble deposits.

Mann-Whitney U Test for Density Measurements on LANDSAT Imagery (MSS Band 7)

RUN 1

Qff = fine grained alluvial fans
Qfc = coarse grained alluvial fans

n_1 = Qff	0.45	0.43	0.50	0.48	0.45	0.45	0.47	0.55
n_2 = Qfc	0.63	0.65	0.60	0.60	0.75	0.89	0.67	0.93

0.43	0.45	0.45	0.45	0.47	0.48	0.50	0.55	0.60	0.60	0.63	0.65	0.67	0.75	0.89	0.93
Qff	Qff	Qff	Qff	Qff	Qff	Qff	Qff	Qfc	Qfc	Qfc	Qfc	Qfc	Qfc	Qfc	Qfc

n_1 = 8

n_2 = 8

α = .05

u = o table value = .000

reject H_o (therefore two samples are different)

Mann-Whitney U Test for Density Measurements on LANDSAT Imagery (MSS Band 7)

RUN 2

Qff = fine grained alluvial fans
Qfc = coarse grained alluvial fans

n_1 = Qff	0.47	0.45	0.44	0.50	0.44	0.40	0.40	0.48
n_2 = Qfc	0.81	0.71	0.94	0.72	0.61	0.60	0.67	0.73

0.40	0.40	0.44	0.44	0.45	0.47	0.48	0.50	0.60	0.61	0.67	0.71	0.72	0.73	0.81	0.94
Qff	Qff	Qff	Qff	Qff	Qff	Qff	Qff	Qfc	Qfc	Qfc	Qfc	Qfc	Qfc	Qfc	Qfc

$n_1 = 8$
$n_2 = 8$
$\alpha = .05$

u = 0 table value = .000

reject H_o (two samples are different)

Mann-Whitney U Test for Density Measurements on LANDSAT Imagery (MSS Band 7)

RUN 3

Qff = fine grained alluvial fans
Qfc = coarse grained alluvial fans

n_1 = Qff	0.49	0.47	0.49	0.46	0.41	0.44	0.37	0.41
n_2 = Qfc	0.71	0.63	0.61	0.72	0.66	0.70	0.65	0.67

0.37	0.41	0.41	0.44	0.46	0.47	0.49	0.49	0.61	0.63	0.65	0.66	0.67	0.70	0.71	0.72
Qff	Qff	Qff	Qff	Qff	Qff	Qff	Qff	Qfc	Qfc	Qfc	Qfc	Qfc	Qfc	Qfc	Qfc

$n_1 = 8$
$n_2 = 8$
$= .05$

$u = 0$ table value = .000

reject H_o (therefore two samples are different)

Mann-Whitney U Test for Density Measurements on LANDSAT Imagery (MSS Band 7)

Run 1

Qgv = varnished gravels
Qfc = coarse grained alluvial fans

n_1 = Qgv	1.24	1.26	1.25	1.16	1.10	1.23	1.13	1.03
n_2 = Qfc	0.63	0.65	0.60	0.60	0.75	0.89	0.67	0.93

0.60	0.60	0.63	0.65	0.67	0.75	0.89	0.93	1.03	1.10	1.13	1.16	1.23	1.24	1.25	1.26
Qfc	Qfc	Qfc	Qfc	Qfc	Qfc	Qfc	Qfc	Qgv	Qgv	Qgv	Qgv	Qgv	Qgv	Qgv	Qgv

n_1 = 8
n_2 = 8
α = .05

u = 0 table value = .000 < .05

reject H_o (therefore two samples are different)

Mann-Whitney U Test for Density Measurements on LANDSAT Imagery (MSS Band 7)

RUN 2

Qgv = varnished gravels
Qfc = coarse grained alluvial fans

n_1 = Qgv	1.19	1.24	1.22	1.18	1.23	0.99	0.99	0.89
n_2 = Qfc	0.81	0.72	0.94	0.72	0.61	0.60	0.67	0.73

0.60	0.61	0.67	0.71	0.72	0.73	0.81	0.89	0.94	0.99	0.99	1.18	1.19	1.22	1.23	1.24
Qfc	Qfc	Qfc	Qfc	Qfc	Qfc	Qfc	Qgv	Qgv	Qgv	Qgv	Qgv	Qgv	Qgv	Qgv	Qgv

n_1 = 8
n_2 = 8
α = .05

u = 0 table value = .000

reject H_o (therefore two samples are different)

Mann-Whitney U Test for Density Measurements on LANDSAT Imagery (MSS Band 7)

Run 3

Qgv = varnished gravels
Qfc = coarse grained alluvial fans

n_1 = Qgv	1.25	1.28	1.23	1.24	0.99	1.06	0.78	1.07
n_2 = Qfc	0.71	0.63	0.61	0.72	0.66	0.70	0.65	0.67

0.61	0.63	0.65	0.66	0.67	0.70	0.71	0.72	0.78	0.99	1.06	1.07	1.23	1.24	1.25	1.28
Qfc	Qfc	Qfc	Qfc	Qfc	Qfc	Qfc	Qfc	Qgv	Qgv	Qgv	Qgv	Qgv	Qgv	Qgv	Qgv

$n_1 = 8$
$n_2 = 8$
$\alpha = .05$

u = 0 table value = .000

reject H_o (therefore two samples are different)

Mann-Whitney U Test for Density Measurements on LANDSAT Imagery (MSS Band 7)

RUN 1

Qcr = caliche rubble
Qfc = coarse grained alluvial fans

n_1 = Qcr	0.63	0.65	0.60	0.60	0.75	0.89	0.67	0.93
n_2 = Qfc	0.66	0.65	0.66	0.75	0.63	0.67	0.61	0.68

0.60	0.60	0.61	0.63	0.63	0.65	0.65	0.66	0.67	0.67	0.68	0.75	0.75	0.89	0.93
Qcr	Qcr	Qfc	Qcr	Qfc	Qcr	Qfc	Qfc	Qfc	Qcr	Qfc	Qfc	Qcr	Qcr	Qcr

$n_1 = 8$

$n_2 = 8$

$\alpha = .05$

$u = 2 + 3 + 4 + 4 + 4 + 5 + 5 = 27$ table value = .323

accept H_o (therefore two samples are same)

Mann-Whitney U Test for Density Measurements on LANDSAT Imagery (MSS Band 7)

RUN 2

Qcr = caliche rubble
Qfc = coarse grained alluvial fans

n_1 = Qcr	0.63	0.63	0.65	0.67	0.68	0.59	0.64	0.63
n_2 = Qfc	0.81	0.71	0.94	0.72	0.61	0.60	0.67	0.73

0.59	0.60	0.61	0.63	0.63	0.63	0.64	0.65	0.67	0.67	0.68	0.71	0.72	0.73	0.81	0.94
Qcr	Qfc	Qfc	Qcr	Qcr	Qcr	Qcr	Qcr	Qcr	Qfc	Qcr	Qfc	Qfc	Qfc	Qfc	Qfc

$n_1 = 8$

$n_2 = 8$

α .05

$u = 1 + 1 + 7 + 8 + 8 + 8 + 8 + 8 = 49$

table value > .520

accept H_o (Therefore two samples are same)

Mann-Whitney U Test for Density Measurements on LANDSAT Imagery (MSS Band 7)

RUN 3

Qcr = caliche rubble
Qfc = coarse grained alluvial fans

n_1 = Qcr	0.65	0.75	0.61	0.63	0.68	0.67	0.64	0.59
n_2 = Qfc	0.71	0.63	0.61	0.72	0.66	0.70	0.65	0.67

0.59	0.61	0.61	0.63	0.63	0.64	0.65	0.65	0.66	0.67	0.67	0.68	0.70	0.71	0.72	0.75
Qcr	Qcr	Qfc	Qfc	Qcr	Qcr	Qcr	Qfc	Qfc	Qcr	Qfc	Qcr	Qfc	Qfc	Qfc	Qcr

$n_1 = 8$

$n_2 = 8$

α .05

$u = 2 + 2 + 5 + 5 + 6 + 7 + 7 + 7 = 41$

table value > .520

accept H_o (therefore two samples are same)

Mann-Whitney U Test for Density Measurements on LANDSAT Imagery (MSS Band 7)

RUN 1

Qal = modern alluvium
Qff = fine grained alluvial fan

n_1 = Qal	0.40	0.37	0.29	0.38	0.46	0.57	0.57	0.68
n_2 = Qff	0.45	0.43	0.50	0.48	0.45	0.45	0.47	0.55

0.29	0.37	0.38	0.40	0.43	0.45	0.45	0.45	0.46	0.47	0.48	0.50	0.55	0.57	0.57	0.68
Qal	Qal	Qal	Qal	Qff	Qff	Qff	Qff	Qal	Qff	Qff	Qff	Qff	Qal	Qal	Qal

$n_1 = 8$

$n_2 = 8$

α .05

$u = 4 + 8 + 8 + 8 = 28$ table value = .360

accept H_o (therefore two samples are same)

Mann-Whitney U Test for Density Measurements on LANDSAT Imagery (Mss Band 7)

RUN 2

Qal = modern alluvium
Qff = fine grained alluvial fans

n_1 = Qal	0.37	0.33	0.35	0.35	0.36	0.56	0.56	0.77
n_2 = Qff	0.47	0.45	0.44	0.50	0.44	0.40	0.40	0.48

0.33	0.35	0.35	0.36	0.37	0.40	0.40	0.44	0.44	0.45	0.47	0.48	0.50	0.56	0.56	0.77
Qal	Qal	Qal	Qal	Qal	Qff	Qff	Qff	Qff	Qff	Qff	Qff	Qff	Qal	Qal	Qal

$n_1 = 8$

$n_2 = 8$

.05

$u = 8 + 8 + 8 = 24$

accept H_o (therefore two samples are same)

Mann-Whitney U Test for Density Measurements on LANDSAT Imagery (MSS Band 7)

RUN 3

Qal = modern alluvium
Qff = fine grained alluvial fans

n_1 = Qal	0.35	0.34	0.33	0.34	0.47	0.47	0.65	0.50
n_2 = Qff	0.49	0.47	0.49	0.46	0.41	0.44	0.37	0.41

0.33	0.34	0.34	0.35	0.37	0.41	0.41	0.44	0.46	0.47	0.47	0.47	0.49	0.49	0.50	0.65
Qal	Qal	Qal	Qal	Qff	Qff	Qff	Qff	Qff	Qff	Qal	Qal	Qff	Qff	Qal	Qal

$n_1 = 8$

$n_2 = 8$

α .05

$u = 6 + 6 + 8 + 8 = 28$ table value = .360

accept H_o (therefore two samples are same)

Mann-Whitney U Test for Density Measurements on LANDSAT Imagery (MSS Bands 4,5 & 7 Color Composite)

RUN 1

Qff = fine grained alluvial fans
Qfc = coarse grained alluvial fans

n_1 = Qff	0.43	0.39	0.40	0.34	0.37	0.38	0.38	0.31
n_2 = Qfc	0.49	0.42	0.44	0.37	0.35	0.47	0.56	0.45

0.31	0.34	0.35	0.37	0.38	0.38	0.39	0.40	0.42	0.43	0.44	0.45	0.47	0.49	0.56
Qff	Qff	Qfc	Qfc	Qff	Qff	Qff	Qff	Qfc	Qff	Qfc	Qfc	Qfc	Qfc	Qfc

n_1 = 8
n_2 = 8
α .05

u = 2 + 2 + 2 + 2 + 3 = 11 table value = .014

reject H_o (therefore two samples are different)

Mann-Whitney U Test for Density Measurements on LANDSAT Imagery (MSS Bands 4,5 & 7 Color Composite)

RUN 1

Qgv = varnished gravels
Qfc = coarse grained alluvial fans

n_1 = Qgv	0.67	0.69	0.71	0.65	0.64	0.68	0.64	0.61
n_2 = Qfc	0.49	0.42	0.44	0.37	0.35	0.47	0.56	0.45

0.35	0.37	0.42	0.44	0.45	0.47	0.49	0.56	0.61	0.64	0.64	0.65	0.67	0.68	0.69	0.71
Qfc	Qfc	Qfc	Qfc	Qfc	Qfc	Qfc	Qfc	Qgv	Qgv	Qgv	Qgv	Qgv	Qgv	Qgv	Qgv

n_1 = 8
n_2 = 8
α .05

u = 0 table value = .000

reject H_o (therefore two samples are different)

Mann-Whitney U Test for Density Measurements on LANDSAT Imagery (MSS Bands 4,5 & 7 Color Composite)

RUN 1

Qcr = caliche rubble
Qfc = coarse grained alluvial fans

n_1 = Qcr	0.47	0.50	0.34	0.33	0.35	0.33	0.37	0.63
n_2 = Qfc	0.49	0.42	0.44	0.37	0.35	0.47	0.56	0.45

0.33	0.33	0.34	0.35	0.35	0.37	0.37	0.42	0.44	0.45	0.47	0.47	0.47	0.49	0.50	0.56	0.63
Qcr	Qcr	Qcr	Qcr	Qfc	Qfc	Qcr	Qfc	Qfc	Qfc	Qcr	Qcr	Qfc	Qfc	Qcr	Qfc	Qcr

n_1 = 8
n_2 = 8
α .05

u = 4 + 4 + 5 + 5 + 5 + 6 + 6 + 7 = 42
table value > .520

accept H_o (therefore two samples are same)

Mann-Whitney U Test for Density Measurements on LANDSAT Imagery (MSS Bands 4,5 & 7 Color Composite)

RUN 1

Qal = modern alluvium
Qff = fine grained alluvial fans

n_1 = Qal	0.19	0.27	0.30	0.43	0.30	0.48	0.30	0.28
n_2 = Qff	0.43	0.39	0.40	0.34	0.37	0.38	0.38	0.31

0.19	0.27	0.28	0.30	0.30	0.30	0.31	0.34	0.37	0.38	0.38	0.39	0.40	0.43	0.43	0.48
Qal	Qal	Qal	Qal	Qal	Qal	Qff	Qff	Qff	Qff	Qff	Qff	Qff	Qff	Qal	Qal

$n_1 = 8$

$n_2 = 8$

α .05

u = 6 + 6 + 6 + 6 + 6 + 6 + 6 + 6 = 48
table value > .520

accept H_o (therefore two samples are same)

APPENDIX II

SIEVE ANALYSIS OF SURFICIAL DEPOSITS

AND WASH DEPOSITS

Sample: Sand Dune

Grain size (mm)	Weight Retained	Weight %	Cumulative %
Greater than 8	0.00	0.00	0.00
2.00-8.00	0.30	0.07	0.07
1.19-1.00	1.88	0.45	0.52
0.59-0.50	10.87	2.59	3.11
.297-.290	104.30	24.82	27.93
.177-.149	132.19	31.43	59.36
.149-.125	42.10	10.02	69.38
.125-.105	28.35	6.75	76.13
.074-.062	58.50	13.92	90.05
Pan	41.80	9.95	100.00
Total	420.29	100.00	100.00

Greater than 8	0.58	0.11	0.11
2.00-8.00	0.80	0.15	0.26
1.19-1.00	2.40	0.44	0.70
0.59-0.50	31.72	5.81	6.51
.297-,290	154.98	28.35	34.86
.177-.149	166.10	30.39	65.25
.149-.125	45.28	8.29	73.54
.125-.105	29.80	5.45	78.99
.074-.062	66.19	12.11	91.10
Pan	48.62	8.90	100.00
Total	546.47	100.00	100.00

Sample: Fine Grained Alluvial Fan

Grain size (mm)	Weight Retained	Weight %	Cumulative %
Greater than 8	8.65	4.38	4.38
2.00-8.00	12.01	6.09	10.47
1.19-1.00	19.70	9.98	20.45
0.59-0.50	24.02	12.17	32.62
.297-.290	28.40	14.39	47.01
.177-.149	16.92	8.57	55.58
.149-.125	6.19	3.14	58.72
.125-.105	4.90	2.48	61.20
.074-.062	15.37	7.79	68.99
Pan	61.20	31.01	100.00
Total	197.36	100.00	100.00

Greater than 8	33.74	14.73	14.73
2.00-8.00	14.10	6.16	20.89
1.19-1.00	16.72	7.30	28.19
0.59-0.50	15.40	6.72	34.91
.297-.290	17.99	7.85	42.76
.177-.149	15.00	6.55	49.31
.149-.125	6.85	2.99	52.30
.125-.105	6.89	3.01	55.31
.074-.062	32.45	14.16	69.47
Pan	70.00	30.53	100.00
Total	229.10	100.00	100.00

Sample: Coarse Grained Alluvial Fan

Grain Size (mm)	Weight Retained	Weight %	Cumulative %
Weathered:			
Greater than 8	266.70	85.56	85.56
2.00-8.00	1.50	0.48	86.04
1.19-1.00	2.20	0.71	86.75
0.59-0.50	2.81	0.90	87.65
.297-.250	3.20	1.03	88.68
.177-.149	2.91	0.93	89.61
.149-.125	1.60	0.51	90.12
.125-.105	1.67	0.54	90.66
.074-.062	9.80	3.14	93.80
Pan	19.32	6.20	100.00
Total	311.71	100.00	100.00
Unweathered:			
Greater than 8	307.49	65.32	65.32
2.00-8.00	58.04	12.33	77.65
1.19-1.00	31.70	6.73	84.38
0.59-0.50	16.83	3.57	87.95
.297-.250	15.87	3.37	91.32
.177-.149	11.30	2.40	93.72
.149-.125	4.30	0.91	94.63
.125-.105	3.29	0.70	95.33
.074-.062	8.50	1.81	97.14
Pan	13.48	2.86	100.00
Total	470.80	100.00	100.00

Sample: CPQ-BI

Grain size (mm)	Weight Retained	Weight %	Cumulative %
Berm:			
Greater than 8	7.78	3.60	3.60
2.00-8.00	4.04	1.90	5.50
1.19-1.00	7.97	3.70	9.20
0.59-0.50	24.15	11.10	20.30
.297-.250	54.46	24.90	45.20
.177-.149	37.19	17.00	62.20
.149-.125	12.09	5.50	67.70
.125-.105	8.99	4.10	71.80
.074-.062	22.72	10.40	82.20
Pan	38.86	17.80	100.00
Total	212.11	100.00	100.00

Channel:			
Greater than 8	358.02	88.06	
2.00-8.00	18.29	4.50	95.56
1.19-1.00	12.92	3.20	95.76
0.59-0.50	10.53	2.60	98.36
.297-.250	4.72	1.20	98.56
.177-.149	0.64	0.20	99.76
.149-.125	0.18	0.04	99.80
.125-.105	0.19	0.05	99.85
.074-.062	0.28	0.07	99.92
Pan	0.52	0.13	100.05
Total	100.00	100.00	100.00

Sample: CPQ-BII

Grain size (mm)	Weight Retained	Weight %	Cumulative %
Berm:			
Greater than 8	0.28	0.13	
2.00-8.00	0.63	0.30	0.43
1.19-1.00	1.81	0.87	1.30
0.59-0.50	5.49	2.62	3.92
.297-.250	19.72	9.42	13.34
.177-.149	29.70	14.19	27.53
.149-.125	15.61	7.46	34.99
.125-.105	13.19	6.30	41.29
.074-.062	43.81	20.93	62.22
Pan	79.08	37.78	100.00
Total	209.32	100.00	100.00
Channel:			
Greater than 8	221.73	78.66	78.66
2.00-8.00	28.91	10.23	88.99
1.19-1.00	19.06	6.74	95.63
0.59-0.50	8.12	2.87	98.50
.297-.250	2.89	1.02	99.52
.177-.149	0.47	0.17	99.69
.149-.125	0.10	0.04	99.73
.125-.105	0.05	0.02	99.75
.074-.062	0.12	0.04	99.79
Pan	0.59	0.21	100.00
Total	282.04	100.00	100.00

Sample: CPQ-BIII

Grain size (mm)	Weight Retained	Weight %	Cumulative %
Berm:			
Greater than 8	14.21	7.56	
2.00-8.00	3.77	2.01	9.57
1.19-1.00	3.76	2.00	11.57
0.59-0.50	5.65	3.01	14.58
.297-.250	15.26	8.12	22.70
.177-.149	21.38	11.37	34.07
.149-.125	10.98	5.84	39.91
.125-.105	9.54	5.07	44.98
.074-.062	34.92	18.57	63.55
Pan	68.57	36.45	100.00
Total	188.04	100.00	100.00
Channel:			
Greater than 8	436.16	90.65	
2.00-8.00	32.94	6.85	97.50
1.19-1.00	7.57	1.59	99.09
0.59-0.50	1.57	0.33	99.42
.297-.250	0.53	0.11	99.53
.177-.149	0.35	0.07	99.60
.149-.125	0.16	0.03	99.63
.125-.105	0.14	0.03	99.66
.074-.062	0.35	0.07	99.73
Pan	1.28	0.27	100.00
Total	481.15	100.00	100.00

Sample: CPQ-BIV

Grain Size (mm)	Weight Retained	Weight %	Cumulative %
Berm:			
Greater than 8	74.20	23.69	23.69
2.00-8.00	46.60	14.88	38.57
1.19-1.00	27.84	8.89	47.46
0.59-0.50	11.20	3.58	51.04
.297-.250	15.37	4.91	55.95
.177-.149	16.78	5.36	61.31
.149-.125	8.38	2.68	63.99
.125-.105	7.38	2.36	66.35
.074-.062	28.46	9.09	75.44
Pan	76.96	24.56	100.00
Total	313.17	100.00	100.00
Channel:			
Greater than 8	287.84	70.78	
2.00-8.00	37.04	9.11	79.89
1.19-1.00	30.95	7.61	87.50
0.59-0.50	27.11	6.67	94.17
.297-.250	14.26	3.51	97.68
.177-.149	2.98	0.73	98.41
.149-.125	0.47	0.12	98.53
.125-.105	0.44	0.11	98.64
.074-.062	1.21	0.30	98.94
Pan	4.31	1.06	100.00
Total	406.61	100.00	100.00

Sample: CPQ-BV

Grain size (mm)	Weight Retained	Weight %	Cumulative %
Berm:			
Channel:			
Greater than 8	115.48	48.37	
2.00-8.00	47.53	19.90	68.27
1.19-1.00	37.07	15.52	83.79
0.59-0.50	21.54	9.02	92.81
.297-.250	8.25	3.45	96.26
.177-.149	1.87	0.78	97.04
.149-.125	0.57	0.24	97.28
.125-.105	0.46	0.19	97.47
.074-.062	1.38	0.58	98.05
Pan	4.65	1.95	100.00
Total	238.80	100.00	100.00

Sample: LMQ-DI (III)

Grain size (mm)	Weight Retained	Weight %	Cumulative %
Berm:			
Greater than 8	26.77	12.18	
2.00-8.00	9.63	4.38	16.56
1.19-1.00	6.46	2.94	19.50
0.71-0.59	7.99	3.63	23.13
.297-.250	21.79	9.91	33.04
.177-.149	26.92	12.24	45.28
.149-.125	12.28	5.59	50.57
.125-.105	10.40	4.73	55.30
.074-.062	19.47	8.86	64.16
Pan	78.15	35.54	99.70
Total	219.86	100.00	100.00
Channel:			
Greater than 8	324.90	80.67	
2.00-8.00	33.00	8.19	88.86
1.19-1.00	20.29	5.04	93.90
0.59-0.50	12.08	3.00	96.90
.297-.250	6.40	1.59	98.49
.177-.149	1.59	0.39	98.88
.149-.125	0.12	0.03	98.91
.125-.105	0.09	0.02	98.93
.074-.062	0.00	0.00	98.93
Pan	4.29	1.07	100.00
Total	402.76	100.00	100.00

Sample: LMQ-DII

Grain size (mm)	Weight Retained	Weight %	Cumulative %
Berm:			
Greater than 8	5.90	2.65	
2.00-8.00	3.58	1.61	4.26
1.19-1.00	4.80	2.16	6.42
0.59-0.50	5.42	2.44	8.86
.297-.250	16.99	7.64	16.50
.177-.149	29.10	13.09	29.59
.149-.125	15.38	6.92	36.51
.125-.105	14.00	6.30	42.81
.074-.062	32.89	14.79	57.60
Pan	94.31	42.41	100.00
Total	222.37	100.00	100.00
Channel:			
Greater than 8	487.00	77.94	
2.00-8.00	32.59	5.22	83.16
1.19-1.00	35.52	5.69	88.85
0.59-0.50	35.09	5.62	94.47
.297-.250	21.02	3.36	97.83
.177-.149	4.81	0.77	98.60
.149-.125	1.07	0.17	98.77
.125-.105	0.69	0.11	98.88
.074-.062	0.06	0.01	98.89
Pan	6.91	1.11	100.00
Total	624.76	100.00	100.00

Sample: LMQ-DIII

Grain size (mm)	Weight Retained	Weight %	Cumulative %
Berm:			
Greater than 8	1.68	0.68	
2.00-8.00	4.58	1.87	2.55
1.19-1.00	6.49	2.64	5.19
0.59-0.50	6.88	2.80	7.99
.297-.250	25.90	10.55	18.54
.177-.149	39.90	16.25	34.79
.149-.125	18.65	7.60	42.39
.125-.105	15.41	6.28	48.67
.074-.062	36.60	14.91	63.58
Pan	89.45	36.42	100.00
Total		100.00	100.00
Channel:			
Greater than 8	444.80	85.46	
2.00-8.00	34.09	6.55	92.01
1.19-1.00	21.08	4.05	96.06
0.59-0.50	9.22	1.77	97.83
.297-.250	4.26	0.82	98.65
.177-.149	2.25	0.43	99.08
.149-.125	0.57	0.11	99.19
.125-.105	0.40	0.08	99.27
.074-.062	1.28	0.25	99.52
Pan	2.50	0.48	100.00
Total	520.45	100.00	100.00

Sample: LMQ-DIV

Grain size (mm)	Weight Retained	Weight %	Cumulative %
Berm:			
Greater than 8	3.09	1.36	
2.00-8.00	3.46	1.52	2.86
1.19-1.00	3.79	1.67	4.55
0.59-0.50	4.72	2.08	6.63
.297-.250	12.79	5.63	12.26
.177-.149	22.20	11.97	24.23
.149-.125	12.80	5.63	29.86
.125-.105	11.99	5.28	35.14
.074-.062	54.91	24.16	59.30
Pan	92.50	40.70	100.00
Total	227.25	100.00	100.00
Channel:			
Greater than 8	362.43	79.13	
2.00-8.00	33.43	7.28	86.41
1.19-1.00	25.53	5.57	91.98
0.59-0.50	13.50	2.95	94.93
.297-.250	9.35	2.04	96.97
.177-.149	4.49	0.98	97.95
.149-.125	1.30	0.28	98.23
.125-.105	0.91	0.20	98.43
.074-.062	2.68	0.59	99.02
Pan	4.50	0.98	100.00
Total	458.03	100.00	100.00

Sample: BHMQ-BI

Grain size (mm)	Weight Retained	Weight %	Cumulative %
Berm:			
Greater than 8	3.50	1.58	1.58
2.00-8.00	9.80	4.43	6.01
1.19-1.00	33.54	15.16	21.17
0.59-0.50	44.37	20.05	41.22
.297-.250	50.43	22.79	64.01
.177-.149	25.40	11.48	75.49
.149-.125	7.98	3.61	79.10
.125-.105	5.60	2.53	81.63
.074-.062	16.62	7.51	89.14
Pan	24.02	10.86	100.00
Total	221.26	100.00	100.00
Channel:			
Greater than 8	71.21	27.91	27.91
2.00-8.00	27.12	10.63	38.54
1.19-1.00	67.20	26.34	64.88
0.59-0.50	51.96	20.36	85.24
.297-.250	24.68	9.67	94.91
.177-.149	6.04	2.37	97.28
.149-.125	1.41	0.55	97.83
.125-.105	0.85	0.33	98.16
.074-.062	1.60	0.63	98.79
Pan	3.10	1.21	100.00
Total	255.17	100.00	100.00

Sample: BMHQ-BII

Grain size (mm)	Weight Retained	Weight %	Cumulative %
Berm:			
Greater than 8	13.69	8.12	8.12
2.00-8.00	10.29	6.11	14.23
1.19-1.00	23.48	13.93	28.16
0.59-0.50	28.39	16.85	45.01
.297-.250	28.40	16.85	61.85
.177-.149	13.68	8.12	69.98
.149-.125	5.02	2.98	72.96
.125-.105	4.08	2.42	75.38
.074-.062	14.78	8.77	84.15
Pan	26.71	15.85	100.00
Total	168.52	100.00	100.00
Channel:			
Greater than 8	43.62	15.42	15.42
2.00-8.00	54.80	19.38	34.80
1.19-1.00	103.56	36.61	71.41
0.59-0.50	45.28	16.01	87.42
.297-.250	17.73	6.27	93.69
.177-.149	5.10	1.80	95.49
.149-.125	1.69	0.60	96.09
.125-.105	1.22	0.43	96.52
.074-.062	3.81	1.35	97.87
Pan	6.01	2.13	100.00
Total	282.82	100.00	100.00

Sample: BHMQ-BIII

Grain size (mm)	Weight Retained	Weight %	Cumulative %
Berm:			
Greater than 8	4.80	2.63	2.63
2.00-8.00	4.20	2.30	4.93
1.19-1.00	6.45	3.53	8.48
0.59-0.50	8.71	4.77	13.25
.297-.250	14.68	8.04	21.29
.177-.149	16.36	8.96	30.25
.149-.125	8.73	4.78	35.03
.125-.105	8.10	4.44	39.47
.074-.062	37.58	20.58	60.05
Pan	72.98	39.97	100.00
Total	182.59	100.00	100.00
Channel:			
Greater than 8	78.69	23.65	23.65
2.00-8.00	58.43	17.56	41.21
1.19-1.00	66.00	19.83	61.04
0.59-0.50	49.61	14.91	75.95
.297-.250	31.10	9.35	85.30
.177-.149	14.62	4.39	89.69
.149-.125	5.70	1.71	91.40
.125-.105	3.59	1.08	92.48
.074-.062	9.95	2.99	95.47
Pan	15.09	4.53	100.00
Total	332.78	100.00	100.00

Sample: BHMQ-BIV

Grain size (mm)	Weight Retained	Weight %	Cumulative %
Berm:			
Greater than 8	16.70	8.11	8.11
2.00-8.00	10.40	5.05	13.16
1.19-1.00	13.78	6.70	19.86
0.59-0.50	10.30	5.00	24.86
.297-.250	10.90	5.30	30.16
.177-.149	12.94	6.29	36.45
.149-.125	8.38	4.07	40.52
.125-.105	8.76	4.26	44.78
.074-.062	42.92	20.85	65.63
Pan	70.73	34.37	100.00
Total	205.81	100.00	100.00
Channel:			
Greater than 8	489.52	50.76	50.76
2.00-8.00	131.17	13.60	64.36
1.19-1.00	118.10	12.24	76.60
0.59-0.50	76.80	7.96	84.56
.297-.250	58.50	6.06	90.62
.177-.149	30.53	3.17	93.79
.149-.125	9.56	0.99	94.78
.125-.105	6.20	0.64	95.42
.074-.062	20.58	2.13	97.55
Pan	23.61	2.45	100.00
Total	964.57	100.00	100.00

Sample: LMQ-AI

Grain size (mm)	Weight Retained	Weight %	Cumulative %
Berm:			
Greater than 8	1.08	0.57	0.57
2.00-8.00	0.40	0.21	0.78
1.19-1.00	0.50	0.26	1.04
0.59-0.50	1.09	0.57	1.61
.297-.250	8.45	4.42	6.03
.177-.149	23.31	12.20	18.23
.149-.125	14.00	7.33	25.56
.125-.105	12.61	6.60	32.16
.074-.062	46.68	24.43	56.59
Pan	82.99	43.41	100.00
Total	191.11	100.00	100.00
Channel:			
Greater than 8	238.59	56.04	56.04
2.00-8.00	37.39	8.78	64.82
1.19-1.00	42.91	10.08	74.90
0.59-0.50	31.81	7.47	82.37
.297-.250	36.90	8.67	91.04
.177-.149	18.61	4.37	95.41
.149-.125	4.28	1.01	96.42
.125-.105	2.47	0.58	97.00
.074-.062	0.45	0.11	97.11
Pan	12.30	2.89	100.00
Total	100.00	100.00	100.00

Sample: LMQ-AII

Grain size (mm)	Weight Retained	Weight %	Cumulative %
Berm:			
Greater than 8	0.05	0.03	0.03
2.00-8.00	0.11	0.06	0.09
1.19-1.00	3.21	1.77	1.86
0.59-0.50	14.21	7.82	9.68
.297-.250	39.69	21.86	31.54
.177-.149	38.38	21.14	52.68
.149-.125	13.81	7.61	60.29
.125-.105	10.21	5.62	65.91
.074-.062	0.31	0.17	66.08
Pan	61.56	33.91	100.00
Total	181.53	100.00	100.00
Channel:			
Greater than 8	242.49	50.43	50.43
2.00-8.00	36.88	7.67	58.10
1.19-1.00	54.05	11.24	69.34
0.59-0.50	63.50	13.21	82.55
.297-0.50	46.75	9.72	92.27
.297-.250	16.10	3.35	95.62
.177-.149	3.90	0.81	96.43
.149-.125	2.42	0.50	96.93
.125-.105	0.00	3.07	96.93
.074-.062	14.76	100.00	100.00
Pan			
Total	480.85	100.00	100.00

Sample: LMQ-AIII

Grain size (mm)	Weight Retained	Weight %	Cumulative %
Berm:			
Greater than 8	0.02	0.01	0.01
2.00-8.00	0.11	0.05	0.06
1.19-1.00	0.60	0.26	0.32
0.59-0.50	2.09	0.91	1.23
.297-.250	9.01	3.91	5.14
.177-.149	21.40	9.28	14.42
.149-.125	14.51	6.29	20.71
.125-.105	15.05	6.52	27.23
.074-.062	58.01	25.15	52.38
Pan	109.89	47.62	100.00
Total	230.69	100.00	100.00
Channel:			
Greater than 8	228.35	48.12	48.12
2.00-8.00	94.23	19.86	67.98
1.19-1.00	84.10	17.72	85.70
0.59-0.50	32.90	6.93	92.63
.297-.250	17.05	3.59	96.22
.177-.149	4.90	1.03	97.25
.149-.125	1.22	0.26	97.51
.125-.105	0.88	0.19	97.70
.074-.062	0.49	0.10	97.80
Pan	10.46	2.20	100.00
Total	474.58	100.00	100.00

Sample: LMQ-AIV

Grain size (mm)	Weight Retained	Weight %	Cumulative %
Berm:			
Greater than 8	0.50	0.24	0.24
2.00-8.00	0.10	0.05	0.29
1.19-1.00	0.14	0.07	0.36
0.59-0.50	0.65	0.31	0.67
.297-.250	6.52	3.10	3.77
.177-.149	24.30	11.56	15.33
.149-.125	15.72	7.48	22.81
.125-.105	14.30	6.80	29.61
.074-.062	44.70	21.26	50.87
Pan	103.32	49.13	100.00
Total	210.25	100.00	100.00
Channel:			
Greater than 8	110.35	27.48	27.48
2.00-8.00	43.00	10.71	38.19
1.19-1.00	87.79	21.87	60.06
0.59-0.50	76.72	19.11	79.17
.297-.250	36.40	9.07	88.24
.177-.149	13.40	3.34	91.58
.149-.125	4.16	1.04	92.62
.125-.105	3.01	0.75	93.37
.074-.062	0.20	0.05	93.42
Pan	26.40	6.58	100.00
Total	401.43	100.00	100.00

Sample: LMQ-AV

Grain size (mm)	Weight Retained	Weight %	Cumulative %
Berm:			
Greater than 8	0.00	0.00	0.00
2.00-8.00	0.00	0.00	0.00
1.19-1.00	0.60	0.22	0.22
0.59-0.50	1.99	0.72	0.94
.297-.250	36.79	13.25	14.19
.177-.149	69.79	25.13	39.32
.149-.125	29.01	10.44	49.76
.125-.105	22.15	7.97	57.73
.074-.062	56.12	20.21	77.94
Pan	61.30	22.07	100.00
Total	277.75	100.00	100.00
Channel:			
Greater than 8	50.79	14.62	14.62
2.00-8.00	26.81	7.72	22.34
1.19-1.00	52.00	14.97	37.31
0.59-0.50	65.31	18.80	56.11
.297-.250	78.23	22.52	78.63
.177-.149	43.70	12.58	91.21
.149-.125	10.25	2.95	94.16
.125-.105	5.32	1.53	95.69
.074-.062	6.45	1.86	97.55
Pan	8.52	2.45	100.00
Total	347.38	100.00	100.00

Sample: LMQ-AVI

Grain size (mm)	Weight Retained	Weight %	Cumulative %
Berm:			
Greater than 8	0.00	0.00	0.00
2.00-8.00	1.32	0.83	0.83
1.19-1.00	6.40	4.05	4.88
0.59-0.50	10.30	6.51	11.39
.297-.250	20.39	12.89	24.28
.177-.149	13.89	8.78	33.06
.149-.125	5.81	3.67	36.73
.125-.105	4.81	3.04	39.77
.074-.062	10.70	6.76	46.53
Pan	84.60	53.47	100.00
Total	158.22	100.00	100.00
Channel:			
Greater than 8	19.85	8.24	8.24
2.00-8.00	24.03	9.98	18.22
1.19-1.00	62.30	25.86	44.08
0.59-0.50	66.19	27.48	71.56
.297-.250	41.90	17.40	88.98
.177-.149	8.41	3.49	92.45
.149-.125	1.85	0.76	93.21
.125-.105	1.25	0.52	93.73
.074-.062	3.50	1.45	95.18
Pan	11.60	4.82	100.00
Total	240.88	100.00	100.00

Sample: CPQ-CI

Grain size (mm)	Weight Retained	Weight %	Cumulative %
Berm:			
Greater than 8	25.31	15.49	15.49
2.00-8.00	3.09	1.89	17.38
1.19-1.00	4.45	2.72	20.10
0.59-0.50	8.70	5.33	25.43
.297-.250	18.25	11.17	36.60
.177-.149	17.25	10.56	47.16
.149-.125	7.63	4.67	51.83
.125-.105	6.78	4.15	55.98
.074-.062	16.10	9.85	65.83
Pan	55.82	34.17	100.00
Total	163.38	100.00	100.00
Channel:			
Greater than 8	595.21	90.13	90.13
2.00-8.00	27.79	4.19	94.32
1.19-1.00	16.09	2.42	96.74
0.59-0.50	7.59	1.15	97.89
.297-.250	3.90	0.59	98.48
.177-.149	1.99	0.30	98.76
.149-.125	0.71	0.11	98.89
.125-.105			98.89
.074-.062	0.62	0.09	98.98
Pan	6.77	1.02	100.00
Total	662.68	100.00	100.00

Sample: CPQ-CII

Grain size (mm)	Weight Retained	Weight %	Cumulative %
Berm:			
Greater than 8	32.65	8.82	8.82
2.00-8.00	31.01	8.38	17.20
1.19-1.00	62.60	16.91	34.11
0.59-0.50	76.33	20.61	54.72
.297-.250	50.49	13.64	68.36
.177-.149	21.79	5.89	74.25
.149-.125	7.89	2.13	76.38
.125-.105	6.75	1.82	78.20
.074-.062	28.70	7.75	85.95
Pan	52.02	14.05	100.00
Total	370.23	100.00	100.00
Channel:			
Greater than 8	363.80	77.53	77.53
2.00-8.00	35.10	7.45	84.98
1.19-1.00	33.10	7.05	92.03
0.59-0.50	24.36	5.19	97.22
.297-.250	7.89	1.68	98.90
.177-.149	1.69	0.36	99.26
.149-.125	0.40	0.09	99.35
.125-.105	0.29	0.06	99.41
.074-.062	0.29	0.06	99.42
Pan	2.65	0.56	100.00
Total	469.57	100.00	100.00

Sample: CPQ-CIII

Grain size (mm)	Weight Retained	Weight %	Cumulative %
Berm:			
Greater than 8	1.40	0.91	0.91
2.00-8.00	2.69	1.75	2.66
1.19-1.00	8.29	5.38	8.04
0.59-0.50	19.25	12.49	20.53
.297-.250	30.30	19.66	40.19
.177-.149	20.10	13.04	53.23
.149-.125	7.53	4.89	58.12
.125-.105	5.98	3.88	62.00
.074-.062	17.75	11.15	73.15
Pan	40.81	26.85	100.00
Total	154.10	100.00	100.00
Channel:			
Greater than 8	239.95	55.59	55.59
2.00-8.00	72.69	16.83	72.42
1.19-1.00	61.25	14.19	86.61
0.59-0.50	28.59	6.62	93.23
.297-.250	10.29	2.38	95.61
.177-.149	3.59	0.83	96.44
.149-.125	1.22	0.28	96.72
.125-.105	1.01	0.23	96.95
.074-.062	3.08	0.71	97.66
Pan	10.11	2.34	100.00
Total	431.78	100.00	100.00

Sample: CPQ-CIV

Grain size (mm)	Weight Retained	Weight %	Cumulative %
Berm:			
Greater than 8	11.38	4.82	4.82
2.00-8.00	9.80	4.15	8.97
1.19-1.00	13.59	5.75	14.72
0.59-0.50	10.93	4.63	19.35
.297-.250	18.69	7.91	27.26
.177-.149	20.20	8.55	35.81
.149-.125	10.10	4.28	40.09
.125-.105	10.39	4.40	44.49
.074-.062	43.38	18.36	62.85
Pan	87.78	37.15	100.00
Total	236.24	100.00	100.00
Channel:			
Greater than 8	289.15	58.53	58.53
2.00-8.00	88.11	17.84	76.37
1.19-1.00	72.42	14.66	91.03
0.59-0.50	33.81	6.85	97.88
.297-.250	8.30	1.68	99.56
.177-.149	0.66	0.13	99.69
.149-.125	0.11	0.02	99.71
.125-.105	0.50	0.01	99.72
.074-.062	0.50	0.01	99.73
Pan	1.31	0.27	100.00
Total	493.97	100.00	100.00

APPENDIX III

SELECTED SLOPE MEASUREMENTS ON INTERFLUVES OF SURFICIAL DEPOSITS

STATION	DISTANCE (ft)	CHANGE IN ELEVATION (ft)	SLOPE
Coarse grained alluvial fans (Qfc):			
1.	815.0	28.5	2.00°
2.	550.0	12.00	1.25°
3.	862.5	27.82	1.84°
4.	1190.0	10.39	0.50°
5.	920.0	2.78	0.17°
6.	1225.0	21.37	1.00°
7.	1120.0	21.96	1.12°
8.	1135.0	6.62	0.33°
9.	1150.0	20.07	1.00°
Fine grained alluvial fans (Qff):			
1.	1342.5	4.16	0.18°
2.	800.0	3.49	0.25°
3.	545.0	7.13	0.75°
Varnished gravels (Qgv):			
1.	395.0	6.89	1.00°
2.	1030.0	15.09	0.84°
3.	545.0	11.89	1.25°
4.	877.5	17.77	1.16°
5.	1205.0	23.71	1.13°
6.	1120.0	4.18	0.21°
7.	1305.0	19.31	0.85°
8	1395.0	21.68	0.89°
Caliche rubble (Qcr):			
1.	845.0	29.47	2.00°
2.	1080.0	40.82	2.16°
3.	1290.0	38.98	1.73°
4.	1047.5	11.69	0.64°
5.	1190.0	18.22	0.88°

APPENDIX IV

SELECTED DATA ON GEOMORPHIC MAPPING INCLUDING SOIL AND SUPFICIAL DEPOSIT DESCRIPTIONS

STATION: HV-1

LOCATION: Cortez Peak Quad, T2N, R8W, Sec 36, SE 1/4, NW 1/4

SURFICIAL DEPOSIT: Qfc

MICRO-RELIEF: very low, up to 20 cm

PERCENT COVER OF LAND SURFACE WITH GRAVELS: greater than 50%

SOIL DESCRIPTION: 2 cm of varnished gravels on surface.

Horizons - A. vesicular layer is 1 to 1.5 cm thick; moderately calcareous.

B. slightly sticky, slightly plastic; thickness 18 cm; tends to break blocky or powdery; moderately calcareous; 5-YR 6/4 Lite brown chroma 4.

C. thickness unknown; calcic horizon - CCA calcareous. Cca may be 40-50 cm thick near toe as seen in gully. Where exposed at surface it appears pc rather than calcic.

STATION: HV-2

LOCATION: Cortez Peak Quad, T2N, R8W, Sec 36, NW 1/4, SE 1/4

SURFICIAL DEPOSIT: Qfc

MICRO-RELIEF: 10-17 cm increasing

PERCENT COVER OF LAND SURFACE WITH GRAVELS: 30-40%

SOIL DESCRIPTION: varnished desert pavement surface 1-3 cm thick.

Horizon - A. vesicular layer 1 cm and less in thickness; moderately calcareous; 5-YR 6/4 Lite brown chroma 4.

B. thickness highly variable, measured as 10 cm thick at station; moderately calcareous; slightly sticky, very slightly plastic; 20-30 cm below top of B horizon breaks up in blocky form; sticky, plastic; appears reddish, iron colored; highly calcareous, white blebs of calcite; also contains gravels.

C. horizon thickness at least 30 cm; light brown color; pieces of white $CaCO_3$; highly calcareous; very plastic, sticky; Chroma 4, 10 YR 7/4 grayish orange.

STATION: HV-3

LOCATION: Cortez Peak Quad; T2N, R8W, Sec 36, NW 1/4, NW 1/4

SURFICIAL DEPOSIT: Qff

MICRO-RELIEF: up to 46 cm, high due to aeolian activity

PERCENT COVER OF LAND SURFACE WITH GRAVELS: up to 10%

SOIL DESCRIPTION:

Horizons - A. poorly developed A horizon; ochric A; 4 cm thick; moderately calcareous; 10YR 7/4 grayish range chroma 4.

B. sticky, slightly plastic; 16 cm thick; slightly calcareous; appears moist; almost breaks in prisms; 5YR 7/2 grayish orange pink chroma 2

C. thickness unknown; slightly calcareous; somewhat hard to dig in; appears dry; breaks into sort of large thick plates; 5YR 6/4 lite brown chroma 4.

STATION: HV-4

LOCATION: Cortez Peak Quad, T2N, R8W, Sec 26, SE 1/4, SE 1/4

SURFICIAL DEPOSIT: Qal

MICRO-RELIEF: up to 2.5 cm moderate

PERCENT COVER OF LAND SURFACE WITH GRAVELS: less than 5%

SOIL DESCRIPTION:

Horizons - A. ochric A; 2 cm thick; not calcareous; 5YR 7/2 grayish range pink chroma 2.

B. approximately 13 cm; not or barely calcareous; sticky, slightly plastic; 5 YR 6/4 lite brown chroma 4.

C. slightly carcareous; variable between slightly plastic and plastic; breaks blocky; 10R 7/4 mod. orange pink chroma 4.

SURFICIAL DEPOSIT DESCRIPTION: gravels increase with depth.

STATION: HV-5

LOCATION: Cortez Peak Quad, T2N, R8W, Sec 26, NW 1/4, NW 1/4

SURFICIAL DEPOSIT: Qfc

MICRO-RELIEF: up to 10 cm, very low

PERCENT COVER OF LAND SURFACE WITH GRAVELS: greater than 50%

SOIL DESCRIPTION: varnished desert pavement surface 1-2 cm thick, gravels

Horizons - A. vesicular layer 1-1/2-2 cm thick; moderate to highly calcareous; 5YR 6/4 brown chroma 4.

B. highly calcareous; slightly plastic, slightly sticky; increases plasticity with depth; thickness approximately 15 cm; 10R 4/6 modern reddish brown chroma 6.

C. depth and thickness unknown, at least 20 cm; breaks into blocky forms; highly calcareous; not solid Cca horizon; 10 RY 4/5 moderate reddish orange chroma 6.

STATION: HV-6

LOCATION: Cortez Peak Quad, T2N, R8W, Sec 24, SW 1/4, SE 1/4

SURFICIAL DEPOSIT: Qal

MICRO-RELIEF: very low, only gullies 10-30 cm deep

PERCENT COVER OF LAND SURFACE WITH GRAVELS: 5%

SOIL DESCRIPTION

Horizons - A. 4 cm; ochric A; maybe think layer silts and gravels; not calcareous; 5YR 6/4 lite brown chroma 4

B. not calcareous; slightly plastic, slightly sticky; about 35 cm thick; more thick platey chunks; 10R 6/6 moderate reddish orange chroma 6.

C. slight to moderately calcareous, white blebs of calcatie; breaks into blocky chunks; depth of C unknown; 10R 6/6 moderate reddish orange chroma 6.

STATION: HV-7

LOCATION: Big Horn Mountains Quad, T2N, R8W, Sec 21, NW 1/4, SE 1/4

SURFICIAL DEPOSIT: Qfc

MICRO-RELIEF: low to moderate

PERCENT COVER OF LAND SURFACE WITH GRAVELS: greater than 50%

SOIL DESCRIPTION: type calciorthid

SURFICIAL DEPOSIT DESCRIPTION:

Unit A - 30 cm; gravels; iron brown color; contact between A and underlying surface very irregular; gravel unit increases in amount of $CaCO_3$ downward, blebs of white $CaCO_3$ near contact of units A and B. Unit A cuts channel into unit B; channel 1 m deep, approximately 5 m wide; 10R 6/6 moderate reddish orange chroma 6.

Unit B - at least 1-1/4 m; mainly a silty unit; calcareous; breaks into large blocks and prisms; almost prismatic in weathering, has vesicles throughout entire unit; small stringers of gravel, may be 3-4 cm in width; has white filaments of $CaCO_3$ throughout.

STATION: HV-9

LOCATION: Cortez Peak Quad, T2N, R8W, Sec 28, SE 1/4, SW 1/4

SURFICIAL DEPOSIT: Qfc

MICRO-RELIEF: low, up to 15 cm

PERCENT COVER OF LAND SURFACE WITH GRAVELS: 20-30%

SOIL DESCRIPTION: type calciorthid or haplargid; 1-2 cm weathered gravels, desert pavement varnish

Horizons - A. 7 cm. thick; light buff color; highly calcareous; 10R 6/6 moderate reddish orange chroma 6.

B. at least 20 cm thick; reddish brown color; moderately calcareous; slightly plastic, sticky; weathers powdery; 10R 4/6 moderate reddish brown chroma 6.

C. horizon weathers angular and blocky; somewhat indurated; highly calcareous, white filaments of caliche present; 10R 5/4 pale reddish brown chroma 4.

Station HV-9 Continued

SURFICIAL DEPOSIT DESCRIPTION:

Unit A - 20 cm thick; desert pavement surface on top; reddish brown silt and gravels; moderately calcareous

Unit B - 1.3 m; weathers and breaks blocky; moderate to highly calcareous, white filaments of $CaCO_3$ visible throughout section; calcareous throughout unit; lower part of B has large lens of gravel approximately 50 cm thick, vary in thickness to approximately 6 cm; gravelly subunit of B overlies C; Unit B increases in gravel downward; vesicular

Unit C - at least 40 cm thick; contact between units C and B is irregular and undulating; highly calcareous; breaks angular; white filaments of $CaCO_3$ visible; vesicular; mainly a silty unit; few gravels.

STATION: HV-12

LOCATION: Cortez Peak Quad, T2N, R8W, Sec 34, NW 1/4, SW 1/4

SURFICIAL DEPOSIT: Qff

MICRO-RELIEF: moderate to low

PERCENT COVER OF LAND SURFACE WITH GRAVELS: 10-15%

SOIL DESCRIPTION:

Horizons - A. poorly developed; ochric A.

B. light buff brown throughout; sticky, slightly plastic; very calcareous; 20 cm thick; breaks into very fine particles, almost powder, occasionally blocks.

C. thickness unknown, very gravelly; highly calcareous; no filaments of $CaCO_3$ visible.

STATION: HV-14

LOCATION: Cortez Peak Quad, T1N, R8W, Sec 7, SW1/4, SW 1/4

SURFICIAL DEPOSIT: Qds

MICRO-RELIEF: high, up to 30 cm

PERCENT COVER OF LAND SURFACE WITH GRAVELS: all sand

SURFICIAL DEPOSIT DESCRIPTION:

Unit A - sand dune; about 2 m high at crest; not indurated; not calcareous; covered with vegetation

Unit B - sandy, well indurated; slightly to moderately calcareous; breaks blocky; may be old soil horizon developed before it was covered by overlying sand dune; approximately 1 m thick; grades laterally into slightly less indurated iron brown sand with white filaments of $CaCO_3$

Unit C - B graded into C; becomes indurated laterally and increases in amount of $CaCO_3$; appears more silty than sandy; white blebs are increasing; appears that amount of clay may be increasing.

APPENDIX V

SELECTED WATER WELL RECORDS PARALLEL TO BASE LINE IN THE HARQUAHALA VALLEY

(Data obtained from files of
Arizona Department of Lands, Phoenix, Arizona)

CPQ - 1

LOCATION: T1S, R8W, Sec 5, SE 1/4, SE 1/4, NW 1/4

SURFACE ELEVATION: 1055 ft

FROM	TO	DESCRIPTION
0	15	soil and silt sand
15	30	sand and gravel
30	45	clay silty
45	50	sand and gravel
50	255	sandy clay and small gravel
255	335	sandy clay, small gravel with firm ribs (reddish brown)
335	385	sandy clay, small gravel with firm ribs (tan)
385	486	small gravel and sand with streaks of clay

CPQ - 2

LOCATION: T1S, R8W, Sec 4, NE 1/4, SE 1/4, NW 1/4

SURFACE ELEVATION: 1050 ft

FROM	TO	DESCRIPTION
0	10	sandy loan
10	100	sand, clay
100	140	pea gravel
140	546	sandy clay-gravel conglomerate
546	748	sedimentary rock type formation, looks like cement when dry

CPQ - 3

LOCATION: T1S, R8W, Sec 6, SW 1/4, SW 1/4, SW 1/4

SURFACE ELEVATION: 1090 ft

FROM	TO	DESCRIPTION
0	20	sandy loam, caliche
20	130	sandy clay
130	180	small gravel and sand
180	800	intermittant streaks of clay with stratas of sand-gravel conglomerate

CPQ - 12

LOCATION: T1S, R8W, Sec 14, SE 1/2, SE 1/4, NE 1/4

SURFACE ELEVATION: 990 ft.

FROM	TO	DESCRIPTION
0	7	topsoil
7	16	hard pan
16	20	malipe sand
20	85	silt snad, hard stke.
85	185	gravel, snad, boulders
185	360	gravel, sand, boulders
360	430	malipe rock, quartz rock
430	450	clay and shale conglomerate
450	520	boulders, quartz-malipe rock
520	615	hard conglomerate, streaks of sand
615	708	blue malipe rock and boulders

CPQ - 50

LOCATION: %1N, R8W, Sec 31, SW 1/4, SW 1/4, SW 1/4

SURFACE ELEVATION: 1081 ft.

FROM	TO	DESCRIPTION
0	60	no samples
60	70	sandy silt, sand grains poorly-moderate rounded
80	90	caliche-cemented sandy silt, sand grains are 98% quartz and feldspars derived from granite; a few epidote grains and few lavas
100	130	sandy silt
140	170	sandy silt, sand grains 50% lavas, 50% granitic, moderate rounding
170	200	moderate rounding
200	210	moderate rounding
210	220	moderately well rounded sand and pea gravel, some silt
220	250	well rounded pea gravels, 75% volcanic
250	270	well rounded
270	310	well rounded sand and pea gravels, 90% in origin
310	340	same but more silt
340	350	same, but contained layer of caliche-cemented silt
350	360	well rounded pea gravel and coarse sand, all volcanic
360	370	same
370	380	same but more fine sand and some silt
380	420	silty, volcanic pea gravel
420	430	same but less silt
430	440	same
440	470	same but more silt
470	500	same but less silt

(CPQ - 50, Continued)

FROM	TO	DESCRIPTION
500	560	same but finer, more silt
560	570	sandy silt
570	580	sandy and gravelly silt
580	590	gravelly silt
590	600	same
600	626	clay

CPQ -84

LOCATION: T1N, R9W, Sec 32, SW 1/4, SW 14/, SW 1/4

SURFACE ELEVATION: 1150 ft.

FROM	TO	DESCRIPTION
0	25	surface clay
25	148	sand, gravel, clay
148	185	sand and gravel
185	195	clay
195	330	sand and gravel
330	391	sand
391	480	sand and gravel with little clay
480	568	sand and gravel
568	583	sand, with streaks of hard shell
583	628	sand with streaks very hard shell
628	780	sand and gravel
780	8k2	sand
812	845	red shale

CPQ - 85

LOCATION: T1N, R9W, Sec 35, SW 1/4, SW 1/4, SE 1/4

SURFACE ELEVATION: 1126 ft.

FROM	TO	DESCRIPTION
0	30	top soil
30	122	shale and sand
122	140	sand
140	250	sand and clay
250	325	sand and gravel with streaks of clay
325	400	sand, gravel, and shale
400	460	sand and gravel
460	520	sand and red shale
520	605	snad, gravel, with streaks of clay
605	700	gravel and clay
700	814	clay
814	875	rock and clay
875	896	red bed and thin shells of red rock
896	910	red bed

CPQ -86

LOCATION: T1N, R9W, Sec 36, SW 1/4, SW 1/4, SW 1/4

SURFACE ELEVATION: 1115 ft.

FROM	TO	DESCRIPTION
0	20	surface silt and sand
20	200	pea to large size gravel and streaks of sand
200	260	same, with lenses of boulders
260	600	clay with streaks of good gravel
600	760	mostly clay with streaks of sand
760	1000	good gravel with streaks of clay
1000	1160	boulders with streaks of clay
1160	1190	granitic boulders with streaks of fine sand

APPENDIX VI

GEOMORPHIC PARAMETERS OF LOW ORDER DRAINAGE BASINS IN THE HARQUAHALA VALLEY AND THE HYDRAULIC GEOMETRY AND COMPUTED HYDROLOGIC PARAMETERS OF THEIR PRINCIPLE WASHES

LMQ - A

STATION	DISTANCE FROM DIVIDE, Km	CUMULATIVE DRAINAGE AREA, Km^2	RATIO OF BAHADA AREA TO AREA OF BEDROCK
I	20.1	256.7	.836
II	21.7	257.8	.836
III	24.1	258.2	.623
IV	27.3	259.6	.631
V	29.9	261.1	.640
VI	33.1	279.5	.757
VII	35.5	290.6	.827

ELEVATION OF HIGHEST POINT IN BASIN: 1731.3 m

ELEVATION OF LOWEST POINT IN BASIN: 437.4 m

RELIEF RATIO: 0.039

ROCK TYPE: Igneous, metamorphic, sedimentary

MEAN BASIN WIDTH: 5.76 km

WASH: LMQ - A

STATION	OVERBANK WIDTH, m Wo	CHANNEL WIDTH, m Wc	MAXIMUM WIDTH, m Wm	MAXIMUM DEPTH, m Dm	MAXIMUM WIDTH/DEPTH RATIO W/D	MAXIMUM X-SECTIONAL AREA, m^2	SLOPE	HYDRAULIC RADIUS, m^3
I	24.5	10.0	34.5	1.11	31.1	38.3	0.010	1.040
II	56.0	13.0	69.0	2.18	31.7	150.4	0.009	2.050
III	60.0	12.0	72.0	2.29	31.4	164.9	0.010	2.150
IV	43.0	14.0	57.0	.99	57.6	56.4	0.010	.980
V	350	15.3	365.3	.70	521.9	255.7	0.0085	.697
VI	500	2.9	502.9	.56	898.0	281.6	0.0066	.559
VII	402	2.3	404.3	.46	878.9	185.0	0.0057	.456

WASH: LMQ - A

STATION	VELOCITY, m/sec $V = 1.5 \frac{R^{2/3} S^{1/2}}{n}$ Vm	VELOCITY, m/sec $V = \sqrt{g D}$ Vg	AVERAGED VELOCITY m/sec $\overline{V}$	MAXIMUM DISCHARGE m^3/sec Qm	TRACTIVE FORCE $Kg/m^3\ sec^2$ To
I	2.95	3.30	3.13	119.7	10.43
II	4.86	4.6	4.73	711.4	18.4
III	4.76	4.7	4.73	780	21.53
IV	3.35	3.10	3.23	182.2	9.56
V	1.95	2.6	2.28	583.0	5.93
VI	2.2	2.3	2.25	633.6	3.7
VII	1.79	2.10	1.95	359.8	2.6

BASIN: LMQ - B

STATION	DISTANCE FROM DIVIDE, Km	CUMULATIVE DRAINAGE AREA, Km^2	RATIO OF BAHADA AREA TO AREA OF BEDROCK
I	20.1	256.7	.836
II	21.7	277.6	.750
III	24.3	279.0	.754
IV	33.3	285.3	.793

ELEVATION OF HIGHEST POINT IN BASIN: 1731.3 m

ELEVATION OF LOWEST POINT IN BASIN: 451.1 m

RELIEF RATIO: 0.040

ROCK TYPE: Igneous, metamorphic, sedimentary, volcanic

MEAN BASIN WIDTH: 5.7 km

WASH: LMQ - B

STATION	OVERBANK WIDTH, m Wo	CHANNEL WIDTH, m Wc	MAXIMUM WIDTH, m Wm	MAXIMUM DEPTH, m Dm	MAXIMUM WIDTH/DEPTH RATIO W/D	MAXIMUM X-SECTIONAL AREA, m^2	SLOPE	HYDRAULIC RADIUS, m^3
I	24.5	10.0	34.5	1.11	31.1	38.3	0.010	1.04
II	24.0	12.5	36.5	1.01	36.1	36.9	0.0084	.970
III	13.7	13.2	26.9	1.35	19.9	36.3	0.009	1.350
IV	90.0	2.0	92	1.83	50.3	3.7	0.0069	--

Selected hydraulic geometry parameters of wash

WASH: LMQ - B

STATION	VELOCITY, m/sec $V = 1.5 \frac{R^{2/3} S^{1/2}}{n}$ Vm	VELOCITY, m/sec $V = \sqrt{g\ D}$ Vg	AVERAGED VELOCITY m/sec $\bar{V}$	MAXIMUM DISCHARGE, m^3/sec Qm	TRACTIVE FORCE $Kg/m^3\ sec^2$ To
I	2.95	3.3	3.13	119.7	10.43
II	2.65	3.1	2.88	106.3	8.15
III	2.5	3.5	3	108.9	12.15

Computed hydrologic parameters for stations along selected wash

BASIN: LMQ - C

STATION	DISTANCE FROM DIVIDE, Km	CUMULATIVE DRAINAGE AREA, Km^2	RATIO OF BAHADA AREA TO AREA OF BEDROCK
I	8.9	16.6	.673
II	10.9	17.0	.712
III	11.1	19.3	.939
IV	14.1	20.4	1.05

ELEVATION OF HIGHEST POINT IN BASIN: 1253.9 m

ELEVATION OF LOWEST POINT IN BASIN: 469.4 m

DRAINAGE DENSITY: 5.35

RELIEF RATIO: 0.065

ROCK TYPE: Metamorphic, sedimentary

DRAINAGE FREQUENCY: 16.14

MEAN BASIN WIDTH: 1.8 km

Selected basin parameters

WASH: LMQ - C

STATION	OVERBANK WIDTH, m Wo	CHANNEL WIDTH, m Wc	MAXIMUM WIDTH, m Wm	MAXIMUM DEPTH, m Dm	MAXIMUM WIDTH/DEPTH RATIO W/D	MAXIMUM X-SECTIONAL AREA, m^2	SLOPE	HYDRAULIC RADIUS, m^3
I	14.7	6	20.7	1.17	17.7	24.2	0.016	1.05
II	21.0	8	29	.81	35.8	23.5	0.015	.760
III	4.5	7	11.5	.76	15.1	8.7	0.015	.640
IV	66.0	5	71	.84	84.5	59.6	0.009	.700

Selected hydraulic geometry parameters of wash

WASH: LMQ - C

STATION	VELOCITY, m/sec $V = 1.5 \frac{R^{2/3} S^{1/2}}{n}$ Vm	VELOCITY, m/sec $V = \sqrt{g D}$ Vg	AVERAGED VELOCITY m/sec $\bar{V}$	MAXIMUM DISCHARGE m^3/sec Qm	TRACTIVE FORCE $Kg/m^3\ sec^2$ To
I	3.74	3.4	3.57	86.4	16.8
II	2.9	2.8	2.85	67	11.4
III	2.6	2.7	2.65	23.1	9.6
IV	3.3	2.9	3.1	184.8	7.2

Computed hydrologic parameters for stations along selected wash

BASIN: LMQ -D

STATION	DISTANCE FROM DIVIDE, Km	CUMULATIVE DRAINAGE AREA, Km^2	RATIO OF BAHADA AREA TO AREA OF BEDROCK
I	0.7	.05	--
II	1.5	.52	--
III	3.5	1.5	--
IV	4.9	3.9	--

ELEVATION OF HIGHEST POINT IN BASIN: 585.2 m

ELEVATION OF LOWEST POINT IN BASIN: 483.1

DRAINAGE DENSITY: 8.01

RELIEF RATIO: 0.018

ROCK TYPE: sedimentary and metamorphic

DRAINAGE FREQUENCY: 23.35

MEAN BASIN WIDTH:

Selected basin parameters

WASH: LMQ - D

STATION	OVERBANK WIDTH, m Wo	CHANNEL WIDTH, m Wc	MAXIMUM WIDTH, m Wm	MAXIMUM DEPTH, m Dm	MAXIMUM WIDTH/DEPTH RATIO W/D	MAXIMUM X-SECTIONAL AREA, m^2	SLOPE	HYDRAULIC RADIUS, m^3
I	2.5	2.7	5.2	1.3	4.0	6.8	0.026	.871
II	13.0	5.0	18.0	.84	21.4	15.1	0.019	.755
III	23.0	5.3	28.3	.66	42.9	18.7	0.011	.638
IV	84.5	2.2	86.7	.79	109.8	68.5	0.009	.770

Selected hydraulic geometry parameters of wash

WASH: LMQ - D

STATION	VELOCITY, m/sec $V = 1.5 \frac{R^{2/3} S^{1/2}}{n}$ Vm	VELOCITY, m/sec $V = \sqrt{g D}$ Vg	AVERAGED VELOCITY m/sec $\overline{V}$	MAXIMUM DISCHARGE, m^3/sec Qm	TRACTIVE FORCE $Kg/m^3\ sec^2$ To
I	4.2	3.6	3.8	25.8	22.6
II	3.3	2.9	3.1	46.8	14.35
III	2.2	2.5	2.3	43	7.02
IV	3.2	2.8	3	205.5	6.93

Computed hydrologic parameters for stations along selected wash

BASIN: BHMQ - A

STATION	DISTANCE FROM DIVIDE, Km	CUMULATIVE DRAINAGE AREA, Km^2	RATIO OF BAHADA AREA TO AREA OF BEDROCK
I	4.0	2.5	.53
II	4.8	3.4	1.06
III	5.8	3.6	1.18
IV	7.0	4.9	1.95

ELEVATION OF HIGHEST POINT IN BASIN: 1060.1 m

ELEVATION OF LOWEST POINT IN BASIN: 378.0

DRAINAGE DENSITY: 6.27

RELIEF RATIO: 0.106

ROCK TYPE: volcanic

DRAINAGE FREQUENCY: 16.72

MEAN BASIN WIDTH: 0.84

Selected basin parameters.

WASH: BHMQ - A

STATION	OVERBANK WIDTH, m Wo	CHANNEL WIDTH, m Wc	MAXIMUM WIDTH, m Wm	MAXIMUM DEPTH, m Dm	MAXIMUM WIDTH/DEPTH RATIO W/D	MAXIMUM X-SECTIONAL AREA, m^2	SLOPE	HYDRAULIC RADIUS, m^3
I	4.8	5.3	10.1	1.25	8.1	12.6	0.040	1.00
II	8.2	3.7	11.9	1.42	8.4	16.9	0.035	1.127
III	16.0	6.0	22.0	.48	45.8	10.6	0.017	.460
IV	55.5	3.4	58.9	.38	155.0	22.4	0.015	.373

Selected hydraulic geometry parameters of wash

WASH: BHMQ - A

STATION	VELOCITY, m/sec $V = 1.5 \frac{R^{2/3} S^{1/2}}{n}$ Vm	VELOCITY, m/sec $V = \sqrt{g D}$ Vg	AVERAGED VELOCITY m/sec $\overline{V}$	MAXIMUM DISCHARGE, m^3/sec Qm	TRACTIVE FORCE $Kg/m^3\ sec^2$ To
I	5.7	3.5	4.6	58	40
II	5.8	3.7	4.75	80.3	39.4
III	2.2	2.2	2.2	23.3	7.8
IV	1.8	1.9	1.85	41.4	5.6

Computed hydrologic parameters for stations along selected wash

BASIN: BHMQ - B

STATION	DISTANCE FROM DIVIDE, Km	CUMULATIVE DRAINAGE AREA, Km^2	RATIO OF BAHADA AREA TO AREA OF BEDROCK
I	6.8	5.7	.129
II	12.6	38.3	.290
III	14.3	38.5	.300
IV	16.2	40.5	.350
V	18.6	44.5	.460

ELEVATION OF HIGHEST POINT IN BASIN: 933.6 m

ELEVATION OF LOWEST POINT IN BASIN: 457.5 m

DRAINAGE DENSITY: 3.17

RELIEF RATIO: .030

ROCK TYPE: volcanic, igneous

DRAINAGE FREQUENCY: 16.10

MEAN BASIN WIDTH: 2.6

Selected basin parameters

WASH: BHMQ - B

STATION	OVERBANK WIDTH, m Wo	CHANNEL WIDTH, m Wc	MAXIMUM WIDTH, m Wm	MAXIMUM DEPTH, m Dm	MAXIMUM WIDTH/DEPTH RATIO W/D	MAXIMUM X-SECTIONAL AREA, m^2	SLOPE	HYDRAULIC RADIUS, m^3
I	16.0	11.5	27.5	.76	36.1	20.9	.014	.708
II	8.5	7.0	15.5	.60	26.0	9.3	0.015	.547
III	2.6	6.7	9.3	1.17	8.0	10.9	0.015	.924
IV	7.7	5.6	13.3	.31	43.6	4.1	0.018	.292
V	22.0	5.4	27.4	.46	60.0	12.6	0.010	.442

Selected hydraulic geometry parameters of wash

WASH: BHMQ - B

STATION	VELOCITY, m/sec $V = 1.5 \frac{R^{2/3} S^{1/2}}{n}$ Vm	VELOCITY, m/sec $V = \sqrt{g D}$ Vg	AVERAGED VELOCITY m/sec $\overline{V}$	MAXIMUM DISCHARGE m^3/sec Qm	TRACTIVE FORCE $Kg/m^3\ sec^2$ To
I	1.5	2.7	2.1	43.9	9.9
II	2.4	2.4	2.4	22.3	8.2
III	3.3	3.4	3.35	36.5	13.9
IV	1.7	1.7	1.7	7.0	5.3
V	1.7	2.1	1.95	24.6	4.4

Computed hydrologic parameters for stations along selected wash

BASIN: CPQ - A

STATION	DISTANCE FROM DIVIDE, Km	CUMULATIVE DRAINAGE AREA, Km^2	RATIO OF BAHADA AREA TO AREA OF BEDROCK
I	0.2	.08	--
II	0.8	.21	--
III	1.4	.31	--
IV	1.8	.41	--
V	2.4	2.15	3.57
VI	2.8	2.18	3.64

ELEVATION OF HIGHEST POINT IN BASIN: 573.0

ELEVATION OF LOWEST POINT IN BASIN: 353.6

DRAINAGE DENSITY: 4.57

RELIEF RATIO: 0.073

ROCK TYPE: volcanic

DRAINAGE FREQUENCY: 11.11

MEAN BASIN WIDTH: .62 km

Selected basin parameters

WASH: CPQ - A

STATION	OVERBANK WIDTH, m Wo	CHANNEL WIDTH, m Wc	MAXIMUM WIDTH, m Wm	MAXIMUM DEPTH, m Dm	MAXIMUM WIDTH/DEPTH RATIO W/D	MAXIMUM X-SECTIONAL AREA, m^2	SLOPE	HYDRAULIC RADIUS, m^3
I	2.9	3.0	5.9	.28	21.2	1.7	0.030	.262
II	5.1	1.8	6.9	.76	9.1	5.2	0.026	.612
III	3.6	5.6	9.2	.53	17.3	4.9	0.0225	.480
IV	4.3	3.6	7.9	.36	22.2	2.8	0.018	.311
V	0.7	4.6	5.3	.60	8.9	3.2	0.017	.492
VI	73.1	3.4	76.5	.51	150.6	39.2	0.015	.506

Selected hydraulic geometry parameters of wash

WASH: CPQ - A

STATION	VELOCITY, m/sec $V = 1.5 \frac{R^{2/3} S^{1/2}}{n}$ Vm	VELOCITY, m/sec $V = \sqrt{g D}$ Vg	AVERAGED VELOCITY m^3/sec $\bar{V}$	MAXIMUM DISCHARGE m^3/sec Qm	TRACTIVE FORCE $Kg/m^3\ sec^2$ τo
I	2	1.6	1.8	3.1	7.86
II	3.3	2.7	3	15.6	15.91
III	2.6	2.3	2.45	12	10.8
IV	1.8	1.9	1.85	5.2	5.6
V	2.3	2.4	2.35	7.4	8.36
VI	2.2	2.2	2.2	86	7.59

Computed hydrologic parameters for stations along selected wash

BASIN: CPQ - B

STATION	DISTANCE FROM DIVIDE, Km	CUMULATIVE DRAINAGE AREA, Km^2	RATIO OF BAHADA AREA TO AREA OF BEDROCK
I	2.4	1.6	.164
II	4.2	5.0	.323
III	5.8	5.2	.384
IV	7.6	6.7	.465
V	8.2	6.8	.469
VI	11.4	11.4	.653

ELEVATION OF HIGHEST POINT IN BASIN: 852.2 m

ELEVATION OF LOWEST POINT IN BASIN: 298.1 m

DRAINAGE DENSITY: 3.40

RELIEF RATIO: 0.063

ROCK TYPE: volcanic

DRAINAGE FREQUENCY: 4.16

MEAN BASIN WIDTH: 1.5 km

Selected basin parameters

WASH: CPQ - B

STATION	OVERBANK WIDTH, m Wo	CHANNEL WIDTH, m Wc	MAXIMUM WIDTH, m Wm	MAXIMUM DEPTH, m Dm	MAXIMUM WIDTH/DEPTH RATIO W/D	MAXIMUM X-SECTIONAL AREA, m^2	SLOPE	HYDRAULIC RADIUS, m^3
I	7.3	6.0	14.3	.91	15.7	13.0	0.025	.797
II	16.5	10.0	26.5	.58	45.4	15.4	0.020	.560
III	14.5	10.3	24.8	.58	42.5	14.4	0.015	.554
IV	3.0	13.0	16.0	.70	22.9	11.2	0.014	.622
V	9.2	13.7	22.9	.95	24.0	21.8	0.013	.822
VI	40.5	16.0	56.5	.51	111.2	28.8	0.0006	.501

Selected hydraulic geometry parameters of wash

WASH: CPQ - B

STATION	VELOCITY, m/sec $V = 1.5\frac{R^{2/3} S^{1/2}}{n}$ Vm	VELOCITY, m/sec $V = \sqrt{g D}$ Vg	AVERAGED VELOCITY m/sec $\overline{V}$	MAXIMUM DISCHARGE m^3/sec Qm	TRACTIVE FORCE $Kg/m^3\ sec^2$ To
I	3.9	3.0	3.45	51.4	19.9
II	2.8	2.4	2.6	40	11.2
III	2.4	2.4	2.4	34.6	8.3
IV	2.5	2.6	2.55	28.6	9.3
V	3.0	3.1	3.05	66.5	11.3
VI	1.4	2.2	1.8	51.8	3.0

Computed hydrologic parameters for stations along selected wash

BASIN: CPQ - C

STATION	DISTANCE FROM DIVIDE, Km	CUMULATIVE DRAINAGE AREA, Km^2	RATIO OF BAHADA AREA TO AREA OF BEDROCK
I	0.7	.47	.310
II	2.3	.85	.520
III	4.3	2.2	1.66
IV	5.9	2.9	2.48
V	7.5	3.0	0.34
VI	9.0	4.3	0.91

ELEVATION OF HIGHEST POINT IN BASIN: 512.1 m

ELEVATION OF LOWEST POINT IN BASIN: 303.3 m

DRAINAGE DENSITY: 9.00

RELIEF RATIO: 0.032

ROCK TYPE: volcanic

DRAINAGE FREQUENCY: 23.30

MEAN BASIN WIDTH: 1.03 Km

Selected basin parameters

WASH: CPQ - B

STATION	OVERBANK WIDTH, m Wo	CHANNEL WIDTH, m Wc	MAXIMUM WIDTH, m Wm	MAXIMUM DEPTH, m Dm	MAXIMUM WIDTH/DEPTH RATIO W/D	MAXIMUM X-SECTIONAL AREA, m^2	SLOPE	HYDRAULIC RADIUS m^3
I	1.6	2.5	4.1	.71	5.8	2.9	0.025	.518
II	1.7	6.0	7.7	.52	14.8	4.0	0.022	.444
III	13.0	7.0	20.0	.81	24.6	16.2	0.0175	.736
IV	12.6	5.2	17.8	.97	18.5	17.3	0.012	.865
V	29.0	4.6	33.6	1.32	25.4	44.4	0.010	1.216
VI	7.3	11.8	19.1	.51	37.6	9.0	0.005	.473

Selected hydraulic geometry parameters of wash

WASH: CPQ - C

STATION	VELOCITY, m/sec $V = 1.5 \frac{R^{2/3} S^{1/2}}{n}$ Vm	VELOCITY, m/sec $V = \sqrt{g D}$ Vg	AVERAGED VELOCITY m/sec $\overline{V}$	MAXIMUM DISCHARGE m^3/sec Qm	TRACTIVE FORCE $Kg/m^3\ sec^2$ τo
I	2.9	2.6	2.75	8.0	13
II	2.5	2.3	2.4	9.8	9.8
III	3.1	2.8	2.95	47.8	12.9
IV	2.9	3.1	3.0	51.9	10.4
V	3.2	3.6	3.3	146.5	12.2
VI	1.2	2.2	1.7	16.5	2.4

Computed hydrologic parameters for stations along selected wash

BASIN: CPQ - D

STATION	DISTANCE FROM DIVIDE, Km	CUMULATIVE DRAINAGE AREA, Km^2	RATIO OF BAHADA AREA TO AREA OF BEDROCK
I	.81	.47	
II	1.4	.52	
III	2.21	.98	
IV	3.0	1.04	

ELEVATION OF HIGHEST POINT IN BASIN: 853.4 m

ELEVATION OF LOWEST POINT IN BASIN: 365.8 m

DRAINAGE DENSITY: 6.25

RELIEF RATIO: 0.156

ROCK TYPE: volcanic

DRAINAGE FREQUENCY: 11.54

MEAN BASIN WIDTH: .38 km

Selected basin parameters

WASH: CPQ - D

STATION	OVERBANK WIDTH, m Wo	CHANNEL WIDTH, m Wc	MAXIMUM WIDTH, m Wm	MAXIMUM DEPTH, m Dm	MAXIMUM WIDTH/DEPTH RATIO W/D	MAXIMUM X-SECTIONAL AREA, m^2	SLOPE	HYDRAULIC RADIUS m^3
I	2	3.5	5.5	2.54	2.2	14.0	0.040	1.330
II	2	3.5	5.5	1.52	2.5	8.4	0.038	.988
III	4	5.5	9.5	1.07	8.9	10.2	0.011	.887
IV	58.5	3.7	62.02	.51	122.0	31.7	0.0108	.502

Selected hydraulic geometry parameters of wash

WASH: CPQ - D

STATION	VELOCITY, m/sec $V=1.5\frac{R^{2/3}\ S^{1/2}}{n}$ Vm	VELOCITY, m/sec $V = \sqrt{g\ D}$ Vg	AVERAGED VELOCITY m^3/sec $\bar{V}$	MAXIMUM DISCHARGE m^3/sec Qm	TRACTIVE FORCE $Kg/m^3\ sec^2$ τo
I	6.9	5.0	5.95	83.3	53.2
II	5.5	3.9	4.7	39.5	37.5
III	2.8	3.2	3.0	30.6	9.8
IV	1.9	2.2	2.1	66.6	5.4

Computed hydrologic parameters for stations along selected wash

BASIN: EMQ - A

STATION	DISTANCE FROM DIVIDE, Km	CUMULATIVE DRAINAGE AREA, Km^2	RATIO OF BAHADA AREA TO AREA OF BEDROCK
I	1.6	1.1	1.140
II	2.2	1.3	1.480
III	3.8	1.4	1.731
IV	4.2	3.4	1.496
V	5.8	3.5	1.601

ELEVATION OF HIGHEST POINT IN BASIN: 823.0 m

ELEVATION OF LOWEST POINT IN BASIN: 446.5 m

DRAINAGE DENSITY: 11.57

RELIEF RATIO: 0.0893

ROCK TYPE: igneous and volcanic

DRAINAGE FREQUENCY: 50.23

Selected basin parameters

WASH: EMQ - A

STATION	OVERBANK WIDTH, m Wo	CHANNEL WIDTH, m Wc	MAXIMUM WIDTH, m Wm	MAXIMUM DEPTH, m Dm	MAXIMUM WIDTH/DEPTH RATIO W/D	MAXIMUM X-SECTIONAL AREA, m^2	SLOPE	HYDRAULIC RADIUS m^3
I	12.7	13.8	26.5	.69	38.5	18.3	0.023	.654
II	0	10.0	10.0	.31	32.8	3.1	0.022	.282
III	16.2	6.9	23.1	.74	31.3	17.1	0.022	.683
IV	10.0	19.6	29.6	.51	58.3	15.1	0.021	.487
V	23.9	9.9	33.8	.61	55.4	29.6	0.016	.589

Selected hydraulic geometry parameters of wash

WASH: EMQ - A

STATION	VELOCITY, m/sec $V = 1.5 \frac{R^{2/3} S^{1/2}}{n}$ Vm	VELOCITY, m/sec $V = \sqrt{g D}$ Vg	AVERAGED VELOCITY m/sec $\bar{V}$	MAXIMUM DISCHARGE m^3/sec Qm	TRACTIVE FORCE $Kg/m^3\ sec^2$ τo
I	3.3	2.6	2.95	54	15
II	1.8	1.7	1.75	5.4	6.2
III	3.3	2.7	3	51.3	15.0
IV	2.6	2.2	2.4	36.2	10.2
V	2.5	2.4	2.45	50.5	9.4

Computed hydrologic parameters for stations along selected wash

BASIN: EMQ - B

STATION	DISTANCE FROM DIVIDE, Km	CUMULATIVE DRAINAGE AREA, Km^2	RATIO OF BAHADA AREA TO AREA OF BEDROCK
I	1.6	1.16	.280
II	2.0	1.09	.310
III	2.6	1.11	.340
IV	3.0	1.29	.550
V	3.6		

ELEVATION OF HIGHEST POINT IN BASIN: 902.2 m

ELEVATION OF LOWEST POINT IN BASIN: 420.6

DRAINAGE DENSITY: 19.33

RELIEF RATIO: 0.184

ROCK TYPE: volcanic

DRAINAGE FREQUENCY: 69.57

MEAN BASIN WIDTH: .39 km

Selected basin parameters

WASH: EMQ - B

STATION	OVERBANK WIDTH, m Wo	CHANNEL WIDTH, m Wc	MAXIMUM WIDTH, m Wm	MAXIMUM DEPTH, m Dm	MAXIMUM WIDTH/DEPTH RATIO W/D	MAXIMUM X-SECTIONAL AREA, m^2	SLOPE	HYDRAULIC RADIUS m^3
I	8.6	4.6	13.2	.48	27.3	6.3	0.030	.444
II	8.0	4.0	12.0	.33	36.4	4.0	0.027	.400
III	6.6	8.6	15.2	.34	44.7	5.2	0.024	.321
IV	0	2.8	2.8	.27	10.5	0.8	0.022	.229
V	4.0	3.0	7.0	.34	20.4	2.4	0.018	.300

Selected hydraulic geometry parameters of wash

WASH: EMQ - B

STATION	VELOCITY, m/sec $V = 1.5 \frac{R^{2/3} S^{1/2}}{n}$ Vm	VELOCITY, m/sec $V = \sqrt{g D}$ Vg	AVERAGED VELOCITY m/sec $\overline{V}$	MAXIMUM DISCHARGE m^3/sec Qm	TRACTIVE FORCE $Kg/m^3\ sec^2$ τo
I	2.9	2.2	2.55	16.1	13.3
II	2.6	1.8	2.2	8.8	10.8
III	2.1	1.8	1.95	10	7.7
IV	2.2	1.6	1.9	1.5	5.0
V	2.4	1.8	2.1	5.0	5.4

Computed hydrologic parameters for stations along selected wash

COMPUTED FROUDE NUMBERS FOR STATIONS ALONG

TRUNK (PRINCIPAL) WASHES IN LOW ORDER BASINS

LOW ORDER DRAINAGE BASIN: LMQ-A

STATION	COMPUTED FROUDE NUMBER
I	.95
II	1.02
III	1.00
IV	1.04
V	.87
VI	.96
VII	.92

LOW ORDER DRAINAGE BASIN: LMQ-B

STATION	COMPUTED FROUDE NUMBER
I	.95
II	1.00
III	.82

LOW ORDER DRAINAGE BASIN: LMQ-C

STATION	COMPUTED FROUDE NUMBER
I	1.05
II	1.01
III	.97
IV	1.10

LOW ORDER DRAINAGE BASIN: LMQ-D

STATION	COMPUTED FROUDE NUMBER
I	1.06
II	1.08
III	0.91
IV	1.08

LOW ORDER DRAINAGE BASIN: CPQ-A

STATION	COMPUTED FROUDE NUMBER
I	1.09
II	1.10
III	1.07

IV	.984
V	.95
VI	.98

LOW ORDER DRAINAGE BASIN: CPQ-B

STATION	COMPUTED FROUDE NUMBER
I	1.32
II	1.09
III	1.01
IV	.973
V	.999
VI	.805

LOW ORDER DRAINAGE BASIN: CPQ-C

STATION	COMPUTED FROUDE NUMBER
I	1.04
II	1.08
III	1.04
IV	.973
V	.917
VI	.76

LOW ORDER DRAINAGE BASIN: CPQ-D

STATION	COMPUTED FROUDE NUMBER
I	1.19
II	1.22
III	.926
IV	.939

LOW ORDER DRAINAGE BASIN: BHMQ-A

STATION	COMPUTED FROUDE NUMBER
I	1.31
II	1.27
III	1.01
IV	0.96

LOW ORDER DRAINAGE BASIN: BHMQ-B

STATION	COMPUTED FROUDE NUMBER
I	1.00
II	.989
III	.988
IV	.975
V	.918

LOW ORDER DRAINAGE BASIN: EMQ-A

STATION	COMPUTED FROUDE NUMBER
I	1.13
II	1.00
III	1.11
IV	1.07
V	1.00

LOW ORDER DRAINAGE BASIN: EMQ-B

STATION	OMPUTED FROUDE NUMBER
I	1.18
II	1.22
III	1.06
IV	1.16
V	1.15

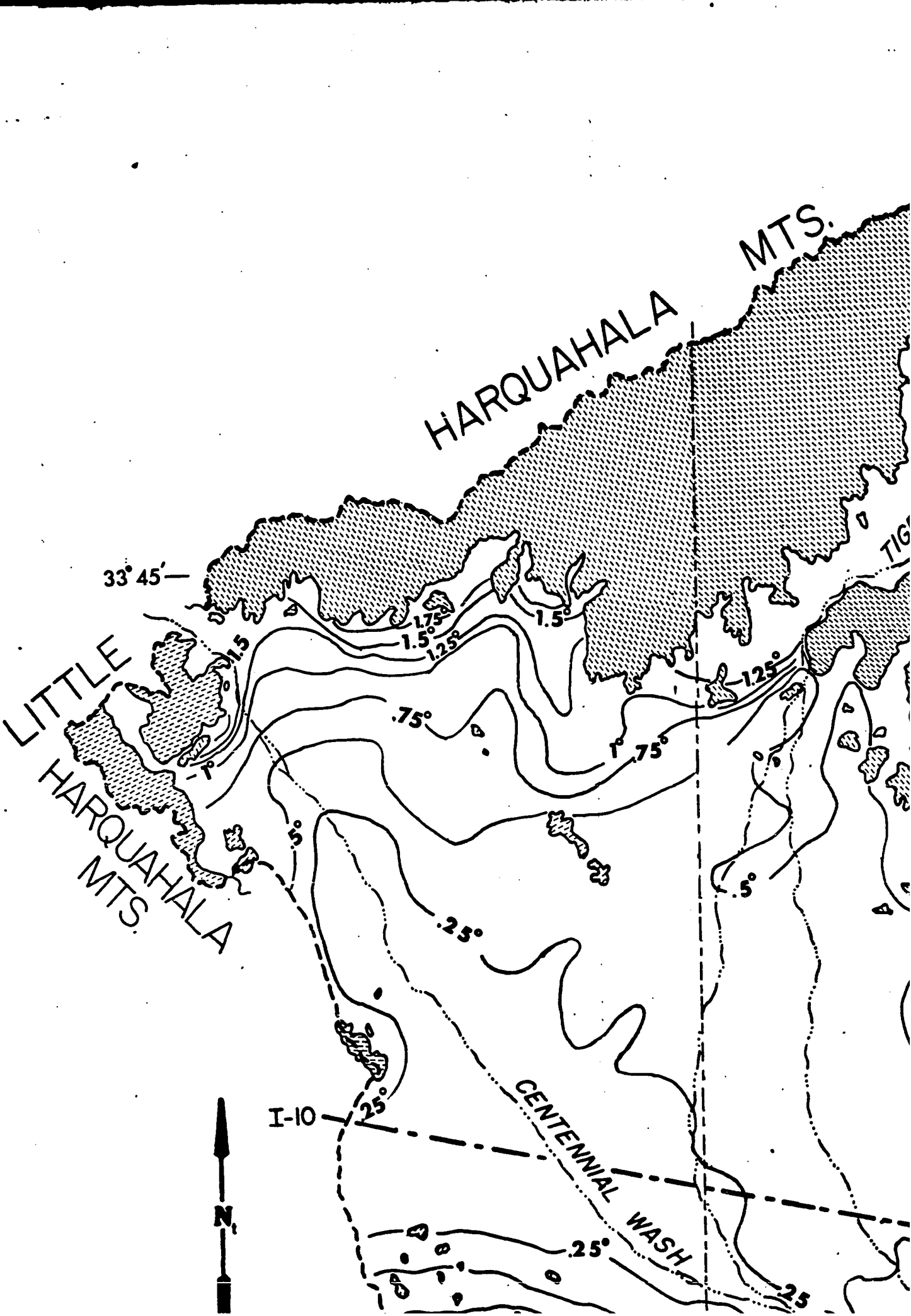

SLOPE MAP

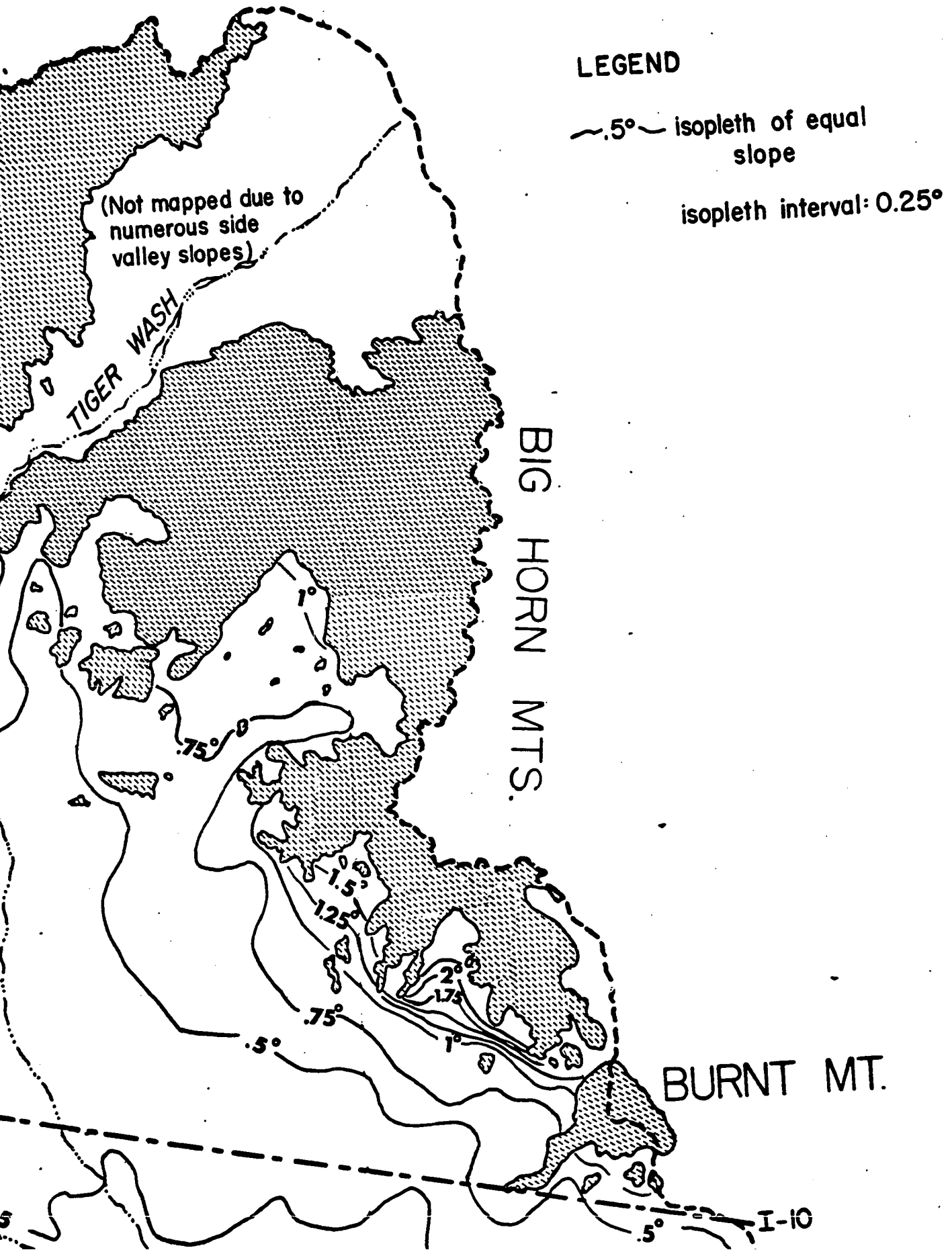

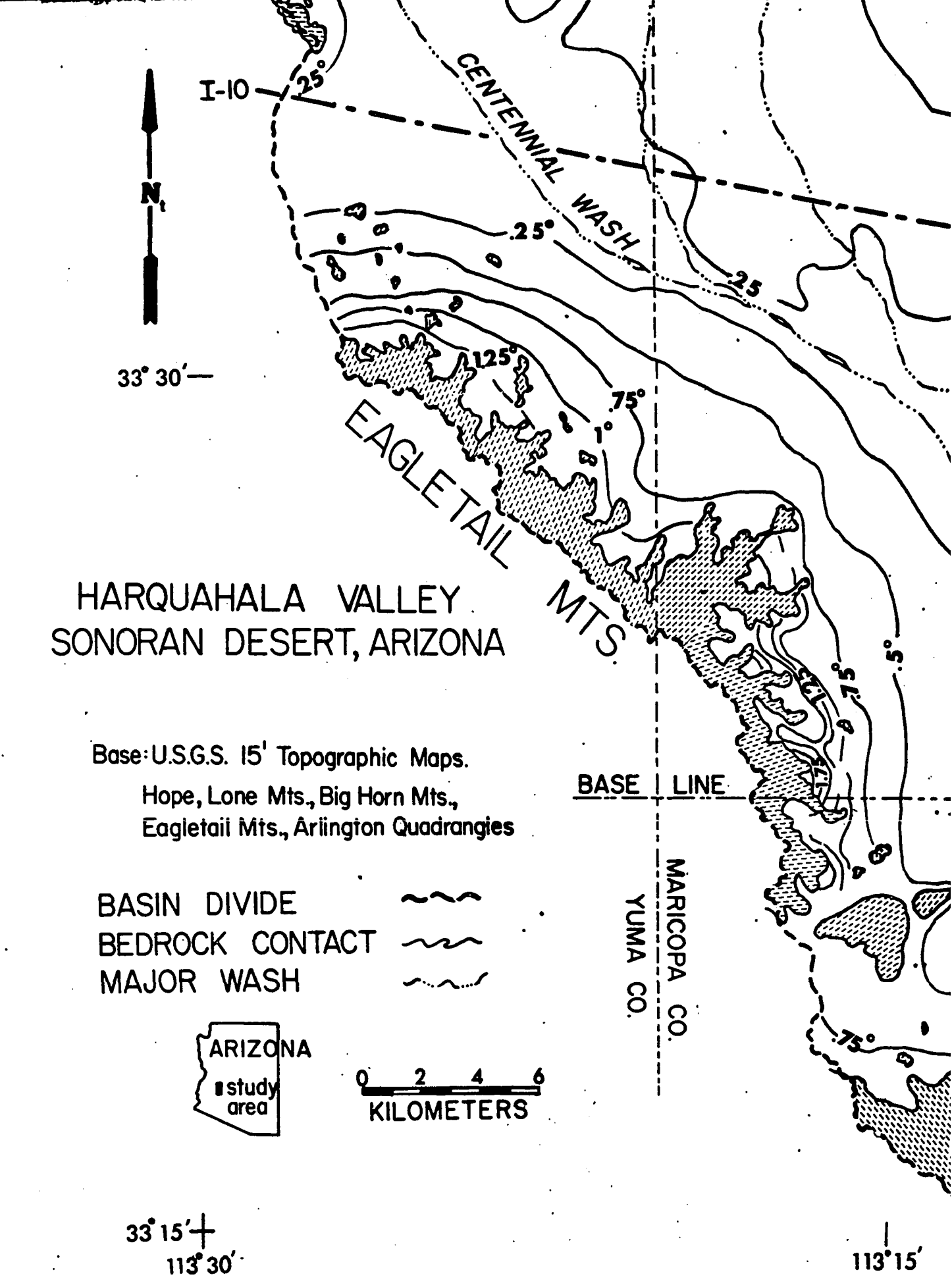

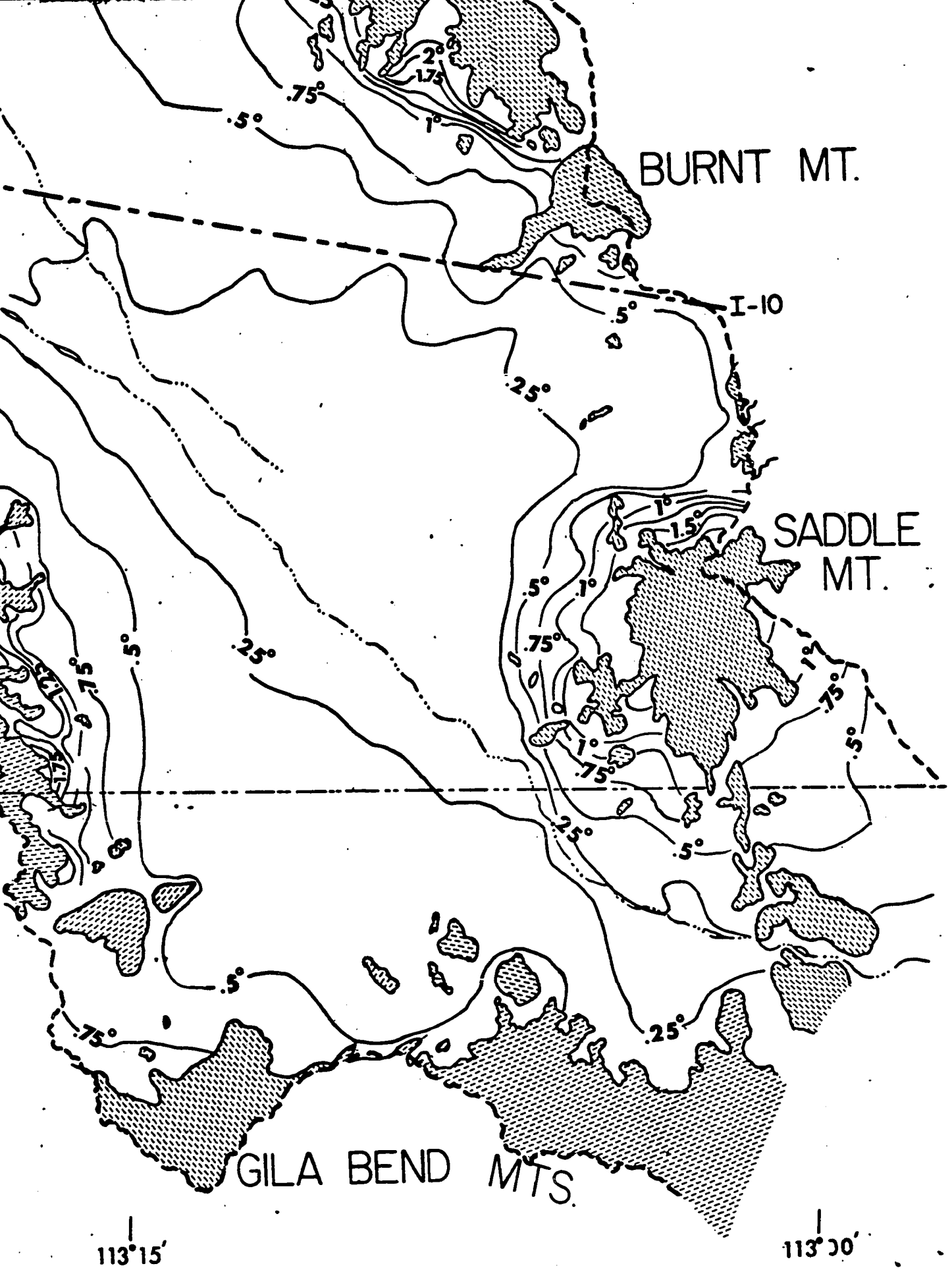

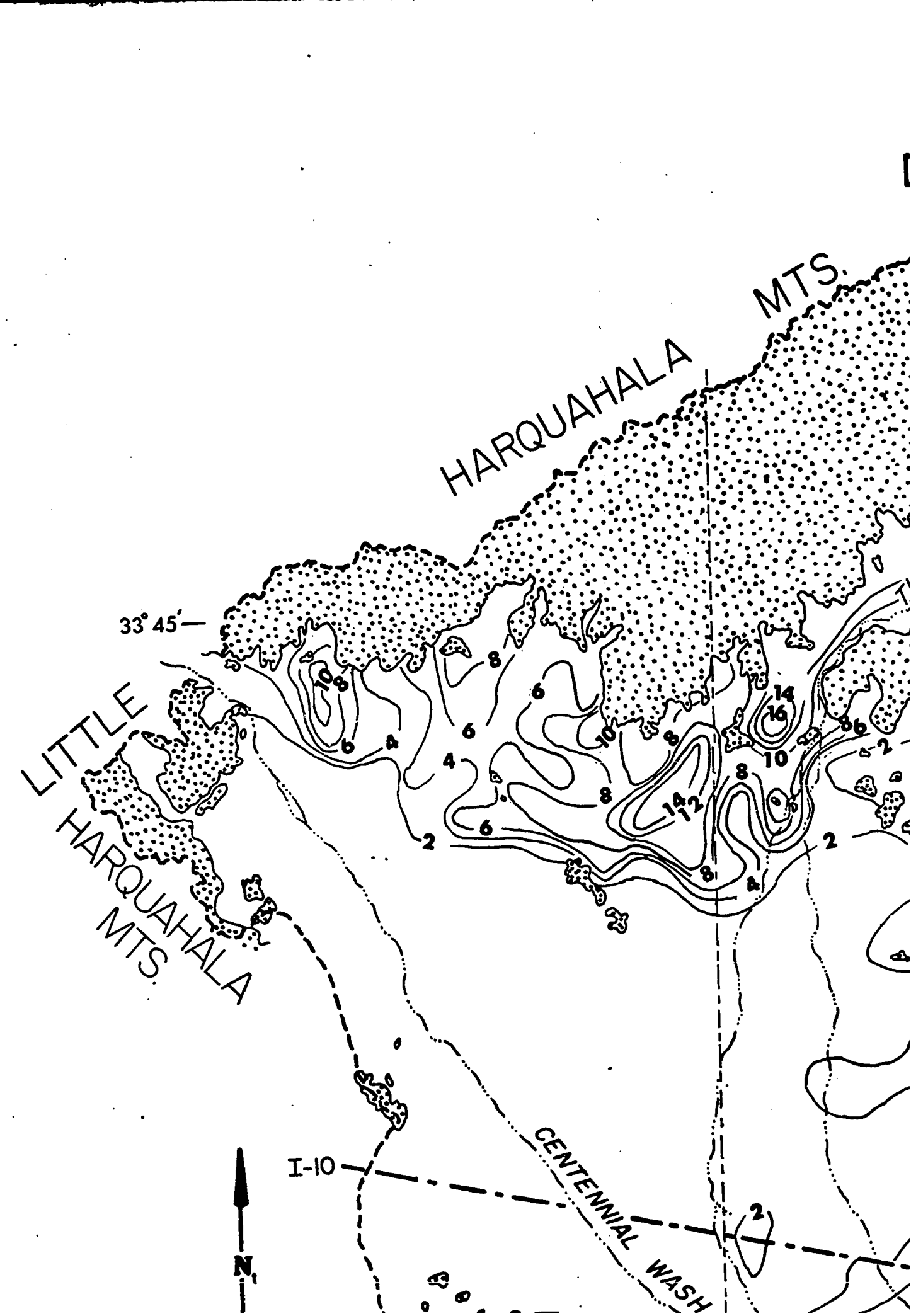

DRAINAGE TEXTURE MAP

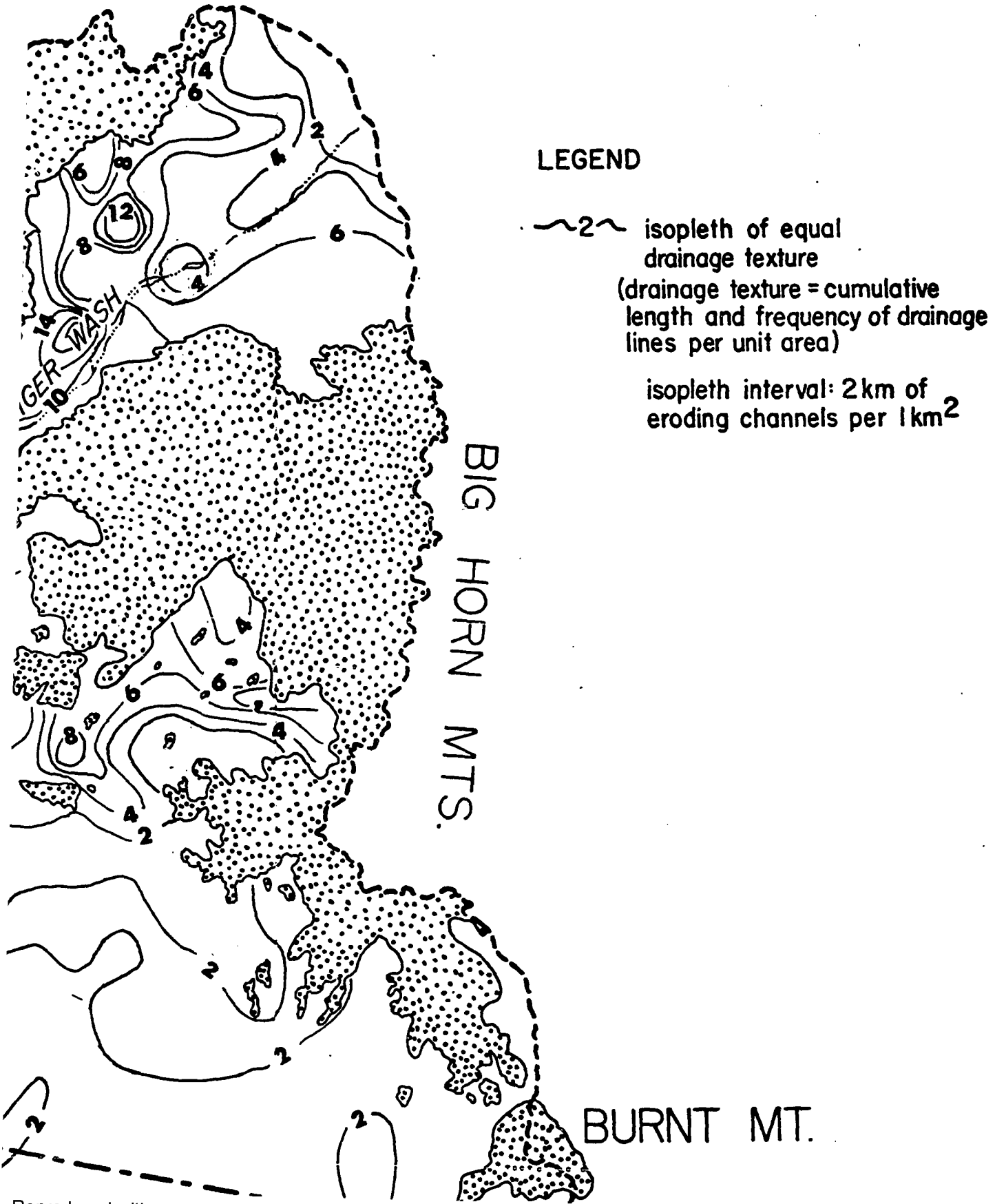

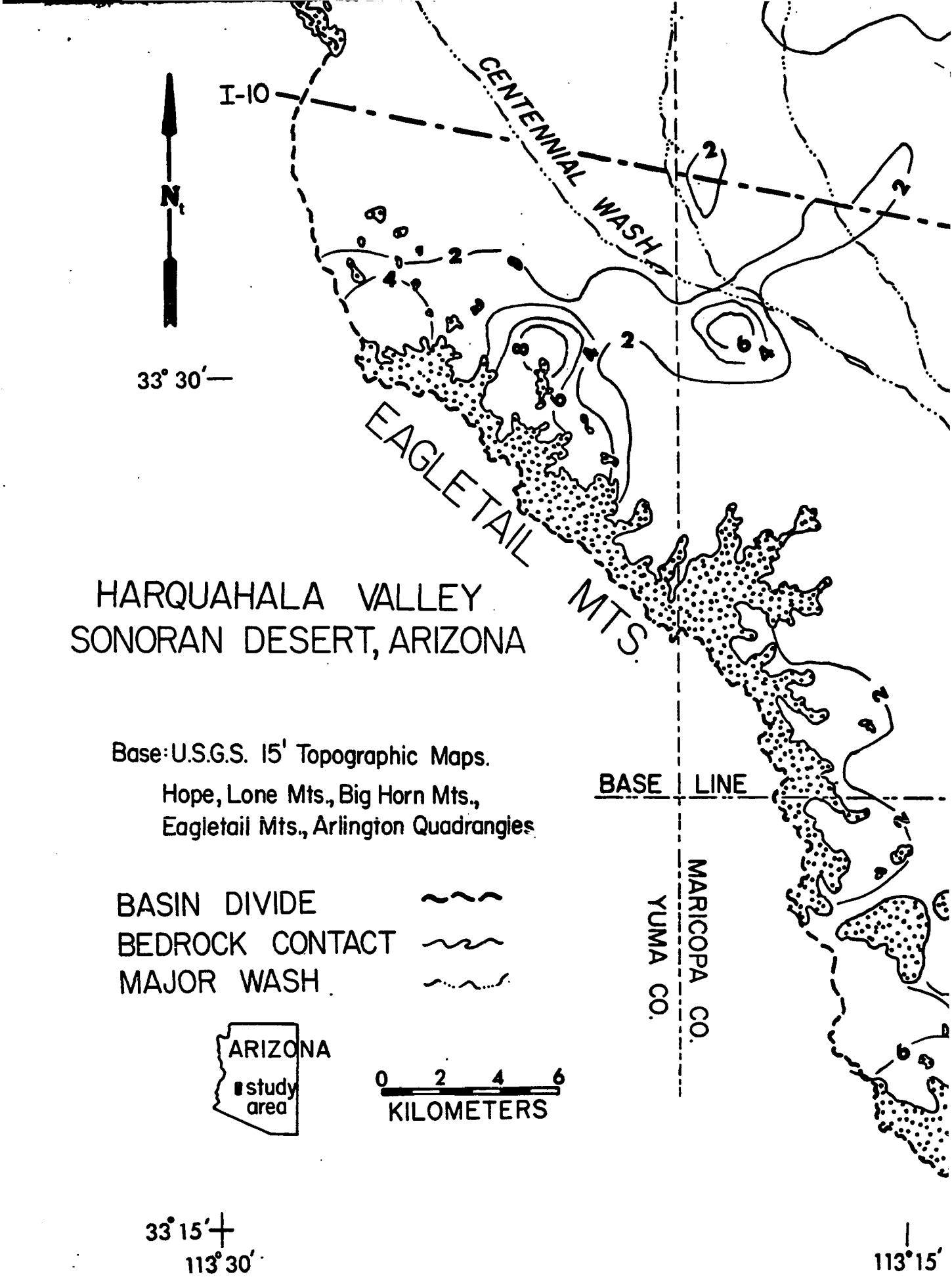

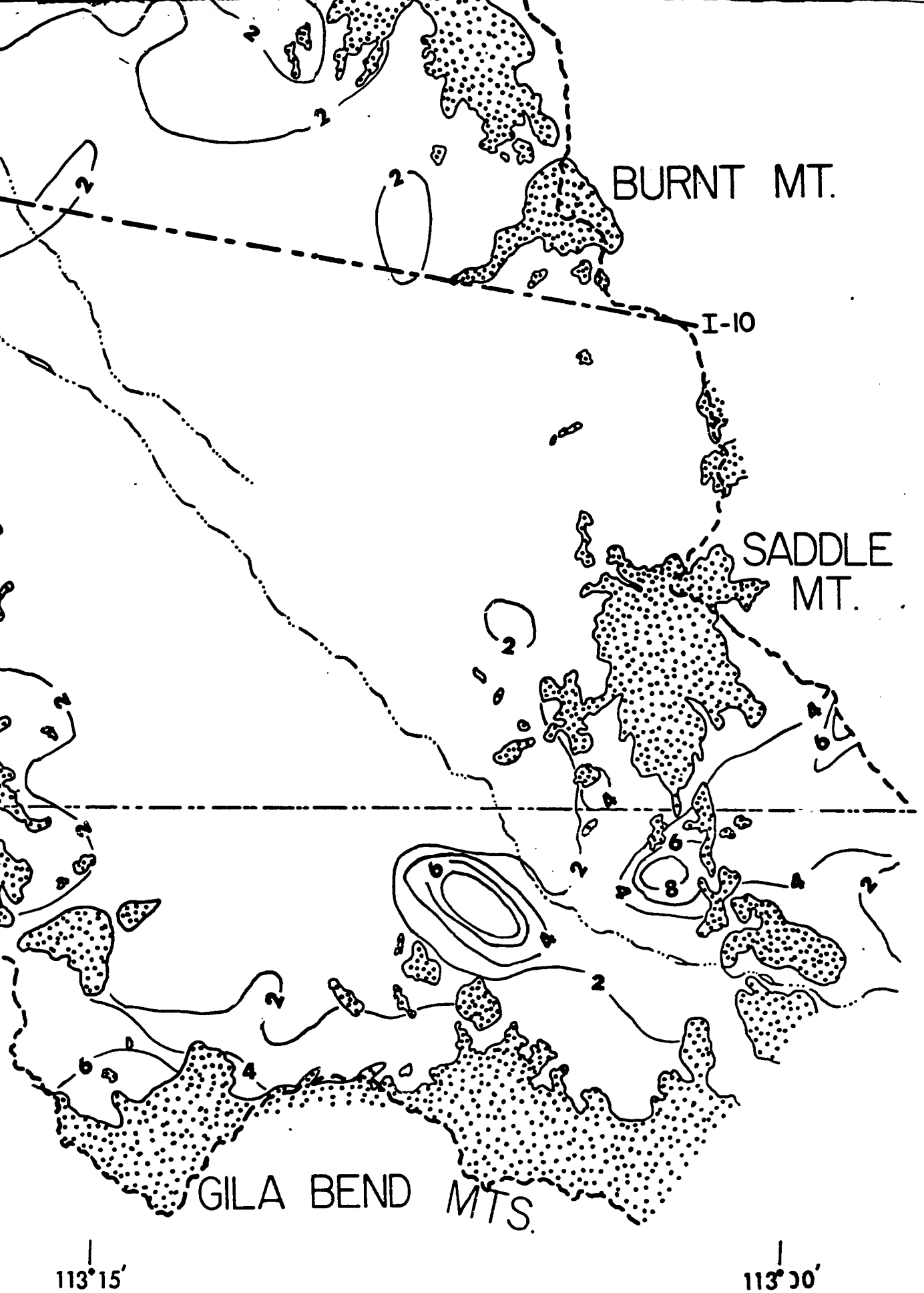

MAP O

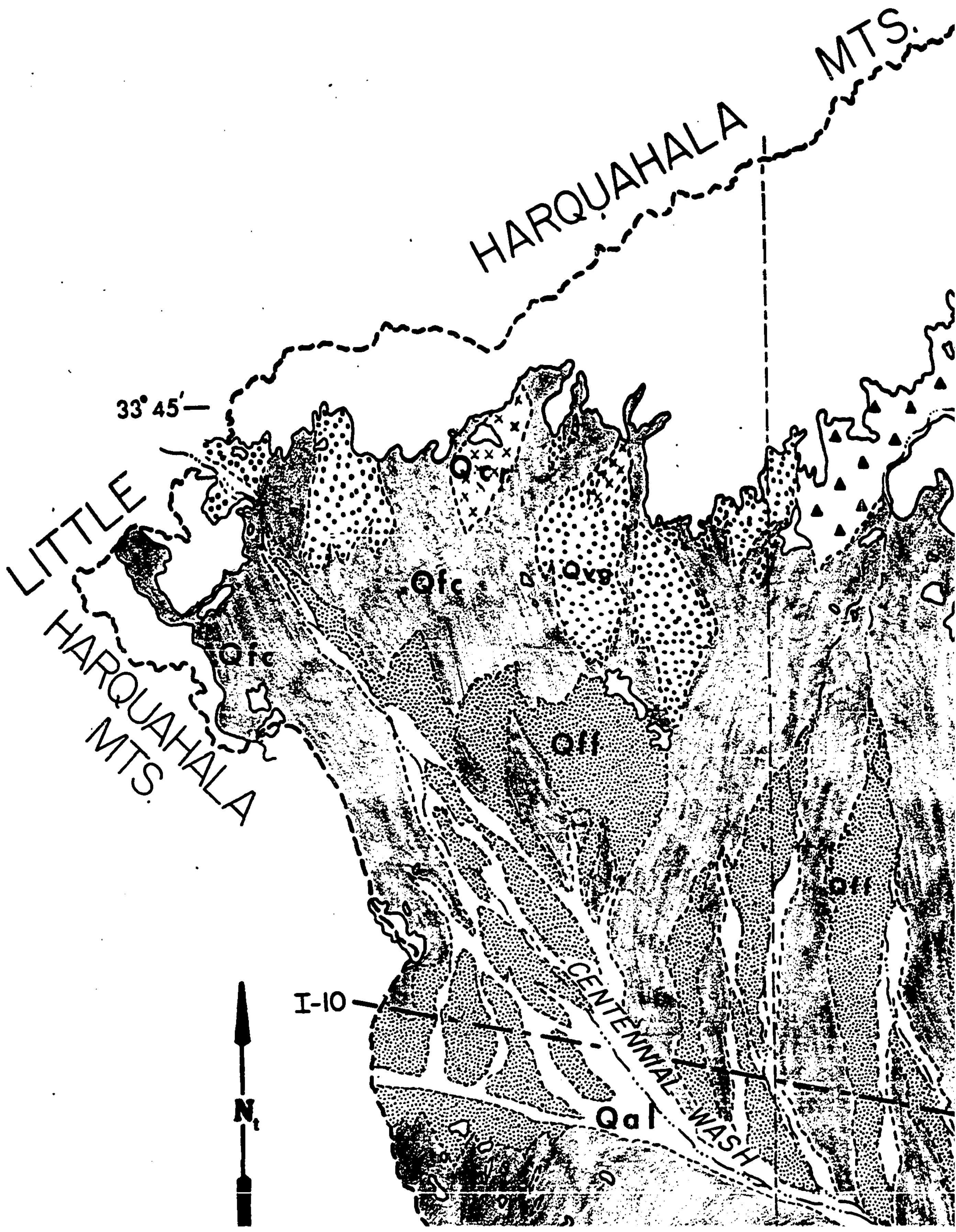

QUATERNARY SURFICIAL DEPOSITS